frontiers | Research Topics

Proceedings of the 9th international symposium on the biology of vertebrate sex determination

2023

Edited by
Dagmar Wilhelm and Talia L. Hatkevich

Published in
Frontiers in Cell and Developmental Biology

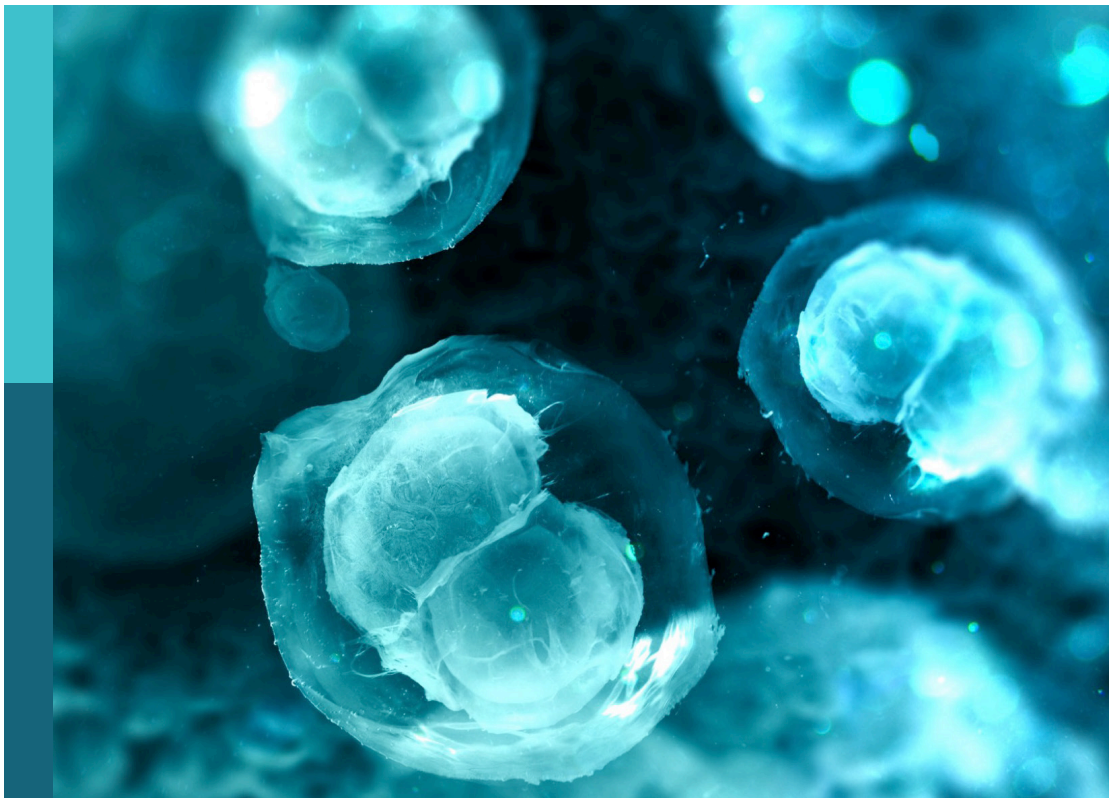

ISSN 1664-8714
ISBN 978-2-8325-5795-2
DOI 10.3389/978-2-8325-5795-2

About Frontiers

Frontiers is more than just an open access publisher of scholarly articles: it is a pioneering approach to the world of academia, radically improving the way scholarly research is managed. The grand vision of Frontiers is a world where all people have an equal opportunity to seek, share and generate knowledge. Frontiers provides immediate and permanent online open access to all its publications, but this alone is not enough to realize our grand goals.

Frontiers journal series

The Frontiers journal series is a multi-tier and interdisciplinary set of open-access, online journals, promising a paradigm shift from the current review, selection and dissemination processes in academic publishing. All Frontiers journals are driven by researchers for researchers; therefore, they constitute a service to the scholarly community. At the same time, the *Frontiers journal series* operates on a revolutionary invention, the tiered publishing system, initially addressing specific communities of scholars, and gradually climbing up to broader public understanding, thus serving the interests of the lay society, too.

Dedication to quality

Each Frontiers article is a landmark of the highest quality, thanks to genuinely collaborative interactions between authors and review editors, who include some of the world's best academicians. Research must be certified by peers before entering a stream of knowledge that may eventually reach the public - and shape society; therefore, Frontiers only applies the most rigorous and unbiased reviews. Frontiers revolutionizes research publishing by freely delivering the most outstanding research, evaluated with no bias from both the academic and social point of view. By applying the most advanced information technologies, Frontiers is catapulting scholarly publishing into a new generation.

What are Frontiers Research Topics?

Frontiers Research Topics are very popular trademarks of the *Frontiers journals series*: they are collections of at least ten articles, all centered on a particular subject. With their unique mix of varied contributions from Original Research to Review Articles, Frontiers Research Topics unify the most influential researchers, the latest key findings and historical advances in a hot research area.

Find out more on how to host your own Frontiers Research Topic or contribute to one as an author by contacting the Frontiers editorial office: frontiersin.org/about/contact

Proceedings of the 9th international symposium on the biology of vertebrate sex determination 2023

Topic editors

Dagmar Wilhelm — The University of Melbourne, Australia

Talia L. Hatkevich — Duke University, United States

Citation

Wilhelm, D., Hatkevich, T. L., eds. (2024). *Proceedings of the 9th international symposium on the biology of vertebrate sex determination 2023*. Lausanne: Frontiers Media SA. doi: 10.3389/978-2-8325-5795-2

Table of contents

frontiers | Frontiers in Cell and Developmental Biology

TYPE Editorial
PUBLISHED 05 December 2024
DOI 10.3389/fcell.2024.1530367

OPEN ACCESS

EDITED AND REVIEWED BY
Fei Liu,
Chinese Academy of Sciences (CAS), China

*CORRESPONDENCE
Talia Hatkevich,
talia.hatkevich@duke.edu
Dagmar Wilhelm,
dagmar.wilhelm@unimelb.edu.au

RECEIVED 18 November 2024
ACCEPTED 22 November 2024
PUBLISHED 05 December 2024

CITATION
Hatkevich T and Wilhelm D (2024) Editorial: Proceedings of the 9th international symposium on the biology of vertebrate sex determination 2023.
Front. Cell Dev. Biol. 12:1530367.
doi: 10.3389/fcell.2024.1530367

Editorial: Proceedings of the 9th international symposium on the biology of vertebrate sex determination 2023

Talia Hatkevich[1]* and Dagmar Wilhelm[2]*

[1]Department of Cell Biology, Duke University Medical Center, Durham, NC, United States, [2]Department of Anatomy and Physiology, The University of Melbourne, Parkville, VIC, Australia

KEYWORDS

sex determination, gonad, gonadal development, Müllerian duct, *Sry*

Editorial on the Research Topic
Proceedings of the 9th international symposium on the biology of vertebrate sex determination 2023

The survival of sexually reproducing species is reliant on proper formation of mature gametes and their subsequent fertilization, and in many organisms, this is dependent upon gonadal sex determination. Gonadal sex determination is the processes in which the bipotential genital ridge differentiates into an ovary or a testis, which can be driven by cues from genetic factors and/or environmental signals (Nagahama et al., 2021). In most mammals, sex determination is genetically dictated, initiated by the expression of the testis-promoting gene *Sry* from the Y chromosome (Koopman et al., 1991; Sinclair et al., 1990). Expression of *Sry* triggers the differentiation of the testes by activating *Sox9* in supporting precursor cells (Sekido and Lovell-Badge, 2008). This initiates a cascade of events, including the formation of Sertoli cells and Leydig cells, which are essential for producing sex hormones that subsequently drive male reproductive organ development (Svingen and Koopman, 2013). In the absence of the Y chromosome, the -KTS splice form of the transcription factor WT1 initiates ovarian development (Gregoire et al., 2023), which is associated with activated canonical WNT/β-catenin signalling and expression of the transcription factor FOXL2 (Chassot et al., 2008; Garcia-Ortiz et al., 2009; Gustin et al., 2016; Maatouk et al., 2008; Yao et al., 2004). Furthermore, to ensure proper gonad development, the testicular and ovarian program suppress each other (Kim et al., 2006). However, the mechanisms surrounding the nuanced processes of sex determination and sex-specific structures throughout vertebrates remain poorly defined. This Special Research Topic, "*Proceedings of the 9th International Symposium on the Biology of Vertebrate Sex Determination 2023*," brings together articles that explore the complex mechanisms underlying sex determination and differentiation in vertebrates. The contributing pieces address key outstanding questions in the field, presenting novel findings and ideology that shed light on genetic, epigenetic, and hormonal regulation of gonadal development and sexual differentiation.

A central question within the field focuses on how genetic and epigenetic mechanisms orchestrate the sex-specific development of the bipotential gonad. Here, Ming et al. introduce a new testicular target gene of SOX9, *Trpc3*. This study shows that *Trpc3* is highly expressed in Sertoli cells during early gonadal development, and in *Sox9* knockout mice, *Trpc3* is downregulated. Inhibiting TRPC3 leads to reduced germ cell proliferation

and endothelial cell apoptosis. Collectively, this work suggests that TRPC3 may mediate SOX9's function in the testis, highlighting the role of *Trpc3* in gonadal development and its potential implications for understanding male infertility.

Expanding on the molecular landscape of sex determination, Stevant et al. explore the role of transposable elements (TEs), mobile genetic elements that can influence gene expression (Percharde et al., 2018). Sophisticated bioinformatics analysis identified TEs as key players in the regulation of sex-specific genes. Further, this study shows that TEs not only regulate gene expression through the production of TE-derived RNAs but also function as cis-regulatory elements that control the expression of sex-specific genes. TEs appear to play a crucial role in gonadal sex determination and differentiation, making TEs integral to the genetic program of sexual differentiation in vertebrates.

Sex determination mechanisms are diverse and can vary significantly across species. While mammals rely heavily on genetic factors, other vertebrates like zebrafish exhibit more flexible sex determination systems (Nagahama et al., 2021). In this research topic, Wilson et al. studied a wild strain of *Danio rerio*, which exhibits a ZZ/ZW chromosomal system. Using single cell sequencing, this work found that the presence of a W chromosome or fewer than two Z chromosomes is crucial for initiating ovarian development. Conversely, gonads with two Z chromosomes develop into testes, bypassing the juvenile ovary stage altogether. This discovery in zebrafish helps expand our understanding of the evolutionary forces that shape sex determination mechanisms across vertebrates.

The development of the Müllerian ducts, which give rise to the female reproductive tract, has long been a subject of study in sexual differentiation. In mammals, the ducts differentiate into the Fallopian tubes, uterus, and upper vagina, while in birds, the ducts form the oviducts. The role of anti-Müllerian hormone (AMH) in the regression of Müllerian ducts in males is well-established (Behringer, 1994; Behringer et al., 1990; Josso, Cate, et al., 1993; Josso, Lamarre, et al., 1993; Josso and Picard, 1986); however, there are remaining questions regarding species that exhibit sexual asymmetry, including chickens (Bakst, 1998). In female chickens, only the left Müllerian duct forms an oviduct. Tan et al. present a literature review on avian Müllerian duct asymmetry and proposes that local interactions between AMH and sex steroids could explain this phenomenon. Furthermore, while Müllerian ducts give rise to oviducts, the Wolffian ducts are precursors of the male reproductive tract. These reproductive tracts export gametes for subsequent fertilization. However, some species, like cyclostomes and basal teleost, lack genital ducts and instead possess genital pores to export gametes (Goodrich, 1930). These differences in gamete-exporting organs across vertebrates are discussed in a comprehensive review by Kanamori and Kobayashi. This review posits outstanding questions on the structure and development of gamete-exporting organs and emphasizes the importance of additional studies on cyclostomes, cartilaginous fishes, basal ray-finned fishes and teleost.

Testicular descent, the movement of testes from near the kidneys to the scrotum, is a key feature of most mammals, believed to be linked to the evolution of endothermy (Werdelin and Nilsonne, 1999). However, certain groups of mammals, particularly within *Afrotheria* and monotremes, exhibit either partial descent or internal testes (Sharman, 1970). Here, Menzies et al. explore the conservation and mechanism of marsupial testicular decent. Using phylogeny and gene analysis of hormone insulin-like peptide 3 (*Insl3*), the authors argue for a therian origin of INSL3 mediated testicular descent in mammals.

A critical aspect of sexual differentiation is the action of steroid hormones, which regulate gonadal function and fertility (De Gendt et al., 2004; Liu et al., 2009; Publicover and Barratt, 2011). Hormones like androgens, estrogens, progesterone, cortisol, and aldosterone influence testicular function through specific receptors, and disruption of these hormonal signals can have profound effects on fertility and sexual development. Matsuyama and DeFalco highlight the complex network of steroid hormones and their receptor function and localization. This review underscores the interplay of these signaling pathways and aims to serve as a resource for further investigation into hormonal mechanisms regulating of male reproductive health.

In addition to the gonad, the brain itself undergoes sexual differentiation, often influenced by steroid hormones released from the gonads (Arnold, 2009; Phoenix et al., 1959). However, genetic factors may also play a role in brain sex differentiation, independent of gonadal influence. Paylar et al. show that in rat brains sex-specific gene expression occurs prior to the onset of gonadal hormone action. The genes *Sry2*, *Eif2s3y*, and *Ddx3y* were found to be expressed at higher levels in males, perhaps contributing to the development of the male brain. These findings suggest that sex-specific genetic programs may contribute to brain differentiation alongside hormonal signals.

In conclusion, the field of vertebrate sex determination is rapidly evolving, with new findings shedding light on the genetic, epigenetic, and hormonal regulation of sexual differentiation. From the identification of novel testicular target genes to the exploration of TEs and homology of sex organs across species, this Special Research Topic highlights the complexity and diversity of sex determination mechanisms.

Author contributions

TH: Conceptualization, Writing–original draft, Writing–review and editing. DW: Writing–original draft, Writing–review and editing.

Funding

The author(s) declare that financial support was received for the research, authorship, and/or publication of this article. We acknowledge funding from NIH grant F32HD113220 to T.H.

Acknowledgments

Generative AI was used in the generation of this Editorial. OpenAI. (2023). ChatGPT (Mar 14 version) [Large language model]. https://chat.openai.com/chat.

Conflict of interest

The authors declare that the research was conducted in the absence of any commercial or financial relationships that could be construed as a potential conflict of interest.

Publisher's note

References

Arnold, A. P. (2009). The organizational-activational hypothesis as the foundation for a unified theory of sexual differentiation of all mammalian tissues. *Horm. Behav.* 55 (5), 570–578. doi:10.1016/j.yhbeh.2009.03.011

Bakst, M. R. (1998). Structure of the avian oviduct with emphasis on sperm storage in poultry. *J. Exp. Zool.* 282 (4-5), 618–626. doi:10.1002/(sici)1097-010x(199811/12)282:4/5<618::aid-jez11>3.3.co;2-d

Behringer, R. R. (1994). The *in vivo* roles of müllerian-inhibiting substance. *Curr. Top. Dev. Biol.* 29, 171–187. doi:10.1016/s0070-2153(08)60550-5

Behringer, R. R., Cate, R. L., Froelick, G. J., Palmiter, R. D., and Brinster, R. L. (1990). Abnormal sexual development in transgenic mice chronically expressing müllerian inhibiting substance. *Nature* 345 (6271), 167–170. doi:10.1038/345167a0

Chassot, A. A., Ranc, F., Gregoire, E. P., Roepers-Gajadien, H. L., Taketo, M. M., Camerino, G., et al. (2008). Activation of beta-catenin signaling by Rspo1 controls differentiation of the mammalian ovary. *Hum. Mol. Genet.* 17 (9), 1264–1277. doi:10.1093/hmg/ddn016

De Gendt, K., Swinnen, J. V., Saunders, P. T., Schoonjans, L., Dewerchin, M., Devos, A., et al. (2004). A Sertoli cell-selective knockout of the androgen receptor causes spermatogenic arrest in meiosis. *Proc. Natl. Acad. Sci. U. S. A.* 101 (5), 1327–1332. doi:10.1073/pnas.0308114100

Garcia-Ortiz, J. E., Pelosi, E., Omari, S., Nedorezov, T., Piao, Y., Karmazin, J., et al. (2009). Foxl2 functions in sex determination and histogenesis throughout mouse ovary development. *BMC Dev. Biol.* 9, 36. doi:10.1186/1471-213x-9-36

Goodrich, E. S. (1930). *Studies on the structure and development of vertebrates*. Macmillan. Available at: https://www.biodiversitylibrary.org/item/155742.

Gregoire, E. P., De Cian, M. C., Migale, R., Perea-Gomez, A., Schaub, S., Bellido-Carreras, N., et al. (2023). The -KTS splice variant of WT1 is essential for ovarian determination in mice. *Science* 382 (6670), 600–606. doi:10.1126/science.add8831

Gustin, S. E., Hogg, K., Stringer, J. M., Rastetter, R. H., Pelosi, E., Miles, D. C., et al. (2016). WNT/β-catenin and p27/FOXL2 differentially regulate supporting cell proliferation in the developing ovary. *Dev. Biol.* 412 (2), 250–260. doi:10.1016/j.ydbio.2016.02.024

Josso, N., Cate, R. L., Picard, J. Y., Vigier, B., di Clemente, N., Wilson, C., et al. (1993). Anti-müllerian hormone: the Jost factor. *Recent Prog. Horm. Res.* 48, 1–59. doi:10.1016/b978-0-12-571148-7.50005-1

Josso, N., and Picard, J. Y. (1986). Anti-Müllerian hormone. *Physiol. Rev.* 66 (4), 1038–1090. doi:10.1152/physrev.1986.66.4.1038

Kim, Y., Kobayashi, A., Sekido, R., DiNapoli, L., Brennan, J., Chaboissier, M. C., et al. (2006). Fgf9 and Wnt4 act as antagonistic signals to regulate mammalian sex determination. *PLoS Biol.* 4 (6), e187. doi:10.1371/journal.pbio.0040187

Koopman, P., Gubbay, J., Vivian, N., Goodfellow, P., and Lovell-Badge, R. (1991). Male development of chromosomally female mice transgenic for Sry. *Nature* 351 (6322), 117–121. doi:10.1038/351117a0

Liu, X., Zhu, P., Sham, K. W., Yuen, J. M., Xie, C., Zhang, Y., et al. (2009). Identification of a membrane estrogen receptor in zebrafish with homology to mammalian GPER and its high expression in early germ cells of the testis. *Biol. Reprod.* 80 (6), 1253–1261. doi:10.1095/biolreprod.108.070250

Maatouk, D. M., DiNapoli, L., Alvers, A., Parker, K. L., Taketo, M. M., and Capel, B. (2008). Stabilization of beta-catenin in XY gonads causes male-to-female sex-reversal. *Hum. Mol. Genet.* 17 (19), 2949–2955. doi:10.1093/hmg/ddn193

Nagahama, Y., Chakraborty, T., Paul-Prasanth, B., Ohta, K., and Nakamura, M. (2021). Sex determination, gonadal sex differentiation, and plasticity in vertebrate species. *Physiol. Rev.* 101 (3), 1237–1308. doi:10.1152/physrev.00044.2019

Percharde, M., Lin, C. J., Yin, Y., Guan, J., Peixoto, G. A., Bulut-Karslioglu, A., et al. (2018). A LINE1-nucleolin partnership regulates early development and ESC identity. *Cell* 174 (2), 391–405.e19. doi:10.1016/j.cell.2018.05.043

Phoenix, C. H., Goy, R. W., Gerall, A. A., and Young, W. C. (1959). Organizing action of prenatally administered testosterone propionate on the tissues mediating mating behavior in the female Guinea pig. *Endocrinology* 65, 369–382. doi:10.1210/endo-65-3-369

Publicover, S., and Barratt, C. (2011). Reproductive biology: progesterone's gateway into sperm. *Nature* 471 (7338), 313–314. doi:10.1038/471313a

Sekido, R., and Lovell-Badge, R. (2008). Sex determination involves synergistic action of SRY and SF1 on a specific Sox9 enhancer. *Nature* 453 (7197), 930–934. doi:10.1038/nature06944

Sharman, G. B. (1970). Reproductive physiology of marsupials. *Science* 167 (3922), 1221–1228. doi:10.1126/science.167.3922.1221

Sinclair, A. H., Berta, P., Palmer, M. S., Hawkins, J. R., Griffiths, B. L., Smith, M. J., et al. (1990). A gene from the human sex-determining region encodes a protein with homology to a conserved DNA-binding motif. *Nature* 346 (6281), 240–244. doi:10.1038/346240a0

Svingen, T., and Koopman, P. (2013). Building the mammalian testis: origins, differentiation, and assembly of the component cell populations. *Genes Dev.* 27 (22), 2409–2426. doi:10.1101/gad.228080.113

Werdelin, L., and Nilsonne, A. (1999). The evolution of the scrotum and testicular descent in mammals: a phylogenetic view. *J. Theor. Biol.* 196 (1), 61–72. doi:10.1006/jtbi.1998.0821

Yao, H. H., Matzuk, M. M., Jorgez, C. J., Menke, D. B., Page, D. C., Swain, A., et al. (2004). Follistatin operates downstream of Wnt4 in mammalian ovary organogenesis. *Dev. Dyn.* 230 (2), 210–215. doi:10.1002/dvdy.20042

frontiers | Frontiers in Cell and Developmental Biology

TYPE Review
PUBLISHED 22 December 2023
DOI 10.3389/fcell.2023.1328024

OPEN ACCESS

EDITED BY
Dagmar Wilhelm,
The University of Melbourne, Australia

REVIEWED BY
Linyan Zhou,
Chinese Academy of Fishery Sciences, China
Christoph Winkler,
National University of Singapore, Singapore

*CORRESPONDENCE
Akira Kanamori,
akirakanamorina@gmail.com

RECEIVED 26 October 2023
ACCEPTED 30 November 2023
PUBLISHED 22 December 2023

CITATION
Kanamori A and Kobayashi Y (2023), Gamete-exporting organs of vertebrates: dazed and confused.
Front. Cell Dev. Biol. 11:1328024.
doi: 10.3389/fcell.2023.1328024

Gamete-exporting organs of vertebrates: dazed and confused

Akira Kanamori[1]* and Yasuhisa Kobayashi[2]

[1]Group of Development and Growth Regulation, Division of Biological Science, Graduate School of Science, Nagoya University, Nagoya, Japan, [2]Laboratory for Aquatic Biology, Department of Fisheries, Faculty of Agriculture, Kindai University, Nara, Japan

Mature gametes are transported externally for fertilization. In vertebrates, the gonads are located within the coelom. Consequently, each species has specific organs for export, which often vary according to sex. In most vertebrates, sperm ducts and oviducts develop from the Wolffian and Müllerian ducts, respectively. However, exceptions exist. Both sexes of cyclostomes, as well as females of basal teleosts, lack genital ducts but possess genital pores. In teleosts of both sexes, genital ducts are formed through the posterior extensions of gonads. These structures appear to be independent of both Wolffian and Müllerian ducts. Furthermore, the development of Wolffian and Müllerian ducts differs significantly among various vertebrates. Are these gamete-exporting organs homologous or not? A question extensively debated around the turn of the 20th century but now largely overlooked. Recent research has revealed the indispensable role of Wnt4a in genital duct development in both sexes of teleosts: zebrafish and medaka. *wnt4a* is an ortholog of mammalian *Wnt4*, which has functions in Müllerian duct formation. These results suggest a potential homology between the mammalian Müllerian ducts and genital ducts in teleosts. To investigate the homology of gamete-exporting organs in vertebrates, more detailed descriptions of their development across vertebrates, using modern cellular and genetic tools, are needed. Therefore, this review summarizes existing knowledge and unresolved questions on the structure and development of gamete-exporting organs in diverse vertebrate groups. This also underscores the need for comprehensive studies, particularly on cyclostomes, cartilaginous fishes, basal ray-finned fishes, and teleosts.

KEYWORDS

Müllerian duct, oviduct, Wolffian duct, sperm duct, *wnt4*, teleosts, cartilaginous fishes, cyclostomes

1 Introduction

The gonads of all vertebrates are suspended dorsally within the coelom (body cavity). Consequently, for sexual reproduction to occur, gametes must find their way out of the body. Vertebrates employ various paths for this purpose, often exhibiting differences based on sex. Some have genital pores, which are very short passages from the coelom to the urogenital sinus. Most jawed vertebrates use the Wolffian ducts (WDs) and Müllerian ducts (MDs) for sperm and ova export, respectively. Finally, most teleosts of both sexes have genital ducts that develop as posterior extensions of the gonads. The anatomical differences among these three

Abbreviations: WD, Wolffian duct, MD, Müllerian duct, GP, genital pore, TD, testicular duct, OD, ovarian duct, OC, ovarian cavity.

types of structures have historically led to their classification as non-homologous organs in textbooks on vertebrate comparative anatomy (e.g., Romer and Parsons, 1977; Wake, 1979; Blüm, 1986; Lombardi, 1998).

Recent studies have revealed that Wnt4a is indispensable for genital duct development in both sexes of two diverse teleost species, zebrafish (Kossack et al., 2019) and the medaka *Oryzias latipes* (Kanamori et al., 2023). Teleost *wnt4a* is an ortholog of mammalian *Wnt4*, which has functions in the MD development (mice, Vainio et al., 1999; humans, Biason-Lauber et al., 2004, Biason-Lauber et al., 2007; see also Mullen and Behringer, 2014; Gonzales et al., 2021). These findings suggested the existence of homologous processes during the development of mammalian MDs and genital ducts in teleosts. This proposition prompted us to question whether homology exists among all gamete-exporting organs across vertebrates. During our literature searches, we were intrigued to find that this specific subject was among the favorites of comparative anatomists around the turn of the 20th century. Their curiosity was likely stimulated by the remarkable diversity observed in both the anatomy and developmental modes of gamete-exporting organs. Darwinian evolutionary theory and Mendelian genetics, combined with advances in microscopy, led to enthusiastic quests for homologies among morphological diversities so prevalent in the animal kingdom. Hoar (1969) noted: "The comparative anatomist has found some of his most interesting problems in the phylogeny of the gonoducts [genital ducts; square brackets represent the authors' annotations] and their relationships to the mesonephric tubules and ducts." Kerr (1919) and Goodrich (1930) provided summaries of the literature up to this period. Particularly, Edwin S. Goodrich made significant contributions to the discussion of genital duct evolution in the animal kingdom, including vertebrates. His enduring interest in the subject is exemplified by a trilogy of papers (Goodrich, 1895; Goodrich, 1930; Goodrich, 1945; see also Holland, 2017). The most debated topics at the time were 1) the origin of genital pores in cyclostomes, 2) the two distinct modes of MD development (cartilaginous fishes vs. other jawed vertebrates), and 3) the origin of teleost genital ducts. Lo and behold, even after a century, these questions remain largely unanswered, with research on the subject tapering off since the 1940s. The sole exception in recent times has been Karl-Heinz Wrobel, who authored a series of exquisite papers on the anatomy and development of the urogenital system in sturgeons during the last few years of his career (Wrobel and Süß, 2000; Wrobel et al., 2002a; Wrobel et al., 2002b; Wrobel, 2003; Wrobel and Jouma, 2004). We believe that these studies provide a roadmap for future investigations, emphasizing the need for detailed and precise descriptions of the structure and development of gamete-exporting organs in several key groups of vertebrates.

How did these seemingly distinct structures, crucial for avoiding extinction, differentiate over the course of vertebrate evolution? This review aims to rekindle general interest in this intriguing, long-unanswered problem. It starts with 1) a summary of the knowledge on vertebrate gamete-exporting organs, followed by 2) detailed discussions addressing pertinent unanswered questions. Finally, we propose 3) the latest methodologies, in addition to classical histology, to address these questions.

2 Anatomy and phylogeny of gamete-exporting organs in vertebrates

As previously outlined, we have broadly categorized the gamete-exporting organs in vertebrates into three main types: genital pores, WDs and MDs, and teleost-specific genital ducts (Figure 1A). Several variations exist within each type, which are not discussed in detail in this review. Interested readers seeking more comprehensive information may refer to textbooks by Goodrich (1930), Romer and Parsons (1977), Wake (1979), Blüm (1986), and Lombardi (1998). Goodrich's work is the oldest and covers a wide array of vertebrate genital duct anatomy and development. The other four offer similar coverage but with the distinctive viewpoints of their respective authors. Below, we provide a summary of the accumulated knowledge on the structures of gamete-exporting organs, along with their distribution within the vertebrate phylogeny.

2.1 Genital pores

Jawless fishes, the earliest vertebrate lineage, include only two extant groups: lampreys and hagfishes (collectively known as cyclostomes). These species lack genital ducts, with mature sperm and oocytes released into the coelom and subsequently exported through genital pores (GPs). These GPs appear only when the individuals have reached maturity and are prepared for copulation. The most recent and informative literature on this topic dates back to Knowles (1939) who demonstrated that gonadotropins and steroid hormones induce GPs from the coelom to the urinary sinus in river lamprey (Figure 2). This hormonal induction led to apoptosis in several cell layers including the coelomic epithelium, mesenchyme, and nephric duct epithelium, resulting in the establishment of GPs (Figure 2B, control; Figure 2C, treated with gonadotropins).

Furthermore, it is worth noting that many basal teleosts, such as elopomorphs (eels and tarpons) and osteoglossomorphs (moon eyes and arowanas), do not possess oviducts in females (Figure 1B). In these species, mature oocytes are directly ovulated into the coelom and, similar to cyclostomes, are exported through the GPs into the urinary sinus. Descriptions of GP structures are available for eels (Syrski, 1876; Tesch, 1977) and have been briefly mentioned for moray eels (Fishelson, 1992), mooneye (*Hiodon tergisus*, Katechis et al., 2007), and pirarucu (Godinho et al., 2005). Unfortunately, comprehensive literature describing the detailed cellular structures or developmental processes of GPs in female basal teleosts is currently lacking.

2.2 WDs and MDs

It is essential to clearly define WD at the outset. During the early stages of development, all vertebrate embryos develop kidneys that facilitate the removal of waste products in the form of urine. The earliest form of the kidney is known as the pronephros, which comprises a few anterior nephrons connected to a duct that extends posteriorly to the urinary sinus (Figure 3; Romer and Parsons, 1977; de Bakker et al., 2019). This duct has been referred to by various

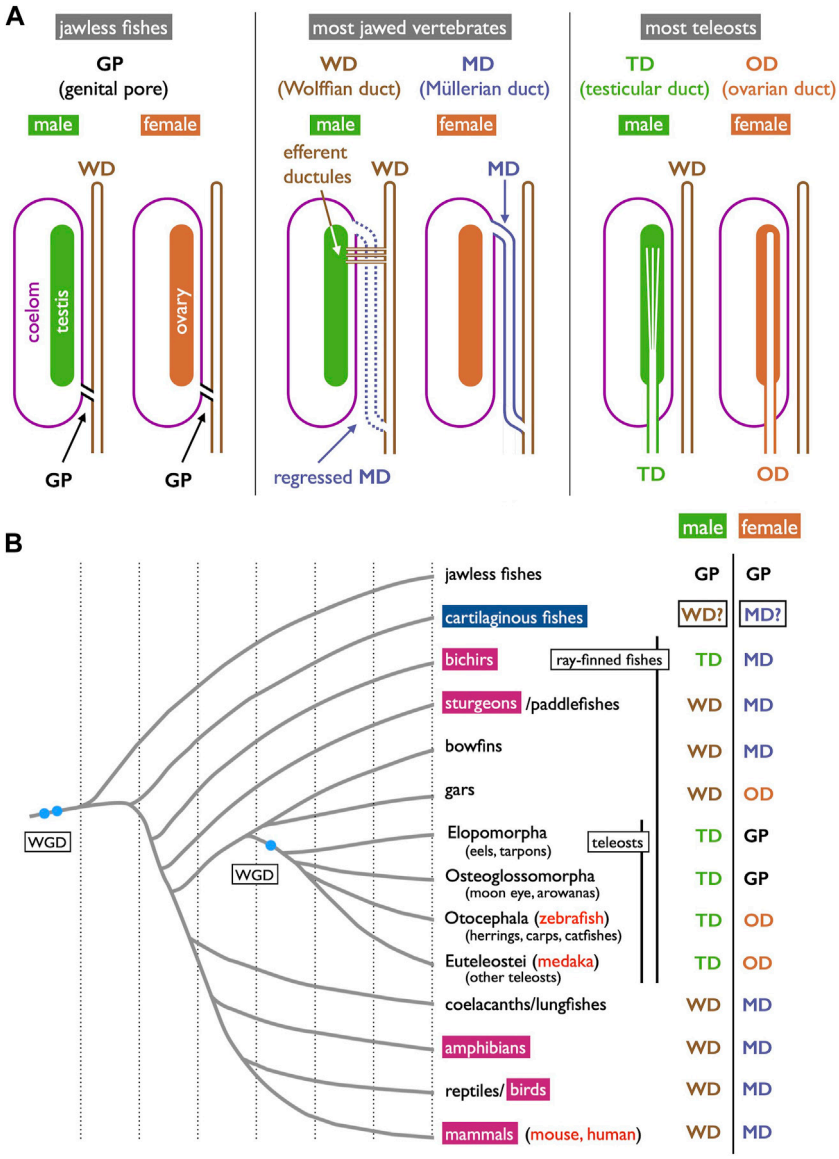

FIGURE 1
Three types of gamete-exporting organs in vertebrates. **(A)** Diagrams illustrating gamete-exporting organs in vertebrates. In jawless fishes, genital ducts are absent, and both sperm and ova are released into the coelom and exported through the genital pores (GPs). In most jawed vertebrates, sperm and ova are exported through the Wolffian ducts (WDs) and Müllerian ducts (MDs), respectively. In males, sperm are exported through the efferent ductules to the WDs; the MDs are developed but later regress in many cases. In females, mature oocytes are shed into the coelom and then exported through the opening of the MDs to the urinary sinus. Finally, most teleosts develop genital ducts as the posterior elongation of gonads: testicular ducts (TDs) and ovarian ducts (ODs). **(B)** Phylogenetic distribution of gamete-exporting organs. The phylogeny of vertebrate groups is based on Hughes et al. (2018), Tekezaki (2021), Koepfli et al. (2015), and Holland and Ocampo Daza (2018). In the species indicated in red letters, *Wnt4* orthologs have been reported to have functions in genital duct development. The **invagination-elongation** mode of MD development is observed in the groups marked in carmine red squares. In cartilaginous fishes (cerulean blue square), the MDs (and the WDs) develop through the **longitudinal splitting** of the pronephric ducts (see Section 3.4 for details).

names, including the pronephric duct, archinephric duct, and WD (as per Romer and Parsons, 1977). As development progresses, the posterior nephrons of the mesonephros (or opisthonephros, posterior kidney) become functional, and the WD is once again utilized to drain urine from the mesonephros, sometimes referred to as the mesonephric duct but identical to the WD. In all male jawed vertebrates, except teleosts and bichirs (Figure 1B), the WD, or at least a portion of the WD, is employed as the duct for exporting sperm. Typically, several thin ducts develop between the testes and WD, serving as sperm canals that transport sperm from the testes to the WDs, referred to as efferent ductules (vasa efferentia) (Figure 4).

In females, all jawed vertebrates, excluding teleosts and gars (Figure 1B), utilize the MDs, also known as paramesonephric ducts, to export ova. In this review, we defined the MD purely anatomically as a duct that opens anteriorly to the coelom, runs alongside the WD, and ultimately opens posteriorly to the urinary sinus (Figure 1A and Figure 4). Mature oocytes are released into the

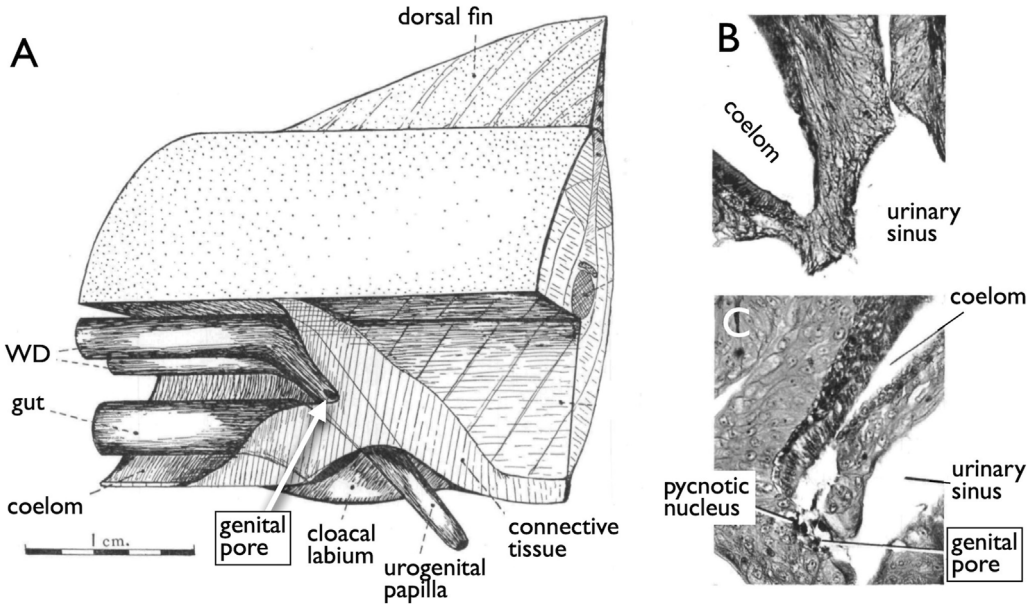

FIGURE 2
Induction of the genital pores in river lamprey by gonadotropins [reproduced from Knowles (1939), with permission from The Company of Biologists]. **(A)** View of the cloacal region of a matured adult *Lampetra fluviatilis*, which has been dissected from the left side. **(B)** Section through the cloacal region of a normal adult male. **(C)** Section through the cloacal region of an adult female, which had been injected with gonadotropins. Several cell layers between the coelom and the urinary sinus undergo apoptosis, forming a path (genital pore) for the oocytes ovulated into the coelom.

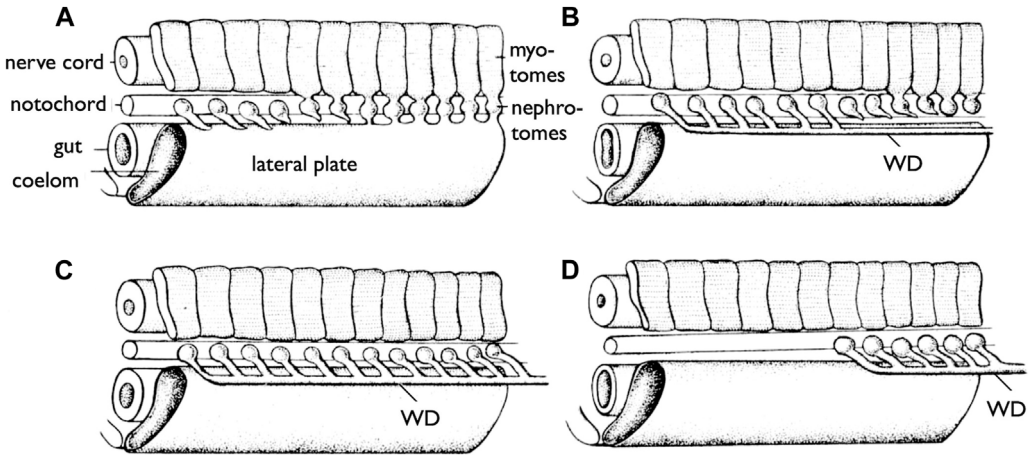

FIGURE 3
Development of the WDs [reproduced from Romer and Parsons (1977), with permission from Elsevier]. Diagrams of the anterior part of the trunk of an embryo (skin removed) to show the development of the WD. **(A)** Most anterior pronephric nephrotomes are budding out tubules that tend to fuse posteriorly. **(B)** The pronephric tubules have formed the duct (WD); the nephrotomes farther posteriorly are forming tubules which are to enter the duct (WD). **(C)** The more posterior tubules have joined the duct (WD). **(D)** The pronephros are lost, but the WD formed by it persists to drain the more posterior part of the kidney (mesonephros).

coelom, transferred to the MD through the coelomic opening, and exported to the urinary sinus. MDs differentiate into various regions, including the uterus that support fetuses in viviparous cartilaginous fishes and mammals. In other groups, they play a role in the production of egg envelopes and other supporting materials for oocytes (see Major et al., 2022). In Section 3.4, we discuss two different modes of MD development reported in vertebrates.

2.3 Genital ducts in teleosts

While Nagahama (1983) provided an overview of the basic structures of genital ducts in teleosts, detailed descriptions of their developmental processes are limited, except in the medaka (Suzuki and Shibata, 2004; Kanamori et al., 2023). In male teleosts, spermatogenesis progresses within tube-like structures (Figure 5A)

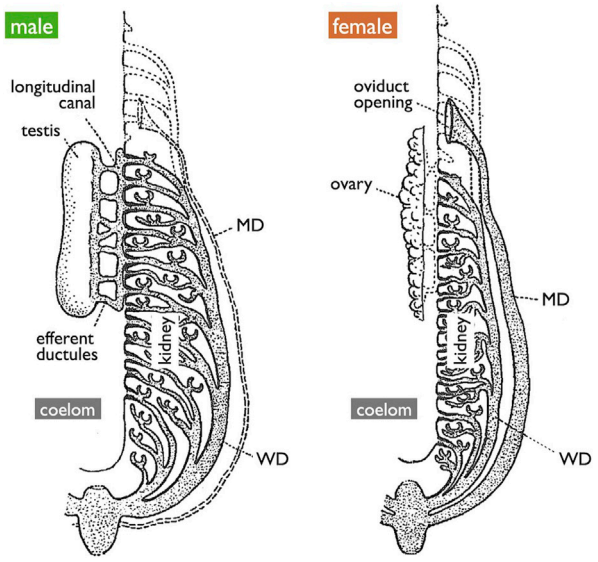

FIGURE 4
Diagrams of the urogenital system of generalized jawed vertebrates [adapted from Goodrich (1945), with permission from The Company of Biologists]. The testis is connected to the kidney through efferent ductules, and subsequently to WDs. Mature oocytes are released into the coelom and expelled through the openings of MDs. Vestigial MDs in males, vestigial networks of efferent ductules in females, and embryonic pronephros in both sexes are depicted by the dotted lines.

(Nagahama, 1983; Uribe et al., 2014). Spermatogonia are localized at the tips of tubes in tubular-type testes. In the lobular-type testes, spermatogonia are distributed at various locations along the tube. In both types of testes, once spermatogonia enter meiosis, they undergo synchronous development within cysts enveloped by Sertoli cells. As the cysts mature, their walls rupture and release mature sperm into the testicular canals. Consequently, the epithelial cells lining these canals are continuous with the Sertoli cells. Moving posteriorly, these canals merge to form a single duct that elongates further posteriorly, exits the coelom, and ultimately opens externally (Figures 6A, C, D; Suzuki and Shibata, 2004; Kanamori et al., 2023). In some species such as the medaka, the sperm duct connects to the urethra (see Dzyuba et al., 2019).

A unique reproductive structure is present in females of most non-basal teleosts (belonging to Otocephala and Euteleostei; Figure 1B). Instead of the direct release of mature oocytes into the coelom, as observed in many other jawed vertebrates, these females possess hollow ovaries. Within these ovaries, mature oocytes ovulate into enclosed spaces, referred to as ovarian cavities (OCs). OC development primarily occurs through two distinct processes: either the ventral ovarian tissue sheets elongate and merge with the coelomic epithelium, resulting in the formation of a parovarian cavity, or both the dorso-lateral and ventro-lateral ovarian tissue sheets elongate and combine to form the entovarian cavity (Figure 5B; see Lepori, 1980 for details). In the medaka, OC development is triggered by estrogen (Suzuki et al., 2004). These cavities extend posteriorly, exit the coelom, and ultimately open externally (Figures 6B, E, F; Suzuki and Shibata, 2004; Kanamori et al., 2023). In certain species, a duct connection is established with the urinary sinus (see Uematsu and Hibiya, 1983). Taken together, in teleosts, both male and female genital ducts develop similarly, involving the posterior elongation of the gonads. In males, there is no direct connection between the testes and urinary ducts (WDs) via the efferent ductules. In females, mature oocytes are not released into the coelom as in other jawed vertebrates. In this review, we

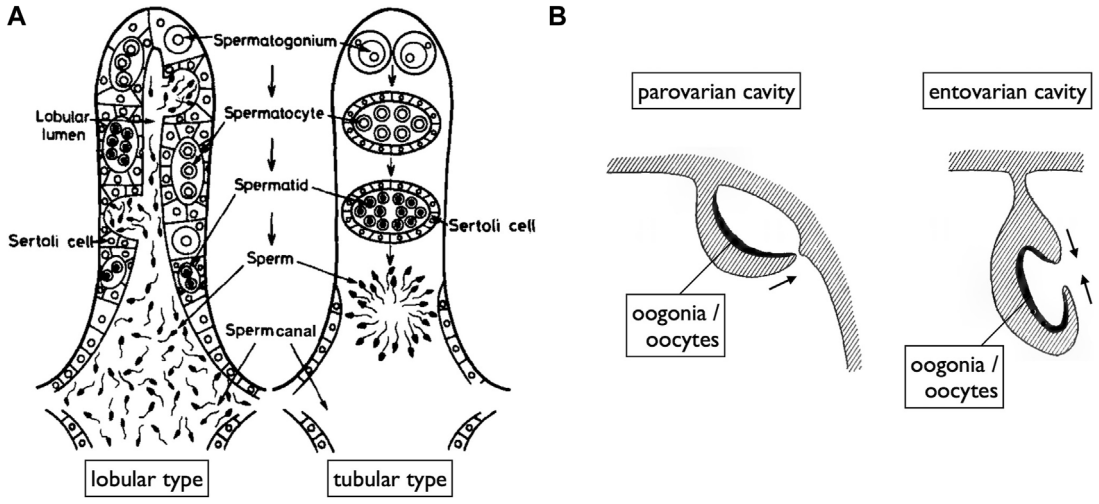

FIGURE 5
Diagrams of teleost gonads illustrating spaces for the release of mature gametes. **(A)** In both lobular type (spermatogonia distributed at various locations along spermatogenic tubes) and tubular type testes (spermatogonia localized at the tips of tubes), spermatogenesis occurs within cysts surrounded by Sertoli cells. Mature sperm are released into spaces (sperm canals) covered by epithelial cells, which are continuous with the Sertoli cells of ruptured spermatogenic cysts [reproduced from Nagahama (1983), with permission from Elsevier]. **(B)** Two modes of OC development [reproduced from Kerr (1919), public domain]. OCs, where ovulated oocytes are released, primarily develop in two ways: the parovarian cavity forms through the fusion of ventral ovarian tissue sheets and the coelomic epithelium, while the entovarian cavity forms through the fusion of dorso-lateral and ventro-lateral ovarian tissue sheets.

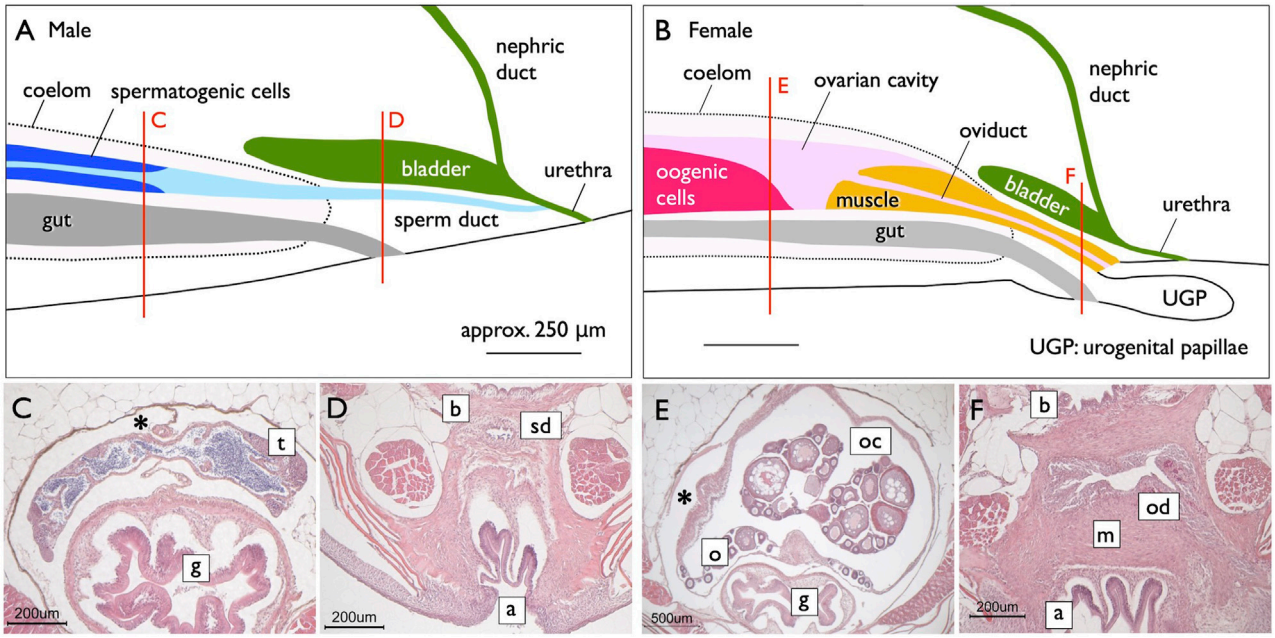

FIGURE 6
Genital ducts of the medaka [adapted from Kanamori et al. (2023), with permission from The Zoological Society of Japan]. Median plane (side view) diagrams illustrating urogenital organs in the medaka, reconstructed from serial histological sections [**(A)**, males; **(B)**, females]. The red lines indicate the levels of cross-sections shown in **(C,D)** (males) and **(E,F)** (females). In males, a single testis (t) is centrally located in the coelom (marked by asterisks) above the gut (g) **(C)**. Mature sperm are released from spermatogenic cysts and are present in canal-like spaces (light blue in A), which fuse posteriorly to form larger lumens. Further posteriorly, the lumens combine to create a single central canal (sperm duct). The sperm duct (sd) exits the coelom beneath the urinary bladder (b) and above the anus (a) **(D)**. Posteriorly, the nephric ducts join the urinary bladder (dark green in A). Subsequently, the sperm ducts fuse with the urethra from its ventral side, and the urinogenital duct opens to the exterior **(A)**. **(B)** In females, a single ovary (o) is centrally situated in the coelom above the gut (g) **(E)**. The ovarian lamella, containing oogonia and developing oocytes, is observed ventrally and at the center of the OC (oc). The posterior part of the OC lacks germ cells, and a sphincter muscle (yellow in B) protrudes from the posterior. A portion of the OC is enveloped by the sphincter muscle (m) to form the oviduct (od) posteriorly. The oviduct then exits the coelom, elongates beneath the urinary bladder **(F)**, and opens dorsally at the well-developed urogenital papillae (ugp) **(B)**.

denote the male and female ducts of teleosts as testicular ducts (TDs) and ovarian ducts (ODs), respectively (Figure 1A).

2.4 Phylogenetic distribution of each gamete-exporting organ

Gamete-exporting organs exhibit varied distributions among vertebrates (Figure 1B). GPs are present in both sexes of cyclostomes and females of basal teleosts. It is evident that the evolution of two critical features occurred at the base of jawed vertebrate radiation: 1) the connection between the testes and WDs and 2) the *de novo* appearance of the MDs. Compelling evidence for the existence of MDs dates back to the Devonian period, approximately 380 million years ago, as indicated by the presence of intrauterine embryos in placoderm fish, an extinct group of cartilaginous fish (Long et al., 2008). Just before the diversification of teleosts, it is conceivable that male TDs evolved through the posterior elongation of the canals within the testes. Among basal teleosts, the presence of TDs has been described in the eel (Bertin, 1958) (Figure 7A). In contrast, basal teleost females have GPs, as described in Section 2.1. There has been a report of two osteoglossomorph fishes possessing OCs (Dymek et al., 2022) without descriptions of their oviducts. It is likely that at the common ancestors of Otocephala (including herrings, carps, and catfishes) and Euteleostei, teleost females acquired OCs and ODs as part of their posterior elongation. Documentation of OCs and ODs is available in Otocephala, including herring (Yamamoto, 1955), carp and goldfish (Uematsu and Hibiya, 1983), zebrafish (Hisaoka and Firlit, 1962), and catfish (Rastogi and Saxena, 1968). In Euteleostei, OCs and ODs are widespread, except in salmonids, where the OCs open secondarily into the coelom (Romer and Parsons, 1977; Lepori, 1980; Blüm, 1986; Lombardi, 1998). Two apparent exceptions to this pattern are noteworthy (Figure 1B): 1) the presence of teleost-like TDs in bichirs (Figure 8A; Budgett, 1901; Budgett, 1902) and 2) the presence of teleost-like ODs in gars (Figure 8D; Budgett, 1902; Pfeiffer, 1933). These exceptions are discussed in the following sections.

3 Long-unanswered questions on homologies among gamete-exporting organs in vertebrates

As mentioned earlier, most of the intriguing questions dating back to the Kerr (1919) and Goodrich (1930) eras remain unanswered. In this section, we provide a comprehensive overview of these questions.

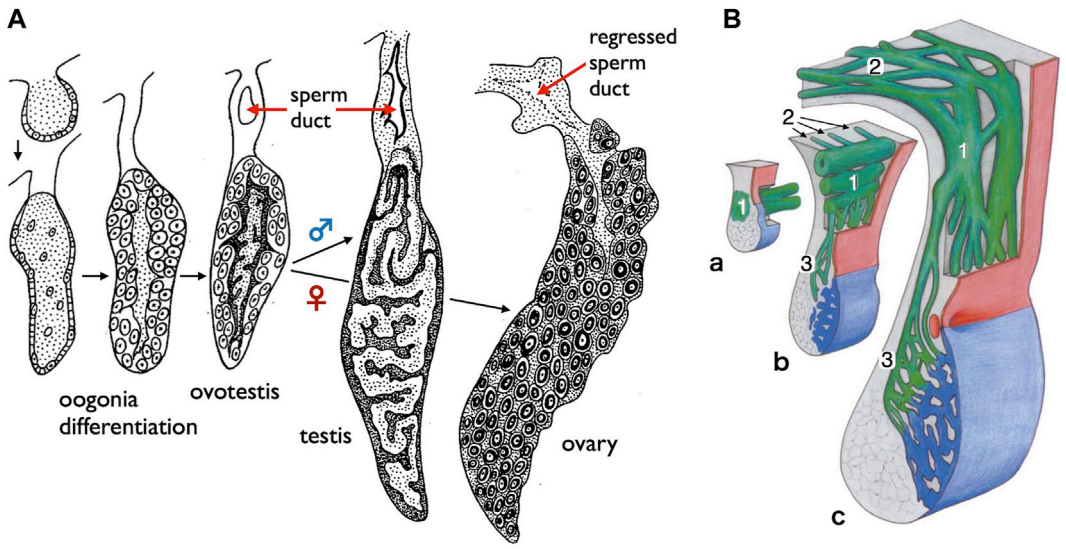

FIGURE 7
Diagrams of the sperm ducts in the European eel (a basal teleost) and the starlet sturgeon (a basal ray-finned fish). **(A)** TD development in the European eel (*Anguilla anguilla*) [adapted from Bertin (1958), with permission from Elsevier Masson SAS]. Oogonia differentiate on the surface of gonads in both sexes, followed by differentiation of spermatogenic cells in the center of gonads. At this hermaphroditic stage, the duct primordium develops dorsally to the gonad within the mesogonadium (tissue sheets suspending gonads from the dorsal wall of the coelom). After sex differentiation, the male primordia develop into the sperm ducts, while the female primordia regress. **(B)** Schematic representation illustrating the development of sperm passageways in 8–18 months-old *Acipenser ruthenus* (starlet sturgeon) [reproduced from Wrobel and Jouma (2004), with permission from Elsevier]. **a**. At 8 months, the pregonadal area of the gonadal fold contains the primary genital duct blastema (1) which grows in the caudal direction as a longitudinal system of solid anastomosing strands situated in the region of the mesogonadal attachment. **b**. At about 9 months, the primary longitudinal strands and tubules of the genital duct apparatus (1) begin to send a series of blinded tubules (2) in the direction of the opisthonephros (posterior kidney). At the same time, narrow anastomosing channels (3) traverse the mesogonadium in the direction of the gonad proper (blue). **c**. Within 12–18 months, the testicular excurrent duct system is completed. The remainders of the partly regressed primary longitudinal strands and tubules are now integrated into the transversal mesorchial ducts and represent here the portions with the largest diameters (1). The solid tubules that leave the primary longitudinal system into the direction of the opisthonephros in b have developed into the marginal longitudinal network of the kidney (2). Close to the gonad itself, the transversal mesorchial channels (3) have widened to form the longitudinal marginal network of the testis.

3.1 Origin of GPs

In both sexes of cyclostomes and females of basal teleosts, mature gametes are released into the coelom and subsequently exported through GPs to reach the urinary sinus. Some comparative anatomists have postulated that these GPs could be homologous to the MDs in jawed vertebrates, proposing that GPs are potentially highly shortened MDs (Kerr, 1919; Goodrich, 1930). Conversely, an alternative perspective is that these pores represent primitive gamete-exporting organs, from which MDs later evolved. Topologically, both the GPs and MDs serve as paths from the coelom to the urinary sinus (Figure 1A). Another interesting hypothesis is that the GPs are homologous to the junction of MDs with the urogenital sinus in mammals. Failure to establish a connection between the MDs and urogenital sinus can lead to various developmental anomalies in the female genital tracts, including vaginal agenesis, as observed in mice (Zhao et al., 2016) and humans (Cunha et al., 2018; Parodi et al., 2022). Although the molecular mechanisms governing this connection are currently unknown, it has been suggested that retinoic acids play a role in this process (Nakajima et al., 2019). Transcriptomic analyses have been employed to study the development of the uterine-vaginal junction in birds, indicating the involvement of the TGF-beta and WNT pathways (Yang et al., 2023). Further research on the molecular and cellular aspects of GP development in cyclostomes and basal teleost females is necessary to elucidate the underlying mechanisms and evolutionary significance of these structures.

3.2 Testis-WD connection and evolution of teleost TDs

Anatomically, males of all jawed vertebrates, excluding teleosts and bichirs, exhibit connections extending from the testes to the WDs (Figure 1A). This urogenital connection is a characteristic feature of jawed vertebrates (Figure 4). In mammals, the rete testis is formed within the testes, and efferent ductules develop from the mesonephric kidney tubules that connect to the WDs (Shaw and Renfree, 2014; Major et al., 2021). Eventually, the rete testis and the efferent ductules are connected. Similar processes have been documented in cartilaginous fishes (see Wourms, 1977). In male gars (a basal ray-finned fish), numerous slender efferent ductules establish connections between the testes and the kidney (Figure 8C). These efferent ductules directly differentiate from the mesonephric tubules (inset of Figure 8C). However, in sturgeons, Wrobel and Jouma (2004) provided a detailed account of a distinct mode of development for the testis-WD connection. Unlike mammals and cartilaginous fishes, the primordium of this connection develops independently of both the testes and WDs (mesonephros) (1 in

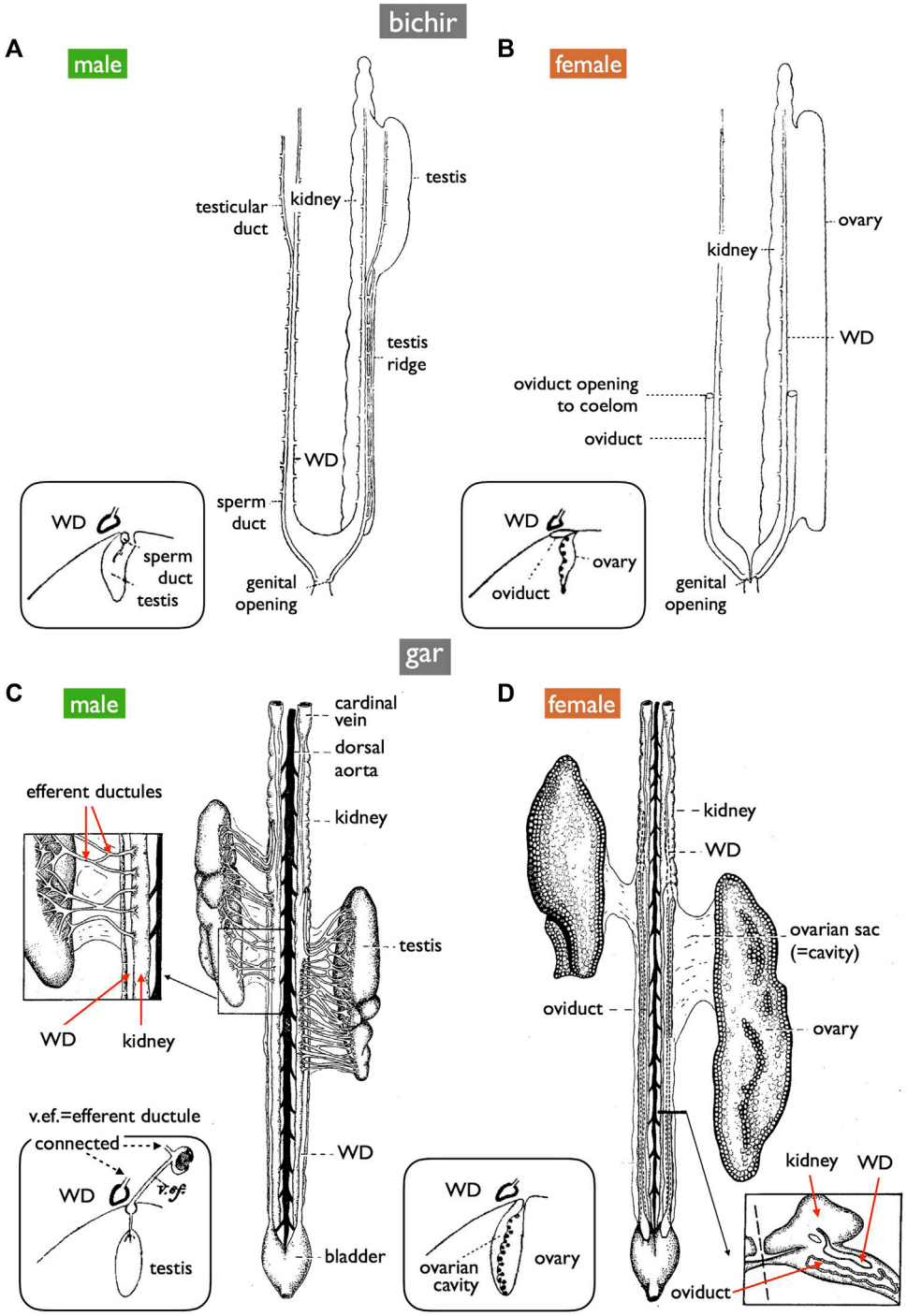

FIGURE 8
Diagrams of the urogenital systems in basal ray-finned fishes (ventral views). **(A,B)** bichir (*Polypterus*) [reproduced from Budgett (1901), with permission from The Company of Biologists]. **(C,D)** shortnose gar (*Lepisosteus platostomus*) [reproduced from Gérard (1958), after Pfeiffer (1933), with permission from Elsevier Masson SAS and John Wiley and Sons]. Insets in **(A–D)** depict cross-section diagrams from developing fishes [adapted from Budgett (1902), with permission from The Company of Biologists]. **(E)** Sketches of cross-sections illustrating OC formation in developing gar [reproduced from Balfour and Parker (1882), public domain]. **(F)** Female bowfin (*Amia*) [reproduced from Romer and Parsons (1977), with permission from Elsevier]. Male bichirs possess teleost-like sperm ducts independent of the WDs **(A)**. In contrast, male gars export sperm via thin efferent ductules, the kidney, and then the WDs **(C)**. In female bichirs and bowfins, oocytes ovulated into the coelom are exported through the openings of the MDs [**(B,F)**, respectively]. In contrast, female gars have OCs and ODs similar to teleosts **(D)**; ova are released into OCs, distinguishing them from other jawed vertebrates [inset of **(D)**]. The developmental processes of OCs resemble those of the parovarian cavities in teleosts [**(E)**, compare to Figure 5B]. OC formation appeared to progress from the anterior to the posterior direction. The anterior, middle, and posterior sections depict completed OC, OC during formation, and no OC, respecively.

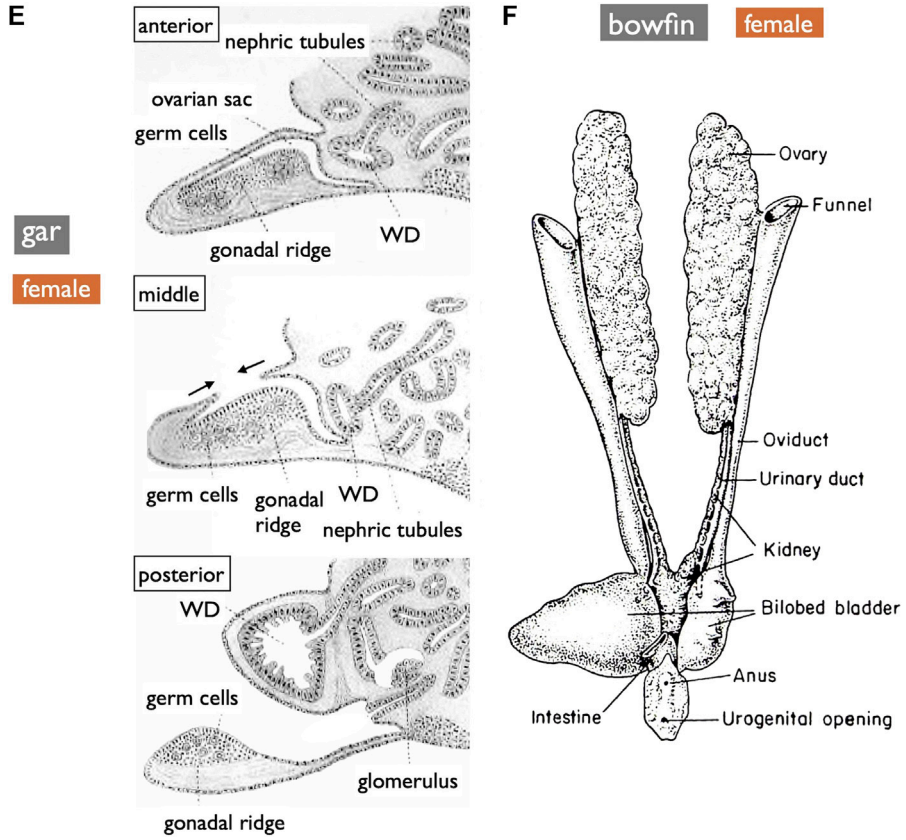

FIGURE 8
(continued).

Figure 7B). This primordium extends its tubules towards both the testes (laterally; 3 in Figure 7B) and WDs (medially; 2 in Figure 7B) to establish a testis-WD connection. A similar duct primordium has been reported in bichirs (De Smet, 1975). The developed sperm ducts in bichirs are not connected to the WD and resemble the anatomical structure of teleost TDs (Figure 8A). It is conceivable that teleost-type TDs evolved independently in both bichirs and teleosts by bypassing tubule elongation towards the WDs from the sturgeon-like duct primordium. This evolutionary event resulted in the loss of the connection between the testes and the WDs in bichirs and teleosts. Wrobel and Jouma (2004) first proposed this hypothesis. Notably, the diagrams illustrating the TDs in the bichirs (inset of Figure 8A) and basal teleost eel (Figure 7A) demonstrate conspicuous similarities. Future research should focus on comprehensive descriptions and investigations of the molecular networks governing TD development in basal ray-finned fishes and basal teleosts.

3.3 Origin of teleost ODs

OC development in gars was first documented in 1882 by Balfour and Parker (Figure 8E). This process bears a striking resemblance to the parovarian cavity formation in teleosts (Figure 5B). In gars, the dorso-lateral tissue sheet elongates medially and eventually fuses with the protrusion of coelomic walls; OC formation appears to progress from the anterior to the posterior direction. In adult gars, the resulting ovarian sac or cavity (Figure 8D and inset) is connected to the oviducts and ovulated oocytes do not enter the coelom, as in other jawed vertebrates. However, in bowfins (*Amia*), a sister group of gars (see Hughes et al., 2018; Koepfli et al., 2015, for phylogeny), the oviducts anatomically resemble those of bichirs (Figure 8B) and sturgeons (Figure 10C) and can be classified as MDs (Figure 8F; Romer and Parsons, 1977). This raises questions about whether MDs were present in the common ancestors of bowfins, gars, and teleosts (Figure 1B). If so, gars and non-basal teleosts may have independently evolved OCs and ODs. If teleost-like ODs were indeed present in the common ancestors of these groups, then bowfins might have regained MDs after diverging from gars, and the GPs in basal teleost females can be interpreted as degenerated ODs, with only the pores remaining to connect to the urinary sinus.

Another hypothesis considers the possibility that MDs and ODs may be homologous organs despite their seemingly different modes of development (Sections 2.3, 3.4 below); Both MDs and ODs are lined by epithelial cells derived from the coelomic epithelium. Functional loss of orthologous genes, *Wnt4* in mice (Vainio et al., 1999) and humans (Biason-Lauber et al., 2004; Biason-Lauber et al., 2007) and *wnt4a* in zebrafish (Kossack et al., 2019)

and the medaka (Kanamori et al., 2023), results in the complete absence of MDs and genital ducts, respectively. However, notable differences exist in the duct shapes and their relationships with the coelom. In mice, the anterior coelomic epithelium undergoes invagination (Figure 10A; see Section 3.4), whereas in teleosts, the genital duct primordia within the gonads elongate posteriorly and exit the coelom at the most posterior end (Figures 1A, 6B). These teleost-specific derived characters present challenges for the interpretation of homology. It is also possible that teleosts and mammals independently co-opted *wnt4a* and *Wnt4* for OD and MD development, respectively. Kanamori et al. (2023) proposed two approaches to discern correct hypotheses. The first approach involves conducting detailed molecular and cellular studies of medaka genital duct elongation to identify common genetic networks between medaka and mice, where detailed studies have already been reported (see Mullen and Behringer, 2014; Gonzales et al., 2021). The second approach adopts an evolutionary developmental biology (evo-devo) perspective as presented in the present review.

Next, we discuss the possibility of homology between teleost TDs and ODs. Notably, the zebrafish and medaka *wnt4a* mutants exhibit nearly identical phenotypes in the development of genital ducts in both sexes, suggesting similar molecular processes in the formation of TDs and ODs. The epithelium lining the lumen of TDs originates from the Sertoli cells, whereas that of ODs arises from the epithelium facing the OCs, which, in turn, is derived from the coelomic epithelium (Figure 5B). Both cell types are differentiated from the lateral plate mesoderm (Nakamura et al., 2006). However, the detailed lineages of these cells have yet to be examined in teleosts. Kanamori et al. (1985) described a group of somatic cells with a distinct basal lamina in developing medaka gonads. These cells give rise to the Sertoli cells, the epithelial cells lining the sperm duct in males, and the epithelial cells lining the OCs, and the granulosa cells in females. In mammals, Sertoli cells are derived from the coelomic epithelium (Karl and Capel, 1998).

Teleosts are the only vertebrate group that includes species capable of functional sex changes during their life cycle. A study on TDs and ODs in hermaphroditic fish species may provide insights into their possible homology. Approximately 400 hermaphroditic fish species have been reported, each exhibiting unique mechanisms of sex change (Devlin and Nagahama, 2002; Kuwamura et al., 2020). Although extensive research has focused on physiological gonadal changes during sex change, our understanding of the sexual transformation of the genital ducts remains relatively limited. The present knowledge regarding three types of sex change is summarized as follows:

3.3.1 Protogynous fish (female-to-male sex change)

Female protogynous wrasse have ovaries devoid of testicular tissue. Mature oocytes are exported from the OCs through the ODs. During sex change, the ovarian tissues completely degenerate and are absorbed, resulting in the emergence of undifferentiated germ and somatic cells that subsequently transform into testicular cells. Importantly, transformed testes do not reuse the former ODs as sperm ducts. Instead, new TDs develop within the connective tissues of the ovarian surface (Hourigan et al., 1991). In some wrasse species, primary males coexist with secondary males, which are derived from females via sex change. Primary males entirely lack OCs, with only TDs observed at the base of the testes. Intriguingly, we successfully induced a reverse sex change, from male to female, in primary males by administering estrogen (Kojima et al., 2008). This induction leads to the differentiation of new OCs. Similarly, in protogynous grouper, new TDs are formed during sex change (Alam and Nakamura, 2007). Initially, these early-stage ducts appear as small, elliptical slits within the stromal tissue of the ovarian surface connective tissues. As the sex change progresses, these slit-like structures expand and fuse, eventually forming well-developed TDs.

3.3.2 Protandrous fish (male-to-female sex change)

Clownfish and black porgy are protandrous hermaphroditic fish capable of transitioning from male to female. These fish exhibit bisexual gonadal structures comprising immature ovaries and mature testes during the male phase (Chang et al., 1994; Nakamura et al., 1994). As they undergo female transformation, their testes regress, facilitating ovarian development. Individuals possessing both male and female gonads maintain a unique "double-canule genital duct" structure, wherein TDs and ODs exist in the testicular and ovarian compartments, respectively (Lee et al., 2011). During male-to-female sex change in the black porgy, the male TDs regress and are replaced by connective tissue. In contrast, immature OCs and ODs develop. Although the precise changes in the genital ducts during sex change in clownfish have not been fully elucidated, the TDs no longer exist within the transformed ovary (Nakamura et al., 1994). To gain further insight into this process, we artificially induced opposite-sex changes (female-to-male) in clownfish females by administering an aromatase inhibitor (Nakamura et al., 2015). This transformation resulted in the emergence of new TDs.

3.3.3 Bi-directional sex change

Okinawa rubble gobiid fish, capable of undergoing serial sex changes, possess ovaries with ODs and testes with TDs simultaneously (Kobayashi et al., 2005; Sunobe and Nakazono, 2010). Observations have shown that this goby develops genital ducts in response to changes in its social environment (Kobayashi et al., 2012).

In summary, it is widely recognized the germ and somatic cells within the gonads of hermaphroditic fish exhibit remarkable sexual plasticity. However, recent results summarized above suggest that the plasticity of genital ducts in these fish is limited and that these ducts are not reused during sex change. Instead, new genital ducts differentiate during sex change. These findings suggest that teleost TDs and ODs are independent structures that are closely associated with the physiological sex of their gonads. TDs and ODs are probably derived solely from the Sertoli cells and the epithelium of the OCs, respectively. Therefore, teleost TDs and ODs may not have homologous structures, and *wnt4a* might have been independently co-opted for their development.

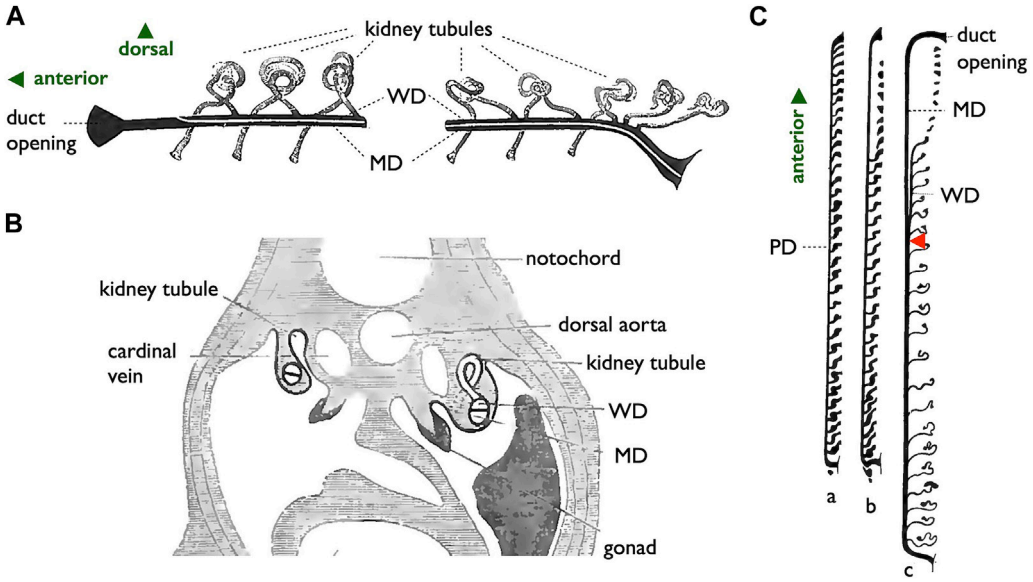

FIGURE 9
Diagrams of the **longitudinal splitting** mode of MD development in sharks. **(A,B)**, adapted from Balfour (1885), public domain. **(A)** Diagram illustrating the primitive condition of the kidney in a shark embryo. The initial pronephric duct is separated into the ventral MD and dorsal WD, which connects to mesonephric tubules. **(B)** Cross-section of a shark embryo demonstrating the WD and MD formation by the **longitudinal splitting** of the pronephric duct. **(C)** Arrangement of the pronephric duct, etc., in embryos of a shark, *Pristiurus*. a, male 17 mm. Pronephros are connected to the pronephric duct (PD). b, female 19 mm. The anterior pronephros degenerated. c, female 27 mm. The PD is split into the ventral MD and dorsal WD. The point of splitting is labeled with a red arrowhead. Presumably, this splitting point moves posteriorly as development proceeds [adapted from Kerr (1919), after Rabl (1896), public domain].

3.4 Origin of MDs

The challenge at hand is to understand the existence of two distinct modes of MD development, a topic that ignited extensive debate among comparative anatomists around the turn of the 20th century (Kerr, 1919; Goodrich, 1930). Wourms (1977) provided a comprehensive summary of MD development in cartilaginous fishes as follows: "Müllerian ducts develop from the pronephros and the pronephric duct. . .The main portion of the Müllerian duct develops from the pronephric duct. The pronephric duct undergoes a gradual **longitudinal splitting** into an anterior-posterior direction to produce a dorsal and ventral tube. The ventral tube is continuous with the pronephric funnel [opening to the coelom] and becomes the Müllerian duct. The dorsal tube receives the kidney tubules. It is a true Wolffian (mesonephric) duct which persists as the functional urinary duct of the opisthonephros. . . . (Kerr, 1919; Goodrich, 1930)." These descriptions were sourced from two classical textbooks and are rooted in original papers from the late 19th century, contributed by notable authors such as Semper (1875), Balfour (1875), and Rabl (1896). Figure 9 shows several original diagrams from these pioneering studies. Importantly, Figure 9C reveals a connection between the posterior kidney tubules and pronephric ducts before the splitting process, a feature not observed in red stingrays or catsharks (Figures 12, 13, as discussed below).

In contrast, an alternative mode of MD development is prevalent among most jawed vertebrates (Figure 10). During this process, the anterior coelomic epithelium near the pronephros undergoes thickening and invagination. The tip of this invaginated cord of cells elongates posteriorly along the WD until it reaches the urinary sinus. This mode, **invagination-elongation**, has been described in various species, including bichirs (Budgett, 1902; De Smet, 1975), sturgeons (Wrobel, 2003), amphibians (Hall, 1904; Wrobel and Süß, 2000), birds (Gruenwald, 1941; Jacob et al., 1999), and mammals (Gruenwald, 1941) (Figure 1B). The process has been most comprehensively documented in mice, including detailed cellular and molecular dynamics (Figure 10A; Orvis and Behringer, 2007; Mullen and Behringer, 2014; Gonzales et al., 2021). In mice, specific coelomic epithelial cells have been identified as the MD epithelium through the expression of several transcription factors such as LHX1, PAX2, and EMX2. These cells subsequently undergo invagination and posterior elongation under the influence of WNT4, which is expressed in the mesenchymal tissue underlying the tips of the elongating MDs. This mode is also highly likely to be applied in bichirs, as indicated by developmental diagrams of the oviducts (Figure 10B; De Smet, 1975). The coelomic epithelium at the dorsolateral base of the genital ridge undergoes invagination (b–c), leading to the formation of a posteriorly extending tubular structure (d–e), which ultimately closes further posteriorly (f). Unfortunately, older specimens that the author did not obtain may reveal an MD connection to the urinary sinus. The development of MDs in sturgeons has been meticulously studied (Figure 10C; Wrobel, 2003). Scanning electron microscopy (SEM) and cross-section images unequivocally illustrate that sturgeon MDs develop in a manner very similar to that observed in mice, involving invagination of the coelomic epithelium (10C-8, 10), followed by posterior elongation (10C-8, 11, 12). In conclusion, the gradual **longitudinal splitting** during MD development is currently

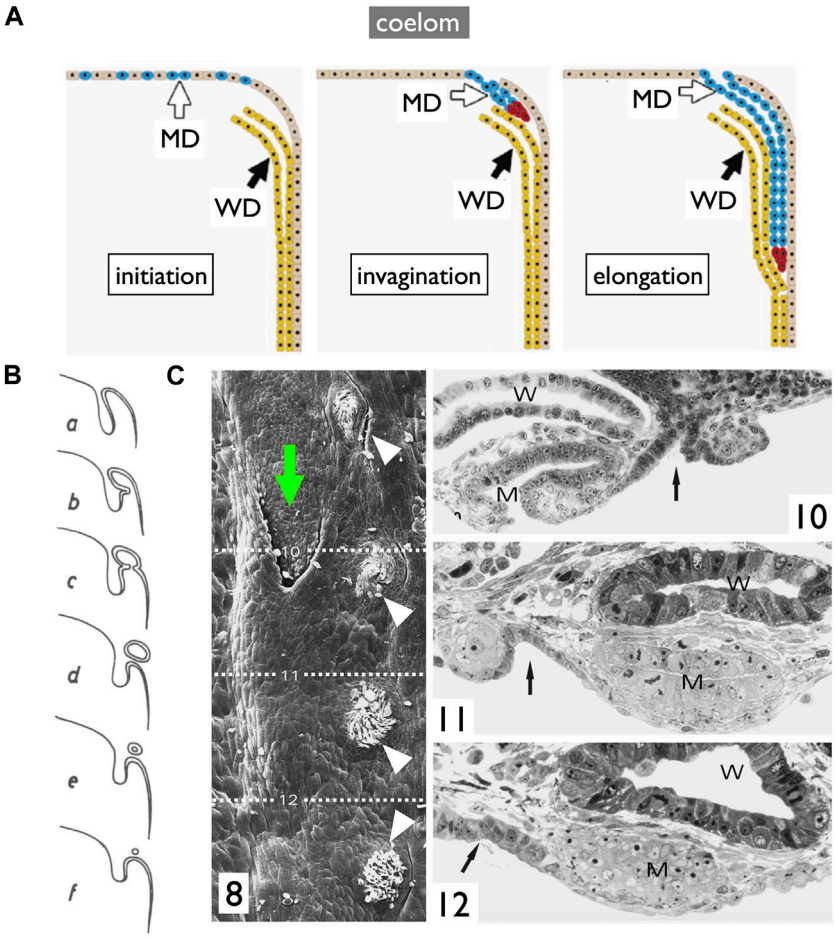

FIGURE 10
Diagrams of the **invagination-elongation** mode of MD development. **(A)** A three-phase model for MD development in mammals. In the first phase (initiation), cells of the coelomic epithelium are specified to become MD cells (blue). After specification, the second phase (invagination) begins and these cells invaginate posteriorly towards the WD. Once the MD comes into contact with the WD, the third phase (elongation) begins and the MD elongates posteriorly, following the WD path, towards the urogenital sinus. Red cells; proliferating MD precursor cells, brown cells; coelomic epithelial cells, yellow cells; WD epithelial cells [reproduced from Orvis and Behringer (2007), with permission from Elsevier]. **(B)** Oviduct development process in bichirs [reproduced from De Smet (1975) with a permission from KMDA] shown in cross-sections from anterior to posterior direction (a–f). Anteriorly, the coelomic epithelium thickens with cuboidal cells (a). At the dorsolateral base of the genital ridge, they undergo invagination (b,c), forming a posteriorly-extending tubular structure (d,e) that ultimately closes farther posteriorly (f). **(C)** Oviduct development in sturgeons [adapted from Wrobel (2003), with permission from Springer Nature]. 8, 28-day-old *Acipenser ruthenus*, SEM. A series of segmentally arranged nephrostomes (coelomic openings of nephrons; white arrowheads) coexists with an opening of the MD (green arrow). The numbers 10–12 with dotted lines represent the locations of cross-sections similar to those in 10C-10, 11, 12: 10, the level of the opening of MD (left body side); 11, the primordium of MD with a slit-like lumen (right body side); 12, the posteriorly growing solid tip of MD primordium (right body side). Arrow, a line of nephrostomes; W, WD; M, MD.

exclusive to cartilaginous fishes. Although this mode was previously described in urodeles (Furbringer, 1878; Romer and Parsons, 1977), it has since faced considerable skepticism (Hall, 1904; Wrobel and Süß, 2000). Distinguishing these two modes based solely on histological sections poses a significant challenge, as shown in Figure 11. In both cases, the anterior cross-sections exhibited striking similarities, with the primary discerning factor residing in the position of the ducts in the posterior cross-sections. This distinction may be difficult to verify, with WDs positioned proximally and MDs positioned distal to the kidney.

Therefore, we reexamined the histological slides originally prepared by one of the authors (YK; Kobayashi et al., 2021). In viviparous red stingrays (*Hemitrygon akajei*), we observed the differentiation of MDs on the ventral side of the kidney primordium in immature fetuses, approximately 1 cm in total length, where gill formation was completed (Figure 12A). When the fetuses reached a length of 2 cm and placental development was initiated, WDs became discernible (Figure 12B). In female fetuses measuring approximately 8 cm in body length, the right MD enlarged and differentiated into the uterus (Figure 12C). In the subsequent developmental stages, we observed growth of the inner uterine wall and myometrium in female fetuses just before birth, at a body length of approximately 10 cm (Figure 12D). Therefore, it is evident that the left-right asymmetry of the genital ducts observed in adult females was already established during intrauterine development. In contrast, we observed only a slight enlargement of both the left and right WDs in male fetuses immediately before birth (Figure 12E). WD differentiation into sperm ducts and seminal

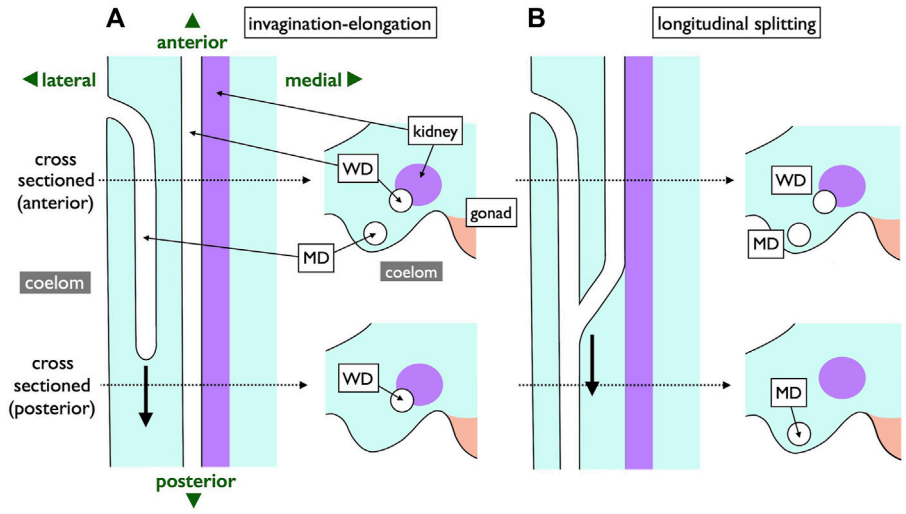

FIGURE 11
Comparison of two MD development modes depicted with ventral views (left) and transverse views (right). Two dotted lines represent levels of cross-sections. In the **invagination-elongation** mode **(A)**, the MD epithelium invaginates and elongates posteriorly (thick arrow). In contrast, the pronephric duct splits into the ventral MD and dorsal WD in the **longitudinal splitting** mode **(B)**. The splitting point moves posteriorly (thick arrow) as development proceeds. The only difference is the location of a duct in posterior sections; WD is proximal, and MD is distal to the kidney within nephric ridges.

vesicles is expected to occur after birth. Importantly, the MDs in male fetuses and WDs in female fetuses did not regress; instead, they persisted as undifferentiated ducts. Besides studies on stingrays, we conducted a comprehensive analysis of the differentiation and developmental processes of genital ducts in the oviparous catshark (*Scyliorhinus torazame*). In embryos examined 45 days after spawning, a pair of left and right MDs originating from the former pronephric ducts were observed on the dorsal side of the body cavity (Figure 13). The most anterior part of the MDs opened into the coelom (Figure 13C). At this stage, the mesonephric kidney had not yet undergone differentiation, and only segmental development of the nephrotomes was observed (Figures 13A, B, D). This observation demonstrates that MD differentiation occurs before mesonephric kidney or WD differentiation in catsharks as well. Subsequently, in female embryos, the anterior part of the MDs undergoes enlargement and differentiation into eggshell glands (Kobayashi et al., 2021). Similar to the stingrays, the WDs in females and the MDs in males persisted without regression, remaining as undifferentiated ducts (Kobayashi et al., 2021). In both species, as reported in previous studies by Balfour (1875), Semper (1875), and Rabl (1896), the pronephric ducts differentiated long before the onset of mesonephros development. During this early stage, the nephrotomes remained undifferentiated, whereas well-developed pronephric ducts (referred to as MDs in our definition, as outlined in Section 2.2) were present (Figure 12, 13). Based on our observations, the pronephric ducts are directly differentiated into the MDs. This inference is primarily based on the spatial arrangement of these ducts, with the MDs consistently situated distally in the nephric ridge, compared to the dorsal and proximal location of the WDs (Figure 12). Thus, the results from the late 19th century were partially confirmed. However, we were unable to identify evidence of pronephric duct splitting in either the red stingrays or the catsharks. Furthermore, the differentiation of WDs in these species and the establishment of their connections to the testes remain elusive. This uncertainty is likely due to the absence of crucial samples in the developmental series examined.

In summary, the confusion persists as Goodrich noted in 1930: "Obviously, there is a striking difference between the development of the Müllerian ducts in Selachii [sharks and rays] and Tetrapoda; indeed, many have doubted its homology in the two groups. Yet so similar are the ducts in the adult condition both in function and in anatomical relationship that it can scarcely be doubted that they are homologous throughout the Gnathostomes [jawed vertebrates] (leaving the Teleostomes [teleosts] aside for the present. . .). . . . Further knowledge of the development in other groups may enable us to solve this problem." Future research focusing on MD development in cartilaginous fishes, such as sharks and rays, is of utmost importance. Wrobel (2003) similarly argued as follows: "In *Acipenser* [a sturgeon], the müllerian ducts unite with the corresponding wolffian ducts before the latter fuse to form the urogenital sinus. Without knowing its embryogenesis, the fully-developed adult condition can easily be misinterpreted as the result of an incomplete longitudinal splitting of the wolffian ducts. This diagnostic error was obviously made by Romer (1960) [see Romer and Parsons (1977)] who considered the müllerian duct of sturgeons to be a side branch of the opisthonephric duct and the starting point of a morphogenetic line leading to the situation seen in elasmobranchs [sharks and rays] and urodeles. In these two groups, the müllerian duct allegedly is the result of a complete longitudinal splitting of the wolffian duct, an assumption, however, that has been

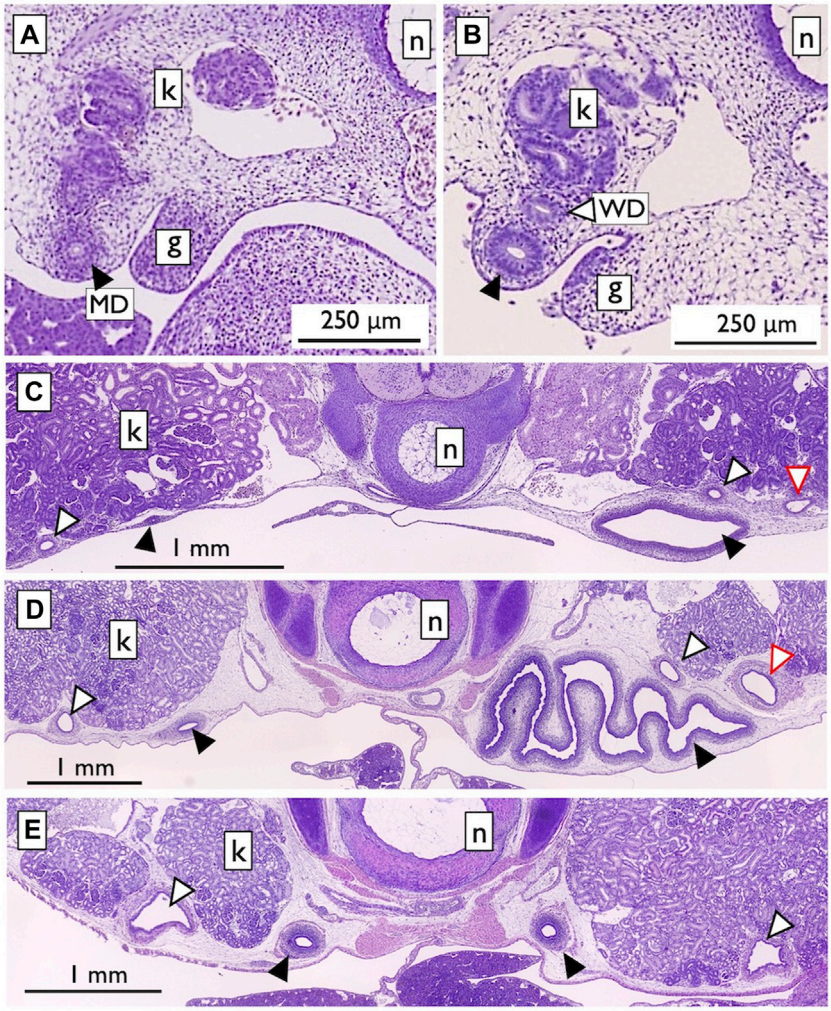

FIGURE 12
Urogenital duct development in the viviparous red stingray fetuses [adapted from Kobayashi et al. (2021), with permission from The Japanese Society of Fisheries Science]. **(A)** Fetus with a total length (TL) of 1 cm. The nephric ridge is shown adjacent to the gonad (g). The kidney (k) was still in the developmental stage, with no associated duct. In contrast, the completed pronephric duct was located distally in the nephric ridge (labeled as MD; closed arrowheads). **(B)** Fetus with a TL of 2 cm. The WD (open arrowheads) was observed near the kidney. **(C)** Female fetus (TL 8.2 cm). The MDs on the right side were enlarged and differentiated into the uterus. No changes were observed in the MDs on the left side, as well as in the left and right WDs. Secondary nephric ducts (red open arrowheads) were also observed. **(D)** Female fetus (TL 10.1 cm). Myometrium muscle development was observed. **(E)** Male fetus (TL 10.3 cm). Slight enlargement of the left and right WDs was observed. n; notochord.

proven untenable for the lower amphibians (Hall, 1904; Wrobel and Süß, 2000) and certainly needs reinvestigation with a suitable methodology for the elasmobranchs."

Finally, we briefly explore the possibility that WDs and MDs are homologous organs. Romer and Parsons (1977) expressed this perspective as follows: "The embryonic course of the oviduct [MD] parallels that of the archinephric duct [WD]. . .. The evidence on the whole thus indicates that the female genital duct (like that of the male. . .) is derived from the urinary system but has become so specialized that embryonic evidence of its origin may be lost." Interestingly, quite a few genes are expressed in either the epithelium or mesenchyme of both MDs and WDs during development (Mullen and Behringer, 2014; Gonzales et al., 2021). This shared expression pattern raises the possibility of a deep homology between MDs and WDs.

In conclusion, we still lack detailed temporal sequences of urogenital development in cartilaginous fishes for comparison with those in mammals.

4 Prospects and proposals

As emphasized throughout this review, a significant knowledge gap persists concerning the fundamental structures and developmental processes of gamete-exporting organs in essential vertebrate groups such as cyclostomes, cartilaginous fishes, basal ray-finned fishes, and basal teleosts. Several factors have contributed to the limited research in this area. Obtaining a sufficient number of samples for analysis poses a significant challenge because of the rarity of many of these species and the difficulties in maintaining them in laboratory settings.

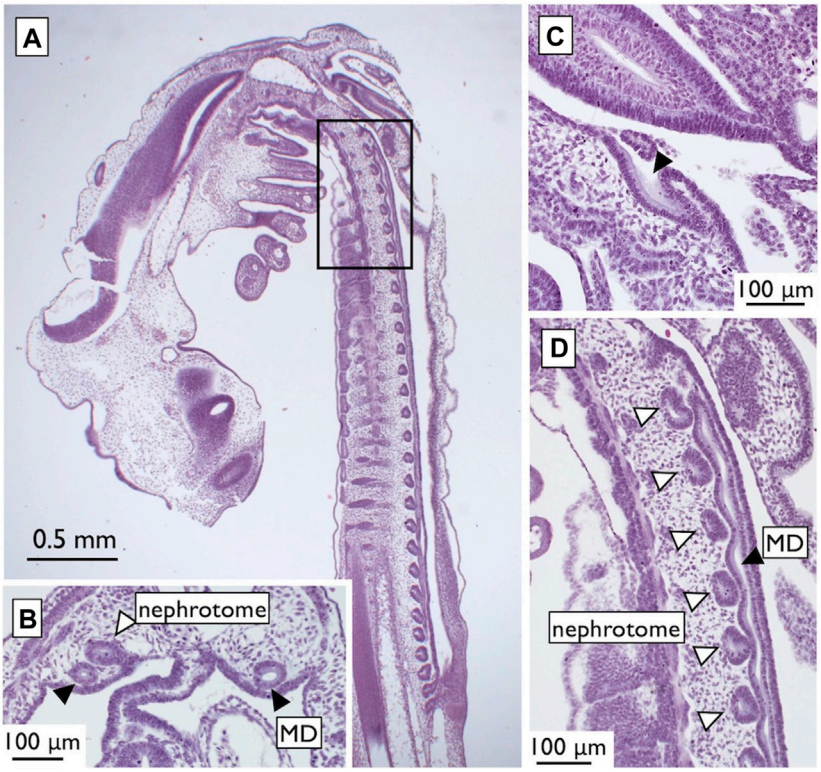

FIGURE 13
Urogenital systems in the catshark embryos at 45 days after spawning [adapted from Kobayashi et al. (2021), with permission from The Japanese Society of Fisheries Science]. **(A)** A low-magnified micrograph of a parasagittal-section. A blow-up of the squared portion is shown in **(D)**. The MDs (closed arrowheads) were formed, but the mesonephric kidney was still undifferentiated and present as segmental nephrotomes (open arrowheads). In a cross-section shown in **(B)**, the MDs were observed in the ventral nephric ridge distal to the nephrotome. In a parasagittal-section near **(A)**, the opening of MD to the coelom was observed [**(C)**, arrowheads].

Historical studies conducted around the turn of the 20th century have often relied on small sample sizes, further complicating our understanding. Moreover, the relatively late genital duct differentiation during development, which sometimes occurs several years after fertilization, poses two distinct challenges. First, determining the precise timing for sampling to analyze duct development is challenging, as the variability in developmental timing increases with prolonged development. Secondly, larger body sizes at the time of sampling create difficulties in histological sectioning, requiring meticulous trimming, a greater number of sections, and more resources.

Given these challenges, we propose three approaches to advance the study of duct structure and development.

4.1 MRI application on living specimens

Observing organ structures in living organisms without sacrificing them would help to overcome the limitations of sample availability. Researchers can utilize the same organism at various developmental time points. Multiple noninvasive imaging techniques, including computed tomography (CT), magnetic resonance imaging (MRI), positron emission tomography (PET), single-photon emission computed tomography (SPECT), and ultrasound (US), are available (see https://encyclopedia.pub/entry/12494; Riehakainen et al., 2021). It is preferable to avoid the use of radioactive tracers or heavy molecular dyes. Therefore, MRI is a promising option among these methods. MRI has been successfully utilized in humans to detect developmental anomalies of MDs owing to its exceptional soft tissue resolution and accuracy (Udayakumar et al., 2023). Moreover, MRI has exhibited outstanding resolution, nearly equivalent to histology, for the imaging of mouse embryos (Turnbull and Mori, 2007). Recent studies have indicated that MRI resolution is sufficient for observing gamete-exporting organs in vertebrates (e.g., Kanahashi et al., 2023). Fortunately, the species we intended to analyse, such as lampreys, sharks, rays, bichirs, bowfins, sturgeons, gars, and basal teleosts such as eels, are sufficiently large to be accommodated in readily available MRI facilities. The living yellowtail specimens (rather large fish, 60–70 cm body length) have been imaged by MRI successfully (Tawara et al., 2022). Observing organ structures *in situ* without sacrificing specimens allows researchers to determine the ideal time for sacrifice and subsequent organ dissection for traditional histological analyses. Nonetheless, challenges may arise due to the accessibility of MRI facilities and the associated expenses for imaging animal specimens.

4.2 Genetic and cellular atlas/dynamics during development of gamete-exporting organs

Recent advances in single-cell RNA sequencing technologies, combined with techniques for mapping cell types in 3D spatial contexts (spatial transcriptomics; see Rao et al., 2021; Moses and Pachter, 2022; Williams et al., 2022; Tian et al., 2023), offer valuable methods for investigating limited sample populations. With prior knowledge of the timing and locations for sampling from non-invasive imaging, researchers can confidently proceed with spatial transcriptomic analyses. These analyses can potentially reveal the genetic networks involved in various cell types during gamete-exporting organ development in vertebrates. By comparing cell types and networks, we can gain insight into the presence or absence of homology among these organs.

4.3 Mutants of *wnt4a* and other genes involved in MD development

One of the most practical approaches currently available involves CRISPR/Cas9-mediated gene knockout of *Wnt4* (*wnt4a*) or other genes implicated in mammalian MD development (Mullen and Behringer, 2014; Gonzales et al., 2021). Researchers can investigate the possible phenotypes arising in gamete-exporting organs following gene knockouts. Importantly, CRISPR/Cas9 systems can theoretically be applied to most organisms, making them suitable for genetic research (see Russell et al., 2017; Matthews and Vosshall, 2020). Notably, CRISPR/Cas9-mediated gene knockout has already been reported in the lamprey, one of our target organisms (Suzuki et al., 2021). Nevertheless, a significant challenge arises due to the relatively long developmental timeline of gamete-exporting organs in the proposed organisms. Successful husbandry methods are required to maintain these animals in laboratories or aquaria for extended periods. In this context, noninvasive imaging methods are indispensable for determining the optimal time to sample duct development in mutants, which is likely to vary among individuals.

5 Concluding remarks

The presence of gamete-exporting organs is vital for the reproductive success and survival of vertebrates. Based on the phylogenetic distribution of these organs (Figure 1B), it is likely that several transitions between the organ types occurred during evolution. For example, there were changes from cyclostome GPs to WDs and MDs in cartilaginous fishes, as well as transitions from WDs and MDs in basal ray-finned fishes to teleost TDs and ODs. How were these evolutionary changes successfully implemented? Are the MDs of sharks and rays truly homologous to those of other jawed vertebrates? If not, what kind of independent genetic networks underlie the development of seemingly identical organs in adults? These questions remain unanswered after a century of limited scientific research. We firmly believe that these challenges are worth pursuing and may be addressed with modern technologies that were unavailable around the turn of the 20th century when the subject was ever so popular.

Author contributions

AK: Conceptualization, Funding acquisition, Investigation, Resources, Visualization, Writing–original draft, Writing–review and editing. YK: Funding acquisition, Investigation, Resources, Visualization, Writing–original draft, Writing–review and editing.

Funding

The author(s) declare financial support was received for the research, authorship, and/or publication of this article. This work was supported in part by a Grant-in-Aid for Scientific Research from the JSPS (19K06738 to AK, 19K06229, 23K05389 to YK).

Acknowledgments

The present review was written upon the retirement of one of the authors (AK). AK dedicates this review to his former mentors/friends, without whose invaluable guidance, support, and encouragement he could not have made it here: Nobuo Egami, Yoshitaka Nagahama, Tokindo S. Okada, Hisato Kondoh, Donald D. Brown, Kazuo Araki, Hirohiko Kagawa, Hiroshi Hori, Takao Kondo, Mitsuru Sakaizumi. The authors thank Masaru Nakamura and Ryo Nozu for the pictures used in Figures 12, 13, and present and past scientists for the figures used in this review. The original illustrations were adapted with permissions obtained via RightsLink (https://www.copyright.com) or the publishers. The authors greatly appreciate the important and invaluable suggestions during the study from the following colleagues (in no particular order): Masumi Nozaki, Yoshitaka Nagahama, Masaru Nakamura, Shinji Adachi, Hirohiko Kagawa, Koichi Okuzawa, Yukinori Kazeto, Toshiomi Tanaka, Daichi Suzuki, Yasunori Murakami, Masashi Kawaguchi, Fumiaki Sugahara, Hiroshi Wada, Hirohumi Kariyayama, Rie Kusakabe, Masaki Takeuchi, Yukiko Ogino, Richard R. Behringer, John H. Postlethwait, Ingo Braasch, Gen Yamada, Aki Murashima, Shigehiro Kuraku, Richard G. Manzon, Donald D. Brown, Margaret F. Docker, John H. Youson. AK is grateful to the following colleagues for their collaboration, discussion, and help in pursuing the roles of Wnt4a in the medaka: Atsuko Oota, Koudai Hirano, Ryota Kitani, Taijun Myosho, Tohru Kobayashi, Kouichi Kawamura, Naoyuki Kato, Satoshi Ansai, Masato Kinoshita, Kenji Kubo, Hiroshi Hori, Hisashi Hashimoto, Rikita Araki, and Masaru Matsuda.

Conflict of interest

The authors declare that the research was conducted in the absence of any commercial or financial relationships that could be construed as a potential conflict of interest.

Publisher's note

References

Alam, M. A., and Nakamura, M. (2007). Efferent duct differentiation during female-to-male sex change in honeycomb grouper *Epinephelus Merra*. *J. Fish. Biol.* 71, 1192–1202. doi:10.1111/j.1095-8649.2007.01592.x

Balfour, F. M. (1875). On the origin and history of urogenital organs of vertebrates. *J. Anat. Physiol.* 10, 17–48.

Balfour, F. M. (1885). "VII on the origin and history of urogenital organs of vertebrates," in *The works of francis maitland Balfour*. Editors M. Foster, and A. Sedgwick (London: Macmillan), 1, 135–167. doi:10.5962/bhl.title.107583

Balfour, F. M., and Parker, W. K. (1882). On the structure and development of *Lepidosteus*. *Phil. Trans. R. Soc.* 173, 359–442. doi:10.1098/rstl.1882.0008

Bertin, L. (1958). "Sexualité et fécondation," in *Traité de Zoologie, Tome XIII, fasc. II, (Agnathes et Poissons. Anatomie, Ethologie, Systématique)*. Editor P.-P. Grassé (Paris: Masson et Cie), 1585–1652.

Biason-Lauber, A., De Filippo, G., Konrad, D., Scarano, G., Nazzaro, A., and Schoenle, E. J. (2007). WNT4 deficiency – a clinical phenotype distinct from the classic Mayer-Rokitansky-Kuster-Hauser syndrome: a case report. *Hum. Reprod.* 22, 224–229. doi:10.1093/humrep/del360

Biason-Lauber, A., Konrad, D., Navratil, F., and Schoenle, E. J. (2004). A WNT4 mutation associated with Mullerian-duct regression and virilization in a 46, XX woman. *N. Engl. J. Med.* 351, 792–798. doi:10.1056/NEJMoa040533

Blüm, V. (1986). *Vertebrate reproduction: a textbook*. Berlin: Springer Verlag.

Budgett, J. S. (1901). On some points in the anatomy of *Polyprerus*. *Trans. Zool. Soc. Lond.* 15, 323–338. doi:10.1111/j.1096-3642.1901.tb00025.x

Budgett, J. S. (1902). On the structure of the larval *Po1ypterus*. *Trans. Zool. Soc. Lond.* 16, 315–340. doi:10.1111/j.1096-3642.1902.tb00033.x

Chang, C. F., Lee, M. F., and Chen, G. R. (1994). Estradiol-17β associated with the sex reversal in protandrous black porgy, *Acanthopagrus schlegeli*. *J. Exp. Zool.* 268, 53–58. doi:10.1002/jez.1402680107

Cunha, G. R., Robboy, S. J., Kurita, T., Isaacson, D., Shen, J., Cao, M., et al. (2018). Development of the human female reproductive tract. *Differentiation* 103, 46–65. doi:10.1016/j.diff.2018.09.001

de Bakker, B. S., van den Hoff, M. J. B., Vize, P. D., and Oostra, R. J. (2019). The Pronephros; a fresh perspective. *Integr. Comp. Biol.* 59, 29–47. doi:10.1093/icb/icz001

De Smet, W. M. A. (1975). Considerations sur le developpement des gonades et des gonoductes chez les polypteres (Pisces). *Acta. Zool. Pathol. antv.* 62, 95–127.

Devlin, R. H., and Nagahama, Y. (2002). Sex determination and sex differentiation in fish: an overview of genetic, physiological, and environmental influences. *Aquaculture* 208, 191–364. doi:10.1016/S0044-8486(02)00057-1

Dymek, A. M., Piprek, R. P., Boroń, A., Kirschbaum, F., and Pecio, A. (2022). Ovary structure and oogenesis in internally and externally fertilizing Osteoglossiformes (Teleostei:Osteoglossomorpha). *Acta Zool.* 103, 346–364. doi:10.1111/azo.12378

Dzyuba, V., Shelton, W. L., Kholodnyy, V., Boryshpolets, S., Cosson, J., and Dzyuba, B. (2019). Fish sperm biology in relation to urogenital system structure. *Theriogenology* 132, 153–163. doi:10.1016/j.theriogenology.2019.04.020

Fishelson, L. (1992). Comparative gonad morphology and sexuality of the muraenidae (Pisces, Teleostei). *Copeia* 1992, 197–209. doi:10.2307/1446552

Fürbringer, M. (1878). Zur vergleichenden anatomie und entwicklungsgeschichte der excretionsorgane der vertebraten. *Morph. Jb.* 4, 1–111.

Gérard, P. (1958). "Organes reproducteurs," in *Traité de Zoologie, Tome XIII, fasc. II, (Agnathes et Poissons. Anatomie, Ethologie, Systématique)*. Editor P.-P. Grassé (Paris: Masson et Cie), 1565–1583.

Godinho, H. P., Santos, J. E., Formagio, P. S., and Guimarães-Cruz, R. J. (2005). Gonadal morphology and reproductive traits of the Amazonian fish *Arapaima gigas* (Schinz, 1822). *Acta Zool.* 86, 289–294. doi:10.1111/j.1463-6395.2005.00213.x

Gonzalez, L. S., Rota, I. A., Artibani, M., Morotti, M., Hu, Z., Wietek, N., et al. (2021). Mechanistic drivers of Müllerian duct development and differentiation into the oviduct. *Front. Cell. Dev. Biol.* 9, 605301. doi:10.3389/fcell.2021.605301

Goodrich, E. S. (1895). Memoirs: on the cœlom, genital ducts, and nephridia. *Q. J. Microsc. Sci.* 37, 477–510. doi:10.1242/jcs.s2-37.148.477

Goodrich, E. S. (1930). *Studies on the structure and development of Vertebrates*. London: Macmillan. doi:10.5962/bhl.title.82144

Goodrich, E. S. (1945). The study of nephridia and genital ducts since 1895. *Q. J. Microsc. Sci.* 86, 113–301. doi:10.1242/jcs.s2-86.342.113

Gruenwald, P. (1941). The relation of the growing Mullerian duct to the Wolffian duct and its importance for the genesis of malformations. *Anat. Rec.* 81, 1–19. doi:10.1002/ar.1090810102

Hall, R. W. (1904). The development of the mesonephras and the Müllerian duct in Amphibia/. *Bull. Mus. Comp. Zool. Harv. Coll.* 45, 32–125. doi:10.5962/bhl.title.52397

Hisaoka, K. K., and Firlit, C. F. (1962). Ovarian cycle and egg production in the zebrafish, *Brachydanio rerio*. *Copeia* 1962, 788–792. doi:10.2307/1440680

Hoar, W. S. (1969). "Reproduction," in *Fish physiology Volume III Reproduction and growth Bioluminescence, pigments, and poisons*. Editors W. S. Hoar, and D. J. Randall (New York: Academic Press), 1–72. doi:10.1016/S1546-5098(08)60111-9

Holland, L. Z., and Ocampo Daza, D. (2018). A new look at an old question: when did the second whole genome duplication occur in vertebrate evolution? *Genome Biol.* 19, 209. doi:10.1186/s13059-018-1592-0

Holland, N. D. (2017). The long and winding path to understanding kidney structure in amphioxus - a review. *Int. J. Dev. Biol.* 61, 683–688. doi:10.1387/ijdb.170196nh

Hourigan, T. F., Nakamura, M., Nagahama, Y., Yamauchi, K., and Grau, E. G. (1991). Histology, ultrastructure, and *in vitro* steroidogenesis of the testes of two male phenotypes of the protogynous fish, *Thalassoma duperrey* (Labridae). *Gen. Comp. Endocrinol.* 83, 193–217. doi:10.1016/0016-6480(91)90023-y

Hughes, L. C., Ortía, G., Huang, Y., Sunc, Y., Baldwin, C. C., Thompson, A. W., et al. (2018). Comprehensive phylogeny of ray-finned fishes (Actinopterygii) based on transcriptomic and genomic data. *Proc. Natl. Acad. Sci. U. S. A.* 115, 6249–6254. doi:10.1073/pnas.1719358115

Jacob, M., Konrad, K., and Jacob, H. J. (1999). Early development of the müllerian duct in avian embryos with reference to the human. An ultrastructural and immunohistochemical study. *Cells Tissues Organs* 164, 63–81. doi:10.1159/000016644

Kanahashi, T., Imai, H., Otani, H., Yamada, S., Yoneyama, A., and Takakuwa, T. (2023). Three-dimensional morphogenesis of the human diaphragm during the late embryonic and early fetal period: analysis using T1-weighted and diffusion tensor imaging. *J. Anat.* 242, 174–190. doi:10.1111/joa.13760

Kanamori, A., Kitani, R., Oota, A., Hirano, K., Myosho, T., Kobayashi, T., et al. (2023). Wnt4a is indispensable for genital duct elongation but not for gonadal sex differentiation in the medaka, *Oryzias latipes*. *Oryzias Latipes. Zool. Sci.* 40, 348–359. doi:10.2108/zs230050

Kanamori, A., Nagahama, Y., and Egami, N. (1985). Development of the tissue architecture in the gonads of the medaka *Oryzias latipes*. *Zool. Sci.* 2, 695–706. doi:10.34425/zs000178

Karl, J., and Capel, B. (1998). Sertoli cells of the mouse testis originate from the coelomic epithelium. *Dev.* Biol. 203, 323–333. doi:10.1006/dbio.1998.9068

Katechis, C. T., Sakaris, P. C., and Irwin, E. R. (2007). Population demographics of *Hiodon tergisus* (Mooneye) in the lower Tallapoosa river. *Southeast. Nat.* 6, 461–470. doi:10.1656/1528-7092(2007)6[461:pdohtm]2.0.co;2

Kerr, J. G. (1919). *Textbook of embryology, vol. 2, vertebrata*. London: Macmillan. doi:10.5962/bhl.title.53985

Knowles, F. G. W. (1939). The influence of anterior-pituitary and testicular hormones on the sexual maturation of lampreys. *J. Exp. Biol.* 16, 535–548. doi:10.1242/jeb.16.4.535

Kobayashi, Y., Nozu, R., and Nakamura, M. (2021). "Reproduction and sexual differentiation in cartilaginous fish," in *Sex determination, sex differentiation and sex change in fishes*. Editors K. Kikuchi, S. Ijiri, and T. Kitano (Tokyo: Kouseisha Kouseikaku).

Kobayashi, Y., Sunobe, T., Kobayashi, T., Nagahama, Y., and Nakamura, M. (2005). Gonadal structure of the serial-sex changing gobiid fish *Trimma Okinawae*. *Dev. Growth Differ.* 47, 7–13. doi:10.1111/j.1440-169x.2004.00774.x

Kobayashi, Y., Usami, T., Sunobe, T., Manabe, H., Nagahama, Y., and Nakamura, M. (2012). Histological observation of the urogenital papillae in the bi-directional sex-changing gobiid fish, Trimma okinawae. *Trimma Okinawae. Zool. Sci.* 29, 121–126. doi:10.2108/zsj.29.121

Koepfli, K. P., Paten, B., and OBrien, S. J. (2015). the genome 10K project: a way forward. *Annu. Rev. Anim. Biosci.* 3, 57–111. doi:10.1146/annurev-animal-090414-014900

Kojima, Y., Bhandari, R. K., Kobayashi, Y., and Nakamura, M. (2008). Sex change of adult initial-phase male wrasse, *Halichoeres trimaculatus* by estradiol-17β treatment. *Gen. Comp. Endocrinol.* 156, 628–632. doi:10.1016/j.ygcen.2008.02.003

Kossack, M. E., High, S. K., Hopton, R. E., Yan, Y., Postlethwait, J. H., and Draper, B. W. (2019). Female sex development and reproductive duct formation depend on Wnt4a in zebrafish. *Genetics* 211, 219–233. doi:10.1534/genetics.118.301620

Kuwamura, T., Sunobe, T., Sakai, Y., Kadota, T., and Sawada, K. (2020). Hermaphroditism in fishes: an annotated list of species, phylogeny, and mating system. *Ichthyol. Res.* 67, 341–360. doi:10.1007/s10228-020-00754-6

Lee, M. F., Huang, J. D., and Chang, C. F. (2011). Development of the genital duct system in the protandrous black porgy, *Acanthopagrus schlegeli*. *Anat. Rec.* 294, 494–505. doi:10.1002/ar.21339

Lepori, N. G. (1980). *Sex differentiation, hermaphroditism and intersexuality in vertebrates including man*. Padova, Italy: Pissin Medical Books.

Lombardi, J. (1998). *Comparative vertebrate reproduction*. Boston: Kluwer Academic Publishers. doi:10.1007/978-1-4615-4937-6

Long, J. A., Trinajstic, K., Young, G. C., and Senden, T. (2008). Live birth in the Devonian period. *Nature* 453, 650–652. doi:10.1038/nature06966

Major, A. T., Estermann, M. A., Roly, Z. Y., and Smith, C. A. (2022). An evo-devo perspective of the female reproductive tract. *Biol. Reprod.* 106, 9–23. doi:10.1093/biolre/ioab166

Major, A. T., Estermann, M. A., and Smith, C. A. (2021). Anatomy, endocrine regulation, and embryonic development of the rete testis. *Endocrinology* 162, bqab046–13. doi:10.1210/endocr/bqab046

Matthews, B. J., and Vosshall, L. B. (2020). How to turn an organism into a model organism in 10 "easy" steps. *J. Exp. Biol.* 223 (1), jeb218198. doi:10.1242/jeb.218198

Moses, L., and Pachter, L. (2022). Museum of spatial transcriptomics. *Nat. Methods.* 19, 534–546. doi:10.1038/s41592-022-01409-2

Mullen, R. D., and Behringer, R. R. (2014). Molecular genetics of Mullerian duct formation, regression and differentiation. *Sex. Dev.* 8, 281–296. doi:10.1159/000364935

Nagahama, Y. (1983). "The functional morphology of teleost gonads," in *Fish Physiology vol.9 pt.A*. Editors W. S. Hoar, D. J. Randall, and E. M. Donaldson (New York: Academic Press), 223–264. doi:10.1016/S1546-5098(08)60290-3

Nakajima, T., Yamanaka, R., and Tomooka, Y. (2019). Elongation of Müllerian ducts and connection to urogenital sinus determine the borderline of uterine and vaginal development. *Biochem. Biophys. Rep.* 17, 44–50. doi:10.1016/j.bbrep.2018.10.013

Nakamura, M., Mariko, T., and Nagahama, Y. (1994). Ultrastructure and *in vitro* steroidogenesis of the gonads in the protandrous anemonefish *Amphiprion frenatus*. *Jpn. J. Ichthyol.* 41, 47–56. doi:10.11369/jji1950.41.47

Nakamura, M., Miura, S., Nozu, R., and Kobayashi, Y. (2015). Opposite-directional sex change in functional Female protandrous anemonefish, *Amphiprion clarkii*: effect of aromatase inhibitor on the ovarian tissue. *Zool. Lett.* 1, 30. doi:10.1186/s40851-015-0027-y

Nakamura, S., Kobayashi, D., Aoki, Y., Yokoi, H., Ebe, Y., Wittbrodt, J., et al. (2006). Identification and lineage tracing of two populations of somatic gonadal precursors in medaka embryos. *Dev. Biol.* 295, 678–688. doi:10.1016/j.ydbio.2006.03.052

Orvis, G. D., and Behringer, R. R. (2007). Cellular mechanisms of Mullerian duct formation in the mouse. *Dev. Biol.* 306, 493–504. doi:10.1016/j.ydbio.2007.03.027

Parodi, L., Hoxhaj, I., Dinoi, G., Mirandola, M., Pozzati, F., Topouzova, G., et al. (2022). Complete uterine septum, double cervix and vaginal septum (U2b C2 V1): hysteroscopic management and fertility outcomes - a systematic review. *J. Clin. Med.* 12, 189. doi:10.3390/jcm12010189

Pfeiffer, C. A. (1933). The anatomy and blood supply of the urogenital system of *Lepidosteus platystomus* Rafinesque. *J. Morphol.* 54, 459–475. doi:10.1002/jmor.1050540304

Rabl, C. (1896). Ueber die entwicklung des urogenitalsystems der Selachier. *Morph. Jahrb.* 24, 632–767.

Rao, A., Barkley, D., França, G. S., and Yanai, I. (2021). Exploring tissue architecture using spatial transcriptomics. *Nature* 596, 211–220. doi:10.1038/s41586-021-03634-9

Rastogi, R. K., and Saxena, P. K. (1968). Annual changes in the ovarian activity of the catfish, *Mystus tengara* (Ham.) (Teleostei). *Jpn. J. Ichthyol.* 15, 28–35. doi:10.11369/jji1950.15.28

Riehakainen, L., Cavallini, C., Armanetti, P., Panetta, D., Caramella, D., and Menichetti, L. (2021). *In vivo* imaging of biodegradable implants and related tissue biomarkers. *Polymers* 13, 2348. doi:10.3390/polym13142348

Romer, A. S. (1960). *The vertebrate body*. 3rd Edition. Philadelphia: W. B. Saunders Co.

Romer, A. S., and Parsons, T. S. (1977). *The vertebrate body*. 5th Edition. Philadelphia: W. B. Saunders Co.

Russell, J. J., Theriot, J. A., Sood, P., Marshall, W. F., Landweber, L. F., Fritz-Laylin, L., et al. (2017). Non-model model organisms. *BMC Biol.* 15, 55. doi:10.1186/s12915-017-0391-5

Semper, C. (1875). Das urogenitalsystem der plagiostomen. *Arb. Zool-zoot. Inst. Würzbg.* 2, 195–509.

Shaw, G., and Renfree, M. B. (2014). Wolffian duct development. *Sex. Dev.* 8, 273–280. doi:10.1159/000363432

Sunobe, T., and Nakazono, A. (2010). Sex change in both directions by alteration of social dominance in *Trimma okinawae* (Pisces: gobiidae). *Ethology* 94, 339–345. doi:10.1111/j.1439-0310.1993.tb00450.x

Suzuki, A., and Shibata, N. (2004). Developmental process of genital ducts in the medaka, *Oryzias latipes*. *Oryzias Latipes. Zool. Sci.* 21, 397–406. doi:10.2108/zsj.21.397

Suzuki, A., Tanaka, M., Shibata, N., and Nagahama, Y. (2004). Expression of aromatase mRNA and effects of aromatase inhibitor during ovarian development in the medaka, *Oryzias latipes*. *J. Exp. Zool. A Comp. Exp. Biol.* 301, 266–273. doi:10.1002/jez.a.20027

Suzuki, D. G., Wada, H., and Higashijima, S. I. (2021). Generation of knock-in lampreys by CRISPR-Cas9-mediated genome engineering. *Sci. Rep.* 11, 19836. doi:10.1038/s41598-021-99338-1

Syrski, A. (1876). Lecture on the organs of reproduction and the fecundation of fishes and especially of eels. *Rep. U. S. Comm. Fish.* 3, 719–734.

Takezaki, N. (2021). Resolving the early divergence pattern of teleost fish using genome-scale data. *Genome Biol. Evol.* 13, evab052. doi:10.1093/gbe/evab052

Tawara, M., Miyati, T., Sawada, R., Ohno, N., Okamoto, R., Maehara, Y., et al. (2022). Magnetic resonance imaging applied to the assessment of intact yellowtail (*Seriola quinqueradiata*): preliminary results. *Aquac. Res.* 53, 1956–1962. doi:10.1111/are.15724

Tesch, F. W. (1977). *The eel*. New York: Chapman and Hall Ltd.

Tian, L., Chen, F., and Macosko, E. Z. (2023). The expanding vistas of spatial transcriptomics. *Nat. Biotechnol.* 41, 773–782. doi:10.1038/s41587-022-01448-2

Turnbull, D. H., and Mori, S. (2007). MRI in mouse developmental biology. *NMR Biomed.* 20, 265–274. doi:10.1002/nbm.1146

Udayakumar, N., Smith, E., Boone, A., and Porter, K. K. (2023). A common path: magnetic resonance imaging of Mullerian and Wolffian duct anomalies. *Curr. Urol. Rep.* 24, 1–9. doi:10.1007/s11934-022-01138-1

Uematsu, K., and Hibiya, T. (1983). Sphincter-like musculature surrounding the urino-genital duct of some teleosts. *Jpn. J. Ichthyol.* 30, 72–79. doi:10.11369/jji1950.30.72

Uribe, M. C., Grier, H. J., and Mejía-Roa, V. (2014). Comparative testicular structure and spermatogenesis in bony fishes. *Spermatogenesis* 4, e983400, e983400. doi:10.4161/21565562.2014.983400

Vainio, S., Heikkilä, M., Kispert, A., Chin, N., and McMahon, A. P. (1999). Female development in mammals is regulated by Wnt-4 signalling. *Nature* 397, 405–409. doi:10.1038/17068

Wake, M. H. (1979). "The comparative anatomy of the urogenital system," in *HYMAN's comparative vertebrate anatomy*. Editor M. H. Wake (Chicago, IL: Univ. Chicago Press), 555–614.

Williams, C. G., Lee, H. J., Asatsuma, T., Vento-Tormo, R., and Haque, A. (2022). An introduction to spatial transcriptomics for biomedical research. *Genome Med.* 14, 68. doi:10.1186/s13073-022-01075-1

Wourms, J. P. (1977). Reproduction and development in chondrichthyan fishes. *Amer. Zool.* 17, 379–410. doi:10.1093/icb/17.2.379

Wrobel, K. H. (2003). The genus *Acipenser* as a model for vertebrate urogenital development: the müllerian duct. *Anat. Embryol.* 206, 255–271. doi:10.1007/s00429-002-0287-0

Wrobel, K. H., Geserer, S., and Schimmel, M. (2002a). The genus *Acipenser* as a model for vertebrate urogenital development: ultrastructure of nephrostomial tubule formation and of initial gonadogenesis. *Ann. Anat.* 184, 443–454. doi:10.1016/S0940-9602(02)80077-2

Wrobel, K. H., Hees, I., Schimmel, M., and Stauber, E. (2002b). The genus *Acipenser* as a model system for vertebrate urogenital development: nephrostomial tubules and their significance for the origin of the gonad. *Anat. Embryol.* 205, 67–80. doi:10.1007/s00429-002-0228-y

Wrobel, K. H., and Jouma, S. (2004). Morphology, development and comparative anatomical evaluation of the testicular excretory pathway in *Acipenser*. *Ann. Anat.* 186, 99–113. doi:10.1016/S0940-9602(04)80020-7

Wrobel, K. H., and Süß, F. (2000). The significance of rudimentary nephrostomial tubules for the origin of the vertebrate gonad. *Anat. Embryol.* 201, 273–290. doi:10.1007/s004290050317

Yamamoto, T. S. (1955). Ovulation in the salmon, herring and lamprey. *Jpn. J. Ichthyol.* 4, 182–192. doi:10.11369/jji1950.4.182

Yang, L., Cai, J., Rong, L., Yang, S., and Li, S. (2023). Transcriptome identification of genes associated with uterus-vagina junction epithelial folds formation in chicken hens. *Poult. Sci.* 102, 102624. doi:10.1016/j.psj.2023.102624

Zhao, F., Zhou, J., Li, R., Dudley, E. A., and Ye, X. (2016). Novel function of LHFPL2 in female and male distal reproductive tract development. *Sci. Rep.* 6, 23037. doi:10.1038/srep23037

frontiers | Frontiers in Cell and Developmental Biology

TYPE Mini Review
PUBLISHED 05 January 2024
DOI 10.3389/fcell.2023.1339385

OPEN ACCESS

EDITED BY
Talia L. Hatkevich,
Duke University, United States

REVIEWED BY
Silvana A. Andric,
University of Novi Sad, Serbia

*CORRESPONDENCE
Tony DeFalco,
tony.defalco@cchmc.org

RECEIVED 16 November 2023
ACCEPTED 15 December 2023
PUBLISHED 05 January 2024

CITATION
Matsuyama S and DeFalco T (2024), Steroid hormone signaling: multifaceted support of testicular function. *Front. Cell Dev. Biol.* 11:1339385. doi: 10.3389/fcell.2023.1339385

Steroid hormone signaling: multifaceted support of testicular function

Satoko Matsuyama[1] and Tony DeFalco[1,2]*

[1]Reproductive Sciences Center, Division of Developmental Biology, Cincinnati Children's Hospital Medical Center, Cincinnati, OH, United States, [2]Department of Pediatrics, University of Cincinnati College of Medicine, Cincinnati, OH, United States

Embryonic development and adult physiology are dependent on the action of steroid hormones. In particular, the reproductive system is reliant on hormonal signaling to promote gonadal function and to ensure fertility. Here we will describe hormone receptor functions and their impacts on testicular function, focusing on a specific group of essential hormones: androgens, estrogens, progesterone, cortisol, and aldosterone. In addition to focusing on hormone receptor function and localization within the testis, we will highlight the effects of altered receptor signaling, including the consequences of reduced and excess signaling activity. These hormones act through various cellular pathways and receptor types, emphasizing the need for a multifaceted research approach to understand their critical roles in testicular function. Hormones exhibit intricate interactions with each other, as evidenced, for example, by the antagonistic effects of progesterone on mineralocorticoid receptors and cortisol's impact on androgens. In light of research findings in the field demonstrating an intricate interplay between hormones, a systems biology approach is crucial for a nuanced understanding of this complex hormonal network. This review can serve as a resource for further investigation into hormonal support of male reproductive health.

KEYWORDS

steroid, testis, hormone receptor, male fertility, sexual development, reproductive endocrinology

Introduction

Steroid hormones are integral to various physiological processes, including cellular metabolism, growth, immune function, and reproduction. It is essential to understand the complex biosynthetic pathways, site-specific production, and diverse actions of these hormones, in particular their roles in supporting the male reproductive system. Originating from cholesterol, these hormones undergo enzymatic transformations to form bioactive steroids, each with unique physiological roles.

The biosynthesis of steroid hormones, involving the conversion of cholesterol into a spectrum of hormones, is a crucial process. The review delves into the roles of steroid hormones in testicular function, emphasizing their interactions with intracellular nuclear receptors. Additionally, it explores the non-genomic signaling pathways of these hormones, highlighting their ability to elicit rapid cellular responses and showcasing their adaptability in cellular signaling (Cooke and Walker, 2022).

We will examine the roles of specific steroid hormones in the testes, such as androgens (including testosterone), estrogens, progesterone, cortisol, and aldosterone. We will also

emphasize each hormone's receptor function, localization within testicular cells, and the physiological impacts of their signaling. The significance of these hormones in male reproductive health is underscored by examining the effects of altered receptor signaling, addressing both deficiencies and excesses in hormonal actions.

By providing a broad overview of the roles of steroid hormones in the male reproductive system, we emphasize the need for a multidisciplinary and systems biology approach to fully understand the complex hormonal interactions in male reproductive health and their broader systemic implications.

Biosynthetic pathway and site of production of steroid hormones

The biosynthesis of steroid hormones (Figure 1) involves a cascade of biochemical reactions that transform cholesterol into various steroid hormones through the action of steroidogenic enzymes. Sources of intracellular cholesterol include free cholesterol, acetic acid, cholesterol esters found in lipid droplets, and cholesterol uptake from low-density lipoproteins (LDL) (Miller and Auchus, 2011; Miller, 2017; Zirkin and Papadopoulos, 2018).

Steroid hormones are immediately released into the blood after their synthesis, unlike peptide hormones that are stored in vesicles. This direct link between biosynthesis and release necessitates a readily available cholesterol pool in steroidogenic cells, since mitochondrial cholesterol, especially in the inner mitochondrial membrane where steroidogenesis starts, is insufficient for sustained hormone production. Recent research indicates that mitochondrial dynamics, autophagy, and associated lipophagy are vital for internal cholesterol uptake and balance in these cells, thereby supporting steroid hormone production essential for physiological functions (Bassi et al., 2021). In recent years, the role of mitochondria in steroid hormone action has been the focus of much attention (Guajardo-Correa et al., 2022; Picard and Shirihai, 2022; Shaia et al., 2023).

Within the mitochondria, the transport and conversion of cholesterol are facilitated by steroidogenic acute regulatory protein (StAR) and cytochrome P450 family 11 subfamily a member 1 (CYP11A1)—the latter being a key enzyme located on the inner mitochondrial membrane responsible for side-chain cleavage. Furthermore, the biosynthetic progression of steroid hormones from pregnenolone necessitates the involvement of cytochrome P450 (CYP) and hydroxysteroid dehydrogenase (HSD) enzymes, which are present in both mitochondria and the endoplasmic reticulum (Miller and Auchus, 2011; Zirkin and Papadopoulos, 2018).

Specifically, 3-beta-hydroxysteroid dehydrogenase (3β-HSD, official name HSD3B1) converts pregnenolone into progesterone. Progesterone is then metabolized into testosterone through the catalytic action of cytochrome P450 17A1 (CYP17A1), among other enzymatic steps. Testosterone undergoes conversion to estradiol by the enzyme aromatase, encoded by cytochrome P450 Family 19 subfamily a member 1 (CYP19A1). Cytochrome P450 family 21 Subfamily A member 2 (CYP21A2) mediates progesterone's transformation to 11-deoxycortisol and deoxycorticosterone (DOC). After that transformation, cytochrome P450 family 11 subfamily B member 1 (CYP11B1) converts 11-deoxycortisol and DOC to the glucocorticoids cortisol and corticosterone, respectively. Finally, corticosterone is metabolized to the potent mineralocorticoid aldosterone by cytochrome P450 family 11 subfamily B member 2 (CYP11B2) (Miller and Auchus, 2011; Chakraborty et al., 2021).

Sex steroid hormones, primarily estrogens (estradiol, estriol, estrone), androgens, and progesterone, are predominantly

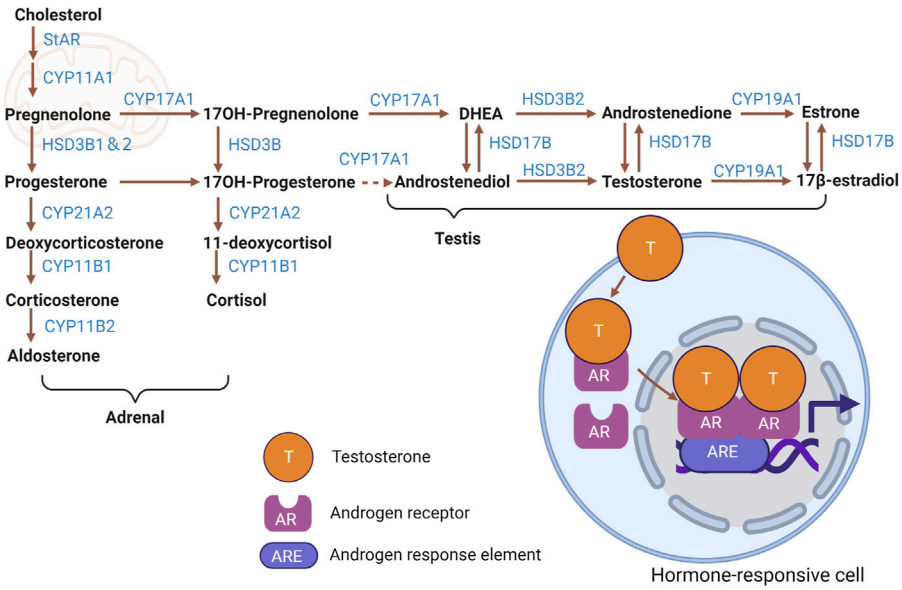

FIGURE 1
Steroid hormone biosynthetic pathways. Cartoon depicting biosynthesis of major adrenal- and testicular-derived steroid hormones from cholesterol, including intermediate molecules and steroidogenic enzymes involved. Testosterone and the resultant change in gene expression mediated by AR in a hormone-responsive cell is shown as an example of signaling activity. Figure created with BioRender.com.

synthesized in the gonads and placenta (Miller and Auchus, 2011). While the adrenal cortex secretes sex hormones, it does so in significantly lesser quantities than gonads. Interestingly, the gonads can also produce adrenal steroids (Chakraborty et al., 2021). In contrast, the adrenal cortex predominantly releases adrenal steroids, comprising glucocorticoids and mineralocorticoids (Miller and Auchus, 2011). In addition to steroid production by mesenchymal-derived Leydig cells in the testis, which are presumed to be the major steroidogenic cells in that organ, the importance of interstitial and peritubular macrophages in testicular steroidogenesis has also been discussed in recent years (Gu et al., 2022).

Feedback mechanisms finely tune steroid hormone biosynthesis. Elevated blood cortisol levels trigger a suppression of adrenocorticotropic hormone (ACTH) secretion from the hypothalamus and pituitary, resulting in a consequent decrease in cortisol release from the adrenal cortex (Schiffer et al., 2019). Other modulatory hormones include luteinizing hormone (LH) and follicle-stimulating hormone (FSH), which orchestrate hormone synthesis within the gonads (Schiffer et al., 2019). Regulation of testicular steroidogenesis is similarly complex, involving a diversity of critical regulatory pathways, including endocrine, paracrine, autocrine, and juxtacrine mechanisms (Bornstein et al., 2004; Hofmann and McBeath, 2022; Huhtaniemi and Toppari, 1995; O'Hara et al., 2015).

Testis-derived androgens and anti-mullerian hormone (AMH) drive male genital (internal and external) differentiation, while their absence leads to female differentiation. Testicular growth, testicular descent, and penile growth occur in response to testicular signals, with early infancy marked by active gonadotropin and steroid secretion. Reduced androgen signaling, characterized by hypogonadism, can inhibit male-specific sexual differentiation, such as penile growth, in boys. The reactivation of the HPG axis during puberty leads to secondary sex characteristic development, with hypogonadism potentially causing incomplete puberty and, later, infertility or sexual dysfunction (Grinspon et al., 2019).

Mechanism of action of steroids in cells via intracellular nuclear receptors

Steroid hormones primarily exert their effects via nuclear signaling pathways (Chan and O'Malley, 1976a). In this cascade, steroid hormones traverse the cell membrane and subsequently associate with specific receptors in the cytoplasm and nucleus (Chan and O'Malley, 1976a). Acting as ligand-activated transcription factors, these receptors form complexes with distinct steroid hormones, such as androgens and estrogens (Chan and O'Malley, 1976b). Once a receptor-ligand complex is established, it interacts with a specialized region on the target gene's regulatory region known as the hormone response element. The ligand-activated receptor dimer then binds specifically to this hormone response element (Devin-Leclerc et al., 1998). This binding prompts the recruitment of co-regulators to enhance gene transcription or co-repressors to inhibit it (Klinge, 2000). Resultant mRNA is then translated into protein, which culminates in characteristic hormonal responses, which include alterations in cell metabolism, growth, or differentiation.

Additionally, certain hormones can elicit rapid cellular responses in mere seconds upon administration, a phenomenon termed membrane or non-genomic signaling (Szego and Davis, 1967; Pietras and Szego, 1975). Interestingly, this non-classical signaling pathway can also elicit genomic effects (Fix et al., 2004).

Androgens

Receptor function

Androgens are essential for testicular function, male reproductive tract differentiation, and maintenance of male fertility (Cunha, 1973; Lasnitzki and Mizuno, 1977; Cunha et al., 1987). Androgens, most commonly testosterone, are ligands for androgen receptor (AR, also known as NR3C4). Androgen signaling is not strictly required for fetal testicular differentiation, as XY humans and mice can undergo fetal testicular differentiation without functional AR (Merlet et al., 2007). Nonetheless, androgens are absolutely essential for spermatogenesis and establishing male secondary sexual characteristics (De Gendt et al., 2004; Davey and Grossmann, 2016).

Receptor localization

Even though androgens are required for spermatogenesis, germ cells do not express a functional androgen receptor (De Gendt et al., 2004), and AR is not required in germ cells in a normal somatic environment (Johnston et al., 2001). Therefore, androgen signaling acts through somatic cells to regulate sperm production. The persistent expression of AR in peritubular and Leydig cells starts from early fetal life and extends well into postnatal stages. In Sertoli cells, nuclear AR expression is first observed by 4–5 days after birth in mice, reaches high expression by 7–9 days of age, and is maintained in adult mice (Edelsztein et al., 2018). AR is expressed strongly in Sertoli cell nuclei but not in spermatogonia, preleptotene and pachytene spermatocytes, or round spermatids (Takada et al., 2023). Nuclear AR localization is linked to active signaling, whereas cytoplasmically-localized AR is considered inactive (Smith and Walker, 2014). Androgens cross the cell membrane and bind to AR in target cells, displacing heat shock proteins (HSP) (Shang et al., 2002). In the classical pathway, ligand-bound AR translocates to the nucleus and forms homodimers that interact with androgen response elements (ARE) in target gene promoters or with other transcription factors (TF), ultimately regulating gene expression (Smith and Walker, 2014). In the non-genomic pathway, the ligand-bound AR migrates to the inner side of the cell membrane, interacts with steroid receptor coactivator (Src), and activates the epidermal growth factor receptor (EGFR) signaling cascade involving downstream pathways such as the mitogen-activated protein kinase (MAPK), extracellular signal-regulated kinase (ERK), and cAMP response element binding protein (CREB) pathways (Konoplya and Popoff, 1992; Benten et al., 1999).

Effects of loss of receptor signaling

Androgen signaling is vital for sperm development in the testis. Specifically, lack of testosterone or its receptor, AR, leads to infertility due to arrest in meiosis, a critical stage in spermatogenesis (Tsai et al., 2006; Walker and Cooke, 2023). This effect is predominantly mediated through Sertoli cells (Chang et al., 2004; Larose et al., 2020). Complete AR knockout (ARKO) in mouse models significantly reduces Sertoli cell numbers (Tan et al., 2005). Milder changes occur in Sertoli cell-selective AR knockout (SCARKO) mice, where meiosis is arrested at specific stages (Tan et al., 2005; Tsai et al., 2006). SCARKO mice also show a disrupted blood testis barrier, which is vital for spermatogenesis (Willems et al., 2010). Direct AR action on Sertoli cells is essential for developing spermatogonia and spermatocytes (O'Shaughnessy et al., 2010). An inducible AR knockout model (iARKO) was developed using a mouse line that ubiquitously expresses a tamoxifen-inducible Cre recombinase (Willems et al., 2011), in which AR inactivation can be temporally controlled, a feature that is lacking in ARKO and SCARKO mice. Both ARKO and iARKO mice exhibit reduced sperm production (Yeh et al., 2002; Willems et al., 2011).

Androgen action via testicular peritubular myoid cells is also essential for normal testis function, spermatogenesis, and male fertility, as well as for normal differentiation and function of adult Leydig cells (Welsh et al., 2012). Sertoli cell function was impaired in peritubular myoid-specific AR-knockout (PTM-ARKO) males, manifested by reduced seminiferous tubule fluid production and reduced expression of some androgen-dependent Sertoli-specific genes (Welsh et al., 2012). Functional AR in Leydig cells is required for steroidogenic function, as spermatogenic arrest predominately at the round spermatid stage was observed when *anti-Müllerian hormone receptor-2* (*Amhr2*) promoter-driven Cre was used to conditionally delete *Ar* in Leydig cells (Xu et al., 2007).

Effects of excess receptor signaling

Prenatal exposure of male rat fetuses to excess testosterone disrupted reproductive function, manifested as a reduction of a number of parameters: testis weight; number of Sertoli cells, spermatocytes, and spermatids; sperm count and motility; and serum concentration of testosterone after puberty (Ramezani Tehrani et al., 2013). Letrozole, an aromatase inhibitor, causes estrogen deficiency and androgen excess. Severe testicular defects, including necrosis and disruption of the seminiferous epithelium, sloughing of epithelial cells, and spermatogenic arrest were observed in prenatal letrozole-treated groups (Shaaban et al., 2023), demonstrating the negative impacts of excess androgens. In the SPARKI (SPecificity-affecting AR KnockIn) mouse model, in which a zinc finger of the AR protein was replaced with that of GR such that only classical, and not selective, androgen response elements can be bound, reproductive capacity and organ size were significantly compromised (Schauwaers et al., 2007).

Estrogens

Receptor function

Two primary pathways dictate estrogen signaling. The classical pathway involves the nuclear estrogen receptors ERα (ESR1) or ERβ (ESR2) (King and Greene, 1984; Green et al., 1986; Greene et al., 1986; Kuiper et al., 1996). These receptors engage with estrogen response elements (EREs) in the DNA to regulate gene expression (Edwards, 2005). The non-classical pathway involves GPER/GPR30, a G protein-coupled receptor, which triggers rapid signaling events such as cAMP production and calcium release upon binding with estrogen (Filardo et al., 2000; Filardo et al., 2002; Revankar et al., 2005). Within the testis, GPER is found on Sertoli cells (Lucas et al., 2010) and sperm (Liu et al., 2009), influencing sperm activation and movement via estrogen's non-genomic effects.

Receptor localization

Numerous studies have reported the presence of ERα in peritubular cells, Leydig cells (Fisher et al., 1997; Pelletier et al., 2000; Mäkinen et al., 2001), and, notably, Sertoli cells (Saunders et al., 2001; Cavaco et al., 2009; Valeri et al., 2020). However, the expression dynamics of ERα in mouse testes show a decline from mid to late puberty (Jefferson et al., 2000). A consistent pattern has been observed in human samples, showing ERα expression in Sertoli cells from childhood through puberty (Valeri et al., 2020). In contrast, ERβ expression in mouse testes reaches its zenith on postnatal days 1–5 and is seldom seen after postnatal day 12 (Cooke et al., 2017). In adult mice, ERβ is found in Leydig and germ cells but is conspicuously absent from Sertoli cells (Cavaco et al., 2009). The most prominent expression was observed in the nucleus of pachytene spermatocytes, but ER expression was also evident in spermatogonia, preleptotene spermatocytes, round spermatids, and Sertoli cells (Takada et al., 2023).

Effects of loss of receptor signaling

Estrogen receptor anomalies stemming from mutations in *Esr1* (encoding ERα) and *Esr2* (encoding ERβ) lead to estrogen insensitivity or resistance conditions. In *Esr1*-deficient mice, fetal testis development is unaffected, but in adulthood they exhibit disrupted spermatogenesis and excess fluid retention in the rete testis, leading to infertility (Lubahn et al., 1993). Also, loss of ER function in ERKO males leads to reduced mating frequency, low sperm numbers, and defective sperm function (Eddy et al., 1996). Patients with aromatase deficiency exhibit symptoms such as Sertoli cell hyperplasia and significant testicular enlargement, likely due to continuous FSH elevation (Morishima et al., 1995). Intriguingly, murine studies suggest ERβ′s minimal role in testicular physiology (Krege et al., 1998; Dupont et al., 2000). An interesting relationship between the decline in endogenous estrogen and testicular cortisol has been observed, hinting at an interconnected signaling pathway impacting Sertoli cell proliferation. For instance, treatment with the aromatase inhibitor letrozole led to a reduction in testicular cortisol

levels, inversely increasing Sertoli cell proliferation (Berger et al., 2019).

Effects of excess receptor signaling

A rare genetic aberration in humans, termed aromatase excess syndrome, results from a chromosome 15 rearrangement that causes an upsurge in CYP19A1 expression (Fukami and Ogata, 2022). Remarkably, male external genitalia and fertility remain unaffected. This suggests elevated estrogen levels do not significantly hamper testicular function (Rochira and Carani, 2009; Bulun, 2014; Miedlich et al., 2016). Following chronic treatment with estradiol, however, a reduced number of germ cells was observed, likely caused by increased germ cell apoptosis (Kaushik et al., 2010b). All these observations were attributed to the negative effect of estradiol on the expression of AR, as estrogen treatment causes an increase in ERα expression and a decrease in AR expression in the rat testis (Kaushik et al., 2010a; b). Analysis of human testicular morphology and function after estradiol treatment revealed decreased seminiferous tubule diameter and induced fatty degeneration in the surrounding connective tissue. Spermatogenesis was impaired, resulting in mainly spermatogonia being present (Leavy et al., 2017). Genetically induced estrogen receptor α mRNA (*Esr1*) overexpression did not adversely affect fertility development in male mice (Heath et al., 2011), revealing a minimal impact of excess estrogen signaling on general testicular function in the absence of an exogenous estrogen exposure.

Progesterone

Receptor function

Traditionally associated with female reproductive physiology for its roles in fertilization, pregnancy, and endometrial receptivity, progesterone also exerts important functions in male reproductive tissues like the prostate and testes. Progesterone rapidly activates intracellular signaling in human sperm, regulating key aspects of their physiology (Publicover and Barratt, 2011). An ion channel unique to the sperm tail seems to relay progesterone's signal (Lishko et al., 2011; Strünker et al., 2011), although it is unclear if progesterone signals through the progesterone receptor (PR; official name PGR) in the testis (Baker and Katsu, 2020).

Receptor localization

Experiments focusing on suppressing spermatogenesis and its effects on receptor expression found that PR-B, a specific isoform of the progesterone receptor, was expressed in the rat testis at both transcriptional and protein levels (Lue et al., 2013). In mice, B-gal expression from a PR knockout allele was reported to be expressed in PRKO mice within Leydig cells, but only under conditions of gonadotropin inhibition (Lue et al., 2013); however, there are caveats in relying on a reporter line, and immunohistochemistry was not performed. There is also some debate about PR expression in primate and human testis, in which some studies report widespread testicular PR expression (Shah et al., 2005), while others show limited expression in few cells (Luetjens et al., 2006). Given some inconsistency between different reports, the localization of PR in the testis, if any is indeed expressed, is unclear.

Effects of loss of receptor signaling

Mice devoid of functional progesterone receptor (PRKO) had significantly larger testes than control mice, and they exhibited increased sperm production accompanied by an increase in Sertoli and Leydig cell numbers (Lue et al., 2013). In general, it appears that PR plays an inhibitory role in testicular function.

Effects of excess receptor signaling

Progesterone treatment suppresses gonadotropin-releasing hormone (GnRH) in the hypothalamus, which in turn lowers the production of LH and FSH by the pituitary gland (Amory, 2004). Synthetic progestins such as levonorgestrel induced germ cell apoptosis (Lue et al., 2013); therefore, progesterone may also act directly on the testes, but the mechanism has not yet been elucidated. Testicular macrophages could also produce progesterone, and steroid production by macrophages may contribute to a local feedback loop between Leydig cells and macrophages that regulate testosterone production (Yamauchi et al., 2022; Ogawa and Isaji, 2023). This interplay suggests that testosterone and progesterone can influence each other's roles in testicular function.

Cortisol

Receptor function

Glucocorticoids regulate major systemic functions, including blood pressure and immune responses. Corticosterone is the major form in mice (Leenaars et al., 2020), whereas it is cortisol in humans (Salehzadeh and Soma, 2021). The primary signaling mechanism involves the glucocorticoid receptor (GR; official name NR3C1), a nuclear receptor family member. GR modulates gene expression when bound to cortisol by interacting with specific DNA elements (Oakley and Cidlowski, 2013). Subcellular trafficking, promoter specificity, cofactor interaction, receptor stability, and turnover further fine-tune the receptor's cellular functions (Whirledge and Cidlowski, 2017). The response to glucocorticoids is regulated by the recruitment of cofactors, which can act in various mechanisms including remodeling of chromatin, facilitating the assembly of transcriptional machinery, or modifying histones or other components of the transcription factor complex (Barnes, 2009; Grøntved et al., 2013; Jones et al., 2014). The testicular role of GR is less well understood. Innate immunity, which is responsive to GR signaling, remains crucial despite the blood-testis barrier and systemic immune tolerance that shield the testis from inflammatory responses normally occurring in other organs. Inflammation can compromise this barrier and induce germ cell death, yet

glucocorticoids' role in testicular function is unclear (Whirledge and Cidlowski, 2017).

Receptor localization

In the testis, the localization and role of GR are less extensively studied as compared to other tissues. GR expression was reported in Leydig, peritubular, Sertoli cells and early germ cells on postnatal day 20 testis in mice (Hazra et al., 2014). In adult mice, GR was expressed in the nuclei of spermatogonia and preleptotene spermatocytes. In contrast, pachytene spermatocytes exhibited weak GR expression, and no apparent GR expression was observed in spermatids (Takada et al., 2023). In mature 70-day-old mice, Sertoli cells do not express detectable levels of GR (Levy et al., 1989; Hazra et al., 2014).

In adult human testis, GR was detected in peritubular cells (Welter et al., 2020), a subset of Leydig cells, Sertoli cells (weak), and spermatogonia, but not in spermatids. The GR expression pattern in fetal testis samples differed, notably by heterogeneous expression in Sertoli cells, lack of expression in gonocytes, and weak expression in nascent peritubular cells, along with detectable expression in a subset of prospermatogonia (Nordkap et al., 2017).

Effects of loss of receptor signaling

Sertoli-specific *Gr* deletion in mice had a limited impact on fertility but did reduce Sertoli cell and spermatocyte numbers (Hazra et al., 2014). A 50% reduction of GR in Leydig cells using AAV9-Cre disrupted steroidogenesis (Gannon et al., 2022), suggesting a role for GR in Leydig cell function. Rat adrenalectomy studies showed decreased sperm counts were partially restored by dexamethasone, but not sperm morphology (Silva et al., 2014). Testosterone production surged after adrenalectomy, which glucocorticoid replacement prevented (Whirledge and Cidlowski, 2017), revealing an interplay between glucocorticoid and testosterone levels. Mice deficient for *Tsc22d3-2*, originally identified as a dexamethasone-induced transcript protecting T lymphocytes from T cell receptor (TCR)/CD3-activated cell death (D'Adamio et al., 1997), exhibited increased germ cell apoptosis, leading to azoospermia and infertility (Romero et al., 2012; Suarez et al., 2012).

Effects of excess receptor signaling

Glucocorticoids like betamethasone and dexamethasone disrupt male reproductive hormones across species. In medaka fish, betamethasone led to feminization (Su et al., 2023). Dexamethasone treatment in mice increased expression of male-specific genes like *Sry* and *Sox9* during critical embryonic stages (Yun et al., 2016). In rats treated with glucocorticoids during prenatal development, expression of nuclear COUP-TFII (official name NR2F2), a marker of Leydig precursors, increased, stem Leydig cell proliferation decreased, and testosterone levels decreased (van den Driesche et al., 2012); in addition, they showed compromised testicular morphology and reduced StAR expression (Liu et al., 2018). Epigenetic programming affecting sperm quality was also observed (Liu et al., 2023).

Postnatal exposure to excess glucocorticoids also has significant impacts. Psychological stress, which increases systemic glucocorticoid levels, impaired Sertoli cell function in adult rats (Medubi et al., 2021). Dexamethasone led to atrophy of the seminiferous tubules and degeneration of spermatocytes but was somewhat mitigated by onion extract, which has the potential to inhibit oxidative stress, in adult rats (Nassan et al., 2021). Following exposure, adult horses showed gene downregulation such as *NR4A1*, *NR5A1,* and *NR5A2* in primary cultures of Leydig cells, but *A. cepa* (onion) extract inhibited oxidative stress induced by dexamethasone (Valdez et al., 2019). In male rats, dexamethasone for 7 days caused severe testicular pathology such as hypospermatogenesis, germ cell degeneration and depletion, epithelial vacuolization, and degenerated Leydig cells (Azimi Zangabad et al., 2023).

In vitro studies indicate dexamethasone suppresses Leydig cell differentiation (Zhang et al., 2019; Liu et al., 2021), an effect reversible with an NR3C1 (GR) antagonist (Zhang et al., 2019). These findings highlight the need for further study on long-term consequences of glucocorticoid treatment (Jeje and Raji, 2017).

Aldosterone

Receptor function

Aldosterone regulates sodium and water homeostasis via the mineralocorticoid receptor (MR; official name NR3C2) and has broader roles in organ development, including the kidneys and heart (Zhang et al., 2018).

Receptor localization

MR is expressed in the testicular Leydig cells of adult rats, where aldosterone modulates stem Leydig cell proliferation and testosterone production (Zhang et al., 2018).

Effects of loss of receptor signaling

The consequences of MR knockout in testes are unclear. Fetal exposure to di-(2-ethylhexyl) phthalate (DEHP) reduced MR mRNA and protein levels and reduced testosterone levels in adulthood (Martinez-Arguelles et al., 2009), suggesting a link between MR and testicular steroidogenesis.

Effects of excess receptor signaling

Low serum testosterone correlates with gonadal dysfunction. Similar observations in rats with renal failure suggest a link between the renin-angiotensin-aldosterone system and gonadal failure (Zhang et al., 2018; Liu et al., 2021). *In vitro* culture of seminiferous tubules from Leydig-cell-depleted testes revealed that aldosterone suppressed stem Leydig cell proliferation and

increased steroidogenesis, which is in direct contrast with dexamethasone's inhibitory effect on stem Leydig cell differentiation (Zhang et al., 2018).

Both aldosterone and progesterone activate their respective receptors at low concentrations, so the antagonistic effect of elevated progesterone on human MR needs further study (Zhang et al., 2018; Baker and Katsu, 2020). A human MR Ser810Leu mutation that is activated by progesterone is associated with high blood pressure (Geller et al., 2000). Furthermore, spironolactone, an aldosterone antagonist, is linked to reduced plasma testosterone in men (Baba et al., 1978). All these data indicate an interplay between aldosterone levels and the production of other steroid hormones.

Future perspectives

Immune cells are not merely passive targets of steroid hormones through their receptors but also possess the potential to convert and metabolize these hormones on their own (Rubinow, 2018). Human alveolar macrophages have been reported to convert androstenedione to testosterone and other steroids through specific enzymatic catalytic activities (Milewich et al., 1983). Moreover, human monocyte-derived macrophages can convert dehydroepiandrosterone (DHEA) to testosterone, estradiol, and other steroids in the presence of LPS (Schmidt et al., 2000). These findings offer insights into the heterogeneity and microenvironment-dependency of steroid hormone conversion in macrophages.

Furthermore, it has been shown that immune cells have the capacity for *de novo* steroidogenesis starting from cholesterol. For instance, the expression of StAR has been detected in macrophages (Ma et al., 2007; Taylor et al., 2010), suggesting at least the ability to import cholesterol into mitochondria and to produce steroidogenic substrates. Primary rat testicular macrophages have been reported to produce corticosterone *in vitro* (Wang et al., 2017), although it remains unclear whether this production is derived from *de novo* steroidogenesis or from the conversion of other steroids. Furthermore, it has been reported that testicular macrophages produce progesterone *de novo*, which is promoted by cAMP and inhibited by M1 polarization inducers (Yamauchi et al., 2022). These discoveries suggest the potential involvement of macrophages in local feedback loops with Leydig cells, thus influencing and contributing to the regulation of testosterone production.

The existence of steroidogenesis and steroid signaling within immune cells presents new possibilities for understanding how immune cells communicate and shape the physiology of immune responses, as well as how they become dysregulated in disease states. The impact of nuclear receptor signaling pathways, such as those mediated by steroid hormone receptors, is profound. Given that the GR alone can regulate up to 20% of genes, these pathways hold the potential to revolutionize our understanding of immune regulation (Galon et al., 2002; Weikum et al., 2017). Technological advancements, particularly improvements in liquid chromatography/tandem mass spectrometry, single-cell transcriptomics, multimodal omics, and spatial resolution techniques, are enhancing our understanding of steroid production and gene expression networks related to steroid responsiveness in immune cells. Chromosome conformation capture assays can analyze changes in genome interactions, contributing to the elucidation of mechanisms by which nuclear receptors bind to chromatin and regulate gene expression (Chakraborty et al., 2021). These developments are poised to deepen our understanding of immune regulation and contribute to the development of new therapeutic strategies.

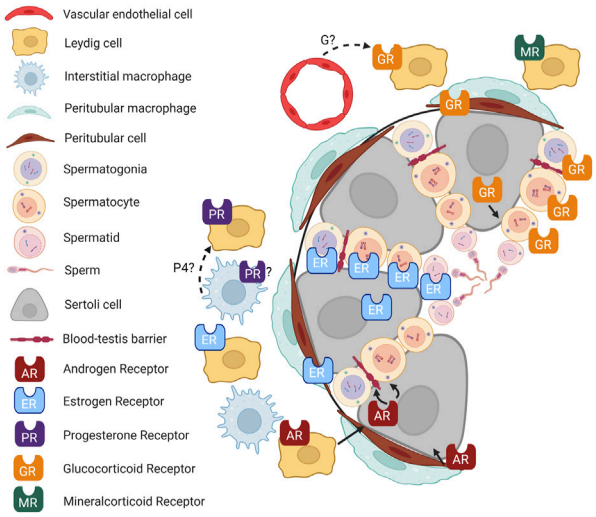

FIGURE 2
Hormone signaling in the testis. Cartoon depicting an adult mouse testis, showing localization of hormone receptors in different cell types and known (solid lines) and putative (dashed lines) interactions between cell types. P4, progesterone; G, glucocorticoid. Figure created with BioRender.com.

Discussion

The multifaceted roles of hormone receptors in testicular function have been the subject of considerable research. Still, the complexity of their interactions and the mechanisms underlying their effects on male reproductive health remain incompletely understood (Figure 2). In particular, the roles of GR, MR, and PR are still unclear. Similarly, hormone receptor localization in testicular cells warrants further study.

Furthermore, hormones often do not function in isolation. Their role in the testes appears modulated by complex feedback loops, crosstalk with other hormones, and possibly interaction with local immune cells (Rubinow, 2018). As immune-mediated endocrinology gains traction in the scientific community, it would be informative to investigate how local immune cells like macrophages interact with testicular hormone production and action.

In addition, dysfunction in hormonal signaling is not without repercussions. Aberrant expression or activities of hormonal receptors can lead to a variety of pathologies, including inflammation-induced infertility, testicular atrophy, and even testicular cancer. Understanding these outcomes necessitates a multi-disciplinary approach that transcends traditional endocrinology.

In conclusion, a systems biology approach integrating these multifactorial interactions will likely provide new insights into male reproductive endocrinology. Such holistic perspectives are imperative not just for solving reproductive health issues but also for advancing our understanding of systemic endocrine functions.

Author contributions

SM: Conceptualization, Writing–original draft, Writing–review and editing, Investigation. TD: Conceptualization, Writing–original draft, Writing–review and editing, Funding acquisition, Supervision.

Funding

The author(s) declare that no financial support was received for the research, authorship, and/or publication of this article. The TD laboratory is supported by Cincinnati Children's Hospital Medical Center internal funding and National Institutes of Health (NIH) grant #R01HD094698 to TD. SM is supported by Japan Society for the Promotion of Science (JSPS) Overseas Research Fellowship #202360521.

Conflict of interest

The authors declare that the research was conducted in the absence of any commercial or financial relationships that could be construed as a potential conflict of interest.

Publisher's note

References

Amory, J. K. (2004). Testosterone/progestin regimens: a realistic option for male contraception? *Curr. Opin. Investig. Drugs* 5 (10), 1025–1030.

Azimi Zangabad, E., Shomali, T., and Roshangar, L. (2023). Effects of pharmacological doses of niacin on subacute glucocorticoid-induced testicular damage in rats. *Pharmacol. Res. Perspect.* 11 (5), e01128. doi:10.1002/prp2.1128

Baba, S., Murai, M., Jitsukawa, S., Hata, M., and Tazaki, H. (1978). Antiandrogenic effects of spironolactone: hormonal and ultrastructural studies in dogs and men. *J. Urol.* 119 (3), 375–380. doi:10.1016/s0022-5347(17)57495-9

Baker, M. E., and Katsu, Y. (2020). Progesterone: an enigmatic ligand for the mineralocorticoid receptor. *Biochem. Pharmacol.* 177, 113976. doi:10.1016/j.bcp.2020.113976

Barnes, P. J. (2009). Histone deacetylase-2 and airway disease. *Ther. Adv. Respir. Dis.* 3 (5), 235–243. doi:10.1177/1753465809348648

Bassi, G., Sidhu, S. K., and Mishra, S. (2021). The expanding role of mitochondria, autophagy and lipophagy in steroidogenesis. *Cells* 10 (8), 1851. doi:10.3390/cells10081851

Benten, W. P., Lieberherr, M., Giese, G., Wrehlke, C., Stamm, O., Sekeris, C. E., et al. (1999). Functional testosterone receptors in plasma membranes of T cells. *FASEB J.* 13 (1), 123–133. doi:10.1096/fasebj.13.1.123

Berger, T., Sidhu, P., Tang, S., and Kucera, H. (2019). Are testicular cortisol and WISP2 involved in estrogen-regulated Sertoli cell proliferation? *Anim. Reprod. Sci.* 207, 44–51. doi:10.1016/j.anireprosci.2019.05.014

Bornstein, S. R., Rutkowski, H., and Vrezas, I. (2004). Cytokines and steroidogenesis. *Mol. Cell. Endocrinol.* 215 (1-2), 135–141. doi:10.1016/j.mce.2003.11.022

Bulun, S. E. (2014). Aromatase and estrogen receptor α deficiency. *Fertil. Steril.* 101 (2), 323–329. doi:10.1016/j.fertnstert.2013.12.022

Cavaco, J. E., Laurentino, S. S., Barros, A., Sousa, M., and Socorro, S. (2009). Estrogen receptors alpha and beta in human testis: both isoforms are expressed. *Syst. Biol. Reprod. Med.* 55 (4), 137–144. doi:10.3109/19396360902855733

Chakraborty, S., Pramanik, J., and Mahata, B. (2021). Revisiting steroidogenesis and its role in immune regulation with the advanced tools and technologies. *Genes Immun.* 22 (3), 125–140. doi:10.1038/s41435-021-00139-3

Chan, L., and O'Malley, B. W. (1976a). Mechanism of action of the sex steroid hormones (first of three parts). *N. Engl. J. Med.* 294 (24), 1322–1328. doi:10.1056/nejm197606102942405

Chan, L., and O'Malley, B. W. (1976b). Mechanism of action of the sex steroid hormones (second of three parts). *N. Engl. J. Med.* 294 (25), 1372–1381. doi:10.1056/nejm197606172942505

Chang, C., Chen, Y. T., Yeh, S. D., Xu, Q., Wang, R. S., Guillou, F., et al. (2004). Infertility with defective spermatogenesis and hypotestosteronemia in male mice lacking the androgen receptor in Sertoli cells. *Proc. Natl. Acad. Sci. U. S. A.* 101 (18), 6876–6881. doi:10.1073/pnas.0307306101

Cooke, P. S., Nanjappa, M. K., Ko, C., Prins, G. S., and Hess, R. A. (2017). Estrogens in male physiology. *Physiol. Rev.* 97 (3), 995–1043. doi:10.1152/physrev.00018.2016

Cooke, P. S., and Walker, W. H. (2022). Nonclassical androgen and estrogen signaling is essential for normal spermatogenesis. *Semin. Cell Dev. Biol.* 121, 71–81. doi:10.1016/j.semcdb.2021.05.032

Cunha, G. R. (1973). The role of androgens in the epithelio-mesenchymal interactions involved in prostatic morphogenesis in embryonic mice. *Anat. Rec.* 175 (1), 87–96. doi:10.1002/ar.1091750108

Cunha, G. R., Donjacour, A. A., Cooke, P. S., Mee, S., Bigsby, R. M., Higgins, S. J., et al. (1987). The endocrinology and developmental biology of the prostate. *Endocr. Rev.* 8 (3), 338–362. doi:10.1210/edrv-8-3-338

D'Adamio, F., Zollo, O., Moraca, R., Ayroldi, E., Bruscoli, S., Bartoli, A., et al. (1997). A new dexamethasone-induced gene of the leucine zipper family protects T lymphocytes from TCR/CD3-activated cell death. *Immunity* 7 (6), 803–812. doi:10.1016/s1074-7613(00)80398-2

Davey, R. A., and Grossmann, M. (2016). Androgen receptor structure, function and biology: from bench to bedside. *Clin. Biochem. Rev.* 37 (1), 3–15.

De Gendt, K., Swinnen, J. V., Saunders, P. T., Schoonjans, L., Dewerchin, M., Devos, A., et al. (2004). A Sertoli cell-selective knockout of the androgen receptor causes spermatogenic arrest in meiosis. *Proc. Natl. Acad. Sci. U. S. A.* 101 (5), 1327–1332. doi:10.1073/pnas.0308114100

Devin-Leclerc, J., Meng, X., Delahaye, F., Leclerc, P., Baulieu, E. E., and Catelli, M. G. (1998). Interaction and dissociation by ligands of estrogen receptor and Hsp90: the antiestrogen RU 58668 induces a protein synthesis-dependent clustering of the receptor in the cytoplasm. *Mol. Endocrinol.* 12 (6), 842–854. doi:10.1210/mend.12.6.0121

Dupont, S., Krust, A., Gansmuller, A., Dierich, A., Chambon, P., and Mark, M. (2000). Effect of single and compound knockouts of estrogen receptors alpha (ERalpha) and beta (ERbeta) on mouse reproductive phenotypes. *Development* 127 (19), 4277–4291. doi:10.1242/dev.127.19.4277

Eddy, E. M., Washburn, T. F., Bunch, D. O., Goulding, E. H., Gladen, B. C., Lubahn, D. B., et al. (1996). Targeted disruption of the estrogen receptor gene in male mice causes alteration of spermatogenesis and infertility. *Endocrinology* 137 (11), 4796–4805. doi:10.1210/endo.137.11.8895349

Edelsztein, N. Y., Racine, C., di Clemente, N., Schteingart, H. F., and Rey, R. A. (2018). Androgens downregulate anti-Müllerian hormone promoter activity in the Sertoli cell through the androgen receptor and intact steroidogenic factor 1 sites. *Biol. Reprod.* 99 (6), 1303–1312. doi:10.1093/biolre/ioy152

Edwards, D. P. (2005). Regulation of signal transduction pathways by estrogen and progesterone. *Annu. Rev. Physiol.* 67, 335–376. doi:10.1146/annurev.physiol.67.040403.120151

Filardo, E. J., Quinn, J. A., Bland, K. I., and Frackelton, A. R., Jr. (2000). Estrogen-induced activation of Erk-1 and Erk-2 requires the G protein-coupled receptor homolog, GPR30, and occurs via trans-activation of the epidermal growth factor

receptor through release of HB-EGF. *Mol. Endocrinol.* 14 (10), 1649–1660. doi:10.1210/mend.14.10.0532

Filardo, E. J., Quinn, J. A., Frackelton, A. R., Jr., and Bland, K. I. (2002). Estrogen action via the G protein-coupled receptor, GPR30: stimulation of adenylyl cyclase and cAMP-mediated attenuation of the epidermal growth factor receptor-to-MAPK signaling axis. *Mol. Endocrinol.* 16 (1), 70–84. doi:10.1210/mend.16.1.0758

Fisher, J. S., Millar, M. R., Majdic, G., Saunders, P. T., Fraser, H. M., and Sharpe, R. M. (1997). Immunolocalisation of oestrogen receptor-alpha within the testis and excurrent ducts of the rat and marmoset monkey from perinatal life to adulthood. *J. Endocrinol.* 153 (3), 485–495. doi:10.1677/joe.0.1530485

Fix, C., Jordan, C., Cano, P., and Walker, W. H. (2004). Testosterone activates mitogen-activated protein kinase and the cAMP response element binding protein transcription factor in Sertoli cells. *Proc. Natl. Acad. Sci. U. S. A.* 101 (30), 10919–10924. doi:10.1073/pnas.0404278101

Fukami, M., and Ogata, T. (2022). Congenital disorders of estrogen biosynthesis and action. *Best. Pract. Res. Clin. Endocrinol. Metab.* 36 (1), 101580. doi:10.1016/j.beem.2021.101580

Galon, J., Franchimont, D., Hiroi, N., Frey, G., Boettner, A., Ehrhart-Bornstein, M., et al. (2002). Gene profiling reveals unknown enhancing and suppressive actions of glucocorticoids on immune cells. *FASEB J.* 16 (1), 61–71. doi:10.1096/fj.01-0245com

Gannon, A. L., Darbey, A. L., Chensee, G., Lawrence, B. M., O'Donnell, L., Kelso, J., et al. (2022). A novel model using AAV9-cre to knockout adult Leydig cell gene expression reveals a physiological role of glucocorticoid receptor signalling in Leydig cell function. *Int. J. Mol. Sci.* 23 (23), 15015. doi:10.3390/ijms232315015

Geller, D. S., Farhi, A., Pinkerton, N., Fradley, M., Moritz, M., Spitzer, A., et al. (2000). Activating mineralocorticoid receptor mutation in hypertension exacerbated by pregnancy. *Science* 289 (5476), 119–123. doi:10.1126/science.289.5476.119

Green, S., Walter, P., Greene, G., Krust, A., Goffin, C., Jensen, E., et al. (1986). Cloning of the human oestrogen receptor cDNA. *J. Steroid Biochem.* 24 (1), 77–83. doi:10.1016/0022-4731(86)90035-x

Greene, G. L., Gilna, P., Waterfield, M., Baker, A., Hort, Y., and Shine, J. (1986). Sequence and expression of human estrogen receptor complementary DNA. *Science* 231 (4742), 1150–1154. doi:10.1126/science.3753802

Grinspon, R. P., Freire, A. V., and Rey, R. A. (2019). Hypogonadism in pediatric health: adult medicine concepts fail. *Trends Endocrinol. Metab.* 30 (12), 879–890. doi:10.1016/j.tem.2019.08.002

Grøntved, L., John, S., Baek, S., Liu, Y., Buckley, J. R., Vinson, C., et al. (2013). C/EBP maintains chromatin accessibility in liver and facilitates glucocorticoid receptor recruitment to steroid response elements. *EMBO J.* 32 (11), 1568–1583. doi:10.1038/emboj.2013.106

Gu, X., Li, S. Y., Matsuyama, S., and DeFalco, T. (2022). Immune cells as critical regulators of steroidogenesis in the testis and beyond. *Front. Endocrinol. (Lausanne)* 13, 894437. doi:10.3389/fendo.2022.894437

Guajardo-Correa, E., Silva-Agüero, J. F., Calle, X., Chiong, M., Henríquez, M., García-Rivas, G., et al. (2022). Estrogen signaling as a bridge between the nucleus and mitochondria in cardiovascular diseases. *Front. Cell Dev. Biol.* 10, 968373. doi:10.3389/fcell.2022.968373

Hazra, R., Upton, D., Jimenez, M., Desai, R., Handelsman, D. J., and Allan, C. M. (2014). *In vivo* actions of the Sertoli cell glucocorticoid receptor. *Endocrinology* 155 (3), 1120–1130. doi:10.1210/en.2013-1940

Heath, J., Abdelmageed, Y., Braden, T. D., Williams, C. S., Williams, J. W., Paulose, T., et al. (2011). Genetically induced estrogen receptor α mRNA (Esr1) overexpression does not adversely affect fertility or penile development in male mice. *J. Androl.* 32 (3), 282–294. doi:10.2164/jandrol.110.010769

Hofmann, M. C., and McBeath, E. (2022). Sertoli cell-germ cell interactions within the niche: paracrine and juxtacrine molecular communications. *Front. Endocrinol. (Lausanne)* 13, 897062. doi:10.3389/fendo.2022.897062

Huhtaniemi, I., and Toppari, J. (1995). Endocrine, paracrine and autocrine regulation of testicular steroidogenesis. *Adv. Exp. Med. Biol.* 377, 33–54. doi:10.1007/978-1-4899-0952-7_3

Jefferson, W. N., Couse, J. F., Banks, E. P., Korach, K. S., and Newbold, R. R. (2000). Expression of estrogen receptor beta is developmentally regulated in reproductive tissues of male and female mice. *Biol. Reprod.* 62 (2), 310–317. doi:10.1095/biolreprod62.2.310

Jeje, S. O., and Raji, Y. (2017). Maternal treatment with dexamethasone during gestation alters sexual development markers in the F1 and F2 male offspring of Wistar rats. *J. Dev. Orig. Health Dis.* 8 (1), 101–112. doi:10.1017/s2040174416000453

Johnston, D. S., Russell, L. D., Friel, P. J., and Griswold, M. D. (2001). Murine germ cells do not require functional androgen receptors to complete spermatogenesis following spermatogonial stem cell transplantation. *Endocrinology* 142 (6), 2405–2408. doi:10.1210/endo.142.6.8317

Jones, C. L., Bhatla, T., Blum, R., Wang, J., Paugh, S. W., Wen, X., et al. (2014). Loss of TBL1XR1 disrupts glucocorticoid receptor recruitment to chromatin and results in glucocorticoid resistance in a B-lymphoblastic leukemia model. *J. Biol. Chem.* 289 (30), 20502–20515. doi:10.1074/jbc.M114.569889

Kaushik, M. C., Misro, M. M., Sehgal, N., and Nandan, D. (2010a). AR versus ER (α) expression in the testis and pituitary following chronic estrogen administration in adult rat. *Syst. Biol. Reprod. Med.* 56 (6), 420–430. doi:10.3109/19396368.2010.501891

Kaushik, M. C., Misro, M. M., Sehgal, N., and Nandan, D. (2010b). Effect of chronic oestrogen administration on androgen receptor expression in reproductive organs and pituitary of adult male rat. *Andrologia* 42 (3), 193–205. doi:10.1111/j.1439-0272.2009.00979.x

King, W. J., and Greene, G. L. (1984). Monoclonal antibodies localize oestrogen receptor in the nuclei of target cells. *Nature* 307 (5953), 745–747. doi:10.1038/307745a0

Klinge, C. M. (2000). Estrogen receptor interaction with co-activators and co-repressors. *Steroids* 65 (5), 227–251. doi:10.1016/s0039-128x(99)00107-5

Konoplya, E. F., and Popoff, E. H. (1992). Identification of the classical androgen receptor in male rat liver and prostate cell plasma membranes. *Int. J. Biochem.* 24 (12), 1979–1983. doi:10.1016/0020-711x(92)90294-b

Krege, J. H., Hodgin, J. B., Couse, J. F., Enmark, E., Warner, M., Mahler, J. F., et al. (1998). Generation and reproductive phenotypes of mice lacking estrogen receptor beta. *Proc. Natl. Acad. Sci. U. S. A.* 95 (26), 15677–15682. doi:10.1073/pnas.95.26.15677

Kuiper, G. G., Enmark, E., Pelto-Huikko, M., Nilsson, S., and Gustafsson, J. A. (1996). Cloning of a novel receptor expressed in rat prostate and ovary. *Proc. Natl. Acad. Sci. U. S. A.* 93 (12), 5925–5930. doi:10.1073/pnas.93.12.5925

Larose, H., Kent, T., Ma, Q., Shami, A. N., Harerimana, N., Li, J. Z., et al. (2020). Regulation of meiotic progression by Sertoli-cell androgen signaling. *Mol. Biol. Cell* 31 (25), 2841–2862. doi:10.1091/mbc.E20-05-0334

Lasnitzki, I., and Mizuno, T. (1977). Induction of the rat prostate gland by androgens in organ culture. *J. Endocrinol.* 74 (1), 47–55. doi:10.1677/joe.0.0740047

Leavy, M., Trottmann, M., Liedl, B., Reese, S., Stief, C., Freitag, B., et al. (2017). Effects of elevated β-estradiol levels on the functional morphology of the testis - new insights. *Sci. Rep.* 7, 39931. doi:10.1038/srep39931

Leenaars, C. H. C., van der Mierden, S., Durst, M., Goerlich-Jansson, V. C., Ripoli, F. L., Keubler, L. M., et al. (2020). Measurement of corticosterone in mice: a protocol for a mapping review. *Lab. Anim.* 54 (1), 26–32. doi:10.1177/0023677219868499

Levy, F. O., Ree, A. H., Eikvar, L., Govindan, M. V., Jahnsen, T., and Hansson, V. (1989). Glucocorticoid receptors and glucocorticoid effects in rat Sertoli cells. *Endocrinology* 124 (1), 430–436. doi:10.1210/endo-124-1-430

Lishko, P. V., Botchkina, I. L., and Kirichok, Y. (2011). Progesterone activates the principal Ca2+ channel of human sperm. *Nature* 471 (7338), 387–391. doi:10.1038/nature09767

Liu, M., Chen, B., Pei, L., Zhang, Q., Zou, Y., Xiao, H., et al. (2018). Decreased H3K9ac level of StAR mediated testicular dysplasia induced by prenatal dexamethasone exposure in male offspring rats. *Toxicology* 408, 1–10. doi:10.1016/j.tox.2018.06.005

Liu, X., Zhu, P., Sham, K. W., Yuen, J. M., Xie, C., Zhang, Y., et al. (2009). Identification of a membrane estrogen receptor in zebrafish with homology to mammalian GPER and its high expression in early germ cells of the testis. *Biol. Reprod.* 80 (6), 1253–1261. doi:10.1095/biolreprod.108.070250

Liu, Y., Liu, Y., Chen, G., and Wang, H. (2023). Epigenetic programming of TBX2/CX43 mediates lower sperm quality in male offspring induced by prenatal dexamethasone exposure. *Toxicol. Sci.* 192, 178–193. doi:10.1093/toxsci/kfad016

Liu, Z. J., Liu, Y. H., Huang, S. Y., and Zang, Z. J. (2021). Insights into the regulation on proliferation and differentiation of stem Leydig cells. *Stem Cell Rev. Rep.* 17 (5), 1521–1533. doi:10.1007/s12015-021-10133-x

Lubahn, D. B., Moyer, J. S., Golding, T. S., Couse, J. F., Korach, K. S., and Smithies, O. (1993). Alteration of reproductive function but not prenatal sexual development after insertional disruption of the mouse estrogen receptor gene. *Proc. Natl. Acad. Sci. U. S. A.* 90 (23), 11162–11166. doi:10.1073/pnas.90.23.11162

Lucas, T. F., Royer, C., Siu, E. R., Lazari, M. F., and Porto, C. S. (2010). Expression and signaling of G protein-coupled estrogen receptor 1 (GPER) in rat sertoli cells. *Biol. Reprod.* 83 (2), 307–317. doi:10.1095/biolreprod.110.084160

Lue, Y., Wang, C., Lydon, J. P., Leung, A., Li, J., and Swerdloff, R. S. (2013). Functional role of progestin and the progesterone receptor in the suppression of spermatogenesis in rodents. *Andrology* 1 (2), 308–317. doi:10.1111/j.2047-2927.2012.00047.x

Luetjens, C. M., Didolkar, A., Kliesch, S., Paulus, W., Jeibmann, A., Böcker, W., et al. (2006). Tissue expression of the nuclear progesterone receptor in male non-human primates and men. *J. Endocrinol.* 189 (3), 529–539. doi:10.1677/joe.1.06348

Ma, Y., Ren, S., Pandak, W. M., Li, X., Ning, Y., Lu, C., et al. (2007). The effects of inflammatory cytokines on steroidogenic acute regulatory protein expression in macrophages. *Inflamm. Res.* 56 (12), 495–501. doi:10.1007/s00011-007-6133-3

Mäkinen, S., Mäkelä, S., Weihua, Z., Warner, M., Rosenlund, B., Salmi, S., et al. (2001). Localization of oestrogen receptors alpha and beta in human testis. *Mol. Hum. Reprod.* 7 (6), 497–503. doi:10.1093/molehr/7.6.497

Martinez-Arguelles, D. B., Culty, M., Zirkin, B. R., and Papadopoulos, V. (2009). *In utero* exposure to di-(2-ethylhexyl) phthalate decreases mineralocorticoid receptor expression in the adult testis. *Endocrinology* 150 (12), 5575–5585. doi:10.1210/en.2009-0847

Medubi, L. J., Akinola, O. B., and Oyewopo, A. O. (2021). Low testicular zinc level, p53 expression and impairment of Sertoli cell phagocytosis of residual bodies in rat subjected to psychological stress. *Andrologia* 53 (3), e13958. doi:10.1111/and.13958

Merlet, J., Moreau, E., Habert, R., and Racine, C. (2007). Development of fetal testicular cells in androgen receptor deficient mice. *Cell Cycle* 6 (18), 2258–2262. doi:10.4161/cc.6.18.4654

Miedlich, S. U., Karamooz, N., and Hammes, S. R. (2016). Aromatase deficiency in a male patient - case report and review of the literature. *Bone* 93, 181–186. doi:10.1016/j.bone.2016.09.024

Milewich, L., Kaimal, V., and Toews, G. B. (1983). Androstenedione metabolism in human alveolar macrophages. *J. Clin. Endocrinol. Metab.* 56 (5), 920–924. doi:10.1210/jcem-56-5-920

Miller, W. L. (2017). Steroidogenesis: unanswered questions. *Trends Endocrinol. Metab.* 28 (11), 771–793. doi:10.1016/j.tem.2017.09.002

Miller, W. L., and Auchus, R. J. (2011). The molecular biology, biochemistry, and physiology of human steroidogenesis and its disorders. *Endocr. Rev.* 32 (1), 81–151. doi:10.1210/er.2010-0013

Morishima, A., Grumbach, M. M., Simpson, E. R., Fisher, C., and Qin, K. (1995). Aromatase deficiency in male and female siblings caused by a novel mutation and the physiological role of estrogens. *J. Clin. Endocrinol. Metab.* 80 (12), 3689–3698. doi:10.1210/jcem.80.12.8530621

Nassan, M. A., Soliman, M. M., Aldhahrani, A., El-Saway, H. B., and Swelum, A. A. (2021). Ameliorative impacts of Allium cepa Linnaeus aqueous extract against testicular damage induced by dexamethasone. *Andrologia* 53 (4), e13955. doi:10.1111/and.13955

Nordkap, L., Almstrup, K., Nielsen, J. E., Bang, A. K., Priskorn, L., Krause, M., et al. (2017). Possible involvement of the glucocorticoid receptor (NR3C1) and selected NR3C1 gene variants in regulation of human testicular function. *Andrology* 5 (6), 1105–1114. doi:10.1111/andr.12418

Oakley, R. H., and Cidlowski, J. A. (2013). The biology of the glucocorticoid receptor: new signaling mechanisms in health and disease. *J. Allergy Clin. Immunol.* 132 (5), 1033–1044. doi:10.1016/j.jaci.2013.09.007

Ogawa, K., and Isaji, O. (2023). Testosterone upregulates progesterone production in mouse testicular interstitial macrophages, whose niche likely provides properties of progesterone production to tissue-resident macrophages. *Reprod. Biol.* 23 (2), 100767. doi:10.1016/j.repbio.2023.100767

O'Hara, L., McInnes, K., Simitsidellis, I., Morgan, S., Atanassova, N., Slowikowska-Hilczer, J., et al. (2015). Autocrine androgen action is essential for Leydig cell maturation and function, and protects against late-onset Leydig cell apoptosis in both mice and men. *FASEB J.* 29 (3), 894–910. doi:10.1096/fj.14-255729

O'Shaughnessy, P. J., Verhoeven, G., De Gendt, K., Monteiro, A., and Abel, M. H. (2010). Direct action through the sertoli cells is essential for androgen stimulation of spermatogenesis. *Endocrinology* 151 (5), 2343–2348. doi:10.1210/en.2009-1333

Pelletier, G., Labrie, C., and Labrie, F. (2000). Localization of oestrogen receptor alpha, oestrogen receptor beta and androgen receptors in the rat reproductive organs. *J. Endocrinol.* 165 (2), 359–370. doi:10.1677/joe.0.1650359

Picard, M., and Shirihai, O. S. (2022). Mitochondrial signal transduction. *Cell Metab.* 34 (11), 1620–1653. doi:10.1016/j.cmet.2022.10.008

Pietras, R. J., and Szego, C. M. (1975). Endometrial cell calcium and oestrogen action. *Nature* 253 (5490), 357–359. doi:10.1038/253357a0

Publicover, S., and Barratt, C. (2011). Reproductive biology: progesterone's gateway into sperm. *Nature* 471 (7338), 313–314. doi:10.1038/471313a

Ramezani Tehrani, F., Noroozzadeh, M., Zahediasl, S., Ghasemi, A., Piryaei, A., and Azizi, F. (2013). Prenatal testosterone exposure worsen the reproductive performance of male rat at adulthood. *PLoS One* 8 (8), e71705. doi:10.1371/journal.pone.0071705

Revankar, C. M., Cimino, D. F., Sklar, L. A., Arterburn, J. B., and Prossnitz, E. R. (2005). A transmembrane intracellular estrogen receptor mediates rapid cell signaling. *Science* 307 (5715), 1625–1630. doi:10.1126/science.1106943

Rochira, V., and Carani, C. (2009). Aromatase deficiency in men: a clinical perspective. *Nat. Rev. Endocrinol.* 5 (10), 559–568. doi:10.1038/nrendo.2009.176

Romero, Y., Vuandaba, M., Suarez, P., Grey, C., Calvel, P., Conne, B., et al. (2012). The Glucocorticoid-induced leucine zipper (GILZ) Is essential for spermatogonial survival and spermatogenesis. *Sex. Dev.* 6 (4), 169–177. doi:10.1159/000338415

Rubinow, K. B. (2018). An intracrine view of sex steroids, immunity, and metabolic regulation. *Mol. Metab.* 15, 92–103. doi:10.1016/j.molmet.2018.03.001

Salehzadeh, M., and Soma, K. K. (2021). Glucocorticoid production in the thymus and brain: immunosteroids and neurosteroids. *Brain Behav. Immun. Health* 18, 100352. doi:10.1016/j.bbih.2021.100352

Saunders, P. T., Sharpe, R. M., Williams, K., Macpherson, S., Urquart, H., Irvine, D. S., et al. (2001). Differential expression of oestrogen receptor alpha and beta proteins in the testes and male reproductive system of human and non-human primates. *Mol. Hum. Reprod.* 7 (3), 227–236. doi:10.1093/molehr/7.3.227

Schauwaers, K., De Gendt, K., Saunders, P. T., Atanassova, N., Haelens, A., Callewaert, L., et al. (2007). Loss of androgen receptor binding to selective androgen response elements causes a reproductive phenotype in a knockin mouse model. *Proc. Natl. Acad. Sci. U. S. A.* 104 (12), 4961–4966. doi:10.1073/pnas.0610814104

Schiffer, L., Barnard, L., Baranowski, E. S., Gilligan, L. C., Taylor, A. E., Arlt, W., et al. (2019). Human steroid biosynthesis, metabolism and excretion are differentially reflected by serum and urine steroid metabolomes: a comprehensive review. *J. Steroid Biochem. Mol. Biol.* 194, 105439. doi:10.1016/j.jsbmb.2019.105439

Schmidt, M., Kreutz, M., Löffler, G., Schölmerich, J., and Straub, R. H. (2000). Conversion of dehydroepiandrosterone to downstream steroid hormones in macrophages. *J. Endocrinol.* 164 (2), 161–169. doi:10.1677/joe.0.1640161

Shaaban, Z., Derakhshanfar, A., Reza Jafarzadeh Shirazi, M., Javad Zamiri, M., Moayedi, J., Vahedi, M., et al. (2023). The effects of letrozole-induced maternal hyperandrogenism on sexual behaviors, testicular histology, and serum biochemical traits in male offspring rats: an experimental study. *Int. J. Reprod. Biomed.* 21 (1), 71–82. doi:10.18502/ijrm.v21i1.12669

Shah, C., Modi, D., Sachdeva, G., Gadkar, S., and Puri, C. (2005). Coexistence of intracellular and membrane-bound progesterone receptors in human testis. *J. Clin. Endocrinol. Metab.* 90 (1), 474–483. doi:10.1210/jc.2004-0793

Shaia, K. L., Harris, B. S., Selter, J. H., and Price, T. M. (2023). Reproductive functions of the mitochondrial progesterone receptor (PR-M). *Reprod. Sci.* 30 (5), 1443–1452. doi:10.1007/s43032-022-01092-w

Shang, Y., Myers, M., and Brown, M. (2002). Formation of the androgen receptor transcription complex. *Mol. Cell* 9 (3), 601–610. doi:10.1016/s1097-2765(02)00471-9

Silva, E. J., Vendramini, V., Restelli, A., Bertolla, R. P., Kempinas, W. G., and Avellar, M. C. (2014). Impact of adrenalectomy and dexamethasone treatment on testicular morphology and sperm parameters in rats: insights into the adrenal control of male reproduction. *Andrology* 2 (6), 835–846. doi:10.1111/j.2047-2927.2014.00228.x

Smith, L. B., and Walker, W. H. (2014). The regulation of spermatogenesis by androgens. *Semin. Cell Dev. Biol.* 30, 2–13. doi:10.1016/j.semcdb.2014.02.012

Strünker, T., Goodwin, N., Brenker, C., Kashikar, N. D., Weyand, I., Seifert, R., et al. (2011). The CatSper channel mediates progesterone-induced Ca2+ influx in human sperm. *Nature* 471 (7338), 382–386. doi:10.1038/nature09769

Su, M., Zhong, Y., Xiang, J., Chen, Y., Liu, N., and Zhang, J. (2023). Reproductive endocrine disruption and gonadal intersex induction in male Japanese medaka chronically exposed to betamethasone at environmentally relevant levels. *J. Hazard. Mat.* 455, 131493. doi:10.1016/j.jhazmat.2023.131493

Suarez, P. E., Rodriguez, E. G., Soundararajan, R., Mérillat, A. M., Stehle, J. C., Rotman, S., et al. (2012). The glucocorticoid-induced leucine zipper (gilz/Tsc22d3-2) gene locus plays a crucial role in male fertility. *Mol. Endocrinol.* 26 (6), 1000–1013. doi:10.1210/me.2011-1249

Szego, C. M., and Davis, J. S. (1967). Adenosine 3',5'-monophosphate in rat uterus: acute elevation by estrogen. *Proc. Natl. Acad. Sci. U. S. A.* 58 (4), 1711–1718. doi:10.1073/pnas.58.4.1711

Takada, M., Fukuhara, D., Takiura, T., Nishibori, Y., Kotani, M., Kiuchi, Z., et al. (2023). Involvement of GLCCI1 in mouse spermatogenesis. *FASEB J.* 37 (1), e22680. doi:10.1096/fj.202101667RR

Tan, K. A., De Gendt, K., Atanassova, N., Walker, M., Sharpe, R. M., Saunders, P. T., et al. (2005). The role of androgens in sertoli cell proliferation and functional maturation: studies in mice with total or Sertoli cell-selective ablation of the androgen receptor. *Endocrinology* 146 (6), 2674–2683. doi:10.1210/en.2004-1630

Taylor, J. M., Borthwick, F., Bartholomew, C., and Graham, A. (2010). Overexpression of steroidogenic acute regulatory protein increases macrophage cholesterol efflux to apolipoprotein AI. *Cardiovasc. Res.* 86 (3), 526–534. doi:10.1093/cvr/cvq015

Tsai, M. Y., Yeh, S. D., Wang, R. S., Yeh, S., Zhang, C., Lin, H. Y., et al. (2006). Differential effects of spermatogenesis and fertility in mice lacking androgen receptor in individual testis cells. *Proc. Natl. Acad. Sci. U. S. A.* 103 (50), 18975–18980. doi:10.1073/pnas.0608565103

Valdez, R., Cavinder, C. A., Varner, D. D., Welsh, T. H., Jr., Vogelsang, M. M., and Ing, N. H. (2019). Dexamethasone downregulates expression of several genes encoding orphan nuclear receptors that are important to steroidogenesis in stallion testes. *J. Biochem. Mol. Toxicol.* 33 (6), e22309. doi:10.1002/jbt.22309

Valeri, C., Lovaisa, M. M., Racine, C., Edelsztein, N. Y., Riggio, M., Giulianelli, S., et al. (2020). Molecular mechanisms underlying AMH elevation in hyperoestrogenic states in males. *Sci. Rep.* 10 (1), 15062. doi:10.1038/s41598-020-71675-7

van den Driesche, S., Walker, M., McKinnell, C., Scott, H. M., Eddie, S. L., Mitchell, R. T., et al. (2012). Proposed role for COUP-TFII in regulating fetal Leydig cell steroidogenesis, perturbation of which leads to masculinization disorders in rodents. *PLoS One* 7 (5), e37064. doi:10.1371/journal.pone.0037064

Walker, W. H., and Cooke, P. S. (2023). Functions of steroid hormones in the male reproductive tract as revealed by mouse models. *Int. J. Mol. Sci.* 24 (3), 2748. doi:10.3390/ijms24032748

Wang, M., Fijak, M., Hossain, H., Markmann, M., Nüsing, R. M., Lochnit, G., et al. (2017). Characterization of the micro-environment of the testis that shapes the phenotype and function of testicular macrophages. *J. Immunol.* 198 (11), 4327–4340. doi:10.4049/jimmunol.1700162

Weikum, E. R., Knuesel, M. T., Ortlund, E. A., and Yamamoto, K. R. (2017). Glucocorticoid receptor control of transcription: precision and plasticity via allostery. *Nat. Rev. Mol. Cell Biol.* 18 (3), 159–174. doi:10.1038/nrm.2016.152

Welsh, M., Moffat, L., Belling, K., de França, L. R., Segatelli, T. M., Saunders, P. T., et al. (2012). Androgen receptor signalling in peritubular myoid cells is essential for normal differentiation and function of adult Leydig cells. *Int. J. Androl.* 35 (1), 25–40. doi:10.1111/j.1365-2605.2011.01150.x

Welter, H., Herrmann, C., Dellweg, N., Missel, A., Thanisch, C., Urbanski, H. F., et al. (2020). The glucocorticoid receptor NR3C1 in testicular peritubular cells is developmentally regulated and linked to the smooth muscle-like cellular phenotype. *J. Clin. Med.* 9 (4), 961. doi:10.3390/jcm9040961

Whirledge, S., and Cidlowski, J. A. (2017). Glucocorticoids and reproduction: traffic control on the road to reproduction. *Trends Endocrinol. Metab.* 28 (6), 399–415. doi:10.1016/j.tem.2017.02.005

Willems, A., Batlouni, S. R., Esnal, A., Swinnen, J. V., Saunders, P. T., Sharpe, R. M., et al. (2010). Selective ablation of the androgen receptor in mouse sertoli cells affects sertoli cell maturation, barrier formation and cytoskeletal development. *PLoS One* 5 (11), e14168. doi:10.1371/journal.pone.0014168

Willems, A., De Gendt, K., Deboel, L., Swinnen, J. V., and Verhoeven, G. (2011). The development of an inducible androgen receptor knockout model in mouse to study the postmeiotic effects of androgens on germ cell development. *Spermatogenesis* 1 (4), 341–353. doi:10.4161/spmg.1.4.18740

Xu, Q., Lin, H. Y., Yeh, S. D., Yu, I. C., Wang, R. S., Chen, Y. T., et al. (2007). Infertility with defective spermatogenesis and steroidogenesis in male mice lacking androgen receptor in Leydig cells. *Endocrine* 32 (1), 96–106. doi:10.1007/s12020-007-9015-0

Yamauchi, S., Yamamoto, K., and Ogawa, K. (2022). Testicular macrophages produce progesterone *de novo* promoted by cAMP and inhibited by M1 polarization inducers. *Biomedicines* 10 (2), 487. doi:10.3390/biomedicines10020487

Yeh, S., Tsai, M. Y., Xu, Q., Mu, X. M., Lardy, H., Huang, K. E., et al. (2002). Generation and characterization of androgen receptor knockout (ARKO) mice: an *in vivo* model for the study of androgen functions in selective tissues. *Proc. Natl. Acad. Sci. U. S. A.* 99 (21), 13498–13503. doi:10.1073/pnas.212474399

Yun, H. J., Lee, J. Y., and Kim, M. H. (2016). Prenatal exposure to dexamethasone disturbs sex-determining gene expression and fetal testosterone production in male embryos. *Biochem. Biophys. Res. Commun.* 471 (1), 149–155. doi:10.1016/j.bbrc.2016.01.161

Zhang, J., Hu, G., Huang, B., Zhuo, D., Xu, Y., Li, H., et al. (2019). Dexamethasone suppresses the differentiation of stem Leydig cells in rats *in vitro*. *BMC Pharmacol. Toxicol.* 20 (1), 32. doi:10.1186/s40360-019-0312-z

Zhang, J., Huang, B., Hu, G., Zhan, X., Xie, T., Li, S., et al. (2018). Aldosterone blocks rat stem Leydig cell development *in vitro*. *Front. Endocrinol. (Lausanne)* 9, 4. doi:10.3389/fendo.2018.00004

Zirkin, B. R., and Papadopoulos, V. (2018). Leydig cells: formation, function, and regulation. *Biol. Reprod.* 99 (1), 101–111. doi:10.1093/biolre/ioy059

frontiers | Frontiers in Cell and Developmental Biology

TYPE Original Research
PUBLISHED 12 January 2024
DOI 10.3389/fcell.2023.1327410

OPEN ACCESS

EDITED BY
Talia L Hatkevich,
Duke University, United States

REVIEWED BY
Daniel Martin Messerschmidt,
Institute of Molecular and Cell Biology (A*STAR), Singapore
Barbara Nicol,
National Institute of Environmental Health Sciences (NIH), United States

*CORRESPONDENCE
Nitzan Gonen,
nitzan.gonen@biu.ac.il
Francis Poulat,
francis.poulat@igh.cnrs.fr

RECEIVED 24 October 2023
ACCEPTED 20 December 2023
PUBLISHED 12 January 2024

CITATION
Stévant I, Gonen N and Poulat F (2024), Transposable elements acquire time- and sex-specific transcriptional and epigenetic signatures along mouse fetal gonad development.
Front. Cell Dev. Biol. 11:1327410.
doi: 10.3389/fcell.2023.1327410

Transposable elements acquire time- and sex-specific transcriptional and epigenetic signatures along mouse fetal gonad development

Isabelle Stévant[1,2], Nitzan Gonen[1]* and Francis Poulat[2]*

[1]The Mina and Everard Goodman Faculty of Life Sciences and the Institute of Nanotechnology and Advanced Materials, Bar-Ilan University, Ramat Gan, Israel, [2]Institute of Human Genetics, CNRS UMR9002 University of Montpellier, Montpellier, France

Gonadal sex determination in mice is a complex and dynamic process, which is crucial for the development of functional reproductive organs. The expression of genes involved in this process is regulated by a variety of genetic and epigenetic mechanisms. Recently, there has been increasing evidence that transposable elements (TEs), which are a class of mobile genetic elements, play a significant role in regulating gene expression during embryogenesis and organ development. In this study, we aimed to investigate the involvement of TEs in the regulation of gene expression during mouse embryonic gonadal development. Through bioinformatics analysis, we aimed to identify and characterize specific TEs that operate as regulatory elements for sex-specific genes, as well as their potential mechanisms of regulation. We identified TE loci expressed in a time- and sex-specific manner along fetal gonad development that correlate positively and negatively with nearby gene expression, suggesting that their expression is integrated to the gonadal regulatory network. Moreover, chromatin accessibility and histone post-transcriptional modification analyses in differentiating supporting cells revealed that TEs are acquiring a sex-specific signature for promoter-, enhancer-, and silencer-like elements, with some of them being proximal to critical sex-determining genes. Altogether, our study introduces TEs as the new potential players in the gene regulatory network that controls gonadal development in mammals.

KEYWORDS

transposable elements, sex determination, gonads, testis, ovary, gene expression regulation

Introduction

Sex determination is the developmental process by which individuals acquire the necessary organs for sexual reproduction. In vertebrates, it starts with the differentiation of the bipotential gonadal primordium into the ovaries or testes. In mice, the bipotential gonad forms around embryonic day (E) 10.0 on the ventral surface of the intermediate mesoderm and comprises multipotent somatic cells and primordial germ cells (Mayere et al., 2022; Neirijnck et al., 2023). At this stage, the XX and XY somatic cells display no autosomal sexual dimorphism at the transcriptional (Stevant et al., 2019) and chromatin levels (Garcia-Moreno et al., 2019). The supporting cell lineage is the first to operate sex fate decision at

E11.5 by differentiating as either Sertoli cells or pre-granulosa cells depending on the presence or absence of the Y chromosome (Albrecht and Eicher, 2001; Chassot et al., 2008). Once specified, Sertoli and pre-granulosa cells instruct other somatic progenitors and the primordial germ cell to commit and differentiate toward the testicular or ovarian cell fates. In XX gonads, the canonical Wnt pathway (WNT4/RSPO1/β-catenin) and the transcription factors (TFs), FOXL2 and RUNX1, induce the differentiation of pre-granulosa cells (Greenfield, 2021). In XY gonads, sex determination is governed by the *Sry* gene located on the Y chromosome (Sinclair et al., 1990; Koopman et al., 1991) that activates the expression of the transcription factor SOX9 at E11.5 (Gonen et al., 2018), which in turn controls the differentiation of Sertoli cells (Vining et al., 2021). In both sexes, the action of master transcription factors induces the activity of sex-specific regulatory networks, controlling the expression and repression of downstream pro-testicular or pro-ovarian genes. Many levels of regulation are expected to play a role in controlling this delicate gene regulatory network. Indeed, it has been shown that prior to sex determination, sex-specific genes carry a bivalent histone mark signature with both active (H3K4me3) and repressive (H3K27me3) markers. As sex differentiation progresses, these genes lose one of these markers and acquire sex-specific expression (Garcia-Moreno et al., 2019). Furthermore, many sex-specific intergenic loci acquire the deposition of H3K27Ac, which characterizes active enhancers (Garcia-Moreno et al., 2019). With two alternative outcomes, the study of sex determination provides an attractive model for studying the epigenetic events involved in cell fate decisions.

We have previously shown that the versatile nuclear-scaffold protein TRIM28 directly interacts and co-localizes with SOX9 on the chromatin of fetal Sertoli cells (Rahmoun et al., 2017). We also discovered that TRIM28 protects adult ovaries from granulosa to Sertoli cell reprogramming through its SUMO E3 ligase activity (Rossitto et al., 2022). Interestingly, in addition to its role on gene regulation as a transcriptional activator or repressor, TRIM28 is a master regulator of transposable element (TE) silencing in somatic cells (Rowe et al., 2010). In mammalian genomes, nearly half of the DNA consists of TEs. TEs are divided into two classes depending on the mechanism by which they transpose. Class I TEs are retrotransposons that propagate via a "copy–paste" mechanism by using an intermediate RNA molecule that is reverse-transcribed as DNA before reinsertion into the host genome. Class II TEs are DNA transposons propagating via a "cut and paste" mechanism. They encode a transposase that excises their flanking inverted terminal repeats and inserts them somewhere else in the host genome. The repression of somatic or germinal TE expression is crucial to block the genetic instability that their uncontrolled expression would induce (Hedges and Deininger, 2007). Therefore, most TE loci are silenced by H3K9me3 or CpG methylation in somatic cells and by the piRNA machinery in male germinal lineages (Zhou et al., 2022). In somatic cells, TRIM28 negatively regulates retrotransposons upon its interaction with KRAB-containing zinc-finger proteins. Consequently, TRIM28 recruits the histone methylase SETDB1 that deposits the heterochromatin mark H3K9me3, contributing to epigenetic retrotransposon silencing (Randolph et al., 2022).

Apart from the potential genomic stability threat, some TEs have become an intrinsic part of the genome during vertebrate evolution and are drivers of genetic innovations, notably in sex determination and reproduction (Dechaud et al., 2019). For instance, TE insertion in sablefish and medaka generated allelic diversification, leading to the creation of a new master sex-determining gene (Schartl et al., 2018; Herpin et al., 2021). More recently, a second exon of the *Sry* gene was identified in mice. This cryptic exon originates from the insertion of four retrotransposons. While the short SRY isoform contains a C-terminal degron, which renders the protein unstable, the long isoform containing the cryptic exon is degron-free and, thus, more stable (Miyawaki et al., 2020). Furthermore, co-option and domestication have repurposed TEs for the benefit of their host and contributed to novel regulatory mechanisms. We distinguish three different mechanisms by which TEs influence gene expression. First, TEs are involved in chromatin organization. TEs containing CCCTC-binding factor (CTCF) motifs were found to be directly involved in the formation of topologically associating domains (TADs) and long-range enhancer–promoter interactions (Lawson et al., 2023). Second, TE sequences are rich in motifs for lineage-specific transcription factors and can be co-opted as *cis*-regulatory elements. For example, endogenous retroviruses (ERVs) were shown to be highly enriched in species-specific placenta development enhancers (Chuong et al., 2013). Finally, TE-derived transcripts were shown to influence gene expression by mechanisms that are still poorly understood. In mice, the transition from the two-cell stage and development progression to the blastocyst stage appeared to depend on LINE-1 expression (Jachowicz et al., 2017; Percharde et al., 2018). TE expression was also shown to be involved in adult neurogenesis, neuronal pathologies, and cancer (Richardson et al., 2014; Jonsson et al., 2020; Jansz and Faulkner, 2021).

In this work, we aimed to characterize TE expression and chromatin landscape as fetal gonads specify as testis or ovary in order to establish the groundwork for further functional studies of TEs in mouse gonadal development. We first identified that common TEs were dysregulated in adult ovaries of *Trim28* KO mice (Rossitto, et al., 2022) and ovarian *Dmrt1* overexpression mice (Lindeman et al., 2015), two models presenting granulosa to Sertoli transdifferentiation, suggesting a sex-specific signature of TE expression in mice. Hence, we reanalyzed transcriptomic and epigenomic data from embryonic gonads and found that the major expression of TE loci is indeed detectable in both sexes with temporal- and sex-dependent variations. We observed that a significant proportion of open chromatin regions contain TE sequences associated to active or repressive histone marks and having enrichment for DNA motifs recognized by transcription factors involved in sex determination. Therefore, our findings suggest that TEs may play a role at several levels during mammalian sex determination.

Results

Quantification of TE expression in mouse developing gonads

We first reanalyzed bulk RNA-seq data from control and mutant adult whole ovaries (7 months old), displaying granulosa to Sertoli cell transdifferentiation upon conditional *Trim28* deletion in the granulosa cells (Rossitto, et al., 2022), and measured the change in TE expression. Due to their highly repetitive nature and low RNA abundance, the evaluation of TE expression requires the use of

10.3389/fcell.2023.1327410

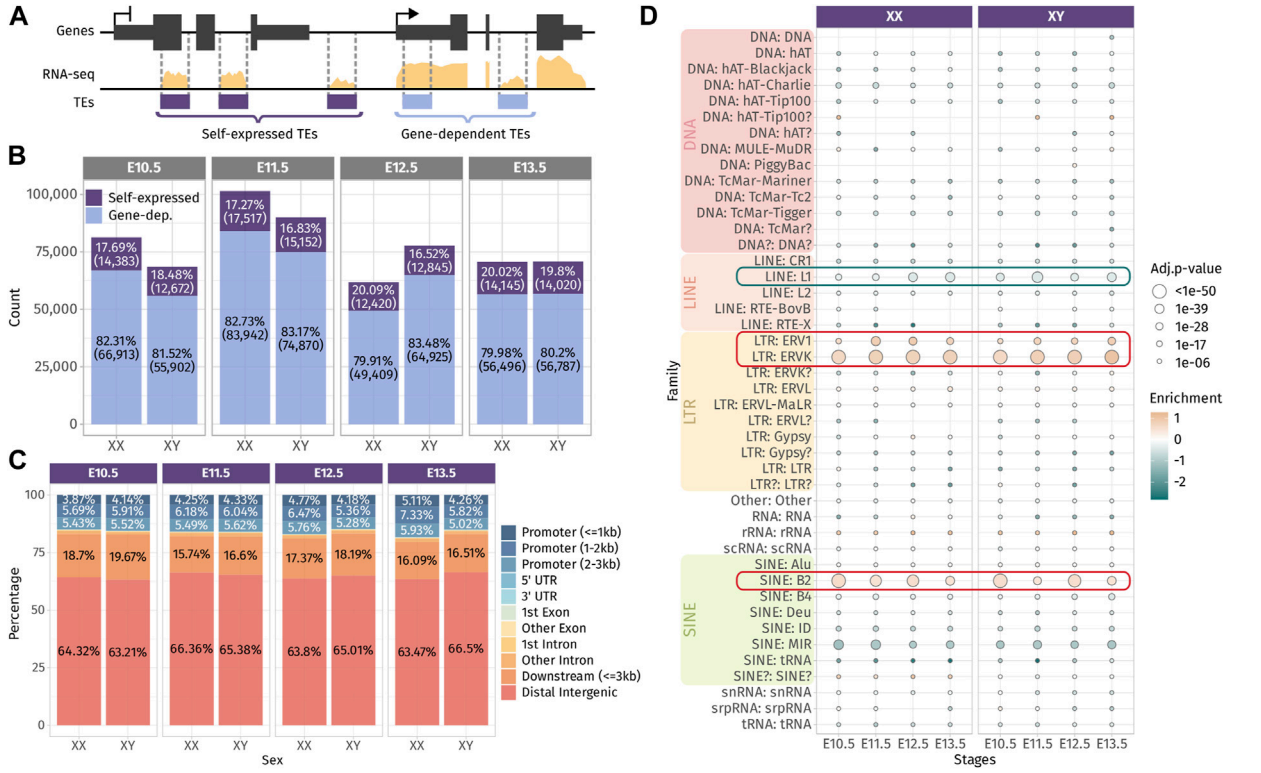

FIGURE 1
Expressed TEs in the developing gonads. **(A)** Classification of TEs as "self-expressed" when they are found in intergenic regions or within a gene that is not expressed or as "gene-dependent" when they are found within a transcribed gene. **(B)** Number of self-expressed and gene-dependent TEs per sex and stage. **(C)** Repartition of the self-expressed TEs in the genome for each sex and stage. **(D)** Enrichment test of the self-expressed TE families compared to their distribution in the mouse genome. Positively enriched TE families are colored in orange, while the under-represented families are colored in green. Enrichment score is represented as the log2 (odds ratio) from Fisher's exact test. The size of the dots reflects the statistical power of their enrichment. Only enrichment with an adj.*p*-value<0.05 are shown.

dedicated tools. TE-specific mapping software re-attributes the sequencing reads, habitually discarded from regular RNA-seq, to the TE family or TE loci, allowing the quantification of their expression levels (Lanciano and Cristofari, 2020). For that aim, we used the SQuIRE suite of tools which is based on an expectation–maximization (EM) algorithm to map RNA-seq data and quantify individual TE copy expression (Yang et al., 2019). We found that 8,110 TEs were upregulated upon cell reprograming, while 2,102 were downregulated (Supplementary Figure S1A). We predicted that TE dysregulation is mainly driven by the absence of the TE master regulator TRIM28, but we hypothesized that TEs could also be dysregulated by the change of cell identity. To verify this hypothesis, we also reanalyzed RNA-seq data stemming from the reprograming of adult granulosa to Sertoli cells upon *Dmrt1* forced expression (Lindeman, et al., 2015). While DMRT1 has no identified role in TE expression regulation, we found that 4,099 TEs were differentially expressed upon cell reprogramming (Supplementary Figure S1B). We compared the differentially expressed TEs in the *Trim28* knockout and the *Dmrt1*-induced cell reprograming and found 935 TEs that are commonly dysregulated (Supplementary Figure S1C), supporting the idea of a sex-specific signature of TE expression in the mouse gonads.

Next, we sought to evaluate the involvement of TE-derived RNAs in the dynamics of gonadal transcriptomes during sex determination. For that aim, we measured TE RNAs at a locus-specific level in mice using the bulk RNA-seq dataset of whole mouse gonads from E10.5, E11.5, E12.5, and E13.5 of both sexes (Zhao et al., 2018). We were able to detect between 61,000 and 101,000 expressed TE loci across all the embryonic stages and sexes (Supplementary Figure S2A). TEs are interspersed throughout the mouse genome and can be located with genes and as such incorporated within gene transcripts. To discriminate TE transcripts induced by their own promoters from passive TE co-transcription with genes, we classified TEs with respect to their environment, as done by others (Chang et al., 2022). We considered expressed TEs found in intergenic regions or inside genes that are not transcribed as "self-expressed" since their expression is likely to be driven by their own promoters, while TEs located within expressed genes are qualified as "gene-dependent" since their transcripts are likely to be part of their host gene RNAs (Figure 1A). Although TEs are relatively rare in gene bodies (Kapusta et al., 2013), we found that up to 83% of the detected TEs were located with expressed genes. On the other hand, self-expressed TEs constitute approximately 17% of the detected TEs, which represents between 12,672 and 17,517 TE loci that are transcribed independently from genes across stages and sexes (Figure 1B). In the present study, we focused our interest on self-expressed TEs as part of autonomously transcribed RNAs

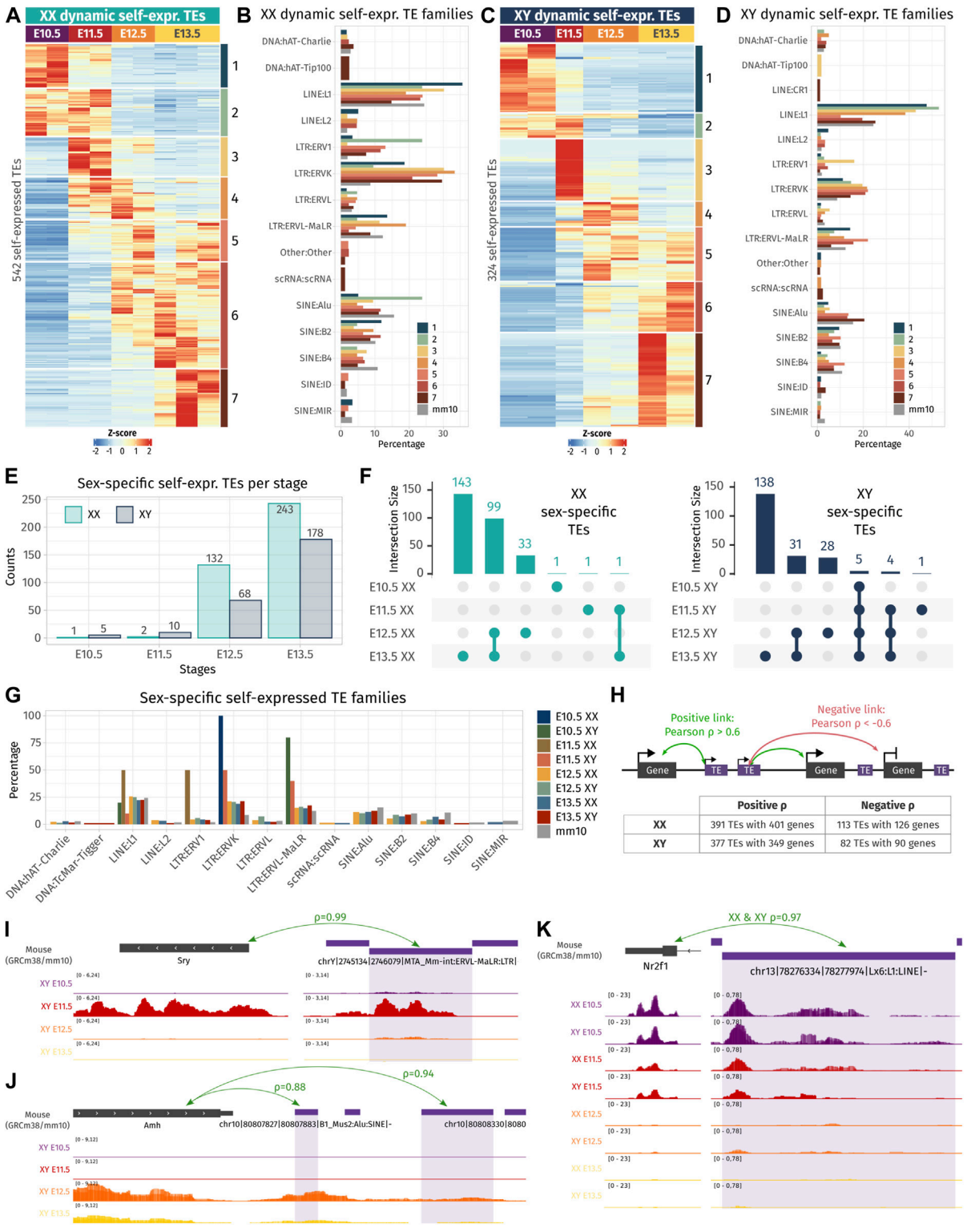

FIGURE 2
Dynamic- and sex-specific TEs along gonadal development. **(A, C)** Heatmap showing the self-expressed TEs that are differentially expressed among different embryonic stages in XX **(A)** and XY **(C)** gonads. The expression is normalized by a z-score. **(B, D)** Percentage of TE families for each cluster of an expression pattern. As reference, the global percentage of TE families in the mouse genome is shown in gray. **(E)** Number of overexpressed self-expressed TEs between sexes for each stage. **(F)** Upset plots representing the overlap of the sex-specific TEs across embryonic stages. The bars on the top represent the number of TEs found in each intersection. The dots linked by lines represent the intersections. **(G)** Percentage of TE families of the sex-specific TEs found at each embryonic stage. **(H)** Schematic representation describing the strategy to find the correlation between TEs and their nearby genes. A TE is correlated to a gene in its 100 kb flanking region if the correlation coefficient is above 0.6 (positive correlation) or below −0.6 (negative correlation). The table shows the number of correlating TE and genes found by the analysis. **(I–K)** Genomic tracks of the RNA-seq signal of three TE-gene positive correlation examples.

susceptible to participate in the gonadal sex differentiation genetic program. As TE expression has been observed in male germ cells (Liu et al., 2014), we verified if self-expressed TEs detected can be expressed by gonadal somatic cells. To this aim, we reanalyzed the only available bulk RNA-seq data from purified somatic cells that was performed at E11.5 in XX and XY gonads (Miyawaki, et al., 2020). We detected 8,696 and 7,479 common self-expressed TEs between whole gonad and somatic cell in XX and XY, respectively, representing nearly half of the self-expressed TEs we detected in whole gonads at E11.5 for both sexes (Supplementary Figure S2C). These results show that self-expressed TEs we detected in the whole gonads are transcribed by both/either the germ cells and/or the somatic cells of the gonads.

We question whether self-expressed TEs were located in a close proximity of genes, in particular to promoter regions and 3′ end regions, as TEs have been described to produce alternative promoters, transcription start sites (TSSs) and transcription termination sites (TTSs) of genes (Conley and Jordan, 2012; Miao et al., 2020). We found that approximately 15% of self-expressed TEs were located in gene promoter regions up to 3 kb from the gene TSS, and 20% of them were found in the 3-kb downstream of the 3′ end of the genes. The vast majority of self-expressed TEs (65%) were distal intergenic, located more than 3 kb away from genes (Figure 1C). Then, we performed an enrichment analysis to detect the over- or under-represented family of self-expressed TEs compared to the distribution of TE families along the mouse genome (Figure 1D). The enrichment test revealed that DNA families were under-represented among self-expressed TEs, which is expected as they are mostly inactive and only exist as the relics of anciently active elements (Platt et al., 2018). We also noticed that the LINE family, in particular the LINE-1 subfamily, was under-represented. LINE-1 represents 24.4% of the mouse TEs, and ~1,000 copies are potentially capable of active retrotransposition (Goodier et al., 2001). While LINE-1 is highly expressed in the mouse preimplantation embryos (Jachowicz, et al., 2017), fewer copies than expected (8% less) were found transcriptionally active in the developing gonads (Figure 1D and Supplementary Figure S2C). Conversely, we observed a positive enrichment for ERV1 and ERVK LTRs, as well as the B2 SINE non-autonomous retrotransposons.

Overall, we found that TEs are broadly expressed along gonadal development and a large proportion of the detected TEs are a constituent part of genes. The detected self-expressed TE loci from the whole gonads are potentially transcribed in both the somatic and germ cell compartment of the gonads. Self-expressed TEs are mostly found in distal intergenic regions and are enriched in ERVs and SINE B2 retrotransposon families.

Mouse gonads exhibit the gradual sex-specific expression of TEs

After having depicted the TE expression landscape in developing gonads, we undertook to identify if the self-expressed TE loci change in expression during gonadal differentiation and if they exhibit sexual dimorphism. First, we performed differential expression analysis across embryonic stages in both sexes separately, and second, between XX and XY gonads for each stage. Regarding TE expression throughout gonadal development, we identified 542 and 324 TEs presenting a dynamic expression along gonadal specification as ovary or testis, respectively, with 124 of them being shared between the two sexes (Figures 2A–D; Supplementary Data S1). Dynamically expressed TEs were classified in seven groups (numbered 1–7) according to their expression profile. We observed that TEs are expressed in successive waves along gonadal development, with some TEs overexpressed at only one stage (groups 1, 3, and 7 in XX and XY), while other TEs overexpressed during several stages (groups 2, 4 to 6 in XX and groups 2 and 5 XY gonads). In XX gonads, we discovered that LTR:ERV1 and ERVK were more represented than expected among different groups of dynamically expressed TEs (Figure 2B), while in XY gonads, only the LTR: ERVK family was more represented than expected in all dynamically expressed TE groups (Figure 2D). We also discovered that TEs specifically overexpressed at early stages (E10.5 and E11.5) are mainly from the LINE: L1 family in both sexes.

Concerning sexual dimorphism, E10.5 and E11.5 gonads showed few sexual dimorphisms in terms of TE expression (Figure 2E). At E10.5, only one self-expressed TE located in chromosome 6 was found overexpressed in XX compared to XY gonads, and five were found overexpressed in XY compared to XX gonads. These five TEs are located on the Y chromosome and are expressed in all the stages (Figure 2F and Supplementary Data S2). At E11.5, two self-expressed TEs were overexpressed in XX gonads, and ten were found overexpressed in XY, including six TEs located on the Y chromosome stages (Figure 2F and Supplementary Data S2). These results show that autosomal TEs are not expressed in a sexually dimorphic manner in gonadal cells prior to sex determination. From E12.5, we observed an increase of sexually dimorphic self-expressed TE loci, with 200 and 421 loci differentially expressed between XX and XY gonads at E12.5 and E13.5, respectively. This progression of TE expression perfectly copies what was previously observed, concerning the dynamics of the expression of the protein-coding genes (Nef et al., 2005; Jameson et al., 2012; Zhao, et al., 2018; Stevant, et al., 2019). Finally, we looked at whether a particular TE family could be expressed in a sexually dimorphic manner, and no drastic difference was observed compared to the normal proportion of TE families in the mouse genome (Figure 2G).

As TE expression can influence the expression level of their nearby genes, we sought to investigate if the expression level of the identified differentially expressed TEs both in time and sex correlates with proximal gene expression. Positive TE-gene correlation can happen for several reasons. The TE transcript can influence the expression of the gene as a non-coding RNA or enhancer RNA (Liang et al., 2023), TE can act as a promoter or an alternative 3′ UTR for the gene, the gene can be silenced as a collateral effect of the TE silencing, or the TE expression is activated by the same *cis* or *trans* regulatory elements as the gene. On the contrary, negative TE–gene correlation can suggest a negative control of the nearby gene by the TE transcript. As most self-expressed TEs were found in a window of 100 kb of a gene TSS (Supplementary Figure S2D), we looked at the genes present in a 100-kb window around each differentially expressed TE in time and sex, and we calculated Pearson's correlation between the gene and TE expression among embryonic stages and sexes (Figure 2H). In XX gonads, 391 TE loci were positively correlated with 401 genes,

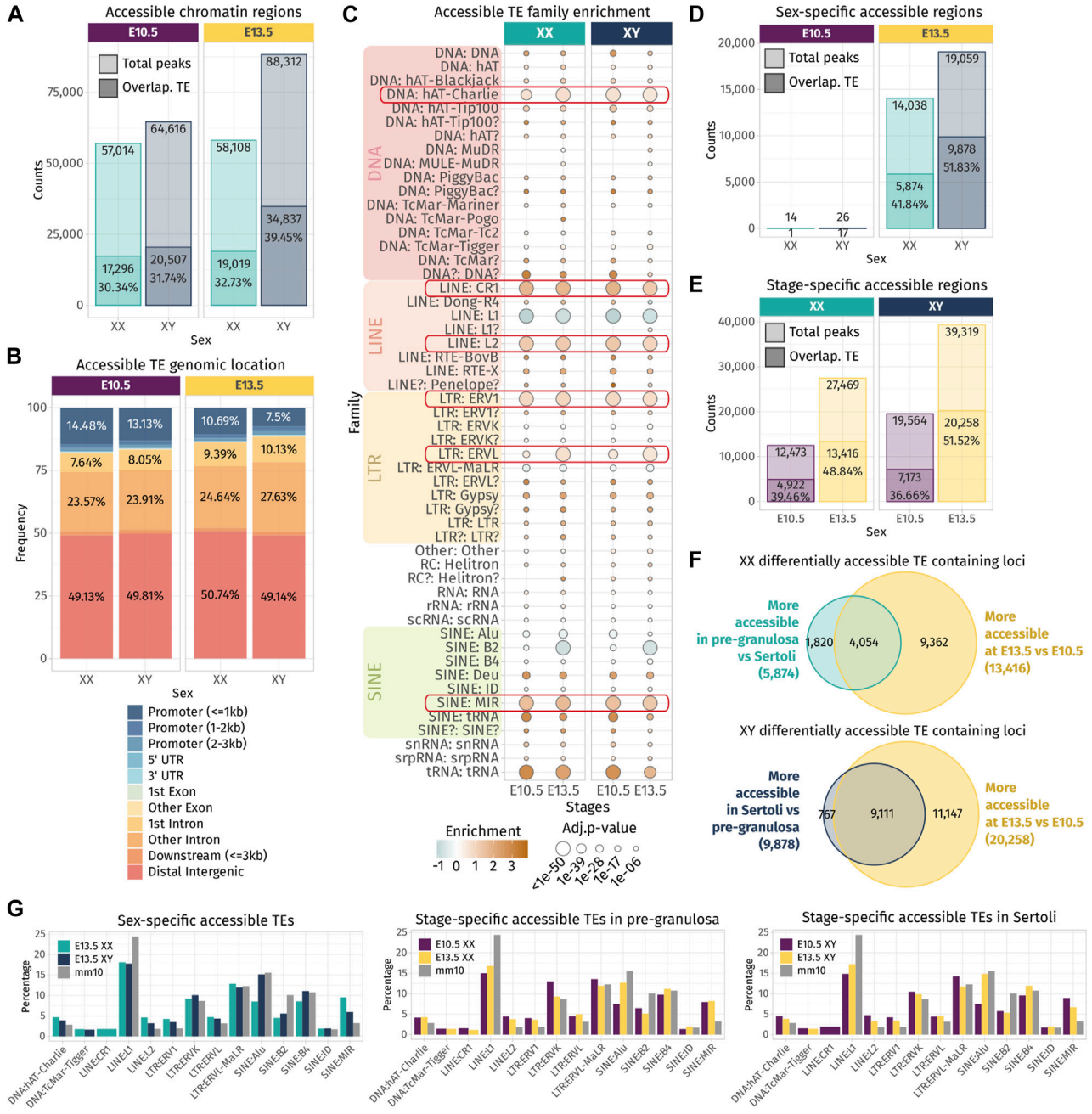

FIGURE 3
Chromatin accessibility landscape of TE loci during gonadal development. **(A)** Number of ATAC-seq peaks detected in total and overlapping TE loci at E10.5 and E13.5 in XX and XY gonadal progenitor and supporting cells. **(B)** Genomic location of the accessible chromatin regions that overlap with a TE sequence. **(C)** Family enrichment analysis of the TE overlapping ATAC-seq peaks. Positively enriched TE families are colored in orange, while the under-represented families are colored in green. Enrichment score is represented as the log2 (odds ratio) from Fisher's exact test. The size of the dots reflects the statistical power of their enrichment. Only enrichment with an adj.*p*-value<0.05 is shown. **(D, E)** Statistically differentially accessible regions in sex and time. The number and the percentage of accessible regions and TE-containing loci showing an increase in accessibility between sex and time are indicated. **(F)** Overlapping of the accessible TE loci that increase in accessibility between sex at E13.5 in either Sertoli and pre-granulosa cells (turquoise and dark blue) with the accessible TE loci that gain accessibility at E13.5 compared to E10.5 (yellow). **(G)** Percentage of TE families in the differentially accessible chromatin regions that overlap with TE sequences (only percentages >1 are shown).

and 113 TEs were negatively correlated with 126 genes. In XY gonads, 377 TEs were positively correlated with 349 genes, while 82 TEs negatively correlated with 90 genes (Supplementary Data S3). Interestingly, among them, we found an LTR ERVL-MaLR retrotransposon located 81 kb upstream of *Sry* expressed with an extremely strong correlation with *Sry* gene expression (ρ = 0.99, Figure 2I). This ERVL-MaLR is separated from *Sry* by one unexpressed gene (*H2al2b*), demonstrating that its expression was produced by a distinct transcript, conversely to the recently identified *Sry* cryptic exon (Miyawaki, et al., 2020). Interestingly, the

expression of this TE was also retrieved in RNA-seq data from XY somatic cells purified at E11.5 (Miyawaki, et al., 2020), which strongly suggests that it is expressed in the same cell lineage as *Sry*. We also found a SINE B4 retrotransposon located 2.9 kb downstream of the *Amh* gene with a correlation coefficient of 0.94 (Figure 2J). This specific transposon was not expressed in XX gonads where *Amh* is silenced. Its proximity with the *Amh* 3′ UTR and the presence of other expressed TEs in the vicinity can suggest that the transcript SINE B4 may be part of an alternative 3′ UTR. Finally, we found five LINE-1 TEs positively correlating with the *Nr2f1* gene (Figure 2K and Supplementary Data S3), also known as *Coup-TFI*, which is expressed in the gonadal somatic cells prior to sex determination in both sexes (Stevant, et al., 2019). *Nr2f1* is a pleiotropic gene capable of activating and repressing target gene expression by interacting with chromatin remodelers. It has been described as a driver of cell fate decision in mouse and human brain development (Bertacchi et al., 2019). The expression of *Nr2f1* has been shown to be regulated by the non-long coding RNA *lnc-Nr2f1* (also referred to as A830082K12Rik), which is located directly upstream of Nr2f1 on the opposite strand and is conserved between mice (Bergeron et al., 2016) and humans (Ang et al., 2019). The five expressed TEs correlating with *Nr2f1* expressed are located in the intronic region of the longest version of *lnc-Nr2f1* (Ensembl mm10 annotation). As *Nr2f1* is expressed only in early gonads prior to gonadal cell differentiation, we speculate that it plays a role in the establishment of the bipotential progenitor cell identity.

To summarize, we found that self-expressed TEs are dynamically expressed and acquire sexual dimorphism during gonadal differentiation. Dynamic and sexually dimorphic TE expression correlates with nearby genes, some of which have a pivotal role in gonadal development. Although we cannot determine with the present data whether TE expression precedes their nearby gene transcription, this suggests that TEs are a whole part of the genetic program driving gonadal specification.

TE loci represent one-third of open chromatin regions in embryonic supporting cells

Independent of their transcription, TE sequences can influence gene expression by acting as *cis*-regulatory elements including promoters or enhancers by providing a large repository of potential transcription factor-binding sites. A comparative study in mouse developing tissues showed that 21% of the open chromatin regions were associated with TEs and half of them were tissue-specific, suggesting an active role in mouse organogenesis (Miao, et al., 2020). We questioned whether the chromatin around TE loci is also specifically opened, while the bipotential gonads differentiate as ovary or testis. We took advantage of the pioneer epigenetic investigations on mouse embryonic gonads performed by Garcia-Moreno et al. (2019) and Garcia-Moreno et al. (2019), and the ATAC-seq data of purified gonadal somatic cells at E10.5 and supporting cells at E13.5 in both sexes were reanalyzed to identify nucleosome-depleted TEs. In total, we identified between 57,014 and 88,312 accessible chromatin regions. Despite inherent mappability issues due to the TE repetitive sequence nature (i.e., multi-mapped reads are filtered out from the ATAC-seq data), we found that 30%–39% of the ATAC-seq peaks were overlapping TE loci across sexes and stages (Figure 3A). In most cases, more than half of the length of TE sequences was covered by an ATAC-peak, showing that most TE sequences are accessible for potential regulatory factor binding (Supplementary Figure S3). Nearly half of the accessible TE-containing loci are found in the distal intergenic compartment, in which approximately 35% of the loci are located within introns and 10% are found in promoter regions (Figure 3B).

The enrichment test shows that many TE families were over-represented in the open chromatin regions compared to their global proportion in the genome (Figure 3C), including the DNA hAT-Charlie, the LINE CR1 and L2, the LTR ERV1, ERVL, and the SINE MIR. These six TE families were also found enriched in TE-derived enhancer-like sequences identified in different human tissue cell lines (Cao et al., 2019), suggesting that they are not necessarily specific to our model and that some TE families are more potent to contribute as *cis*-regulatory elements than others across mammals. We also noticed that the SINE B2 family, which was enriched among the transcribed TE loci in the whole developing gonad (Figure 1D), is under-represented among the open chromatin regions in supporting cells for both sexes. As we assume transcribed TE loci to be accessible, we can speculate that the B2 family is not preferentially transcribed in the supporting cells.

Next, we performed differential chromatin accessibility analysis between sexes and stages in order to identify the regions that gain in accessibility while gonadal progenitor cells differentiate as either pre-granulosa or Sertoli cells. As previously reported, almost no differences were found in open chromatin regions between XX and XY at E10.5 when the cells are multipotent (Garcia-Moreno, Futtner, et al., 2019). In contrast, at E13.5, we observed 14,038 genomic regions with increased accessibility in pre-granulosa cells compared to Sertoli, and 41.84% of them were overlapping with TE loci. On the other hand, 19,059 genomic regions showed increased accessibility in Sertoli cells compared to pre-granulosa, and 51.83% of them contained TE loci (Figure 3D). We also looked at the genomic regions that increased in accessibility in a time-specific manner in both sexes and found that 27,469 and 39,319 regions were more accessible at E13.5 in pre-granulosa and Sertoli cells, respectively, compared to the E10.5 progenitor cells (Figure 3E). Among them, 48.84% and 51.52% were overlapping TE loci in pre-granulosa and Sertoli cells, respectively. Finally, we found that 30% and 45% of TE loci increasing in accessibility at E13.5 in pre-granulosa and Sertoli cells, respectively, were also sexually dimorphic (Figure 3F). Finally, we investigated whether a particular TE family could be enriched in a sex- or time-specific manner, but we observed no noticeable differences in their proportion among the differentially accessible TE-containing loci, apart for the SINE:Alu elements, which are more prevalent in the Sertoli-specific open loci compared to pre-granulosa, in the pre-granulosa compared to E10.5 XX progenitor cells, and in the Sertoli compared to XY progenitor cells (Figure 3G).

Altogether, these results show that TE loci are increasing in accessibility in a time- and sex-specific manner as supporting cells differentiate as pre-granulosa or Sertoli cells. The fact that more than half of the accessible TEs are located in the intergenic region suggests they could participate in the acquisition of the supporting cell-type identity as active *cis*-regulatory regions.

10.3389/fcell.2023.1327410

FIGURE 4
Epigenetic landscape of pre-granulosa cell-accessible TE loci. **(A)** Density plots and heatmaps representing the ATAC-seq and the ChIP-seq signals for histone marks H3K4me3, H3K27ac, and H3K27me3 around the TE loci that gained accessibility in a sex- or time-specific manner in pre-granulosa cells. Accessible TEs were grouped according to the histone marks they display. The groups of histone marks with fewer than 500 TEs were grouped in the "Other" section, as the groups were not clearly visible on the final heatmap. **(B)** Percentage of TE families in different groups of histone marks in pre-granulosa cells (only percentages >1 are shown). **(C)** Genomic location for each chromatin landscape group of TE loci that gains accessibility in a sex- or time-specific manner in pre-granulosa cells. **(D)** Genomic tracks showing the ATAC-seq signal and H3k4me3, H3K27ac, and H3K27me3 ChIP-seq peaks on accessible TE showing enhancer-like chromatin markers and that are close to important gonadal genes. **(E)** Percentage of mouse accessible TE loci conserved among rats, humans, cows, and chickens. TEs are classified according to their histone marks. As a reference, we show the percentage of conservation of 50,000 random TE loci (in gray).

TEs acquire the sex-specific enhancer- and promoter-like chromatin landscape as supporting cells differentiate

To reveal the potential roles of TE sequences that became accessible in pre-granulosa and Sertoli cells in a time- and sex-specific manner, we explored the histone post-transcriptional modifications present in their vicinity. We reanalyzed ChIP-seq data for H3K4me3 (marker of promoters), H3K27ac (marker of active promoters and enhancers), and H3K27me3 (marker of silencers and transcriptionally silenced genes by PRC2) performed on purified gonadal somatic cells at E10.5 and supporting cells at E13.5 in both sexes (Garcia-Moreno et al., 2019; Garcia-Moreno et al., 2019). We classified accessible TEs according to the combination of histone mark peaks overlapping with the TE sequences +/-200 bp to have an overview of the chromatin landscape at a one nucleosome resolution (Supplementary Data S4). Finally, we represented ATAC-seq and the different ChIP-seq signals on accessible TEs and up to 2 kb around them as juxtaposed heatmaps for the pre-granulosa and Sertoli cells (Figures 4A, 5A).

In pre-granulosa cells, TEs were classified into six histone combination groups (Figure 4A), and we determined TE families present in each groups (Figure 4B). The first two groups contain open TEs displaying histone marks specific for promoters (H3K4me3 and H3K4me3 + H3K27ac). They represent 25.6% of the total pre-granulosa-enriched accessible TEs (5,727 out of 22,328 TEs). Surprisingly, only 6.3% of them (360 TEs) were

10.3389/fcell.2023.1327410

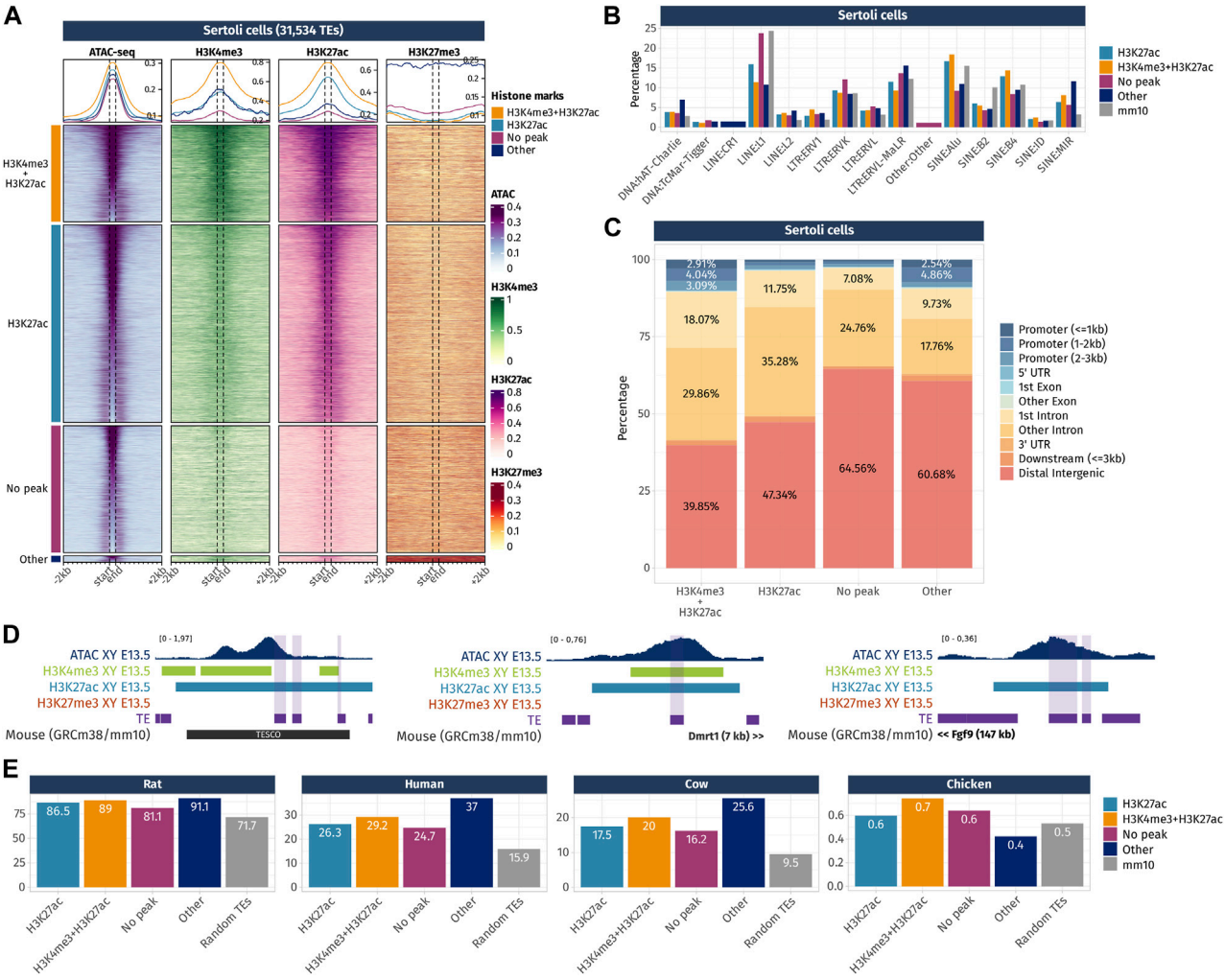

FIGURE 5
Epigenetic landscape of Sertoli cell-accessible TE loci. **(A)** Density plots and heatmaps representing the ATAC-seq and the ChIP-seq signals for histone marks H3K4me3, H3K27ac, and H3K27me3 around the TE loci that gained accessibility in a sex- or time-specific manner in Sertoli cells. Accessible TEs were grouped according to the histone marks they display. The groups of histone marks with fewer than 500 TEs were grouped in the "Other" section as the groups were not clearly visible on the final heatmap. **(B)** Percentage of TE families in the different groups of histone marks in Sertoli cells (only percentages >1 are shown). **(C)** Genomic location for each chromatin landscape group of the TE loci that gains accessibility in a sex- or time-specific manner in Sertoli cells. **(D)** Genomic tracks showing the ATAC-seq signal and H3k4me3, H3K27ac, and H3K27me3 ChIP-seq peaks on accessible TE showing enhancer-like chromatin markers and that are close to important gonadal genes. **(E)** Percentage of mouse accessible TE loci conserved among rats, humans, cows, and chickens. TEs are classified according to their histone marks. As a reference, we show the percentage of conservation of 50,000 random TE loci (in gray).

found in a gene promoter region (up to 3 kb upstream of a gene TSS) (Figure 4C), but no biological GO term was statistically enriched among these genes. We examined whether the genes having TEs that increased in accessibility in their promoter showed a concomitant increase in expression. Although RNA-seq was performed in whole gonads and not purified granulosa cells, we found that 55% (181 out of 333 genes) showed an increase in expression between E10.5 and E13.5 [log2 (fold change)>0]. We investigated the closest genes of 5,727 H3K4me3 and H3K4me3 + H3K27ac TEs and found critical pre-granulosa cell markers, such as *Wnt4*, *Fst*, *Runx1*, *Lef1*, and *Kitl* (Figure 4E, Supplementary Data S4). GO term analysis confirmed the statistical enrichments of terms related to reproductive development and Wnt signaling (Supplementary Data S5). The third group of pre-granulosa-enriched accessible TEs displays the H3K27ac histone mark which suggests that they are potential enhancers (3,725 out of 22,382). The proximal genes were enriched for the biological process GO term of sex differentiation and included *Gata4*, *Cited2*, *Kitl*, and *Lhcgr* (Supplementary Data S5). Next, the fourth group contains accessible TEs with the H3K27me3 histone mark that labels silenced genes and silencer elements (638 out of 22,328). Most of them are found in distal intergenic regions (Figure 4C). Interestingly, we found two H3K27me3 TEs (a SINE B4 and a DNA TcMar-Tigger) in close proximity with *Sox9* (Figure 4E), which are located within TESCO (testis-specific enhancer of the *Sox9* core) (Sekido and Lovell-Badge, 2008). We also found a negative regulator of the Wnt pathway, *Sfrp1*, that is expressed in the gonadal progenitor cells but silenced upon the differentiation of the supporting cell lineage of both sexes

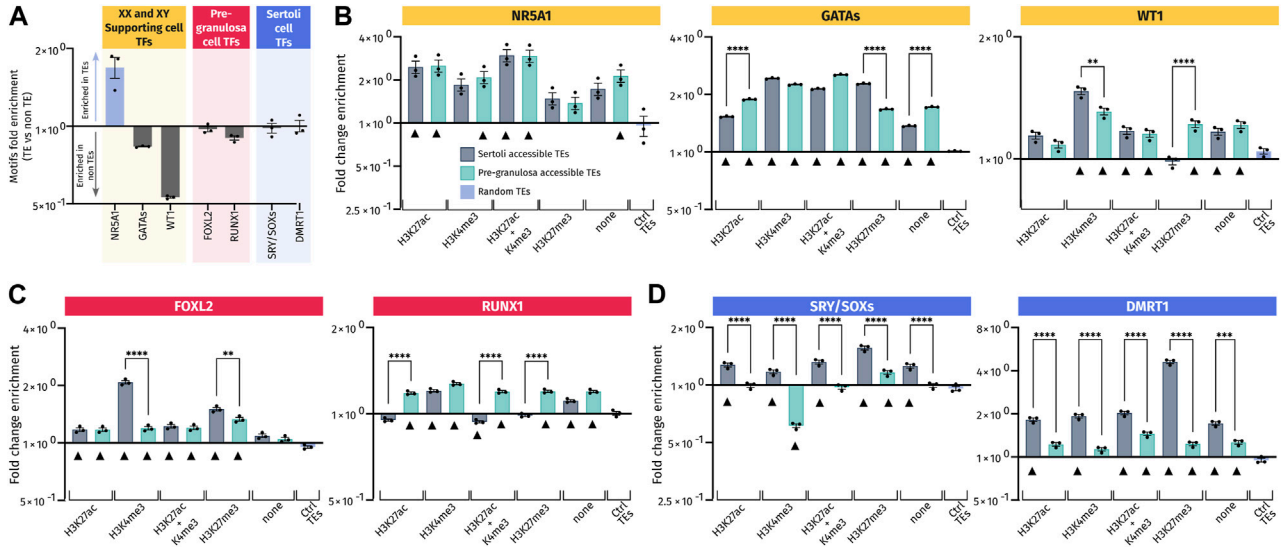

FIGURE 6
Transcription factor-binding motif enrichment in pre-granulosa- and Sertoli cell-accessible TE loci. **(A)** Ratio of the number of the transcription factor motifs found in three sets of 10,000 randomly picked TE or non-TE sequences. For each set of sequences, motifs analyzed were normalized in matches per kb and were expressed (in Log2) by the ratio of matches per kb in TE/matches per kb in non-TE. **(B–D)** Enrichment for the transcription factor motif in motifs per kb of the different analyzed sets of accessible TEs reported to the motifs per kb of three different sets of 10,000 control TEs. Black triangles mark the accessible TEs having a significant enrichment of each motif compared to control TEs (ctrl TEs) (see details of significance in Supplementary Data S6). Motifs in **(B)** are those recognized by transcription factors involved in the specification of XY and XX somatic progenitor cells. Motifs in **(C)** are those for transcription factors involved in the differentiation of pre-granulosa cells, and motifs in **(D)** are corresponding to Sertoli cells.

(Stevant, et al., 2019 17133, Warr et al., 2009). Finally, 53.8% of the pre-granulosa-accessible TEs were not overlapping with any of the investigated histone marks. The proximal genes of these TEs were enriched for female sex differentiation and regulation of canonical Wnt signaling pathway GO terms (Supplementary Data S5). Finally, we investigated whether sex and time differentially accessible TEs were conserved among different species (Figure 4E). We found that independent of their histone marks, the accessible TEs were more conserved than expected among the mammals (rat, human, and cow), but poorly conserved in chickens. Moreover, we observed that most of the accessible TEs were conserved with rats, but to a lesser extent with humans and cows, implying that most of the accessible TEs are rodent-specific.

In Sertoli cells, TEs were classified into four histone combination groups (Figure 5A), and we investigated TE families present in each groups (Figure 5B). The first group is composed of TEs displaying promoter-like histone marks H3K4me3 + H3K27ac (7,124 out of 31,534 TEs). As observed in pre-granulosa, only 10% (715 TEs) of them are found in the promoter region of genes (Figure 5C and Supplementary Data S4). The second group shows TEs with enhancer histone mark H3K27ac (17,570 out of 31,534). Similarly, for the pre-granulosa-enriched accessible TEs, the proximal genes were statistically enriched not only for sex determination-related GO terms but also for terms reflecting Sertoli cell functions, such as epithelium morphogenesis and angiogenesis, among other terms (Supplementary Data S5). Notably, TESCO SINE B4 observed in the pre-granulosa cells and marked with H3K27me3 is present in the H3K27ac Sertoli-accessible TEs (Figure 5D). Although the chromatin state of the present TE is most likely a consequence of its presence within TESCO, the presence of TE loci within a known cell-type-specific enhancer questions on their involvement in the enhancer activity. Interestingly, we found accessible TEs harboring H3K4me3 and H3K27ac histone marks with a 7 kb upstream of *Dmrt1* and 10 kb upstream of *Sox9*. We also found several accessible TEs marked with H3K27ac (Figure 5D), with three of them located 525 kb downstream of *Fgf9* (Supplementary Data S4). These three TEs are contained within the 306 kb locus previously identified as an *Fgf9* enhancer-containing locus using the 3D genome enhancer hub prediction tool. The deletion of the 306-kb region causes partial to complete male-to-female sex reversal (Mota-Gómez et al., 2022). The last group contains TEs showing none of the investigated histone marks (9,367 out of 31,534). Finally, we investigated the accessible TE conservation (Figure 5E) and found that, similar to what was observed in pre-granulosa, TEs were more conserved than expected among the mammals (rat, human, and cow), but poorly conserved in chickens.

Together, these results show that TEs that gain accessibility in a time- and sex-specific manner in pre-granulosa and Sertoli cells upon sex determination are also showing promoter- and enhancer-like properties, which implies they are acting as *cis*-regulatory elements during cell differentiation. The presence of TEs within known critical sex determination enhancer loci such as TESCO or the downstream *Fgf9* enhancer suggest the presence of other TE sequences involved in the process. The absence of either H3K4me3 or H3K27ac on a large fraction of accessible TEs interrogates on the possibility of the presence of other histone marks, such as the recently described H4K16ac that contributes to TE transcription and *cis*-regulatory activity (Pal et al., 2023). Finally, both pre-granulosa and Sertoli cell sex- and time-specific accessible TEs show a higher conservation than expected among mammalian species, suggesting that these specific TEs could have

functional significance in mammalian genomes, such as taking part in the genome 3D structure or in cis-regulatory regions.

Pre-granulosa and Sertoli-accessible TEs are enriched in gonad transcription factor-binding motifs

TE frequently contains sequences that can attract cell-specific transcription factors to promote their expression and, hence, their transposition. Consequently, TE transposition has dispersed transcription factor-binding sites throughout mammalian genomes over evolution. Numerous studies on TE expression in stem cells and early embryos showed that the active TE families were enriched in binding motifs for pluripotency transcription factors, such as NANOG, OCT4, or SOX2. Furthermore, tissue-specific TE transcription and *cis*-regulatory element activity revealed they contain lineage-specific transcription factor-binding sites (Fueyo et al., 2022). As such, we questioned whether TE loci that gain accessibility in a time- and sex-specific manner in pre-granulosa and Sertoli cells are enriched in motifs for the gonadal transcription factors and, in particular, if the motif enrichment changes depending on the chromatin landscape or the sex. We first carried out *de novo* pattern analyses (Santana-Garcia et al., 2022) that did not provide easily interpretable results due to the low quantitative aspect of this method (Supplementary Table S1). Then, we performed a specific transcription factor motif enrichment analysis for known critical gonadal factors: GATA4/6 (Padua et al., 2014; Padua et al., 2015), NR5A1 (Luo et al., 1994), WT1 (Kreidberg et al., 1993), FOXL2 (Schmidt et al., 2004), RUNX1 (Nicol et al., 2019), SRY/SOX (Sinclair, et al., 1990; Wagner et al., 1994; Portnoi et al., 2018), and DMRT1 (Raymond et al., 2000) (Supplementary Figure S5). We used an approach of motif-scanning that calculates the enrichment of motif occurrence per kb compared to control sequences. We first examined if TE sequences are naturally enriched in gonadal transcription factor motifs. To this aim, we selected 3 × 10,000 random TE loci across the genome and compared their sequence composition to motifs with 3 × 10,000 random DNA regions that are not TEs (Figure 6A). We found that the motif recognized by NR5A1, which is involved throughout gonadal differentiation in mammals, was enriched in randomly selected TE loci (control TEs) from the mouse genome when compared to regions containing no repeated elements (non-TE control). For the other motifs analyzed, we did not find any significant enrichment in TE; some motifs such as GATAs, WT1, and RUNX1 are even under-represented in TEs. However, by analyzing TEs by classes (LINEs, LTRs, SINEs, etc.) for the same datasets, we found that the enrichment of NR5A1 motifs was essentially obtained from SINEs and to a lesser extent from LTRs (Supplementary Figure S4A), while LINEs and others were depleted for this motif. Interestingly, SINEs also display enrichment for FOXL2 and DMRT1 motifs. Our results suggest that if certain motifs pre-exist in TEs, it may be in specific classes of TEs, as we observed here for SINEs.

Then, we compared the accessible TEs harboring or not harboring some histone marks to the control TEs randomly distributed in the genome. All the gonadal motifs examined were enriched in almost all the analyzed TE regions compared to the control TEs, regardless of the associated histone mark (Figures 6B–D). This suggests that TEs recruited during gonadal differentiation may have acquired these motifs *de novo*. It is particularly the case for the NR5A1 motif (Figure 6B) that is already enriched when compared to the non-TE control (Figure 6A). By dissociating the datasets in TE classes, we also observed global enrichments for each class in all TE regions compared to control TEs, especially for NR5A1 and GATA motifs (Supplementary Figure S4B). For other motifs, the enrichment is less obvious, sowing some specificity of classes.

Importantly, we also found sexual dimorphism between Sertoli and pre-granulosa in TEs bearing the same histone marks. Interestingly, motifs for male-specific transcription factors, such as SRY/SOX and DMRT1, were more represented in Sertoli-accessible TEs than in pre-granulosa cells independent of their associated histone marks (Figure 6D) with similar results when analyzing different classes (Supplementary Figure S4B). Likewise, pre-granulosa-specific transcriptions factors (FOXL2 and RUNX1) also displayed some sexual dimorphisms (Figure 6C and Supplementary Figure S4B), but to less extent than what we observed for the Sertoli-specific motifs. However, FOXL2 motifs present a different pattern when analyzed by classes; indeed, this motif has mostly depleted in SINEs of open TEs while being more present in other classes. Finally, motifs for transcription factors involved in the formation of the primordial gonads, and later on the maintenance of both Sertoli and pre-granulosa cells, displayed less sexual dimorphism such as GATA, WT1, and NR5A1, which were present at the same frequency in both Sertoli- and pre-granulosa cell-accessible TEs regardless of their classes (Figure 6B and Supplementary Figure S4B).

Our results demonstrate that accessible TEs in Sertoli and pre-granulosa cells are enriched in motifs recognized by the major transcription factors involved during gonadal differentiation. In addition, the motifs recognized by male transcription factors are globally more present in TEs opened in Sertoli cells than in pre-granulosa cells in all subsets of accessible TEs. As random TEs are not naturally enriched for gonadal transcription factor motifs, this suggest that these TEs in male and female supporting cells may have evolved to acquire *de novo* motifs recognized by transcription factors involved in the regulation of their respective transcriptional programs.

Discussion

In this work, we analyzed, for the first time, the TE ecosystem in mouse developing gonads during the time window of sex determination. We observed that approximately 17,000 individual TE loci are transcribed independent of gene promoters and that their expression is tightly regulated in a sex- and time-specific manner as the bipotential gonads adopt their ovarian or testicular identity. Some of the differentially expressed TE loci are found in close proximity to protein-coding genes (100 kb) and their expression correlates with their proximal genes. At the chromatin level, we showed that TE loci are acquiring cell-type-specific enhancer- and promoter-like characteristics while the gonadal somatic cells specify as pre-granulosa or Sertoli cells in XX and XY gonads, respectively. DNA motif analysis revealed that TE loci are displaying potential

binding sites for the critical gonadal development and sex-determining transcription factors. This study resulted in the identification of TE-derived regulatory elements that can participate and contribute to the complex gene regulatory network controlling gonadal development in mice.

The unbiased measurement of TE expression at a locus-specific level remains a challenge using shotgun sequencing technologies. Due to their repetitive nature, short reads cannot be easily attributed to a specific locus, unless TEs have accumulated mutations along evolution. As such, despite the use of EM algorithms that re-allocate multi-mapped reads, TE quantification is biased toward ancient TEs compared to recently inserted TEs displaying fewer mutations. The same challenge is even aggravated when analyzing genomic sequencing data, such as ATAC-seq and ChIP-seq, as no specific tool exists to attempt to re-allocate the multi-mapped reads. Hence, the current analysis is underestimating the number of individual TE loci that are transcribed or accessible in mouse gonads. The use of long-read sequencing technologies would allow unambiguously mapping individual TE loci with fragments longer than TEs and would result in a more resolutive overview of the TE landscape.

Our analyses are based on RNA sequencing of whole gonads and raised the question as to whether TEs might be expressed in a cell-type-specific manner. We first intended to reanalyze single-cell transcriptomic data (Stevant et al., 2018; Stevant, et al., 2019); however, such technologies revealed to not be sensitive enough to efficiently detect TE expression (10,000 total expressed TE loci in an average per stage, against 75,000 in the present bulk RNA-seq, data not shown). Using publicly available bulk RNA-seq data, we could not evaluate whether the expressed TEs we measured in the whole gonads were originating from somatic cells or germline compartments. We reanalyzed the datasets obtained at E11.5 from purified somatic precursor cells and showed that at this stage, half of the self-expressed TEs expressed in the whole gonads were commonly expressed in the purified somatic cells. Moreover, previous analysis at E13.5 (Liu, et al., 2014) suggests that some endogenous retroviruses are much more expressed in somatic cells than in the germ cells of fetal testes. Ultimately, the high-quality RNA-seq data of purified cell types composing the developing gonads of both sexes, similar to what has been done using microarray technology (Jameson, et al., 2012), would greatly contribute to the field to study unexplored aspects of the gonadal transcriptome, with a better sensitivity than the currently existing single-cell data.

An important question is what might be the role of these expressed TEs during gonadal development? In the early embryo, which is the most investigated model for TE expression to date, it has been shown that the activation of LINE-1 expression is required for global chromatin accessibility, independent of the coding nature of the transcript (Jachowicz, et al., 2017). While rarely present in protein-coding genes, co-opted TEs, particularly retrotransposons, constitute a source of lncRNAs (Kelley and Rinn, 2012; Kapusta, et al., 2013) known to be necessary for the correct execution of cellular processes. The endogenous MERVL, expressed in the two-cell stage (Svoboda et al., 2004), is a marker of totipotent cells (Macfarlan et al., 2012). The TE transcript, but not the encoded protein, is required for the correct development of the pre-implantation embryo, possibly through chromatin remodeling during the totipotent–pluripotent transition. At the mechanistic level, it has been shown that LINE-1 RNA recruits nucleonin and TRIM28 to regulate some target genes in embryonic stem cells (Percharde, et al., 2018). During neurogenesis, TE RNAs are associated with chromatin and regulate the activity of polycomb repressor complexes PRC2 (Mangoni et al., 2023). The dynamics of TE expression suggests that some TEs expressed uniquely at E10.5 could contribute to the multipotent state of the cells prior to sex determination, while TEs expressed during and after cell specification and in a sex-specific manner might be involved in the cell differentiation process. Targeted transcriptomic silencing or ablation of these TE loci using CRISPR technologies would allow to functionally explore their role and understand the mechanism of action.

Chromatin architecture influences gene transcription by modulating the access of *cis*-regulatory elements to transcription factors. In this study, we identified that half of the DNA regions that gain accessibility while the gonadal progenitor cells differentiate as pre-granulosa and Sertoli cells overlap with TE loci. A large proportion of these TEs are displaying distinctive histone marks for enhancers and promoters (H3K4me3 and H3K27ac). Using a similar approach, previous studies have identified lineage-specific TE-derived *cis*-regulatory elements (Fueyo, et al., 2022). However, a functional evaluation survey in mouse embryonic and trophoblast stem cells using genome-editing technologies revealed that few of them are critical for gene regulatory networks (Todd et al., 2019). We predict that most candidate TE-derived cis-regulatory regions identified in this study are not critical players of supporting cell differentiation, but rather redundant or shadow enhancers that help sustain the gene regulatory network. However, we cannot exclude that specific TE loci may have become the key players of the gonadal sex determination process. The presence of TEs within TESCO suggests their role in its enhancer activity. The TESCO sequence is highly conserved across mammals (Bagheri-Fam et al., 2010). In mice, TESCO contains four different TE sequences [one DNA TcMar-Tigger and three LINEs, including a B4 and two mammalian-wide interspersed regions (MIRs)]. These four TEs are conserved in rats, while only two LINEs from the MIR family are found across multiple mammalian species, such as rat, rabbit, human, and tree shrew (cf. https://genome.ucsc.edu). These TEs contain predicted binding motifs for the SOX and GATA family of transcription factors (cf. https://genome.ucsc.edu). As such, they potentially contribute to the specie-specific characteristics of TESCO activity. In the same line, several studies have shown that TEs are highly heterogeneous between mouse strains (Nellaker et al., 2012; Jung et al., 2023) that can modify gene expression (Zhou et al., 2021) and chromatin dynamics (Ferraj et al., 2023). Therefore, we can speculate that strain-specific TEs could be involved in the sensitivity of a C57BL/6J background to sex reversal (Eicher et al., 1982; Eicher et al., 1996; Munger et al., 2009).

The enrichment of critical gonadal transcription factor-binding motifs in these accessible TE loci in the differentiating supporting cells further substantiates that TEs could have been co-opted as *cis*-regulatory elements in the context of gonadal sex determination. The enrichment of TE sequences in NR5A1-binding motifs, regardless of their chromatin landscapes, shows that this motif is seemingly already present in the ancestral TE sequences and will be even more enriched in the accessible TEs of both sexes. In contrast, the specific enrichment of gonadal transcription factor motifs in the

accessible TE loci in a time- or sex-specific manner could be explained by *de novo* motif acquisition and/or by a co-optation of a particular TE subfamily that naturally displays these motifs (Garcia-Perez et al., 2016). To support this, our results show a clear enrichment for male-specific transcription factors (SRY/SOX and DMRT1) for the TEs specifically accessible in Sertoli cells compared to pre-granulosa cells. Our refine study of motif enrichment in TE classes shows a global conservation of the enrichment for SRY/SOX and DMRT1. It is also the case for TF motifs involved in the formation of early gonads such as NR5A1, GATA, and WT1; for the same sets of TEs, motifs are mostly enriched in the same manner when they are analyzed by class. One exception is FOXL2 motifs, linked to pre-granulosa cell differentiation, where we observed significant differences between the different classes analyzed. Concerning strain specificity, the motif composition might vary depending of the mouse strain and influence subsequent recognition by DNA-binding proteins as it has been shown for CTCF in the mouse CD-1 strain (Jung, et al., 2023).

In light of our findings, suggesting that TEs may participate in sex determination, it will be interesting to reanalyze human patients suffering from difference in sexual development (DSD) with unexplained etiology (more than 50%: (Rakover et al., 2021)) to investigate whether the reshuffle of TE loci is the cause for their phenotypes. Indeed, the development of long-read technologies of sequencing and dedicated bioinformatics tools for analysis of repeated sequenced would allow better resolving these questions.

Materials and methods

RNA-seq mapping and quantification

RNA-seq FastQ files from the *Trim28* knockout mouse ovaries (Rossitto, et al., 2022) (GSE166385), the *Dmrt1* ovarian reprogramming (Lindeman, et al., 2015) (GSE64960), the whole embryonic gonad splicing event (Zhao, et al., 2018) (SRP076584), and Nr5a1-GFP+ purified somatic cells at E11.5 (Miyawaki, et al., 2020) (GSE151474) studies were downloaded from Gene Expression Omnibus using the nf-core/fetchngs pipeline v1.10.0 (Ewels et al., 2020; Patel et al., 2023a).

Gene- and locus-specific TE expressions were measured using SQuIRE v0.9.9.92 (Yang, et al., 2019). In brief, FastQ files were mapped with STAR v2.5.3a on the 10-mm mouse reference genome obtained from the UCSC. Gene and TE quantification were performed using the 10-mm gene annotation and RepeatMasker TE annotation from the UCSC. First, uniquely mapped reads were assigned to their corresponding TE loci. Then, the multi-mapped reads were assigned to TE loci using an EM algorithm. A score was calculated for each TE locus to account for the proportion of reads uniquely mapped and re-attributed multi-mapped reads in the total TE read count. As TEs with few uniquely aligning reads and numerous re-attributed multi-mapped reads may be prone to low confidence quantification, we considered TEs displaying a score >95 and a minimum of five reads covering the TE locus. We also excluded TEs located outside the conventional chromosomes. Subsequent analysis was performed with R version 4.2.2 "Innocent and Trusting." TE counts together with gene counts were normalized by library size using DESeq2 prior to analysis (Love et al., 2014).

Expressed TE classification and annotation

TEs were classified as gene-dependent or self-expressed if they were found within expressed genes or in intergenic regions or non-expressed genes. To proceed, SQuIRE read counts for genes and TEs were loaded in R. TE loci and 10-mm gene annotation GTF files were transformed as genomic range objects using the GenomicRanges (Lawrence et al., 2013) and the rtracklayer packages, respectively (Lawrence et al., 2009). TE and gene overlaps were computed using "GenomicRanges::findOverlaps" with the option "ignore.strand = TRUE." For each sex and embryonic stage, we investigated whether the genes overlapped by TEs are expressed with a minimum of 10 reads per gene. TEs located within an expressed gene were classified as gene-dependent, as we consider their expression driven by the gene promoter, and the rest of the TEs were classified as self-expressed.

The annotation of TEs as intergenic, exonic, or intronic was performed using "ChIPseeker::annotatePeak" (Wang et al., 2022) using the same 10-mm GTF file as the TE quantification with SQuIRE for genome annotation version consistency.

TE family enrichment test

The TE family enrichment test was performed using the "fisher.test" R function as described by Chang, et al. (2022). For each TE family, we created a contingency table with the number of expressed TEs that belong or do not belong to the family, as well as all annotated TEs that belong or do not belong to the family, and we used Fisher's exact test. *p*-values were corrected for a false discovery rate using the "p.adjust" function with the Benjamini–Hochberg method.

TE differential expression analysis

Differential TE expression analysis by embryonic stage and sex was performed using DESeq2 using both TE and gene quantification for a correct normalization of the data. First, a sample sheet was built with the "stage_sex" sample annotation (e.g., "E10.5_XX") for each sample. A DESeq2 object was created using "DESeqDataSetFromMatrix" with "~stage_sex" as design.

Sexually dimorphic TEs were obtained with the "DESeq" function with default parameters (Wald test). XX and XY overexpressed genes per stage were recovered using the "results" function with "stage_XX" and "stage_XY" contrast for each stage. Dynamically expressed TEs computed sex independently. For each sex, dynamic TEs were obtained using the "DESeq" function with test = "LRT," reduced = ~1′ options (likelihood-ratio test). In both differential expression analyses, we considered a TE statistically differentially expressed with an adj.pval<0.05.

Dynamically expressed TEs per sex were then represented as a heatmap with ComplexHeatmap (Gu et al., 2016) with rows normalized with z-scores and classified into seven clusters using

the "Ward.D2" clustering method. The number of clusters was chosen by visual inspection of the heatmap split.

TE-gene correlation

To inspect whether TE expression was correlating with nearby gene expression, we calculated TE-gene expression correlation per sex across different embryonic stages. To identify the genes located near the time and sex differentially expressed TEs, we first checked the average distance of TE and the nearest gene TSS. We observed that most TEs are located up to 100 kb away from a gene TSS (Supplementary Figure S2D). We defined a window of 100 kb upstream and downstream of the time and sex differentially expressed TEs and selected all the genes overlapping these windows. Then, we calculated Pearson's correlation between TEs and their nearby gene expression across all embryonic stages. We considered a positive correlation with $\rho > 0.6$ and p-value<0.05 and a negative correlation with $\rho < -0.6$ and p-value<0.05.

To visualize the expression correlation between TEs and their nearby genes, we used the bigWig files generated with SQuIRE with the "draw" script. In order to have a clean representation of TE expression and avoid seeing other nearby TEs that were previously excluded by our quality filters described above, we used the bigWig files containing the uniquely mapped reads only and not the re-attributed reads. The genomic track visualization was built using the Gviz R package (Hahne and Ivanek, 2016).

ATAC-seq mapping and analysis

FastQ files for the ATAC-seq data from E10.5 and E13.5 early gonadal progenitors and supporting cells, respectively (Garcia-Moreno, Futtner, et al., 2019), were downloaded from Gene Expression Omnibus (GSE118755) using the nf-core/fetchngs pipeline v1.10.0. Data were mapped on the 10-mm reference genome and analyzed using the nf-core/atacseq v2.1.2 (Patel et al., 2023b). Sequencing data quality was assessed using FastQC, sequencing adapters were removed with cutadapt, and reads were mapped using BWA. Reads were filtered with Picard to remove unmapped and duplicated reads. Peaks were called with MACS2 using the "narrow peak" parameter. For the subsequent analysis, we selected the peaks found in at least two replicates.

Differential accessibility analysis between XX and XY for each stage as well as E10.5 and E13.5 for each sex was performed using DESeq2. First, a consensus table of the read counts per accessible regions was built with featureCounts using the nf-core/atacseq pipeline. Time-specific and sexually dimorphic accessible regions were obtained with the "DESeq" function with default parameters. Sex-biased accessible regions per stage and stage-biased accessible regions per sex were recovered using the "results" function with "stage_XX' and "stage_XY" contrast for each stage and "E10.5_sex" and "E13.5_sex," respectively. A region was defined as differentially accessible with an adj.pval<0.05 and |log2 (foldChange)|>1.

TE overlapping the differentially accessible regions were recovered using "GenomicRanges::findOverlaps" with the option "ignore.strand = TRUE."

ChIP-seq mapping and analysis

FastQ files for the ChIP-seq data (H3K4me3, H3K27ac, and H3K27me3) from E10.5 and E13.5 early gonadal progenitors and supporting cells, respectively (Garcia-Moreno, Futtner, et al., 2019), were downloaded from Gene Expression Omnibus (GSE118755 and GSE130749) using the nf-core/fetchngs pipeline v1.10.0. Data were mapped on the 10-mm reference genome and analyzed using the nf-core/chipseq v2.0.0 (Ewels et al., 2022). Similar to the ATAC-seq analysis, sequencing data quality was assessed using FastQC, sequencing adapters were removed with cutadapt, and reads were mapped using BWA. Reads were filtered with Picard to remove unmapped and duplicated reads. Peaks were called with MACS2 with the respective input controls using the "narrow peak" parameter for H3K4me3 and "broad peaks" for H3K27ac and H3K27me3. Because of the differences of sequencing depth, mapped reads, and peak numbers between the replicates, we considered all the peaks called from any replicates for the rest of the analysis.

TE loci epigenetic classification

We first selected TEs that contributes to the differentiation of the supporting cells as either Sertoli or pre-granulosa cells. To proceed, for each sex, we selected the TE displaying an accessible chromatin region that is statistically more accessible at E13.5 than E10.5, as well as the accessible chromatin regions that are sexually dimorphic at E13.5. We extended the coordinates of the obtained TEs by 200 bp to look for ChIP-seq peaks in the direct vicinity of the TEs, at a one nucleosome resolution. We overlapped the obtained TE regions with the ChIP-seq peaks from E13.5 H3K4me3, H3K27ac, and H3K27me3 for both sexes. For each TE, we binarized the presence of either H3K4me3, H3K27ac, or H3K27me3, i.e., we marked 1 if one or more peaks were found or 0 if no peak was found, and checked the presence of the following combination of histone marks that are biologically relevant: only H3K4me3 (promoters), H3K4me3 and H3K27ac (promoters), only H3K27ac (active enhancer), only H3K27me3 (silencer), and H3K4me3 and H3K27me3 (poised promoters). The other possible combinations were labeled as "Others," and the loci overlapping none of these histone marks were labeled as "No peak." The histone marks overlapping the open TEs were represented on heatmaps with EnrichedHeatmap (Gu et al., 2018) using merged replicate bigWig files produced with WiggleTools and bedGraphToBigWig utilities. For visualization clarity, the combinations of histone marks with fewer than 500 open TEs were grouped in the "Other" section as the groups were not clearly visible on the final heatmap.

GO-term enrichment analysis

Biological process GO-term enrichment analysis was performed using the g:profiler website (https://biit.cs.ut.ee/gprofiler/gost) using the mouse genome as the background, Benjamini–Hogberg FDR <0.5. Because of the large amount of genes present in different analyses, GO terms were displaying various general processes, such as

"Developmental processes." For the concision of the reported results, we filtered the obtained statistically enriched GO terms to maintain biologically relevant terms containing not only "sex," "reproduction/reproductive," and "gonad" but also "Wnt" in female-related gene lists and "angiogenesis" and "epithelium" for male-related gene lists.

TE conservation

The conservation of mouse (10 mm) TE sequences between rat (rn7), human (Hg38), cow (bosTau9), and chicken (galGal6) was performed using LiftOver from the UCSC website (https://genome.ucsc.edu/cgi-bin/hgLiftOver) with default parameters. As a reference, we selected 50,000 random TE sequences and checked which percentage was found conserved in all the species mentioned above. We then repeated the same procedure with all groups of sex- and time-specific accessible TEs carrying different combinations of histone marks in pre-granulosa and Sertoli cells.

TF motif enrichment analysis

Binding sites for transcription factors involved in mammalian sex determination/differentiation were counted using the matrix scan (full options) algorithm from the RSAT suite (http://www.rsat.eu) (Santana-Garcia et al., 2022). The DNA-binding preferences for the transcription factor analyzed were modeled as matrices and analyzed with default settings and a *p*-value set to 10^{-4}. Matrices for transcription factors were obtained from the JASPAR database (https://jaspar.genereg.net): SRY (MA0084.1); SOX9 (MA0077.1); SOX8 (MA0868.2); SOX10 (MA0442.2); SF1, also known as NR5A1 (MA1540.1); GATA4 (MA0482.1); GATA6 (MA1104.1); DMRT1 (MA1603.1); FOXL2 (MA1607.1); RUNX1 (MA0002.2); and WT1 (MA1627.1). GATA4 and GATA6 are redundant during gonadal differentiation (Padua, et al., 2014; Padua, et al., 2015), and the HMG domain of SOX proteins displays related functions (Bergstrom et al., 2000; Polanco et al., 2010). Therefore, the pooled results of matrices scanning for GATA4 and GATA6 were expressed as "GATAs" and "SRY/SOX" for pooled scanning with SRY, SOX8/SOX9/SOX10 matrices. To normalize counts, each motif was expressed in the number of matches per kilobases of the total length of the datasets. Statistical analyses were made using GraphPad Prism 10 with ordinary one-way ANOVA and Tukey's multiple comparison test. The detailed results of statistical tests are provided in Supplementary Table (Supplementary Data S6). *De novo* motif analyses were performed using peak-motifs from the RSAT suite.

Data availability statement

The original contributions presented in the study are included in the article/Supplementary Material; further inquiries can be directed to the corresponding authors.

Author contributions

IS: conceptualization, writing–original draft, and writing–review and editing. NG: funding acquisition, supervision, and writing–review and editing. FP: conceptualization, funding acquisition, supervision, writing–original draft, and writing–review and editing.

Funding

The authors declare that financial support was received for the research, authorship, and/or publication of this article. This work was co-funded by the Israel Science Foundation (ISF_710_2020) and the European Union (ERC, *EnhanceSex*, 101039928). IS and NG were funded by the ISF and ERC. FP was funded by Agence Nationale de la Recherche (ANR): ANR-21-CE14-0061-01 and ANR-23-CE14-0012-01.

Acknowledgments

The authors are grateful to the genotoul bioinformatics platform Toulouse Occitanie (Bioinfo Genotoul, https://doi.org/10.15454/1.5572369328961167E12) for providing the computing resources necessary for the current study. They thank Stéphanie Le Gras from the GenomEast platform of the IGBMC in Strasbourg for her preliminary work on the TE expression analysis. They also thank all the members of Poulat's and the Gonen's teams for the constructive discussions and comments.

Conflict of interest

The authors declare that the research was conducted in the absence of any commercial or financial relationships that could be construed as a potential conflict of interest.

The authors declare that they were editorial board members of Frontiers, at the time of submission. This had no impact on the peer review process and the final decision.

Publisher's note

Author disclaimer

Supplementary material

The Supplementary Material for this article can be found online at: https://www.frontiersin.org/articles/10.3389/fcell.2023.1327410/full#supplementary-material

SUPPLEMENTARY FIGURE 1
Differential TE expression analysis of two cases of granulosa-to-Sertoli transdifferentiation in adult ovaries. **(A, B)** Heatmap representing the differentially expressed TEs in the *Trim28* knock-out ovaries **(A)** and the *Dmrt1* over-expression ovaries **(B)** models compared to control ovaries, respectively. Expression data were normalized using z-scores. **(C)** Overlap of the differentially expressed TEs in the *Trim28* knock-out and the *Dmrt1* over-expression models. Despite the differences in mouse strain genetic background, RNA-seq library, and sequencing protocols, 655 and 251 TEs were found commonly up and down regulated after granulosa-to-Sertoli transdifferentiation.

SUPPLEMENTARY FIGURE 2
Characteristics of the TE found expressed in mouse fetal gonads. **(A)** Number of TE loci detected as expressed across sexes and stages. **(B)** Comparison of the self-expressed TEs detected in whole gonads (Zhao's dataset) and purified somatic cells (Miyawaki's dataset) at E11.5 in XX and XY gonads. Due to the difference in the RNA-seq library preparation protocols and sequencing sensitivity, more self-expressed are detected in the Miyawaki's dataset. However, half of the Zhao's self-expressed TEs were also found in Miyawaki's dataset. **(C)** Proportion of the self-expressed TE families across sexes and stages. **(D)** Distance of the sex- or time-differentially expressed self-expressed TEs relatively to the nearest gene TSS. The red square shows a magnification of the TSS region, +/- 100 kb where most of the TEs were found.

SUPPLEMENTARY FIGURE 3
Characteristics of the ATAC-seq peaks overlapping TEs. Number of TEs contained within ATAC-seq peaks (green) and percentage of the TE sequences overlapping with ATAC-seq peaks (salmon) are reported for each sex and stage. The ATAC-seq peaks can contain up to eight TEs but most of them contains one or two individual TE loci. Most of the TE sequences are entirely embedded within the ATAC-seq peak (100%).

SUPPLEMENTARY FIGURE 4
Transcription factor binding motif enrichment in pre-granulosa and Sertoli cell per classes of accessible TE loci. **(A)** Ratio of the number of the respective transcription factor motifs found in 3 sets of 10,000 randomly picked TE dissociated in four different classes (LINEs, LTRs, SINEs and others) or non-TE sequences, respectively. Motifs were analyzed and normalized as described in Figure 6A. **(B)** Same analyses as in Figure 6B-D for the different set of accessible TEs dissociated in four different classes (LINEs, LTRs, SINEs and others) and reported to corresponding classes of three different sets of 10,000 control TEs. XY and XX correspond to accessible TEs from Sertoli and pre-granulosa cells respectively.

SUPPLEMENTARY FIGURE 5
Expression level of the gonad transcription factors. Expression of the transcription factors used for the motif enrichment analysis across fetal gonad development. Data are expressed as TPM (transcript per million).

SUPPLEMENTARY TABLE 1
De novo motifs analysis for each set of the accessible TEs from Sertoli (XY) and pre-granulosa cells (XX). Are reported all transcription factors motifs others than those already used in Figure 6.

SUPPLEMENTARY DATASHEET 1
Temporally differentially expressed self-expressed TEs. Results of the differential expression analysis across embryonic stages for XX and XY gonads using DESeq2. Only results with padj < 0.05 are reported. The column "TE name" refers to the TE locus identifier which is represented as chromosome|start|end|TEsubfamily:TEfamily:TEclass|size|strand. The "baseMean" is the mean of normalized counts for all samples. "pvalue" column is the *p*-values resulted from the LRT test, and "padj" is the *p*-value corrected for false discovery rate using Benjamini-Hochberg. The column "cluster" refers to the TE clustering presented on the heatmaps from Figure 2A. XX and XY results are reported in separated tabs of the spreadsheet.

SUPPLEMENTARY DATASHEET 2
Sexually differentially expressed self-expressed TEs. Results of the differential expression analysis between XX and XY gonads for each embryonic stages using DESeq2. Only results with padj < 0.05 are reported. Similarly to Sup. Data 1, the column "name" refers to the TE locus identifiers, the "baseMean" is the mean of normalized counts for all samples, "log2FoldChange" of the fold change in expression of XX vs XY normalized expression conditions transformed with log2. Positive values indicate over-expression in XX, and conversely, negative values indicate overexpression in XY. "lfcSE" columns gives the standard error of the log2FoldChange. "pvalue" is the *p*-values resulted from the WALD test, and "padj" is the *p*-value corrected for false discovery rate using Benjamini-Hochberg. The columns "sex" and "stage" refer to the sex and stage in which the TE is overexpressed.

SUPPLEMENTARY DATASHEET 3
Sex- and time-differentially expressed TE correlation with genes in their 100 kb neighborhood. Results of the TE-gene correlation analysis. "TE" column refers to the TE locus identifiers, the "Gene" column are the symbol of the genes present in the 100 kb regions around the TEs. The distance of the gene TSS to the TE is referred in the "distance_to_gene" column. XX and XY Pearson correlation coefficients and their respective p-values are referred. Mathematically impossible correlation test (*i.e.* when the gene expression value is equal to 0) were annotated with a correlation coefficient of 0 and a *p*-value noted "NA". The "TE_coord" column gives the TE loci coordinates in a format usable in IGV genome browser for convenience.

SUPPLEMENTARY DATASHEET 4
Classification of the TEs gaining accessibility in a sex- or time-specific manner in pre-granulosa and Sertoli cells according to histone marks. The spreadsheet presents three different tabs. The first tab contains the number of accessible TEs for each different biologically relevant histone mark classification. The second and third tabs contain the classification details for the pre-granulosa and Sertoli accessible TEs respectively. The first five columns refer to the TE coordinates and their identifier, columns six to eight refers to the presence or not of the respective histone marks as binary data (*i.e.* "0" if no peak was found in the ChIP-seq data, "1" if one or more peaks were found). The "category" column refers to the classification of the TE according to the histone marks found in their sequence. "annotation" are the genomic locations of the TEs, *e.g.* exonic, intronic or intergenic. "geneid" and "distanceToTSS" refer to the nearest gene TSS and the distance from the TE loci.

SUPPLEMENTARY DATASHEET 5
GO-term enrichment for the proximal genes to the sex- and time-accessible TEs found in pre-granulosa and Sertoli cells according to histone marks. The spreadsheet presents two tabs. The first shows the results for the pre-granulosa accessible TEs, while the second the results for the Sertoli cell. GO-term enrichment results were filtered to show biologically relevant terms.

SUPPLEMENTARY DATASHEET 6
Details of the statistical tests used to compare the enrichments of motifs between the different sets of open TE and control TE. The spreadsheet presents two tabs. The first shows the summary of all statistical tests and the seconds the details of each test. $P < 0.032$ (*), < 0.0021 (**), < 0.0002 (***), < 0.0001 (****). The performed was ordinary one-way ANOVA. Multiple comparisons with no matching and pairing was performed using Tukey's test.

References

Albrecht, K. H., and Eicher, E. M. (2001). Evidence that Sry is expressed in pre-Sertoli cells and Sertoli and granulosa cells have a common precursor. *Dev. Biol.* 240, 92–107. doi:10.1006/dbio.2001.0438

Ang, C. E., Ma, Q., Wapinski, O. L., Fan, S., Flynn, R. A., Lee, Q. Y., et al. (2019). The novel lncRNA lnc-NR2F1 is pro-neurogenic and mutated in human neurodevelopmental disorders. *Elife. Jan.* 10, e41770. doi:10.7554/eLife.41770

Bagheri-Fam, S., Sinclair, A. H., Koopman, P., and Harley, V. R. (2010). Conserved regulatory modules in the Sox9 testis-specific enhancer predict roles for SOX, TCF/LEF, Forkhead, DMRT, and GATA proteins in vertebrate sex determination. *Int. J. Biochem. Cell. Biol. Mar.* 42, 472–477. doi:10.1016/j.biocel.2009.07.001

Bergeron, K. F., Nguyen, C. M., Cardinal, T., Charrier, B., Silversides, D. W., and Pilon, N. (2016). Upregulation of the Nr2f1-A830082K12Rik gene pair in murine neural crest cells results in a complex phenotype reminiscent of Waardenburg syndrome type 4. *Dis. Model. Mech.* 9 (9), 1283–1293. doi:10.1242/dmm.026773

Bergstrom, D. E., Young, M., Albrecht, K. H., and Eicher, E. M. (2000). Related function of mouse SOX3, SOX9, and SRY HMG domains assayed by male sex

determination. *Genes. Nov-Dec* 28, 111–124. doi:10.1002/1526-968x(200011/12)28:3/4<111::aid-gene40>3.0.co;2-5

Bertacchi, M., Parisot, J., and Studer, M. (2019). The pleiotropic transcriptional regulator COUP-TFI plays multiple roles in neural development and disease. *Brain Res. Feb* 15, 75-94. doi:10.1016/j.brainres.2018.04.024

Cao, Y., Chen, G., Wu, G., Zhang, X., McDermott, J., Chen, X., et al. (2019). Widespread roles of enhancer-like transposable elements in cell identity and long-range genomic interactions. *Genome Res. Jan.* 29, 40–52. doi:10.1101/gr.235747.118

Chang, N. C., Rovira, Q., Wells, J., Feschotte, C., and Vaquerizas, J. M. (2022). Zebrafish transposable elements show extensive diversification in age, genomic distribution, and developmental expression. *Genome Res. Jul* 32, 1408–1423. doi:10.1101/gr.275655.121

Chassot, A. A., Ranc, F., Gregoire, E. P., Roepers-Gajadien, H. L., Taketo, M. M., Camerino, G., et al. (2008). Activation of beta-catenin signaling by Rspo1 controls differentiation of the mammalian ovary. *Hum. Mol. Genet.* 17, 1264–1277. doi:10.1093/hmg/ddn016

Chuong, E. B., Rumi, M. A., Soares, M. J., and Baker, J. C. (2013). Endogenous retroviruses function as species-specific enhancer elements in the placenta. *Nat. Genet. Mar.* 45, 325–329. doi:10.1038/ng.2553

Conley, A. B., and Jordan, I. K. 2012. Cell type-specific termination of transcription by transposable element sequences. *Mob. DNA* 3:15. doi:10.1186/1759-8753-3-15

Dechaud, C., Volff, J. N., Schartl, M., and Naville, M. (2019). Sex and the TEs: transposable elements in sexual development and function in animals. *Mob. DNA* 10, 42. doi:10.1186/s13100-019-0185-0

Eicher, E. M., Washburn, L. L., Schork, N. J., Lee, B. K., Shown, E. P., Xu, X., et al. (1996). Sex-determining genes on mouse autosomes identified by linkage analysis of C57BL/6J-YPOS sex reversal. *Nat. Genet. Oct.* 14, 206–209. doi:10.1038/ng1096-206

Eicher, E. M., Washburn, L. L., Whitney, J. B., 3rd, and Morrow, K. E. (1982). *Mus poschiavinus* Y chromosome in the C57BL/6J murine genome causes sex reversal. *Science* 217 (217), 535–537. doi:10.1126/science.7089579

Ewels, P., Peltzer, A., Fillinger, S., Patel, H., Alneberg, J., Wilm, A., et al. (2022). *The nf-core framework for community-curated bioinformatics pipelines*. Available at: https://doiorg/105281/zenodo7139814.

Ewels, P. A., Peltzer, A., Fillinger, S., Patel, H., Alneberg, J., Wilm, A., et al. (2020). The nf-core framework for community-curated bioinformatics pipelines. *Nat. Biotechnol. Mar.* 38, 276–278. doi:10.1038/s41587-020-0439-x

Ferraj, A., Audano, P. A., Balachandran, P., Czechanski, A., Flores, J. I., Radecki, A. A., et al. (2023). Resolution of structural variation in diverse mouse genomes reveals chromatin remodeling due to transposable elements. *Cell. Genom* 3, 100291. doi:10.1016/j.xgen.2023.100291

Fueyo, R., Judd, J., Feschotte, C., and Wysocka, J. (2022). Roles of transposable elements in the regulation of mammalian transcription. *Nat. Rev. Mol. Cell. Biol. Feb* 28, 481–497. doi:10.1038/s41580-022-00457-y

Garcia-Moreno, S. A., Futtner, C. R., Salamone, I. M., Gonen, N., Lovell-Badge, R., and Maatouk, D. M. (2019). Gonadal supporting cells acquire sex-specific chromatin landscapes during mammalian sex determination. *Dev. Biol. Feb* 15 (446), 168–179. doi:10.1016/j.ydbio.2018.12.023

Garcia-Moreno, S. A., Lin, Y. T., Futtner, C. R., Salamone, I. M., Capel, B., and Maatouk, D. M. (2019). CBX2 is required to stabilize the testis pathway by repressing Wnt signaling. *PLoS Genet. May* 15, e1007895. doi:10.1371/journal.pgen.1007895

Garcia-Perez, J. L., Widmann, T. J., and Adams, I. R. (2016). The impact of transposable elements on mammalian development. *Dev.* 143:4101–4114. doi:10.1242/dev.132639

Gonen, N., Futtner, C. R., Wood, S., Garcia-Moreno, S. A., Salamone, I. M., Samson, S. C., et al. (2018). Sex reversal following deletion of a single distal enhancer of Sox9. *Science* 360 (360), 1469–1473. doi:10.1126/science.aas9408

Goodier, J. L., Ostertag, E. M., Du, K., and Kazazian, H. H., Jr (2001). A novel active L1 retrotransposon subfamily in the mouse. *Genome Res. Oct.* 11, 1677–1685. doi:10.1101/gr.198301

Greenfield, A. (2021). The molecular genetic basis of fetal granulosa cell development. *Curr. Opin. Endocr. Metab. Res.* 18, 1–7. doi:10.1016/j.coemr.2020.11.010

Gu, Z., Eils, R., and Schlesner, M. (2016). Complex heatmaps reveal patterns and correlations in multidimensional genomic data. *Bioinforma. Sep.* 15 (32), 2847–2849. doi:10.1093/bioinformatics/btw313

Gu, Z., Eils, R., Schlesner, M., and Ishaque, N. (2018). EnrichedHeatmap: an R/Bioconductor package for comprehensive visualization of genomic signal associations. *BMC Genomics. Apr* 4 (19), 234. doi:10.1186/s12864-018-4625-x

Hahne, F., and Ivanek, R. (2016). Visualizing genomic data using Gviz and bioconductor. *Methods Mol. Biol.* 1418, 335–351. doi:10.1007/978-1-4939-3578-9_16

Hedges, D. J., and Deininger, P. L. (2007). Inviting instability: transposable elements, double-strand breaks, and the maintenance of genome integrity. *Mutat. Res. Mar.* 1, 46-59. doi:10.1016/j.mrfmmm.2006.11.021

Herpin, A., Schartl, M., Depince, A., Guiguen, Y., Bobe, J., Hua-Van, A., et al. (2021). Allelic diversification after transposable element exaptation promoted gsdf as the master sex determining gene of sablefish. *Genome Res. Aug* 31, 1366–1380. doi:10.1101/gr.274266.120

Jachowicz, J. W., Bing, X., Pontabry, J., Boskovic, A., Rando, O. J., and Torres-Padilla, M. E. (2017). LINE-1 activation after fertilization regulates global chromatin accessibility in the early mouse embryo. *Nat. Genet. Oct.* 49, 1502–1510. doi:10.1038/ng.3945

Jameson, S. A., Natarajan, A., Cool, J., DeFalco, T., Maatouk, D. M., Mork, L., et al. (2012). Temporal transcriptional profiling of somatic and germ cells reveals biased lineage priming of sexual fate in the fetal mouse gonad. *PLoS Genet.* 8, e1002575. doi:10.1371/journal.pgen.1002575

Jansz, N., and Faulkner, G. J. (2021). Endogenous retroviruses in the origins and treatment of cancer. *Genome Biol.* 22, 147. doi:10.1186/s13059-021-02357-4

Jonsson, M. E., Garza, R., Johansson, P. A., and Jakobsson, J. (2020). Transposable elements: a common feature of neurodevelopmental and neurodegenerative disorders. *Trends Genet. Aug* 36, 610–623. doi:10.1016/j.tig.2020.05.004

Jung, Y. H., Wang, H. V., Ali, S., Corces, V. G., and Kremsky, I. (2023). Characterization of a strain-specific CD-1 reference genome reveals potential inter- and intra-strain functional variability. *BMC Genomics* 24 (24), 437. doi:10.1186/s12864-023-09523-x

Kapusta, A., Kronenberg, Z., Lynch, V. J., Zhuo, X., Ramsay, L., Bourque, G., et al. (2013). Transposable elements are major contributors to the origin, diversification, and regulation of vertebrate long noncoding RNAs. *PLoS Genet. Apr* 9, e1003470. doi:10.1371/journal.pgen.1003470

Kelley, D., and Rinn, J. (2012). Transposable elements reveal a stem cell-specific class of long noncoding RNAs. *Genome Biol. Nov.* 26 (13), R107. doi:10.1186/gb-2012-13-11-r107

Koopman, P., Gubbay, J., Vivian, N., Goodfellow, P., and Lovell-Badge, R. (1991). Male development of chromosomally female mice transgenic for Sry. *Nature* 351, 117–121. doi:10.1038/351117a0

Kreidberg, J. A., Sariola, H., Loring, J. M., Maeda, M., Pelletier, J., Housman, D., et al. (1993). WT-1 is required for early kidney development. *Cell.* 74, 679–691. doi:10.1016/0092-8674(93)90515-r

Lanciano, S., and Cristofari, G. (2020). Measuring and interpreting transposable element expression. *Nat. Rev. Genet. Dec* 21, 721–736. doi:10.1038/s41576-020-0251-y

Lawrence, M., Gentleman, R., and Carey, V. (2009). rtracklayer: an R package for interfacing with genome browsers. *Bioinforma. Jul* 15 (25), 1841–1842. doi:10.1093/bioinformatics/btp328

Lawrence, M., Huber, W., Pages, H., Aboyoun, P., Carlson, M., Gentleman, R., et al. (2013). Software for computing and annotating genomic ranges. *PLoS Comput. Biol.* 9, e1003118. doi:10.1371/journal.pcbi.1003118

Lawson, H. A., Liang, Y., and Wang, T. (2023). Transposable elements in mammalian chromatin organization. *Nat. Rev. Genet. Jun* 7, 712–723. doi:10.1038/s41576-023-00609-6

Liang, L., Cao, C., Ji, L., Cai, Z., Wang, D., Ye, R., et al. (2023). Complementary Alu sequences mediate enhancer-promoter selectivity. *Nat. Jul* 619, 868–875. doi:10.1038/s41586-023-06323-x

Lindeman, R. E., Gearhart, M. D., Minkina, A., Krentz, A. D., Bardwell, V. J., and Zarkower, D. (2015). Sexual cell-fate reprogramming in the ovary by DMRT1. *Curr. Biol. Mar.* 16 (25), 764–771. doi:10.1016/j.cub.2015.01.034

Liu, S., Brind'Amour, J., Karimi, M. M., Shirane, K., Bogutz, A., Lefebvre, L., et al. (2014). Setdb1 is required for germline development and silencing of H3K9me3-marked endogenous retroviruses in primordial germ cells. *Genes. Dev. Sep.* 15 (28), 2041–2055. doi:10.1101/gad.244848.114

Love, M. I., Huber, W., and Anders, S. (2014). Moderated estimation of fold change and dispersion for RNA-seq data with DESeq2. *Genome Biol.* 15, 550. doi:10.1186/s13059-014-0550-8

Luo, X., Ikeda, Y., and Parker, K. L. (1994). A cell-specific nuclear receptor is essential for adrenal and gonadal development and sexual differentiation. *Cell.* 77, 481–490. doi:10.1016/0092-8674(94)90211-9

Macfarlan, T. S., Gifford, W. D., Driscoll, S., Lettieri, K., Rowe, H. M., Bonanomi, D., et al. (2012). Embryonic stem cell potency fluctuates with endogenous retrovirus activity. *Nature* 487, 57–63. doi:10.1038/nature11244

Mangoni, D., Simi, A., Lau, P., Armaos, A., Ansaloni, F., Codino, A., et al. (2023). LINE-1 regulates cortical development by acting as long non-coding RNAs. *Nat. Commun.* 14 (14), 4974. doi:10.1038/s41467-023-40743-7

Mayere, C., Regard, V., Perea-Gomez, A., Bunce, C., Neirijnck, Y., Djari, C., et al. (2022). Origin, specification and differentiation of a rare supporting-like lineage in the developing mouse gonad. *Sci. Adv. May* 27 (8), eabm0972. doi:10.1126/sciadv.abm0972

Miao, B., Fu, S., Lyu, C., Gontarz, P., Wang, T., and Zhang, B. (2020). Tissue-specific usage of transposable element-derived promoters in mouse development. *Genome Biol. Sep.* 28 (21), 255. doi:10.1186/s13059-020-02164-3

Miyawaki, S., Kuroki, S., Maeda, R., Okashita, N., Koopman, P., and Tachibana, M. (2020). The mouse Sry locus harbors a cryptic exon that is essential for male sex determination. *Science* 370, 121–124. doi:10.1126/science.abb6430

Mota-Gómez, I., Rodríguez, J. A., Dupont, S., Lao, O., Jedamzick, J., Kuhn, R., et al. (2022). Sex-determining 3D regulatory hubs revealed by genome spatial auto-correlation analysis. *bioRxiv* 2022, 516861. doi:10.1101/2022.11.18.516861

Munger, S. C., Aylor, D. L., Syed, H. A., Magwene, P. M., Threadgill, D. W., and Capel, B. (2009). Elucidation of the transcription network governing mammalian sex determination by exploiting strain-specific susceptibility to sex reversal. *Genes. Dev. Nov.* 1 (23), 2521–2536. doi:10.1101/gad.1835809

Nef, S., Schaad, O., Stallings, N. R., Cederroth, C. R., Pitetti, J. L., Schaer, G., et al. (2005). Gene expression during sex determination reveals a robust female genetic program at the onset of ovarian development. *Dev. Biol. Nov.* 15 (287), 361–377. doi:10.1016/j.ydbio.2005.09.008

Neirijnck, Y., Sararols, P., Kuhne, F., Mayere, C., Weerasinghe Arachchige, L. C., Regard, V., et al. (2023). Single-cell transcriptomic profiling redefines the origin and specification of early adrenogonadal progenitors. *Cell. Rep.* 42 (42), 112191. doi:10.1016/j.celrep.2023.112191

Nellaker, C., Keane, T. M., Yalcin, B., Wong, K., Agam, A., Belgard, T. G., et al. (2012). The genomic landscape shaped by selection on transposable elements across 18 mouse strains. *Genome Biol.* 13 (13), R45. doi:10.1186/gb-2012-13-6-r45

Nicol, B., Grimm, S. A., Chalmel, F., Lecluze, E., Pannetier, M., Pailhoux, E., et al. (2019). RUNX1 maintains the identity of the fetal ovary through an interplay with FOXL2. *Nat. Commun. Nov.* 11;5116. doi:10.1038/s41467-019-13060-1

Padua, M. B., Fox, S. C., Jiang, T., Morse, D. A., and Tevosian, S. G. (2014). Simultaneous gene deletion of gata4 and gata6 leads to early disruption of follicular development and germ cell loss in the murine ovary. *Biol. Reprod. Jul* 91, 24. doi:10.1095/biolreprod.113.117002

Padua, M. B., Jiang, T., Morse, D. A., Fox, S. C., Hatch, H. M., and Tevosian, S. G. (2015). Combined loss of the GATA4 and GATA6 transcription factors in male mice disrupts testicular development and confers adrenal-like function in the testes. *Endocrinology* 156, 1873–1886. doi:10.1210/en.2014-1907

Pal, D., Patel, M., Boulet, F., Sundarraj, J., Grant, O. A., Branco, M. R., et al. (2023). H4K16ac activates the transcription of transposable elements and contributes to their cis-regulatory function. *Nat. Struct. Mol. Biol. Jun* 12, 935–947. doi:10.1038/s41594-023-01016-5

Patel, H., Beber, M. E., Joshi, E., Han, D. W., bot, nf-core, Manning, J., et al. (2023a). *nf-core/fetchngs: nf-core/fetchngs v1.10.0 - manganese Monkey*. Available at: https://doiorg/105281/zenodo7941940.

Patel, H., Espinosa-Carrasco, J., Langer, B., Ewels, P., bot, nf-core, Garcia, M. U., et al. (2023b). *nf-core/atacseq*. [2.1.2] - 2022-08-07. Available at: https://doiorg/105281/zenodo8222875.

Percharde, M., Lin, C. J., Yin, Y., Guan, J., Peixoto, G. A., Bulut-Karslioglu, A., et al. (2018). A LINE1-nucleolin partnership regulates early development and ESC identity. *Cell.* 174, 391–405. doi:10.1016/j.cell.2018.05.043

Platt, R. N., Vandewege, M. W., and Ray, D. A. (2018). Mammalian transposable elements and their impacts on genome evolution. *Chromosome Res. Mar.* 26, 25–43. doi:10.1007/s10577-017-9570-z

Polanco, J. C., Wilhelm, D., Davidson, T. L., Knight, D., and Koopman, P. (2010). Sox10 gain-of-function causes XX sex reversal in mice: implications for human 22q-linked disorders of sex development. *Hum. Mol. Genet.* 19, 506–516. doi:10.1093/hmg/ddp520

Portnoi, M. F., Dumargne, M. C., Rojo, S., Witchel, S. F., Duncan, A. J., Eozenou, C., et al. (2018). Mutations involving the SRY-related gene SOX8 are associated with a spectrum of human reproductive anomalies. *Hum. Mol. Genet. Apr* 1 (27), 1228–1240. doi:10.1093/hmg/ddy037

Rahmoun, M., Lavery, R., Laurent-Chaballier, S., Bellora, N., Philip, G. K., Rossitto, M., et al. (2017). In mammalian foetal testes, SOX9 regulates expression of its target genes by binding to genomic regions with conserved signatures. *Nucleic Acids Res. Jul* 7 (45), 7191–7211. doi:10.1093/nar/gkx328

Rakover, Y. T., Admoni, O., Elias-Assad, G., London, S., Barhoum, M. N., Ludar, H., et al. (2021). The evolving role of whole-exome sequencing in the management of disorders of sex development. *Endocr. Connect.* 10, 620–629. doi:10.1530/EC-21-0019

Randolph, K., Hyder, U., and D'Orso, I. (2022). KAP1/TRIM28: transcriptional activator and/or repressor of viral and cellular programs? *Front. Cell. Infect. Microbiol.* 12, 834636. doi:10.3389/fcimb.2022.834636

Raymond, C. S., Murphy, M. W., O'Sullivan, M. G., Bardwell, V. J., and Zarkower, D. (2000). Dmrt1, a gene related to worm and fly sexual regulators, is required for mammalian testis differentiation. *Genes. Dev.* 14 (14), 2587–2595. doi:10.1101/gad.834100

Richardson, S. R., Morell, S., and Faulkner, G. J. (2014). L1 retrotransposons and somatic mosaicism in the brain. *Annu. Rev. Genet.* 48, 1–27. doi:10.1146/annurev-genet-120213-092412

Rossitto, M., Dejardin, S., Rands, C. M., Le Gras, S., Migale, R., Rafiee, M. R., et al. (2022). TRIM28-dependent SUMOylation protects the adult ovary from activation of the testicular pathway. *Nat. Commun. Jul* 29 (13), 4412. doi:10.1038/s41467-022-32061-1

Rowe, H. M., Jakobsson, J., Mesnard, D., Rougemont, J., Reynard, S., Aktas, T., et al. (2010). KAP1 controls endogenous retroviruses in embryonic stem cells. *Nature* 463, 237–240. doi:10.1038/nature08674

Santana-Garcia, W., Castro-Mondragon, J. A., Padilla-Galvez, M., Nguyen, N. T. T., Elizondo-Salas, A., Ksouri, N., et al. (2022). RSAT 2022: regulatory sequence analysis tools. *Nucleic Acids Res.* 50 (50), W670–W676. doi:10.1093/nar/gkac312

Schartl, M., Schories, S., Wakamatsu, Y., Nagao, Y., Hashimoto, H., Bertin, C., et al. (2018). Sox5 is involved in germ-cell regulation and sex determination in medaka following co-option of nested transposable elements. *BMC Biol. Jan.* 29 (16), 16. doi:10.1186/s12915-018-0485-8

Schmidt, D., Ovitt, C. E., Anlag, K., Fehsenfeld, S., Gredsted, L., Treier, A. C., et al. (2004). The murine winged-helix transcription factor Foxl2 is required for granulosa cell differentiation and ovary maintenance. *Dev. Feb* 131, 933–942. doi:10.1242/dev.00969

Sekido, R., and Lovell-Badge, R. (2008). Sex determination involves synergistic action of SRY and SF1 on a specific Sox9 enhancer. *Nature* 453, 930–934. doi:10.1038/nature06944

Sinclair, A. H., Berta, P., Palmer, M. S., Hawkins, J. R., Griffiths, B. L., Smith, M. J., et al. (1990). A gene from the human sex-determining region encodes a protein with homology to a conserved DNA-binding motif. *Nature* 346, 240–244. doi:10.1038/346240a0

Stevant, I., Kuhne, F., Greenfield, A., Chaboissier, M. C., Dermitzakis, E. T., and Nef, S. (2019). Dissecting cell lineage specification and sex fate determination in gonadal somatic cells using single-cell transcriptomics. Cell reports 26, 3272–3283. doi:10.1016/j.celrep.2019.02.069

Stevant, I., Neirijnck, Y., Borel, C., Escoffier, J., Smith, L. B., Antonarakis, S. E., et al. (2018). Deciphering cell lineage specification during male sex determination with single-cell RNA sequencing. *Cell. Rep.* 22 (22), 1589–1599. doi:10.1016/j.celrep.2018.01.043

Svoboda, P., Stein, P., Anger, M., Bernstein, E., Hannon, G. J., and Schultz, R. M. (2004). RNAi and expression of retrotransposons MuERV-L and IAP in preimplantation mouse embryos. *Dev. Biol.* 269, 276–285. doi:10.1016/j.ydbio.2004.01.028

Todd, C. D., Deniz, O., Taylor, D., and Branco, M. R. (2019). Functional evaluation of transposable elements as enhancers in mouse embryonic and trophoblast stem cells. *Elife. Apr* 23, e44344. doi:10.7554/eLife.44344

Vining, B., Ming, Z., Bagheri-Fam, S., and Harley, V. (2021). Diverse regulation but conserved function: SOX9 in vertebrate sex determination. *Genes.Genes. (Basel). Mar.* 26, 486. doi:10.3390/genes12040486

Wagner, T., Wirth, J., Meyer, J., Zabel, B., Held, M., Zimmer, J., et al. (1994). Autosomal sex reversal and campomelic dysplasia are caused by mutations in and around the SRY-related gene SOX9. *Cell.* 79, 1111–1120. doi:10.1016/0092-8674(94)90041-8

Wang, Q., Li, M., Wu, T., Zhan, L., Li, L., Chen, M., et al. (2022). Exploring epigenomic datasets by ChIPseeker. *Curr. Protoc.* 2, e585. doi:10.1002/cpz1.585

Warr, N., Siggers, P., Bogani, D., Brixey, R., Pastorelli, L., Yates, L., et al. (2009). Sfrp1 and Sfrp2 are required for normal male sexual development in mice. *Dev. Biol.* 15 (326), 273–284. doi:10.1016/j.ydbio.2008.11.023

Yang, W. R., Ardeljan, D., Pacyna, C. N., Payer, L. M., and Burns, K. H. (2019). SQuIRE reveals locus-specific regulation of interspersed repeat expression. *Nucleic Acids Res. Mar.* 18, 47:e27. doi:10.1093/nar/gky1301

Zhao, L., Wang, C., Lehman, M. L., He, M., An, J., Svingen, T., et al. (2018). Transcriptomic analysis of mRNA expression and alternative splicing during mouse sex determination. *Mol. Cell. Endocrinol.* 478, 84–96. doi:10.1016/j.mce.2018.07.010

Zhou, S., Sakashita, A., Yuan, S., and Namekawa, S. H. (2022). Retrotransposons in the mammalian male germline. *Sex. Dev. Mar.* 1, 404–422. doi:10.1159/000520683

Zhou, X., Sam, T. W., Lee, A. Y., and Leung, D. (2021). Mouse strain-specific polymorphic provirus functions as cis-regulatory element leading to epigenomic and transcriptomic variations. *Nat. Commun. Nov.* 9 (12), 6462. doi:10.1038/s41467-021-26630-z

frontiers | Frontiers in Cell and Developmental Biology

TYPE Original Research
PUBLISHED 02 February 2024
DOI 10.3389/fcell.2024.1353598

OPEN ACCESS

EDITED BY
Talia L. Hatkevich,
Duke University, United States

REVIEWED BY
Sarah Scalercio,
Instituto de Ciência e Tecnologia em Biomodelos (ICTB), Brazil
Ciro Amato,
National Institute of Environmental Health Sciences (NIH), United States

*CORRESPONDENCE
Brandon R. Menzies,
menziesb@unimelb.edu.au

RECEIVED 11 December 2023
ACCEPTED 18 January 2024
PUBLISHED 02 February 2024

CITATION
Menzies BR, Tarulli GA, Frankenberg SR and Pask AJ (2024), Therian origin of INSL3/RXFP2-driven testicular descent in mammals. *Front. Cell Dev. Biol.* 12:1353598. doi: 10.3389/fcell.2024.1353598

Therian origin of INSL3/RXFP2-driven testicular descent in mammals

Brandon R. Menzies*, Gerard A. Tarulli, Stephen R. Frankenberg and Andrew J. Pask

School of BioSciences, Faculty of Science, The University of Melbourne, Melbourne, VIC, Australia

Introduction: During early development in most male mammals the testes move from a position near the kidneys through the abdomen to eventually reside in the scrotum. The transabdominal phase of this migration is driven by insulin-like peptide 3 (INSL3) which stimulates growth of the gubernaculum, a key ligament connecting the testes with the abdominal wall. While all marsupials, except the marsupial mole (*Notoryctes typhlops*), have a scrotum and fully descended testes, it is unclear if *INSL3* drives this process in marsupials especially given that marsupials have a different mechanism of scrotum determination and position relative to the phallus compared to eutherian mammals.

Methods: To understand if INSL3 plays a role in marsupial testicular descent we have sequenced and curated the *INSL3* gene and its receptor (*RXFP2*) in a range of marsupials representing every order. Furthermore, we looked at single cell RNA-seq and qPCR analysis of INSL3 in the fat-tailed dunnart testis (*Sminthopsis crassicaudata*) to understand the location and timing of expression during development.

Results: These data show a strong phylogenetic similarity between marsupial and eutherian orthologues, but not with monotreme INSL3s which were more similar to the ancestral RLN3 gene. We have also shown the genomic location of *INSL3*, and surrounding genes is conserved in a range of marsupials and eutherians. Single cell RNA-seq and qPCR data show that *INSL3* mRNA is expressed specifically in Leydig cells and expressed at higher levels during the testicular descent phase in developing marsupials.

Discussion: Together, these data argue strongly for a therian origin of INSL3 mediated testicular descent in mammals and suggests that a coordinated movement of the testes to the abdominal wall may have preceded externalization in marsupials and therian mammals.

KEYWORDS

testicular descent, scrotum, marsupial, dunnart, development

Introduction

Testicular descent is present in more than 99% of extant mammals and is thought to have arisen due to the evolution of endothermy and the resulting temperature-induced negative effects on sperm production (Werdelin and Nilsonne, 1999; Kleisner et al., 2010). However, there are numerous eutherian mammals, namely within Afrotheria, with either partial testicular descent or internal testes (testicond), while both living species of monotremes are testicond (Sharma et al., 2018). Thus, the evolution of testicular

10.3389/fcell.2024.1353598

TABLE 1 Species and associated accession numbers for sequences used in phylogenetic analyses.

Species	*RLN1*	*RLN3*	*INSL3*	*RXFP2*
Human	NM_006911.4	AF_447451.1	NM_001265587.2	NM_130806.3
Mouse	NM_011272.2	NM_173184.1	NM_013564.7	NM_080468.2
Dog	NM_001003132.1	XM_038567067.1	NM_001002962.1	NM_001005870.1
Rabbit	NM_001082320.1	NM_001122941.1	NM_001122941.1	XM_017350149.2
Wombat	N/A	XM_027851320.1	XM_043980545.1	XM_027877598.1
Koala	XM_021006313.1	XM_020995055.1	XM_021009096.1	XM_020997197.1
Tasmanian devil	XM_02349710.2	XM_031947695.1	XM_003762760.4	XM_003764504.3
Opossum	XM_007499309.3	XM_001377431.4	XM_007489659.3	XM_007495281.3
Monito del monte	XM_043974591.1	XM_043995161.1	XM_043980545.1	XM_043997436.1
Agile gracile opossum	N/A	XM_044658451.1	XM_044658657.1	XM_044668960.1
Brushtail possum	XM_036738887.1	XM_036752124.1	XM_036751821.1	XM_036744005.1
Platypus	XM_007655587.2	NM_001122689.1	NM_001122688.1	XM_039915010.1
Echidna	XM_038769380.1	XM_038771772.1	XM_038771846.1	XM_038762176.1

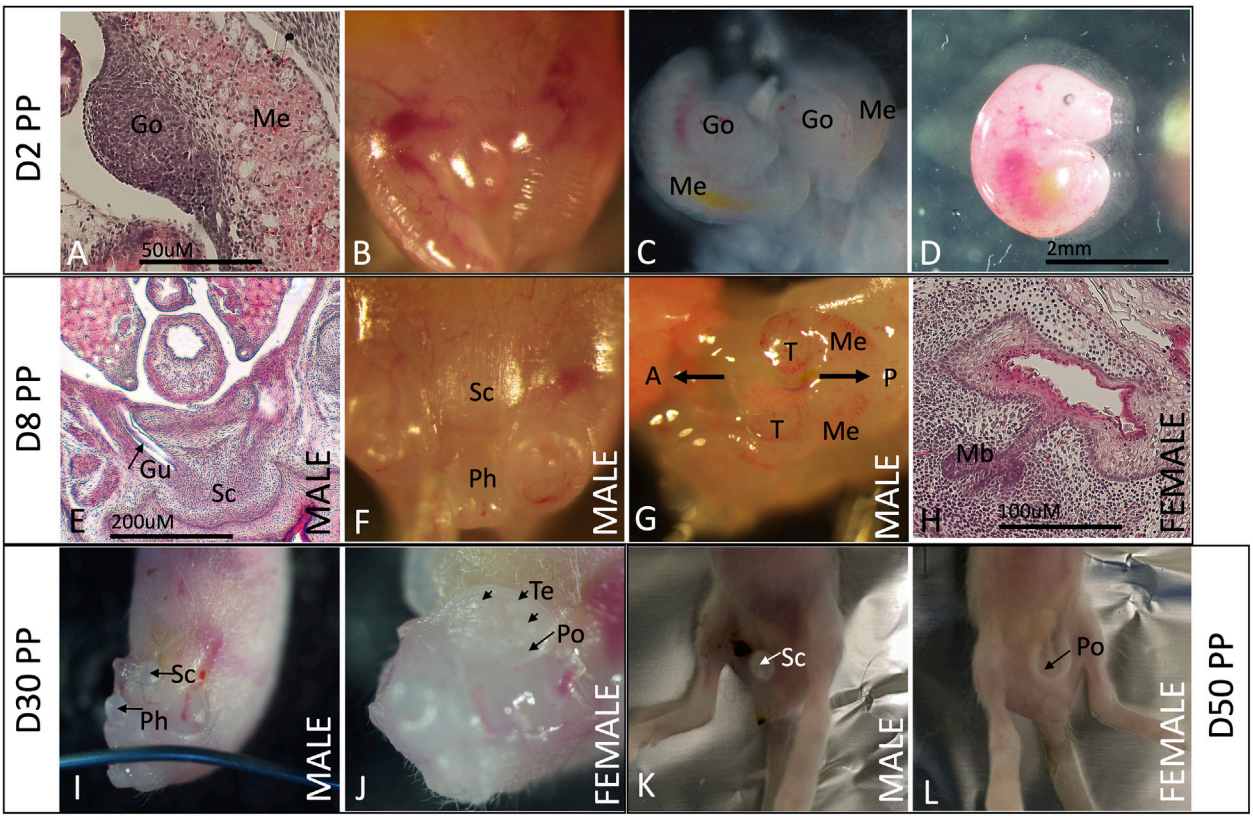

FIGURE 1
Testicular descent and scrotum/mammary region development in the fat-tailed dunnart. From D2–8 PP, the gonads are intra-abdominal, while the developing scrotal bulge is visible in males by D8 **(A, C, D, E–G)**. At D2, there is very little differentiation of the epidermis that will later form the scrotum in males or the mammary glands and pouch in females **(B)**. In D8 females, the mammary primordia are well differentiated, and mammary buds have started to form **(H)**. By D30, the testes are descending transabdominally, and the scrotum is fully formed **(I)**. Females have visible teats and a pouch lip by D30 PP **(J)**. By D50 PP the testes are inguinal, and the scrotum/pouch is are clearly visible **(K, L)**. Testes fully descend into the scrotum by D60 PP. A: anterior, P: posterior, Go: gonad, Gu: gubernaculum, Me: mesonephros, Mb: mammary buds, Ph: phallus, Po: pouch, T: testis, and Te: teat.

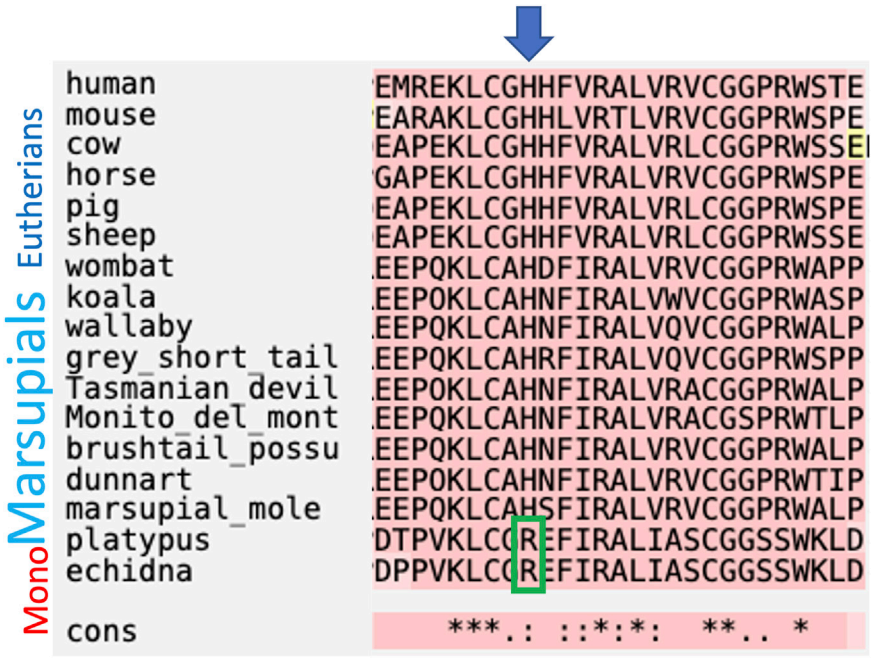

FIGURE 2
Comparison of amino acid sequences for the INSL3 beta chain between mammals. INSL3 binding to its receptor (RXFP2) is conferred by a single R to H amino acid substitution that is absent present in monotremes.

descent and externalization of the testes in mammals is complex and difficult to reconstruct phylogenetically.

Testicular descent occurs in two phases: a transabdominal phase where the testes migrate from a position near the kidneys to the lower abdomen, and an inguinal phase where they move through the abdomen via the inguinal canal into the scrotum (Foresta et al., 2008; Hutson et al., 2015). Insulin-like peptide-3 (INSL3) is expressed by Leydig cells of the testis and is crucial for the transabdominal phase of testicular descent, and loss of function causes the testes to remain in the ovarian position near the kidneys in mice (Zimmermann et al., 1999). Furthermore, the overexpression of INSL3 in female mice results in sub-abdominal ovaries (Adham et al., 2002). A number of afrotherian mammals that have lost testicular descent have premature stop or nonsense mutations in either *INSL3* or its receptor *RXFP2*, making them non-functional (Sharma et al., 2018), demonstrating a secondary loss of this pathway as opposed to its absence in these species.

INSL3 is most closely related to the relaxin-3 peptide in mammals and evolved via the duplication of a specific relaxin-like family locus (RFLC-I) that occurred in the last common ancestor of teleosts and tetrapods approximately 450 million years ago (Park et al., 2008). RFLC-I was the ancestral locus that became the *RLN3* gene in mammals. Its duplication created RLFC-II, which became *INSL3* in therian mammals. The role of INSL3 in testicular descent appears to have evolved in the ancestor of therian mammals not only because monotremes have internal testes and lack a gubernaculum but also because monotreme *INSL3* does not group with therian *INSL3* sequences phylogenetically and is more similar to mammalian *RLN3* sequences (Park et al. 2008). Furthermore, a specific amino acid substitution from arginine (R) to histidine (H) at residue 12 of the INSL3 beta chain is crucial for RXFP2-specific binding and is absent in monotremes (Park et al., 2008).

While all marsupials appear to have some form of testicular descent, the role of INSL3 in this pathway has not yet been evaluated other than to show that *INSL3* is present in the genome of the gray short-tailed opossum (Park et al., 2008). Furthermore, marsupials have a different genetic mechanism for scrotum specification than that of eutherian mammals, whereby its development is genetically regulated and based on X-chromosome dosage and not hormonally dependent as in eutherians (Sharman et al., 1970; Watson et al., 1997). As a result, intersex XXY marsupials have a pouch, phallus, and internal testes, while XO marsupials have a scrotum, ovaries, and no pouch. Furthermore, treatment of neonatal marsupials with either androgens or estrogens does not affect the development of either the mammary glands, pouch, or scrotum (Shaw et al., 1988). Finally, the location of the scrotum in all marsupials is cranial to the penis as opposed to caudal as in all eutherians (Sharman, 1970). Given that the marsupial scrotum may be analogous to that of eutherians but not homologous, it is entirely possible that marsupials may have a different mechanism of testicular descent.

Here, we curated the *INSL3* and *RXFP2* sequences from representatives of every order of marsupials and show that marsupial *INSL3* sequences group phylogenetically with eutherians but not monotremes, while all marsupials have the crucial amino acid substitution that allows RXFP2-specific binding (Arg to His at position 12 of the *INSL3* beta chain). We demonstrated genomic synteny in the *INSL3* position within the genomes of five marsupials. We also showed the Leydig cell-

10.3389/fcell.2024.1353598

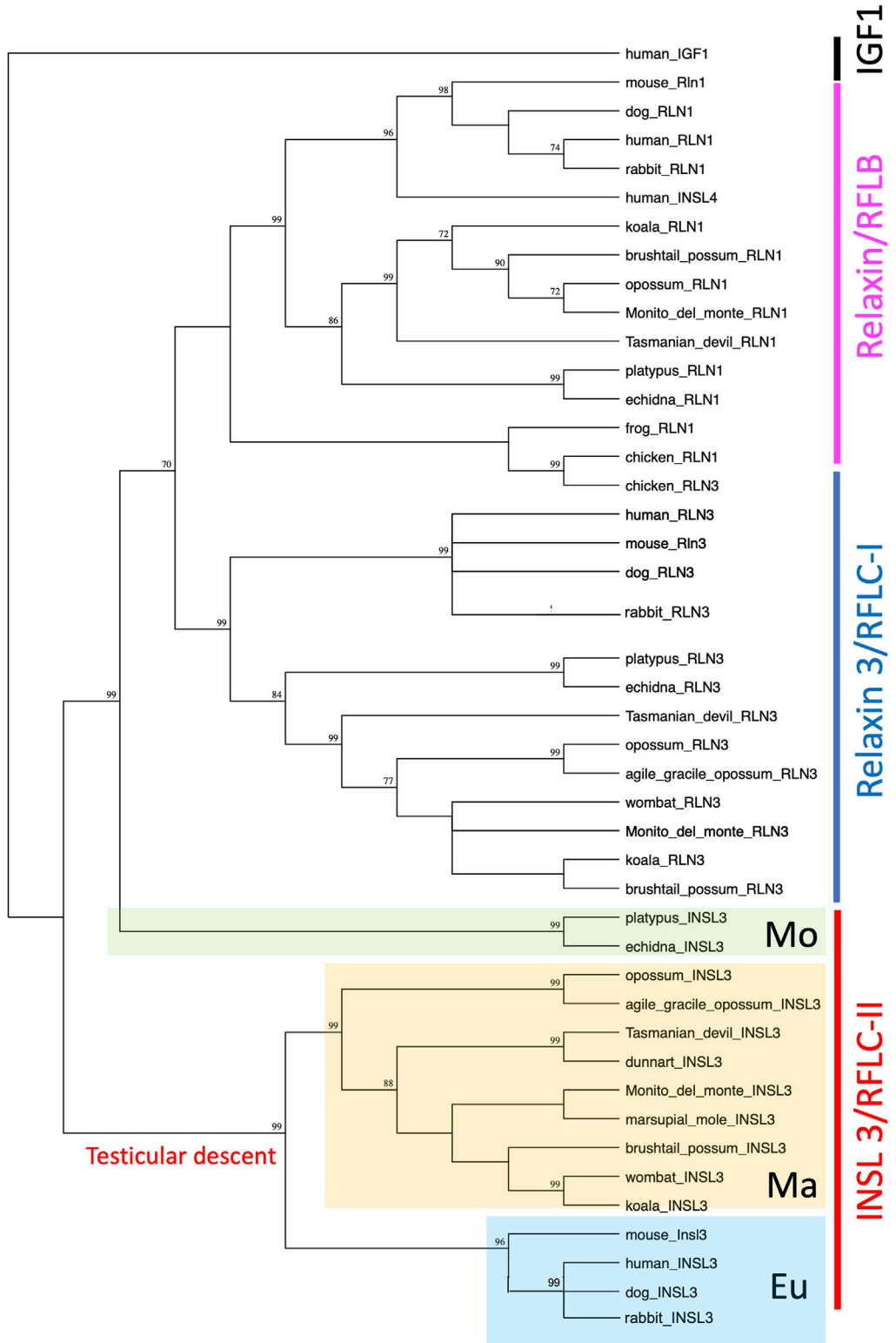

FIGURE 3
Phylogenetic comparison of the RLN1/RLN3/INSL3 family of sequences in vertebrates. Phylogenetic analysis shows that all therian *INSL3* sequences group together, while monotreme *INSL3s* group separately.

specific expression of *INSL3* mRNA in the fat-tailed dunnart (*Sminthopsis crassicaudata*) and a significant upregulation of *INSL3* mRNA expression during the key period of testicular descent in this species [D30–60 post-partum (pp)]. Combined, these data clearly demonstrate a similar role for INSL3 in marsupial testicular descent and show conclusively that this

10.3389/fcell.2024.1353598

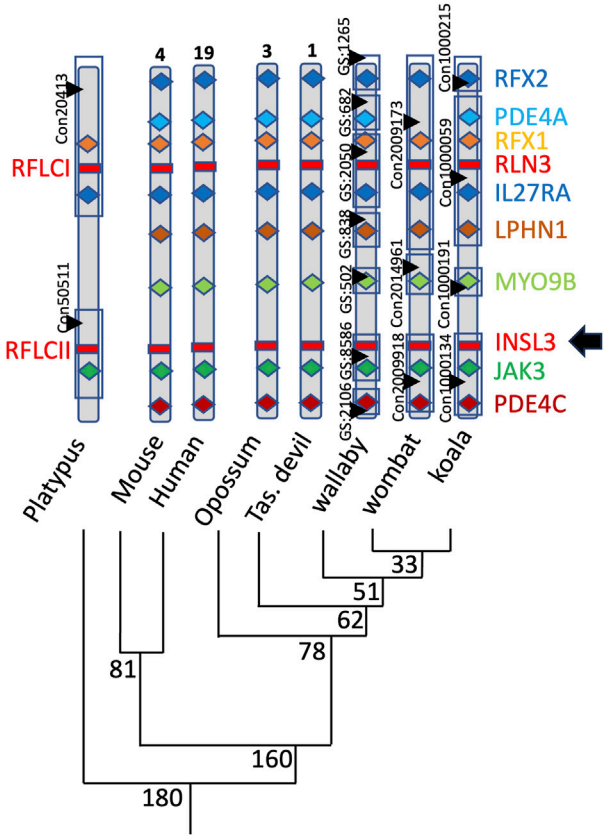

FIGURE 4
Position of INSL3 within the genomes of a range of marsupials. Mammalian *INSL3* genes are all located in the same position within the genome between the *Myosin 9B* and *Janus Kinase 3* genes, indicating a likely conserved regulation and function.

process evolved in the ancestor of therian mammals at least 160 million years ago.

Methods

Collection of pouch young/tissues

All animal procedures, including laboratory breeding, were conducted in accordance with the current Australian Code for the Care and Use of Animals for Scientific Purposes and were approved by the University of Melbourne Institutional Animal Ethics Committee (#10206) and with the appropriate wildlife permits from the Department of Environment, Land, Water, and Planning. Animals were housed in a breeding colony at the University of Melbourne School of BioSciences. Pouch young (PY) were aged from the approximate day (D) of birth and were removed by exposing the mother's pouch and applying gentle traction between the nipple and mouth while supporting/cradling the head/body using fingertips. PY were placed on a Petri dish on ice to provide ice anesthesia and then decapitated using a razor blade. Gonads were immediately dissected from the PY, snap-frozen in liquid nitrogen, and stored at −80°C for later analysis. These tissues were collected opportunistically from PY killed for other ethically approved experiments. The sex of PY and gonads was determined at the earliest ages (D2 pp and D5 pp) by SRY PCR of genomic DNA and at later ages by visualization of the developing pouch or scrotum.

Histological analyses

Whole dunnart PY were fixed in 4% paraformaldehyde for 24 h and then washed three times in 1x phosphate-buffered saline for 30 min each wash and then stored at 4°C until processing into wax blocks for sectioning. Sections were taken at 10 µm intervals, mounted on glass slides, and stained with hematoxylin and eosin.

RNA extraction, cDNA synthesis, primers, and qPCR methods

Total RNA was extracted from frozen gonads using the Sigma GenElute Total Mammalian RNA Tissue Kit (#RTN70-1KT). RNA was then converted to cDNA using the Superscript IV system (Thermo Fisher Scientific, Massachusetts) and OligoDT primers. Primer sequences for this study included dunnart *INSL3* forward (TCTGTGCCCACAACTTCATC) and reverse (AGGCCAGCA GGTCTTGTTT), *RXFP2* forward (AACATTCGTCCAGGAAAA CG) and reverse (TGTTCTCTGATGCCATCTGC), TATA-box binding protein forward (TBP; TTTCCCATAAGATTAGAAGGG CTGG) and reverse (GCTTCATAGATCTCTGCTCTGACC), and pumilio RNA binding family member 1 forward (PUM1; ATGGAG CATGTTGGCATGGA) and reverse (CCTATGTGAGGCTGA TGGGC) and were designed to span introns to eliminate amplification of gDNA. We chose these genes as they have previously been used to compare gene expression levels in the testis. Quantification was performed using a QuantStudio 5 Real-Time PCR System (Applied Biosystems, Massachusetts) and PowerTrack SYBR Green Master Mix (Thermo Fisher Scientific, Massachusetts) in a 10 µL reaction containing 5 µL SYBR, 3 uL sterile water, 0.5 µL each of 10 µL forward and reverse primers, respectively, and 1 µL of diluted cDNA (1:5 in sterile water). Quantitative PCR was conducted with an initial step of 95°C for 20 s, 40 cycles of 95°C for 1 s, and then 56°C for 20 s. Results were calculated using the delta CT method, and the expression was shown relative to the dunnart *PUM1* housekeeping gene. We also compared the expression relative to the dunnart TBP housekeeping gene, which showed the same general pattern (Supplementary Figure S1). Data are presented as the mean +/- the standard error, with significant differences determined by the two-sample *t*-test.

RNA-seq data

Dunnart single-cell RNA-seq data were derived from a larger study to be published in another manuscript. Dissociated single cells from juvenile and adult male dunnarts (n = 2 total, pooled) were processed using the Clontech SMART-Seq v4 3' DE kit. Libraries were prepared using the Illumina Nextera XT DNA Sample Preparation Kit and sequenced at 1 million reads per cell (12 cells per multiplexed library) on an Illumina Nextseq

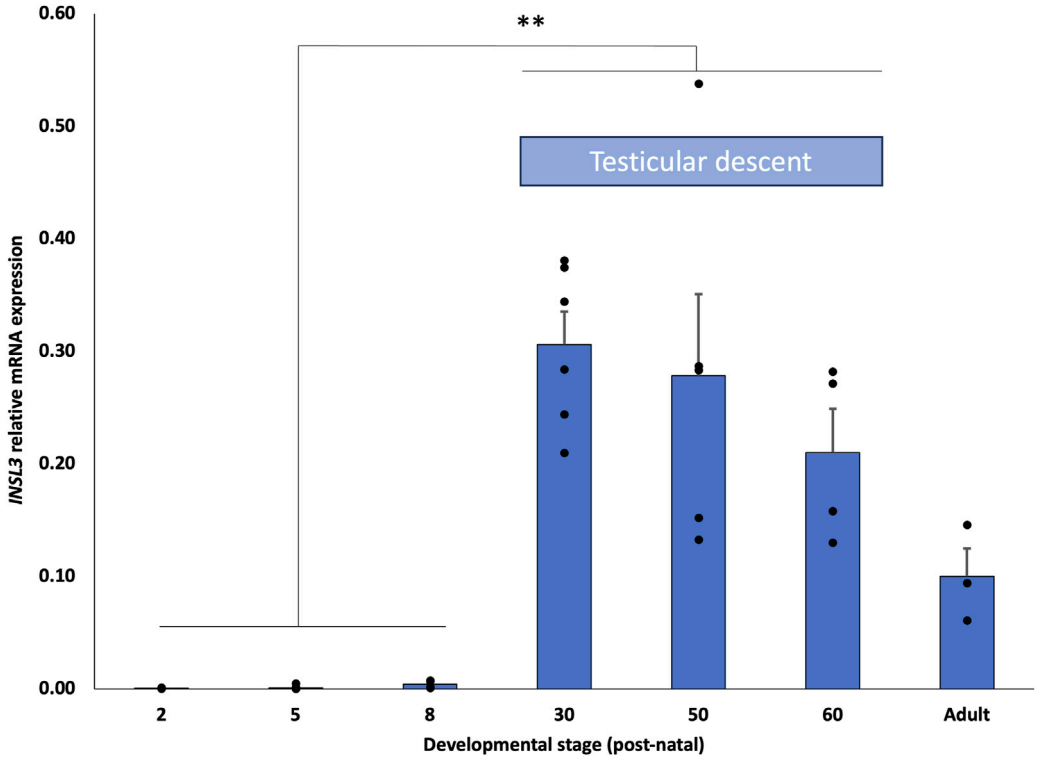

FIGURE 5
Developmental expression profile of *INSL3* mRNA in dunnart testis. *INSL3* mRNA expression is significantly elevated in developing marsupial testes during the critical period of testicular descent (D15–60 PP).

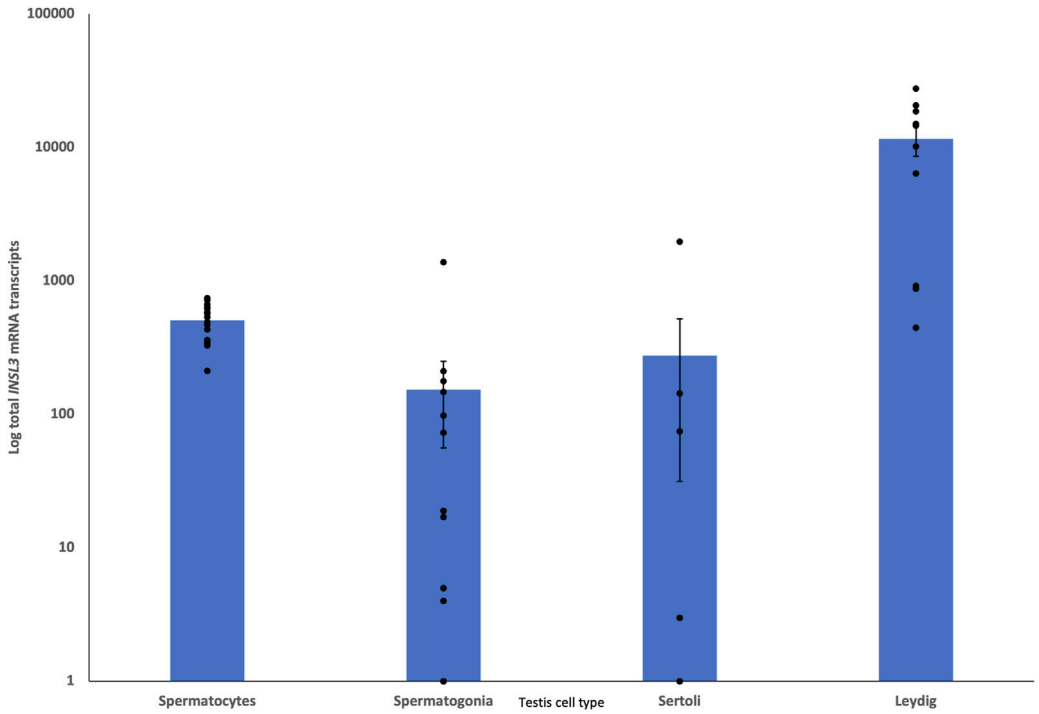

FIGURE 6
Single-cell RNA-seq comparison of presumptive testis cells for *INSL3* expression. *INSL3* expression is at least 30 times higher in Leydig cells than in other testis cell types, demonstrating that *INSL3* originates from a similar cell type (Leydig) as the eutherian species.

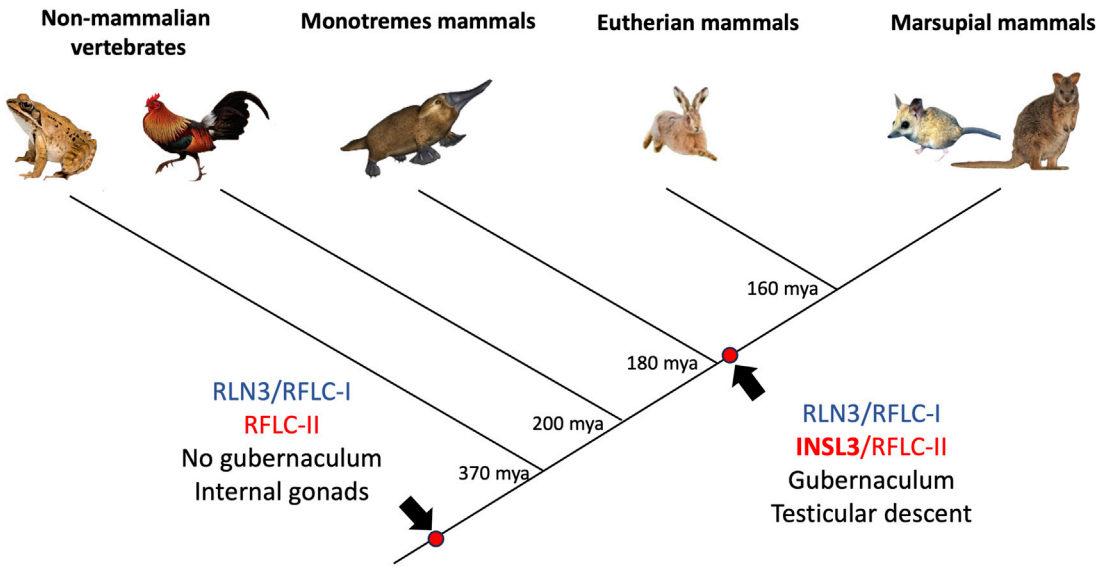

FIGURE 7
Phylogenetic reconstruction of the relaxin family locus (RFL) and the origin of INSL3/RXFP2-mediated testicular descent in vertebrates. Monotremes and non-mammalian vertebrates (after the split from tetrapods) possess two *RFLC* genes denoted as *RFLC-I* and *RFLC-II*. These genes encode *RLN3* and *INSL3* in therian mammals, respectively. However, the monotreme *RFLC-II* gene groups phylogenetically with the ancestral *RLN3* gene as opposed to all therian (eutherian and marsupial) *INSL3* genes, which suggests it arose independently in a therian ancestor to drive testicular descent (a character trait of 99.9% of therian mammals).

500 platform. Using the Galaxy web-based analysis platform (https://usegalaxy.org/), de-multiplexed reads were mapped to dunnart genomic scaffolds (S.R.F. and A.J.P., unpublished) using Bowtie for Illumina (default parameters) and assembled into transcripts using StringTie and StringTie merge. StringTie was then reapplied to the mapped reads using the StringTie merge output as a transcript reference file to produce the TPM (transcripts per million) dataset reported here. *INSL3* was identified among the StringTie merge-assembled transcripts using BLASTn. Presumptive somatic and germ cells were identified using the following established markers: Leydig cells (10 in total) were identified by the expression of *steroidogenic acute regulatory protein* (*STAR*), *luteinizing hormone receptor* (*LHR*), and *nuclear receptor subfamily 2 group F member 2* (*NR2F2*), Sertoli cells (8 in total) by *SRY-box transcription factor-9* (*SOX9*), and *claudin-11* (*CLDN11*), spermatocytes (16 cells in total) by *synaptonemal complex protein-1* (*SYCP1*) and *piwi-like RNA-mediated gene silencing-2* (*PIWIL2*), and spermatogonia (14 cells in total) by two or more of the following *POU class 5 homeobox-1* (*POU5F1*), *inhibitor of DNA binding-4* (*ID4*), *NANOG*, *NANOS3*, *GDNF family receptor alpha-1* (*GFRA1*), and *CXC motif chemokine receptor-4* (*CXCR4*). The data are presented as an average of total *INSL3* transcripts per cell between presumptive cell types.

Sequence curation and phylogenetic analysis

INSL3, *RLN3*, and *RLN1* nucleotide sequences for human (*Homo sapiens*), mouse (*Mus musculus*), rabbit (*Oryctolagus cuniculus*), dog (*Canis lupus familiaris*), wombat (*Vombatus ursinis*), koala (*Phascolarctus cinereus*), opossum (*Monodelphis domestica*), Tasmanian devil (*Sarcophilus harrisii*), Monito del monte (*Dromiciops gliroides*), brushtail possum (*Trichosurus vulpecula*), agile gracile opossum (*Gracilanus agilis*), platypus (*Ornythorynchus anatinus*), and echidna (*Tachyglossus aculeatus*) were curated by BLAST search of publicly accessible genomes using NCBI (Table 1). *INSL3* nucleotide sequences for *S. crassicaudata* (GenBank: OR839190) and *Notoryctes typhlops* (GenBank: OR839192) and *RXFP2* nucleotide sequences for *S. crassicaudata* (GenBank: OR839191) were curated by searching unpublished genomes in our laboratory. These sequences have been submitted to GenBank. Sequences were aligned using MUSCLE, and phylogeny was determined using the neighbor-joining method with 1,000 bootstrap replicate analyses using human *IGF1* as an outgroup (MacVector).

Results

Histological and macroscopic description of testicular descent and the development of the pouch and scrotum in the fat-tailed dunnart

Some details regarding testicular descent in the fat-tailed dunnart have been documented previously from micro-CT data (Cook et al., 2021), including that the mammary primordia differentiate at about D2 PP while the scrotum starts to differentiate at about D4 PP and that the testes are fully

descended into the scrotum by D60 PP. Here, we added to that developmental profile with post-natal pictures and descriptions of the gonads and external development of the pouch and scrotum in the dunnart. At D2, the gonads (Go) can be seen as small translucent spheres that sit in an anterior-medial position in the abdomen next to the mesonephros (Figures 1A, C; Me). There is no overt pouch (Po) or scrotum (Sc) structure at this stage (Figures 1B, D). At D8 PP, there is a well-defined scrotal bulge both histologically (Figure 1E) and macroscopically (Figure 1F), and the gubernaculum (Gu) can clearly be seen linking the scrotum with the testes. Up until D8, the gonads and mesonephros increase slightly in size but do not change their position at all within the body cavity (Figure 1G). At D8, the mammary buds are well-developed histologically, but the pouch area is not yet visible on the surface of the abdomen except for some minute indentations of the developing teats (Figure 1H). At D30, the testes are located much lower in the abdomen, separate from the mesonephros but not yet inguinal, while the scrotum is fully formed (Figure 1I). The D30 PP female has a well-defined pouch ring and teats (Figure 1J). By D50, the scrotum and pouch region are very well differentiated (Figures 1K, L).

Nucleotide sequence and genomic comparisons of marsupial INSL3 and RXFP2

The full-length coding *INSL3* cDNA and predicted amino acid sequences were not highly conserved among therian mammals overall (approximately 40% and 45% identity, respectively). However, the nucleotide and amino acid sequences for the *INSL3* beta chain, which confers specific binding to RXFP2, were 75% and 80% identical, respectively. Importantly, a key amino acid residue substitution from arginine (R) to histidine (H) at position 12 of the INSL3 beta chain, was demonstrated to confer specificity to RXFP2 (as opposed to both RXFP1 and -2 in monotremes and non-mammalian vertebrates), was conserved in all marsupials relative to eutherians but absent in monotremes (Figure 2).

Phylogenetically, all therian *INSL3* (*RFLC-II*) sequences, apart from monotremes, grouped together with strong bootstrap support (99; Figure 3). Monotreme INSL3s then branched off separately to the *relaxin* (*RLN1/RFLB*) and *relaxin-3* (*RLN3/RFLC-I*) sequences, also with strong bootstrap support (99; Figure 3). All mammalian RLN1 and RLN3 sequences were grouped separately, except for chicken *RLN3,* which was grouped with the other non-mammalian *RLN1* sequences.

The genomic *INSL3* locus is also conserved in marsupials relative to eutherians and monotremes located between the Myosin 9B (MYO9B) and Janus Kinase 3 (JAK3) genes in koala, wombat, tammar wallaby, Tasmanian devil, and grey short-tailed opossum (Figure 4). The marsupial RXFP2 nucleotide and amino acid sequences were highly conserved with eutherian species and showed approximately 90% and 95% sequence identity among therians, respectively.

INSL3 mRNA expression in the developing marsupial testes

We compared *INSL3* mRNA expression at seven different developmental stages in the fat-tailed dunnart (*S. crassicaudata*), D2, 5, 8, 30, 50, and 60, and adults (D200+). Expression was barely detectable from D2–8 post-partum, a developmental stage prior to testis migration from the mesonephros (Figure 5). By D30, a developmental stage in the middle of transabdominal descent, the expression was significantly higher ($p < 0.01$) than in earlier stages and had the highest nominal expression throughout early development. The expression at D50 and D60, the later stages of testicular descent, was also significantly higher than at D2–8 but progressively lower and not statistically different from that at D30. The general relative expression pattern of *INSL3* was identical in two separate housekeeping genes, with the expression relative to TPB lower than that of PUM1 from D30 to adult stages (Supplementary Figure S1).

Single-cell RNA-seq data from juvenile and adult dunnart testes showed *INSL3* expression in presumptive Leydig cells that was ×30 greater than that in the next highest cell type (presumptive spermatocytes; Figure 6).

Discussion

Taken together, these data provide considerable evidence for a therian origin of testicular descent driven by INSL3 and its receptor, RXFP2 (Figure 7). Genomic analyses show that a wide range of marsupial orders that have descended testes, namely, the Diprotodontia, Dasyuromorphia, Notoryctemorphia, Microbiotheria, and Didelphimorphia, have an *INSL3* gene located at the same genomic position as the Eutheria. Marsupial *INSL3* genes also group phylogenetically with eutherian *INSL3*, but not monotreme orthologs. The *INSL3* beta chain was very highly conserved among mammals (90% amino acid identity), probably because it is involved in RXFP2 receptor binding. Critically, all marsupials possess a key amino acid substitution in the beta chain, absent in monotremes, that confers specificity to RXFP2 as opposed to the ancestral INSL3 gene, which binds both RXFP-1 and -2 with low affinity (Park et al., 2008). The *RXFP2* gene was also highly conserved among all mammals (95% amino acid sequence identity), which may indicate a broader generalized function for RXFP2 in RLN/INSL signaling throughout the body.

In addition to the genomic evidence, we demonstrated the mRNA expression of *INSL3* in the developing testis and described the process of testicular migration and pouch/scrotum differentiation in this species. Importantly, the *INSL3* expression was predominantly from the Leydig cells and increased in the developing marsupial testes after D8 once they had started their transabdominal migration. This is consistent with data from the mouse and suggests that INSL3 is driving this process in an identical way in marsupials, by stimulation of gubernaculum growth (Zimmerman et al., 1999).

The gubernaculum connects the caudal epididymis of the testis to the scrotal wall and eventually pulls the testis into the scrotum due to its own growth and regression of the caudal suspensory ligament. The fact that marsupials appear to have the same molecular mechanism of transabdominal testicular descent and the presence of a scrotum, as in eutherians (i.e., growth of the gubernaculum via *INSL3/RXFP2* binding), but a different mechanism and location of scrotum differentiation (i.e., X-Ch dosage and pre-penial position), suggests that the presence of a scrotum may have originated in a therian ancestor, but then the position and mechanism of

determination changed after the split between eutherians and marsupials. The alternative hypothesis is that the gubernaculum originally evolved to bring the testes to the abdominal wall, after which marsupials and eutherians developed analogous scrotal structures independently. Consistent with this hypothesis, the marsupial mole (*N. typhlops*), which has subdermal testes, presumably due to the evolutionary loss of the scrotum, still has a functional *INSL3* gene, which demonstrates the continued importance of this pathway in bringing the testes to this subdermal position.

In conclusion, our data provide strong evidence for a therian origin of testicular descent and confirm the evolutionary benefit of this mechanism given the retention of this trait in the majority of therian mammals, including all marsupials.

Data availability statement

The datasets presented in this study can be found in online repositories. The names of the repository/repositories and accession number(s) can be found in the article/Supplementary Material.

Ethics statement

The animal study was approved by the Institutional Animal Ethics Committee of the University of Melbourne. The study was conducted in accordance with local legislation and institutional requirements.

Author contributions

BM: conceptualization, data curation, formal analysis, investigation, methodology, writing–original draft, and writing–review and editing. GT: methodology, resources, and writing–review and editing. SF: data curation, formal analysis, methodology, software, visualization, and writing–review and editing. AP: conceptualization, funding acquisition, methodology, resources, supervision, and writing–original draft.

Funding

The authors declare that financial support was received for the research, authorship, and/or publication of this article. Special thanks go to the Wilson Family Trust for supporting this project.

Acknowledgments

The authors thank Gaile D'Souza and Lee Whitehead for their assistance with animal husbandry and handling.

Conflict of interest

The authors declare that the research was conducted in the absence of any commercial or financial relationships that could be construed as a potential conflict of interest.

Publisher's note

Supplementary material

The Supplementary Material for this article can be found online at: https://www.frontiersin.org/articles/10.3389/fcell.2024.1353598/full#supplementary-material

References

Adham, I. M., Steding, G., Thamm, T., Bullesbach, E. E., Schwabe, C., Paprotta, I., et al. (2002). The overexpression of the insl3 in female mice causes descent of the ovaries. *Mol. Endocrinol.* 16, 244–252. doi:10.1210/mend.16.2.0772

Cook, L. E., Newton, A. H., Hipsley, C. A., and Pask, A. J. (2021). Postnatal development in a marsupial model, the fat-tailed dunnart (*Sminthopsis crassicaudata*; Dasyuromorphia: dasyuridae). *Commun. Biol.* 4 (4), 1028. Sep 2 Epub 20210902. doi:10.1038/s42003-021-02506-2

Foresta, C., Zuccarello, D., Garolla, A., and Ferlin, A. (2008). Role of hormones, genes, and environment in human cryptorchidism. *Endocr. Rev.* 29, 560–580. Epub 20080424. doi:10.1210/er.2007-0042

Hutson, J. M., Li, R., Southwell, B. R., Newgreen, D., and Cousinery, M. (2015). Regulation of testicular descent. *Pediatr. Surg. Int.* 31, 317–325. Epub 20150218. doi:10.1007/s00383-015-3673-4

Kleisner, K., Ivell, R., and Flegr, J. (2010). The evolutionary history of testicular externalization and the origin of the scrotum. *J. Biosci.* 35, 27–37. doi:10.1007/s12038-010-0005-7

Park, J. I., Semyonov, J., Chang, C. L., Yi, W., Warren, W., and Hsu, S. Y. (2008). Origin of INSL3-mediated testicular descent in therian mammals. *Genome Res.* 18, 974–985. Epub 20080507. doi:10.1101/gr.7119108

Sharma, V., Lehmann, T., Stuckas, H., Funke, L., and Hiller, M. (2018). Loss of RXFP2 and INSL3 genes in Afrotheria shows that testicular descent is the ancestral condition in placental mammals. *PLoS Biol.* 16, e2005293. Epub 20180628. doi:10.1371/journal.pbio.2005293

Sharman, G. B. (1970). Reproductive physiology of marsupials. *Science* 27 (167), 1221–1228. doi:10.1126/science.167.3922.1221

Sharman, G. B., Robinson, E. S., Walton, S. M., and Berger, R. J. (1970). Sex chromosomes and reproductive anatomy of some intersexual marsupials. *J. Reprod. Fertil.* 21, 57–68. doi:10.1530/jrf.0.0210057

Shaw, G., Renfree, M. B., Short, R. V., and Ws, O. (1988). Experimental manipulation of sexual differentiation in wallaby pouch young treated with exogenous steroids. *Dev. Dec* 104, 689–701. doi:10.1242/dev.104.4.689

Watson, C. M., Johnston, P. G., Rodger, K. A., McKenzie, L. M., O'Neill, R. J., and Cooper, D. W. (1997). SRY and karyotypic status of one abnormal and two intersexual marsupials. *Reprod. Fertil. Dev.* 9, 233–241. doi:10.1071/r96107

Werdelin, L., and Nilsonne, A. (1999). The evolution of the scrotum and testicular descent in mammals: a phylogenetic view. *J. Theor. Biol.* 7 (196), 61–72. doi:10.1006/jtbi.1998.0821

Zimmermann, S., Steding, G., Emmen, J. M., Brinkmann, A. O., Nayernia, K., Holstein, A. F., et al. (1999). Targeted disruption of the Insl3 gene causes bilateral cryptorchidism. *Mol. Endocrinol.* 13, 681–691. doi:10.1210/mend.13.5.0272

frontiers | Frontiers in Cell and Developmental Biology

TYPE Mini Review
PUBLISHED 05 February 2024
DOI 10.3389/fcell.2024.1347711

OPEN ACCESS

EDITED BY
Jae Yong Han,
Seoul National University, Republic of Korea

REVIEWED BY
Toshihiko Fujimori,
National Institute for Basic Biology, Japan
Fei Zhao,
National Institute of Environmental Health Sciences (NIH), United States
Bichun Li,
Yangzhou University, China

*CORRESPONDENCE
Craig A. Smith,
craig.smith@monash.edu

RECEIVED 01 December 2023
ACCEPTED 17 January 2024
PUBLISHED 05 February 2024

CITATION
Tan JL, Major AT and Smith CA (2024), Mini review: Asymmetric Müllerian duct development in the chicken embryo. *Front. Cell Dev. Biol.* 12:1347711. doi: 10.3389/fcell.2024.1347711

Mini review: Asymmetric Müllerian duct development in the chicken embryo

Juan L. Tan, Andrew T. Major and Craig A. Smith*

Department of Anatomy and Developmental Biology, Monash Biomedicine Discovery Institute, Monash University, Clayton, VIC, Australia

Müllerian ducts are paired embryonic tubes that give rise to the female reproductive tract. In humans, the Müllerian ducts differentiate into the Fallopian tubes, uterus and upper portion of the vagina. In birds and reptiles, the Müllerian ducts develop into homologous structures, the oviducts. The genetic and hormonal regulation of duct development is a model for understanding sexual differentiation. In males, the ducts typically undergo regression during embryonic life, under the influence of testis-derived Anti-Müllerian Hormone, AMH. In females, a lack of AMH during embryogenesis allows the ducts to differentiate into the female reproductive tract. In the chicken embryo, a long-standing model for development and sexual differentiation, Müllerian duct development in females in asymmetric. Only the left duct forms an oviduct, coincident with ovary formation only on the left side of the body. The right duct, together with the right gonad, becomes vestigial. The mechanism of this avian asymmetry has never been fully resolved, but is thought to involve local interplay between AMH and sex steroid hormones. This mini-review re-visits the topic, highlighting questions in the field and proposing a testable model for asymmetric duct development. We argue that current molecular and imaging techniques will shed new light on this curious asymmetry. Information on asymmetric duct development in the chicken model will inform our understanding of sexual differentiation in vertebrates more broadly.

KEYWORDS

Müllerian duct, chicken sexual differentiation, AMH, Amhr2, oestrogen, sex determination, sexual differentiation

1 Introduction

Morphogenesis of the female reproductive tract is critical for sexual reproduction. Understanding how the female reproductive tract develops provides important information on a critical organ system and can also broadly inform other areas biology. The female reproductive tract of amniotic vertebrates (reptiles, birds and mammals) derives from a pair of embryonic tubes called the Müllerian ducts. Early embryos of both sexes develop two pairs of undifferentiated ducts is close association with the mesonephric kidneys and the gonads; these are the Wolffian and Müllerian ducts. In male mammals, under the influence of testis-derived androgens, the Wolffian ducts become the vas deferens and epididymis of the male reproductive tract, while the Müllerian ducts disintegrate under the influence of the testis-derived factor, Anti-Müllerian Hormone (AMH). Conversely, in females, the Wolffian ducts regress and the absence of AMH allows differentiation of the Müllerian ducts into the oviduct (in mouse and chicken) and homologous structures in humans:

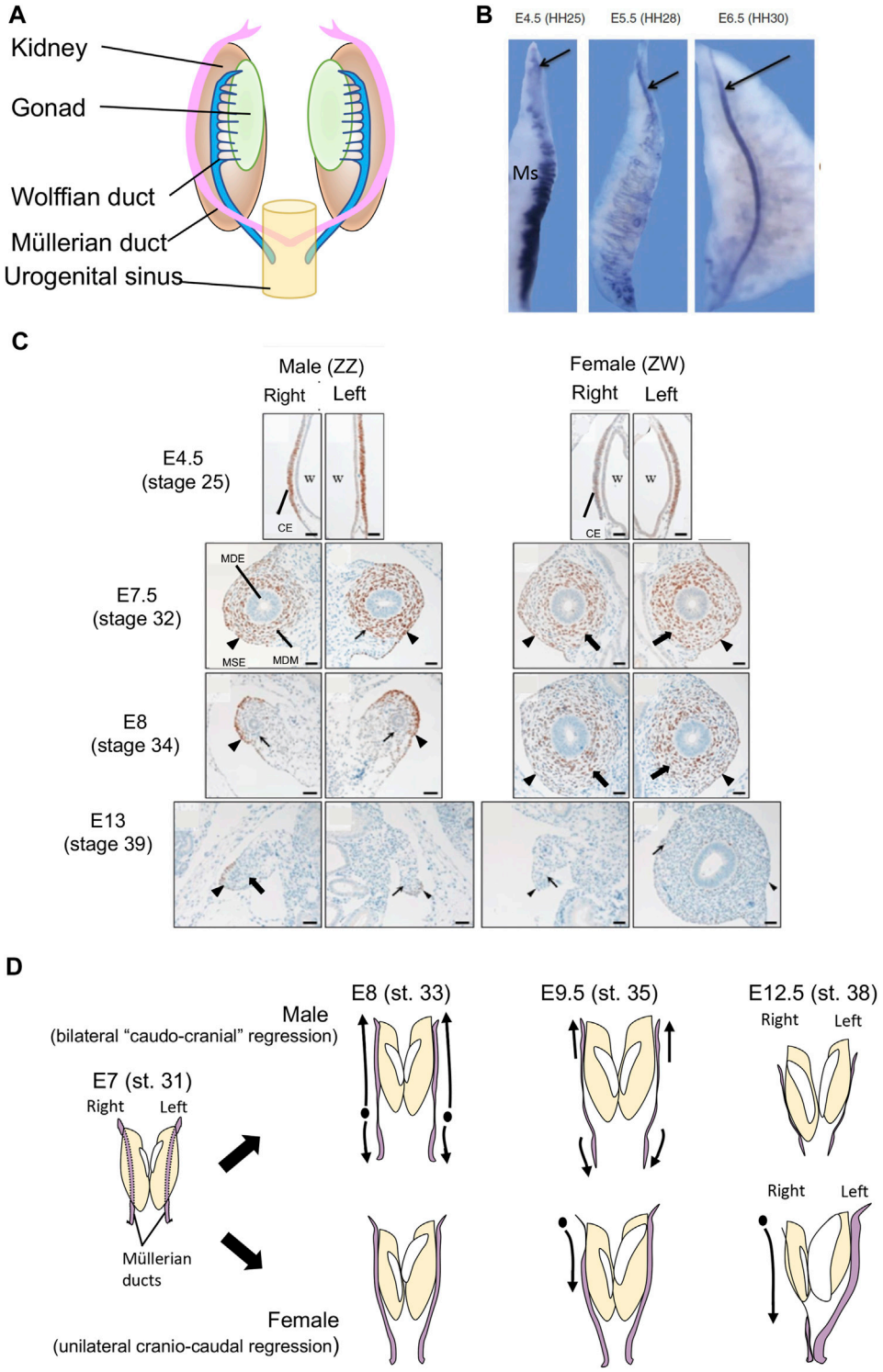

FIGURE 1
(A) Schematic of Müllerian ducts in amniotic vertebrate embryos. Müllerian ducts form in close association with the Wolffian ducts, on the surface of the embryonic kidneys (mesonephric kidneys). **(B)** Formation of the Müllerian duct in the chicken embryo, based on expression of the marker, *LIM1* (arrow). At E4.,5 (HH stage 25) the duct anlagen appears as a group of LIM1+ cells at the cranial pole of the mesonephric kidney (Ms), which also expresses some Lim1 in its tubules. AT E5.5 (HH stage 28), the duct elongates caudally through cell proliferation and caudal expansion. By E6.5 (HH stage 6.5) the duct has migrates to the posterior end of the urogenital system. **(C)** Transverse histological sections showing chicken Müllerian duct development, based on immunohistochemical staining for the marker protein, DMRT1. The ducts first form as DMRT$^+$ thickenings of coelomic epithelium (CE) overlying the Wolffian duct (W) at E4.5 (stage 25). In both the left and right sides of both sexes, this thickening gives rise to cells that migrate to form the inner Müllerian duct epithelium (MDE) and surrounding Müllerian duct mesenchyme (MDM) by E7.5 (stage 32). Both the Müllerian surface epithelium (MSE; arrowhead) and the MDM (arrow) express DMRT1. At E8 (stage 34) both male ducts undergo regression, marked by diminished mesenchyme (arrowhead) and smaller MDE (arrow). At E13 (stage 39), both male ducts are regressed and no longer express DMRT1. In females, the right duct has also regressed
(*Continued*)

FIGURE 1 (Continued)
(arrowhead and arrow), while the left duct is enlarged. It has an expanded mesenchymal domain and duct lumen, and no longer expresses DMRT1. Modified from Omotehara et al. (2014), with permission. **(D)** Schematic of chicken Müllerian duct development and regression in male and female embryos. In males, bilateral duct regression commenced from E7-E8 (stage 31–33). Regression of both ducts occur simultaneously and largely progresses in a caudo-cranial direction. In females, right duct regression commences slightly later, from E9.5 (stage 35) and progressed in a cranio-caudal direction. From the same stage, the left female duct increases in size. By E12.5, both male ducts and the right female duct have regressed, while the left female duct is well developed.

Fallopian tubes, uterus and upper vagina) (Wilson, 1978; van Tienhoven, 1983; Cate, 2022; Machado et al., 2022). Hence, proper sexual differentiation of the Müllerian ducts during embryogenesis is central to female reproductive tract development. Formation of these structures also provides a model for understanding how tubes form in biological systems more broadly (tubulogenesis).

2 AMH and sexual differentiation of the Müllerian ducts

In vertebrate embryos, the Müllerian ducts initially form in both sexes as tubes that run from the cranial to caudal pole on either side of the embryonic kidneys (mesonephric kidneys) (Figure 1A). The ducts derive from a thickened placode of cells in the coelomic epithelium overlying the cranial pole of the mesonephros. This placode comprises Müllerian epithelial and mesenchymal progenitor cells. The cells proliferate and invaginate, giving rise to a meso-epithelial tube (the Müllerian epithelium) and surrounding mesenchyme (Jacob et al., 1999; Guioli et al., 2007; Orvis and Behringer, 2007). As development proceeds, the Müllerian epithelium elongates by caudal extension through the mesenchyme, until it reaches the urogenital sinus reviewed in (Klattig and Englert, 2007; Santana Gonzalez et al., 2021). This is a conserved process among amniotic vertebrates, exemplified by the chicken embryo (Figure 1B). In mouse and/or chicken models, several genes and signalling pathways have been identified that regulate early duct specification, invagination and elongation, including the transcription factors, Lim1, Pax2, Emx2 and Dach1/2, together with Fgf, Bmp and Wnt4 signaling (Miyamoto et al., 1997; Bouchard et al., 2002; Kobayashi et al., 2004; Biason-Lauber and Konrad, 2008; Davis et al., 2008; Atsuta and Takahashi, 2016; Prunskaite-Hyyrylainen et al., 2016). Genetic manipulation of these factors blocks or impairs Müllerian duct formation (Torres et al., 1995; Vainio et al., 1999; Kobayashi et al., 2004; Orvis and Behringer, 2007; Huang et al., 2014). By embryonic day (E)13.5 in mouse and E6.5 in chicken, the ducts are well formed in both sexes. Subsequently, the fate of the Müllerian ducts in males and females diverges dramatically. Figure 1C shows Müllerian duct formation and sexual differentiation in the chicken embryo, based on transverse histological sections stained for the marker, DMRT1. As in mouse, the Müllerian duct anlagen in chicken appears as a DMRT + thickening of coelomic epithelium adjacent to the Wolffian duct. This occurs as embryonic day (E)4.5. By E7.5, proliferation and inward migration of coelomic epithelial cells has given rise to centrally located Müllerian epithelium surrounded by DMRT1+ mesenchyme. Bilateral duct regression in male embryos commences from E7.5-8 (stage 33–34). By E13 (stage 39) both male ducts are largely completely regressed (Figure 1C). In most birds, only the left duct develops into an oviduct (Figure 1D). The right Müllerian duct regresses in females, commencing from E9.5, slightly later than in male embryos (Hutson et al., 1983). This is in parallel with regression of the right gonad, which becomes vestigial. (Figures 1C, D).

In mammals, regression of the Müllerian ducts occurs in male but not female embryos under the direction of Anti-Müllerian Hormone (AMH, also called Müllerian Inhibiting Substance, MIS) (Josso and Picard, 1986; Behringer et al., 1990; Josso et al., 1993a; Josso et al., 1993b; Behringer, 1994; Behringer et al., 1994). In the mammalian embryo, AMH expression is first detectable in developing Sertoli cells of the nascent testis, regulated by factors such as Sox9, Wt1 and Sf1 (De Santa Barbara et al., 1998). In the mouse model, the *Amh* gene is expressed from E12.5, soon after the onset of the master testis-determinant, *Sry*, and pre-Sertoli cell differentiation (Munsterberg and Lovellbadge, 1991). *Amh* is not expressed in the female mouse embryos. Müllerian duct regression commences in the male mouse embryo from E13.5. It is assumed that Amh enters the embryonic blood stream from the nascent testes to exert its effects upon the adjacent Müllerian ducts, although diffusion from the gonads through the mesonephros to the duct is also possible. To induce regression, Amh must bind its cognate receptor, Amhr2, which recruits type I receptor (Josso et al., 1998; Mishina et al., 1999). These TGF-β receptors are serine-threonine kinase receptors that engage intracellular SMAD signalling to induce duct regression in males. In mouse, it has been shown that activation of Amhr2 recruits either Bmpr1a (Alk3) or Acvr1 (Alk2) type I receptors, and the three BMP receptor-Smads (Smad1, Smad5, and Smad8) function redundantly in transducing the Amh signal required for Müllerian duct regression (Visser et al., 2001; Jamin et al., 2002; 2003; Orvis et al., 2008). In mammals, the *Amhr2* gene is expressed in duct mesenchymal cells of both sexes from E12.5, based on LacZ reporter studies. However, only male embryos produce Amh, from E12.5, resulting in male-specific bilateral duct regression commencing from E13.5-E14.5 (Arango et al., 2008). *Amh*-induced regression involves activation of Wnt signaling through β-catenin, expression of metalloproteases and apoptosis (Moses and Behringer, 2019) reviewed in (Klattig and Englert, 2007; Mullen and Behringer, 2014).

3 AMH and Müllerian duct regression in the chicken embryo

The chicken embryos exhibits an unusual pattern of duct regression that serves to broaden our understanding of female reproductive tract formation. The Müllerian ducts form in the chicken embryo in the same way as in mammals, involving specification, invagination and elongation (Guioli et al., 2007; Atsuta and Takahashi, 2016; Roly et al., 2018; Roly et al., 2020b).

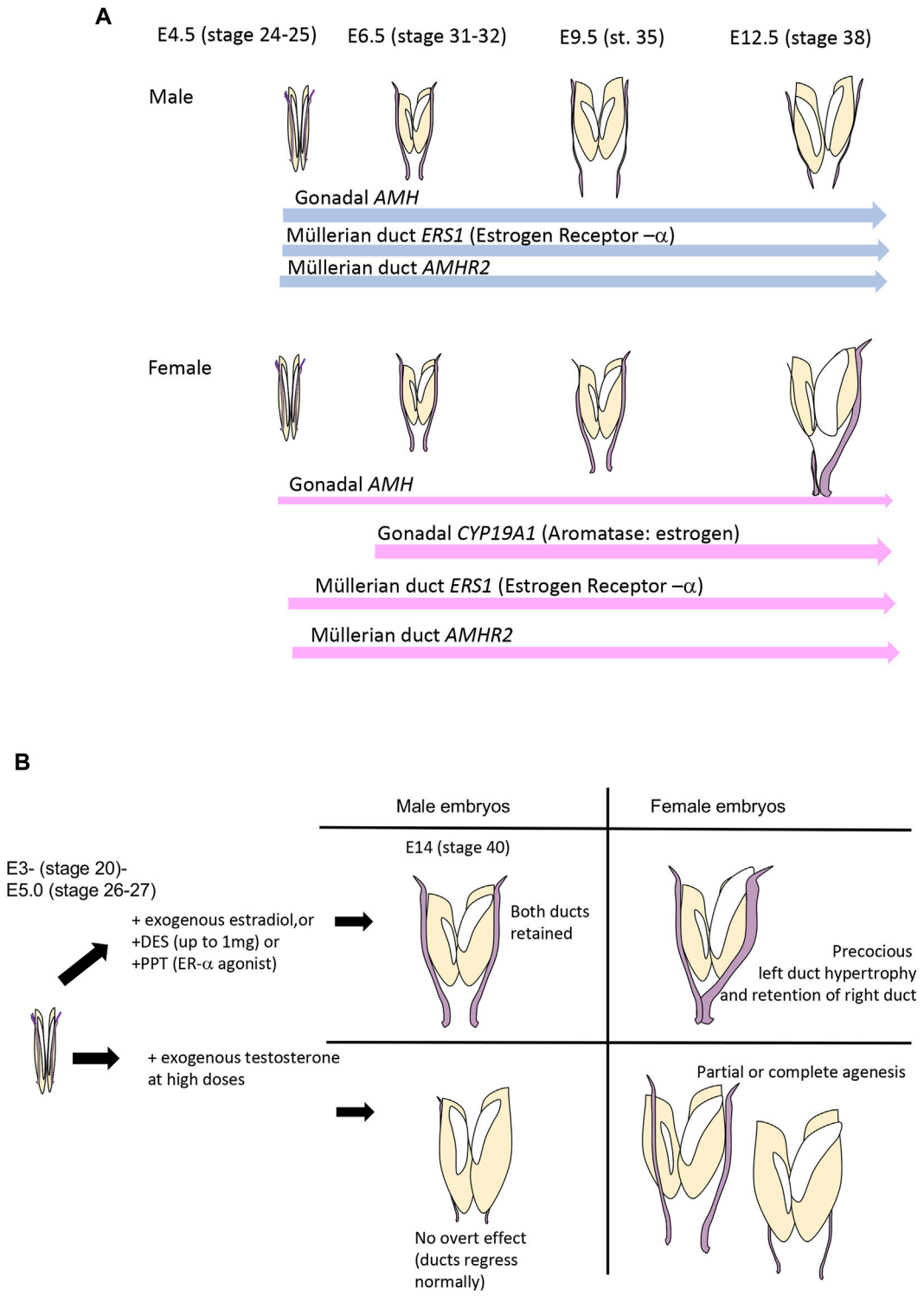

FIGURE 2
(A) Timeline of critical gene expression relevant to Müllerian duct regression in the chicken embryo. AMH is expressed in the gonads of both sexes at E4.5 (stage 25) even before the onset of gonadal sex differentiation at E6.0-E6.5. Expression is always higher in males. Expression of *AMHR2* occurs in the ducts of both sexes, and in both sides, from E4.5. Precise quantification has not been reported. *ESR1*, encoding estrogen receptor-α, is also expressed in both ducts of both sexes, from E4.5, but, again, precise quantification has not been reported. Estrogen is only produced in female embryos, as *CYP19A1*, encoding Aromatase enzyme, is only expressed in (both) female gonads from E6.0—E6.5 (HH stage 31–32). Data from Smith et al. (1997) and Cutting et al. (2014). **(B)** Effects of sex steroid hormones, their agonists and antagonists on avian Müllerian ducts. Estrogens have a stimulatory effect and testosterone (at high doses) has an inhibitory effect.

The Müllerian duct of birds, like that of mammals, becomes regionally differentiated after hatching. In birds, it gives rise to the oviduct that has specialised shell gland, isthmus and other compartments (Bakst, 1998) reviewed in (Major et al., 2022). While both ducts regress in male chicken embryos, the right duct also regresses in females, accompanying regression of the right gonad. Why the right female gonad and its associated duct regress is not entirely clear. It has been hypothesised that such unilateral regression of the right duct and gonad makes birds lighter, an energetic advantage for flight, or that bilateral gravid ovaries and ducts would cause mechanical damage to developing eggs [reviewed in (Guioli et al., 2014)]. Gonadectomy in early chicken embryos results in the retention of both ducts in both sexes, showing that intact gonads are required for duct regression (Hutson et al., 1983). The gonads must secrete hormones that regulate duct regression–bilaterally in males and asymmetrically in females. As in mammals, AMH is expressed in the embryonic gonads of male chicken embryos from the onset of gonadal sex differentiation, from E4.5, equivalent to Hamilton-Hamburger (HH) stage 21 (Eusebe et al., 1996; Oreal et al., 1998) (Figure 2A). AMH, or an implanted testis secreting AMH or viral vector over-expressing AMH, can induce Müllerian duct regression in chicken embryos, as in mammals (Maraud et al., 1982; Rashedi et al., 1983; Lambeth et al., 2016). However, unlike in mammals, the female avian gonad also produces AMH at embryonic stages. In the chicken embryo, AMH expression in female embryonic gonads commences at the same time as in males, but at a lower level (Hutson et al., 1981) (Figure 2A) Based on immunostaining and organ culture assays, it has been shown that the left female chicken gonad produces a higher level of AMH than the right gonad, which ultimately loses the ability to secrete AMH (Hutson et al., 1981; Oreal et al., 1998). AMH expression female gonads provides the mechanism of right duct regression in that sex. The higher level of AMH activity in left versus right female gonads most likely reflects the larger size of the left gonad, and regression of the right gonad. Higher levels of AMH in the left versus right female gonad are unlikely to be the mechanism underpinning right duct regression, as right duct regression occurs despite lower levels of gonadal AMH in the right gonad. Hence, while the left female gonad produces more AMH then the right, it must enter the bloodstream to induce regression of the right (contralateral) duct.

Several studies have shown that left-right asymmetry of the avian gonad is mediated by the *PITX2* transcription factor, which regulates a molecular cascade that triggers enhanced cell proliferation in the left gonad (Guioli and Lovell-Badge, 2007; Ishimaru et al., 2008; Rodriguez-Leon et al., 2008). This molecular pathway contributes to the smaller size of the right female gonad, and hence a lower level of AMH output. However, there is no evidence to suggest that such a mechanism also underpins the left-right asymmetry of the female Müllerian ducts. *PITX2* is not expressed in the ducts and, indeed, both left and right ducts initially develop in both sexes. Rather, the asymmetric fate of the left versus right female Müllerian ducts is hormonally driven, based on the endocrine output of the gonads.

Early anatomical studies conducted on chicken and Pekin duck embryos showed that the right duct of female embryos regresses in a different manner to that of the bilateral regression in males. In the female, the right duct regresses cranio-caudally (i.e., disintegration starts at the anterior pole and progresses down) (Figure 1D) (Lillie, 1919; Lewis, 1946). In males, regression commences slightly earlier and first occurs in the lower medial half of the duct, then largely progresses cranially (so-called "caudo-cranial" regression) (Figure 1D) (Romanoff, 1960; Groenendijk-Huijbers, 1962). Furthermore, bilateral regression is rapid in males, spanning days 8–10, while it is more gradual in females, from E9.5 through E16 (Hutson et al., 1983). These differences between the sexes in the directionality of regression are intriguing and have not been explained at a molecular level. The left female duct of female chicken embryos continues to grow in length and thickness through days 10–21, during which time it enlarges caudally to form the future shell gland (Hutson et al., 1983).

In the chicken embryo, *AMHR2* is expressed in the Müllerian ducts and gonads of both sexes from early stages, prior to subsequent duct regression (Cutting et al., 2014). (Figure 2A). Expression of AMH by female gonads provides the mechanism of duct regression in that sex. However, no studies have been conducted to suggest that different sensitivity to AMH or level of AMHR2 expression could explain the sex differences in the directionality of duct regression shown in Figure 1D. However, in females, the question emerges as to how the left duct is protected from the regressive effects of AMH, despite expressing both AMH from the gonad and AMHR2 in the duct. Several lines of evidence indicate a protective effect of estrogen, which is produced by the gonads at high levels only in females (Figure 2A).

4 Sex steroid hormones and asymmetric chicken Müllerian duct development

Sex steroid hormones do not play an overt role in Müllerian duct formation or regression in mammals. However, several lines of evidence invoke sex steroids, primarily estrogen, in mediating the left-right asymmetry of chicken Müllerian duct development. The effects of sex steroid hormones, their analogues and antagonists on chicken Müllerian ducts, are shown in Figure 2B. Given that both sexes of chicken embryos produce AMH, and the right female duct regresses due to AMH (or a surgically implanted testis) (Stoll et al., 1975; Maraud et al., 1982; Hutson et al., 1983), the question arises as to why the left female duct does not also regress? Several lines of evidence invoke a protective effect of estrogen, which is synthesised by female but not male embryonic chicken gonads from E6 (stage 29) (Smith et al., 1997; Nomura et al., 1999; Smith and Sinclair, 2004; Hirst et al., 2018) (Figure 2A). Exposure of male avian embryos to exogenous 17β-estradiol or estrogen analogues such as increasing doses of diethylstilbestrol (DES) at early stages completely prevents bilateral duct regression (Hutson et al., 1982; Hutson et al., 1985; Doi and Hutson, 1988; Stoll et al., 1993) (Figure 2B). Administration of ER-α agonists has a similar effect (Mattsson et al., 2011)This is consistent with the known expression of estrogen receptor-α in male (and female) ducts (Andrews et al., 1997). In females, early exposure to exogenous estrogen at E2-3 causes precocious differentiation of the left duct, characterised by thickened epithelia and mesenchyme and the appearance of tubular glands (Andrews and Teng, 1979) (Figure 1B). This indicates that estrogen plays a role in left female duct differentiation. The striking effects of estrogen administration

to male embryos indicates that estrogen in some way antagonises the action of AMH in directing duct regression, and would be the putative mechanism by which the left female duct is retained.

The mechanism by which estrogen antagonsies AMH function in the context of asymmetric Müllerian duct regression has been controversial. This antagonism may be in the gonad, where estrogen may repress AMH gene expression or function, or at the level of the duct, where estrogen may block AMH action. In the chicken, implantation of a day 13 testis into the coelom of an early (day 3) female embryo causes complete regression of both Müllerian ducts (Maraud et al., 1982). This firstly confirms that AMHR2 is expressed in both female ducts (as in males) but it also shows that high levels of AMH from the older stage testis can direct duct regression if it pre-empts estrogen action, (Stoll et al., 1987). Stoll and colleagues argue that the role of estrogen in females is downregulation of AMH secretion by the gonads, based on earlier observations that the estrogen-induced maintenance of ducts in males is blocked by the potent estrogen antagonist, tamoxifen, but tamoxifen treatment alone cannot cause duct regression in females (as might be expected if estrogen acted protectively at the level of the duct) (Stoll et al., 1993). One issue with this interpretation is that, in some contexts, tamoxifen may act as an estrogen agonist, not an antagonist, as can occur, for example, in reptile embryos (Lance and Bogart, 1991). The alternative view, which has more experimental support, is that estrogen acts to antagonise AMH function at the level of the duct itself. Using *in vitro* organ culture experiments, Hutson, Doi and colleagues found that pre-treatment of male chicken embryos with the estrogen analogue, DES, protects ducts for regression *in vitro* when exposed to an older stage testis secreting AMH. (Hutson et al., 1982; Doi and Hutson, 1988). This suggests that duct retention is not caused by suppression of AMH secretion by DES, but by direct antagonism of AMH action in the ducts themselves. The molecular details of this interaction are currently unknown, but would provide insight into the interaction between sex steroid and AMH function more broadly. Activated estrogen receptor may directly downregulate *AMHR2* gene expression in the left female duct, for example, although evidence for this is lacking. Both left and right males and female ducts appear to express *AMHR2* throughout embryogenesis (Cutting et al., 2014). Alternatively, ERα may act in competition with the AMHR2 effectors, SMADs, directly at target genes involved in duct regression (e.g., apoptosis and matrix metalloproteases).

The next question that arises is why estrogen does not also protect the right duct from regression in females, as it does in the left? A logical possibility would be a lack of estrogen receptor expression the right duct. We and others have shown that *ERα* mRNA expression or E2 binding occurs in both left and right Müllerian ducts in both sexes of chicken embryos, at least up to E7.5 (Hutson et al., 1983; Andrews et al., 1997). ER-β is not expressed in the ducts (Mattsson et al., 2011). It is possible that ER-*α* expression becomes asymmetric beyond E7.5. The presence of estrogen receptors in chicken Müllerian ducts has been inferred from studies conducted in the 1970's and 1980's using radio-labelled estradiol binding assays. Using this approach, it has been reported that ER is expressed in the left female Müllerian duct from E8 (Teng and Teng, 1975). Furthermore, one study published in 1983 used ^{3}H-estradiol binding to show an apparent difference in E2 binding between left and right embryonic chicken Müllerian ducts, where binding was higher in the left compared to the right ducts (MacLaughlin et al., 1983). This may explain the differential actions of E2 on the left versus right ducts in females. However, an independent study found no difference in the biochemical characteristics of E2 binding in left vs. right ducts (Reichhart et al., 1980). Modern molecular tools need to be applied to answer this question. The other converse possibility is that AMHR2 protein (or the type I receptor) is not expressed in the left female duct, although we do note *AMHR2* mRNA expression both left and right female (and male) ducts over development in the chicken embryo (Cutting et al., 2014). Furthermore, type I receptors (*ACVR1* and *BMPR1a*) are expressed in chicken embryonic ducts, at least at early stages (Roly et al., 2020a). However relative quantification of type I and type II proteins in male vs. female and in left vs. right ducts has never been assayed.

In chicken, it has been shown that the embryonic gonads of both sexes produce measurable amounts of 17β-estradiol and testosterone during the period of Müllerian duct sexual differentiation (from E7-8 onwards). The early synthesis of estrogen by female gonads has been well documented (Woods and Erton, 1978; Woods and Brazzill, 1981). Androgens are synthesised in the gonads of both sexes and could, in theory, influence duct development (Woods and Podczaski, 1974; Woods et al., 1975). When very high doses of exogenous testosterone are administered to female chicken embryos *in vitro* or *in ovo*, the Müllerian ducts can disintegrate, but some other studies found no effect or partial effects at lower doses [reviewed in (Hutson et al., 1983)] (Figure 2A). This most likely reflects the timing, dosage and route of administration of testosterone. It has been considered that many studies examining the effects of testosterone have used pharmacological doses. At physiological doses, testosterone appears to augment AMH-induced duct regression (Ikawa et al., 1982). Androgen receptor is expressed in chicken Müllerian duct (Reichhart et al., 1980; Katoh et al., 2006). In the chicken embryo, Autoradiography and gene expression analysis indicate that AR is expressed in the mesenchyme from the early stages of duct formation (E5.5- E6.5) through regression and differentiation (E10.5+) (Gasc, 1981).

5 Answering questions of Müllerian duct development with modern molecular and imaging approaches

The studies on avian Müllerian duct development described above have largely involved gross anatomy, histology and approaches such radio-labelled sex hormone binding, conducted in the last century. Today, we have access to genomic and transcriptomic tools and advanced imaging methods that will shed new light on duct formation and, especially, the molecular basis of the curious asymmetry seen in most birds. These tools will be very useful in teasing out the hormonal interplay that underpins asymmetric duct development in the avian model. This, in turn, will provide further insights into duct formation and sexual differentiation in vertebrates more broadly. For example, advances in whole mount immunofluorescent staining of ducts allows the visualisation and quantification of duct development

and regression on a global level, using methods such as multi-plane whole mount confocal imaging. Such approaches can now be applied to the study of ERα and AMHR2 expression along the entire duct, to discern the mechanism of asymmetry in females (different patterns of ERα or different AMHR2 protein expression?) and the cranio-caudal (female) vs. caudo-cranial (male) regression profiles. Single cell RNA-seq and ATAC-seq studies can also be performed to elucidate the different cell populations and global gene regulatory landscape of duct development.

Comparisons can be drawn between natural Müllerian duct asymmetry in birds and atypical duct formation among mammals. Such comparisons highlight shared and diverged molecular mechanisms. In the chicken, for example, AMH levels are higher in the left gonad than in the right, yet it is the right duct that regresses. This is presumably because AMH enters the bloodstream or diffuses to the ducts regardless of its site of origin (where the left duct is protected via secreted estrogen). In mice, unusal unilateral Müllerian duct regression has been reported in mutants such as B6N-XY^{POS} (retarded *Sry* expression) and in *M33* and *jumonji domain-containing protein 1a* (Jmjd1a)-knockout mice (Katoh-Fukui et al., 1998; Kuroki et al., 2013; Yamamoto et al., 2018). In these mice, a percentage develop as, true hermaphrodites, characterised in which the left gonad is an ovary, with neighbouring left Müllerian duct, and the right gonad is a testis and the right duct regresses. At least in the case of the B6N-XY^{POS} mice, has been shown that this asymmetry involves local diffusion of AMH on the right side of the urogenital system only (Yamamoto et al., 2018). Such ipsilateral effects of AMH are also evident in rabbit embryos in which the testis is removed from one side: the Mullerian duct on the operated side is maintained (Jost, 1953). This is different to the contralateral mechanism inferred in birds. In human females, one Mullerian duct can sometime fail to develop, leading to a so-called unicornate uterus (a small uterus with only one Fallopian tube). While the incidence of unicornate uterus is sporadic and rare (0.3% of the population), the cause is unknown (Trad and Palmer, 2013). Studies on the asymmetric sensitivity of the paired Müllerian ducts to AMH or oestrogen in chicken may shed light on asymmetric defects in human Müllerian duct formation.

6 Conclusion

In mammals, it is the presence or absence of AMH that underpins sexually dimorphic fate of the Müllerian ducts. In the chicken embryo, the picture is more complex, with asymmetric duct regression occurring in females. This pattern can shed light on the molecular mechanisms of duct regression more broadly among animals, as outlined above. The chicken model offers several novel perspectives on the roles of AMH and sex steroid hormones in the vertebrate reproductive tract. Firstly, during embryonic life, the ovary in addition to the testis produces AMH. Secondly, the female right duct regresses as do both males ducts. Thirdly, the pattern of regression differs between the sexes (cranio-caudal in females vs. largely caudo-cranial in males). These features make the chicken embryo an attractive model for studying genetic and hormonal regulation of the developing Müllerian ducts. In the chicken model, duct development can now be readily manipulated *in ovo*, using modern molecular methods such as electroporation of genes for over-expression, or shRNAs for gene knockdown or Cas9/guide RNAs for gene knockout (Guioli et al., 2007; Atsuta and Takahashi, 2016; Roly et al., 2020b). These rapid functional approaches will provide new information on how the Müllerian ducts grow and undergo sexual differentiation. Furthermore, studies on the hormonal regulation of Müllerian duct formation in egg-laying species such as the chicken are be important for understanding the effects of teratogens and xenoestrogens on sexual differentiation (Mattsson et al., 2011).

Author contributions

JT: Writing–review and editing. AM: Data curation, Formal Analysis, Investigation, Methodology, Supervision, Writing–review and editing. CS: Writing–original draft.

Funding

The author(s) declare financial support was received for the research, authorship, and/or publication of this article. This work is funded by an Australian Research Council (ARC) Discovery Project # DP240100491 grant awarded to CS.

Conflict of interest

The authors declare that the research was conducted in the absence of any commercial or financial relationships that could be construed as a potential conflict of interest.

Publisher's note

References

Andrews, G. K., and Teng, C. S. (1979). Studies on sex-organ development. Prenatal effect of oestrogenic hormone on tubular-gland cell morphogenesis and ovalbumin-gene expression in the chick Mullerian duct. *Biochem. J.* 182, 271–286. doi:10.1042/bj1820271

Andrews, J. E., Smith, C. A., and Sinclair, A. H. (1997). Sites of estrogen receptor and aromatase expression in the chicken embryo. *Gen. Comp. Endocrinol.* 108, 182–190. doi:10.1006/gcen.1997.6978

Arango, N. A., Kobayashi, A., Wang, Y., Jamin, S. P., Lee, H. H., Orvis, G. D., et al. (2008). A mesenchymal perspective of Mullerian duct differentiation and regression in Amhr2-lacZ mice. *Mol. Reprod. Dev.* 75, 1154–1162. doi:10.1002/mrd.20858

Atsuta, Y., and Takahashi, Y. (2016). Early formation of the Mullerian duct is regulated by sequential actions of BMP/Pax2 and FGF/Lim1 signaling. *Development* 143, 3549–3559. doi:10.1242/dev.137067

Bakst, M. R. (1998). Structure of the avian oviduct with emphasis on sperm storage in poultry. *J. Exp. Zool.* 282, 618–626. doi:10.1002/(sici)1097-010x(199811/12)282:4/5<618::aid-jez11>3.0.co;2-m

Behringer, R. R. (1994). The *in vivo* roles of mullerian-inhibiting substance. *Curr. Top. Dev. Biol.* 29, 171–187. doi:10.1016/s0070-2153(08)60550-5

Behringer, R. R., Cate, R. L., Froelick, G. J., Palmiter, R. D., and Brinster, R. L. (1990). Abnormal sexual development in transgenic mice chronically expressing mullerian inhibiting substance. *Nature* 345, 167–170. doi:10.1038/345167a0

Behringer, R. R., Finegold, M. J., and Cate, R. L. (1994). Mullerian-inhibiting substance function during mammalian sexual development. *Cell* 79, 415–425. doi:10.1016/0092-8674(94)90251-8

Biason-Lauber, A., and Konrad, D. (2008). WNT4 and sex development. *Sex. Dev.* 2, 210–218. doi:10.1159/000152037

Bouchard, M., Souabni, A., Mandler, M., Neubuser, A., and Busslinger, M. (2002). Nephric lineage specification by Pax2 and Pax8. *Genes Dev.* 16, 2958–2970. doi:10.1101/gad.240102

Cate, R. L. (2022). Anti-Mullerian hormone signal transduction involved in mullerian duct regression. *Front. Endocrinol. (Lausanne)* 13, 905324. doi:10.3389/fendo.2022.905324

Cutting, A. D., Ayers, K., Davidson, N., Oshlack, A., Doran, T., Sinclair, A. H., et al. (2014). Identification, expression, and regulation of anti-Mullerian hormone type-II receptor in the embryonic chicken gonad. *Biol. Reprod.* 90, 106. doi:10.1095/biolreprod.113.116491

Davis, R. J., Harding, M., Moayedi, Y., and Mardon, G. (2008). Mouse Dach1 and Dach2 are redundantly required for Mullerian duct development. *Genesis* 46, 205–213. doi:10.1002/dvg.20385

De Santa Barbara, P., Bonneaud, N., Boizet, B., Desclozeaux, M., Moniot, B., Sudbeck, P., et al. (1998). Direct interaction of SRY-related protein SOX9 and steroidogenic factor 1 regulates transcription of the human anti-Mullerian hormone gene. *Mol. Cell Biol.* 18, 6653–6665. doi:10.1128/mcb.18.11.6653

Doi, O., and Hutson, J. M. (1988). Pretreatment of chick embryos with estrogen in ovo prevents mullerian duct regression in organ culture. *Endocrinology* 122, 2888–2891. doi:10.1210/endo-122-6-2888

Eusebe, D., Di Clemente, N., Rey, R., Pieau, C., Vigier, B., Josso, N., et al. (1996). Cloning and expression of the chick anti-Mullerian hormone gene. *J. Biol. Chem.* 271, 4798–4804. doi:10.1074/jbc.271.9.4798

Gasc, J. M. (1981). Autoradiographic studies of steroid receptor sites in embryonic tissues (1), (2). *J. Histochem Cytochem* 29, 181–189. doi:10.1177/29.1A_SUPPL.7288153

Groenendijk-Huijbers, M. M. (1962). The cranio-caudal regression of the right Mullerian duct in the chick embryo as studied by castration experiments ad estrogen treatment. *Anat. Rec.* 142, 9–19. doi:10.1002/ar.1091420103

Guioli, S., and Lovell-Badge, R. (2007). PITX2 controls asymmetric gonadal development in both sexes of the chick and can rescue the degeneration of the right ovary. *Development* 134, 4199–4208. doi:10.1242/dev.010249

Guioli, S., Nandi, S., Zhao, D., Burgess-Shannon, J., Lovell-Badge, R., and Clinton, M. (2014). Gonadal asymmetry and sex determination in birds. *Sex. Dev.* 8, 227–242. doi:10.1159/000358406

Guioli, S., Sekido, R., and Lovell-Badge, R. (2007). The origin of the Mullerian duct in chick and mouse. *Dev. Biol.* 302, 389–398. doi:10.1016/j.ydbio.2006.09.046

Hirst, C. E., Major, A. T., and Smith, C. A. (2018). Sex determination and gonadal sex differentiation in the chicken model. *Int. J. Dev. Biol.* 62, 153–166. doi:10.1387/ijdb.170319cs

Huang, C. C., Orvis, G. D., Kwan, K. M., and Behringer, R. R. (2014). Lhx1 is required in Mullerian duct epithelium for uterine development. *Dev. Biol.* 389, 124–136. doi:10.1016/j.ydbio.2014.01.025

Hutson, J., Ikawa, H., and Donahoe, P. K. (1981). The ontogeny of Mullerian inhibiting substance in the gonads of the chicken. *J. Pediatr. Surg.* 16, 822–827. doi:10.1016/s0022-3468(81)80827-5

Hutson, J. M., Donahoe, P. K., and Maclaughlin, D. T. (1985). Steroid modulation of Mullerian duct regression in the chick embryo. *Gen. Comp. Endocrinol.* 57, 88–102. doi:10.1016/0016-6480(85)90204-7

Hutson, J. M., Ikawa, H., and Donahoe, P. K. (1982). Estrogen inhibition of Mullerian inhibiting substance in the chick embryo. *J. Pediatr. Surg.* 17, 953–959. doi:10.1016/s0022-3468(82)80474-0

Hutson, J. M., Maclaughlin, D. T., Ikawa, H., Budzik, G. P., and Donahoe, P. K. (1983). Regression of the Mullerian ducts during sexual differentiation in the chick embryo. A reappraisal. *Int. Rev. Physiol.* 27, 177–224.

Ikawa, H., Hutson, J. M., Budzik, G. P., Maclaughlin, D. T., and Donahoe, P. K. (1982). Steroid enhancement of Mullerian duct regression. *J. Pediatr. Surg.* 17, 453–458. doi:10.1016/s0022-3468(82)80088-2

Ishimaru, Y., Komatsu, T., Kasahara, M., Katoh-Fukui, Y., Ogawa, H., Toyama, Y., et al. (2008). Mechanism of asymmetric ovarian development in chick embryos. *Development* 135, 677–685. doi:10.1242/dev.012856

Jacob, M., Konrad, K., and Jacob, H. J. (1999). Early development of the mullerian duct in avian embryos with reference to the human. An ultrastructural and immunohistochemical study. *Cells Tissues Organs* 164, 63–81. doi:10.1159/000016644

Jamin, S. P., Arango, N. A., Mishina, Y., Hanks, M. C., and Behringer, R. R. (2002). Requirement of Bmpr1a for Mullerian duct regression during male sexual development. *Nat. Genet.* 32, 408–410. doi:10.1038/ng1003

Jamin, S. P., Arango, N. A., Mishina, Y., Hanks, M. C., and Behringer, R. R. (2003). Genetic studies of the AMH/MIS signaling pathway for Mullerian duct regression. *Mol. Cell Endocrinol.* 211, 15–19. doi:10.1016/j.mce.2003.09.006

Josso, N., Cate, R. L., Picard, J. Y., Vigier, B., Di Clemente, N., Wilson, C., et al. (1993a). Anti-mullerian hormone: the Jost factor. *Recent Prog. Horm. Res.* 48, 1–59. doi:10.1016/b978-0-12-571148-7.50005-1

Josso, N., Lamarre, I., Picard, J. Y., Berta, P., Davies, N., Morichon, N., et al. (1993b). Anti-mullerian hormone in early human development. *Early Hum. Dev.* 33, 91–99. doi:10.1016/0378-3782(93)90204-8

Josso, N., and Picard, J. Y. (1986). Anti-Mullerian hormone. *Physiol. Rev.* 66, 1038–1090. doi:10.1152/physrev.1986.66.4.1038

Josso, N., Racine, C., Di Clemente, N., Rey, R., and Xavier, F. (1998). The role of anti-Mullerian hormone in gonadal development. *Mol. Cell Endocrinol.* 145, 3–7. doi:10.1016/s0303-7207(98)00186-5

Jost, A. (1953). Problems of fetal endocrinology: the gonadal and hypophyseal hormones. *Recent Prog. Horm. Res.* 1953, 379–418.

Katoh, H., Ogino, Y., and Yamada, G. (2006). Cloning and expression analysis of androgen receptor gene in chicken embryogenesis. *FEBS Lett.* 580, 1607–1615. doi:10.1016/j.febslet.2006.01.093

Katoh-Fukui, Y., Tsuchiya, R., Shiroishi, T., Nakahara, Y., Hashimoto, N., Noguchi, K., et al. (1998). Male-to-female sex reversal in M33 mutant mice. *Nature* 393, 688–692. doi:10.1038/31482

Klattig, J., and Englert, C. (2007). The Mullerian duct: recent insights into its development and regression. *Sex. Dev.* 1, 271–278. doi:10.1159/000108929

Kobayashi, A., Shawlot, W., Kania, A., and Behringer, R. R. (2004). Requirement of Lim1 for female reproductive tract development. *Development* 131, 539–549. doi:10.1242/dev.00951

Kuroki, S., Matoba, S., Akiyoshi, M., Matsumura, Y., Miyachi, H., Mise, N., et al. (2013). Epigenetic regulation of mouse sex determination by the histone demethylase Jmjd1a. *Science* 341, 1106–1109. doi:10.1126/science.1239864

Lambeth, L. S., Morris, K., Ayers, K. L., Wise, T. G., O'neil, T., Wilson, S., et al. (2016). Overexpression of anti-mullerian hormone disrupts gonadal sex differentiation, blocks sex hormone synthesis, and supports cell autonomous sex development in the chicken. *Endocrinology* 157, 1258–1275. doi:10.1210/en.2015-1571

Lance, V. A., and Bogart, M. H. (1991). Tamoxifen sex reverses Alligator embryos at male producing temperature, but is an antiestrogen in female hatchlings. *Experientia* 47, 263–266. doi:10.1007/bf01958155

Lewis, M. R. (1946). A study of some effects of sex hormones upon the embryonic reproductive system ofthe white Pekin duck. *Physiol. Zool.* 13, 282–329. doi:10.1086/physzool.19.3.30151914

Lillie, F. R. (1919). *The development of the chick*. New York: Henry Holt and Co.

Machado, D. A., Ontiveros, A. E., and Behringer, R. R. (2022). Mammalian uterine morphogenesis and variations. *Curr. Top. Dev. Biol.* 148, 51–77. doi:10.1016/bs.ctdb.2021.12.004

Maclaughlin, D. T., Hutson, J. M., and Donahoe, P. K. (1983). Specific estradiol binding in embryonic Mullerian ducts: a potential modulator of regression in the male and female chick. *Endocrinology* 113, 141–145. doi:10.1210/endo-113-1-141

Major, A. T., Estermann, M. A., Roly, Z. Y., and Smith, C. A. (2022). An evo-devo perspective of the female reproductive tract. *Biol. Reprod.* 106, 9–23. doi:10.1093/biolre/ioab166

Maraud, R., Rashedi, M., and Stoll, R. (1982). Influence of a temporary embryonic testis graft on the regression of mullerian ducts in female chick-embryo. *J. Embryology Exp. Morphol.* 67, 81–87. doi:10.1242/dev.67.1.81

Mattsson, A., Olsson, J. A., and Brunstrom, B. (2011). Activation of estrogen receptor alpha disrupts differentiation of the reproductive organs in chicken embryos. *Gen. Comp. Endocrinol.* 172, 251–259. doi:10.1016/j.ygcen.2011.03.010

Mishina, Y., Whitworth, D. J., Racine, C., and Behringer, R. R. (1999). High specificity of Mullerian-inhibiting substance signaling *in vivo*. *Endocrinology* 140, 2084–2088. doi:10.1210/endo.140.5.6705

Miyamoto, N., Yoshida, M., Kuratani, S., Matsuo, I., and Aizawa, S. (1997). Defects of urogenital development in mice lacking Emx2. *Development* 124, 1653–1664. doi:10.1242/dev.124.9.1653

Moses, M. M., and Behringer, R. R. (2019). A gene regulatory network for Mullerian duct regression. *Environ. Epigenet* 5, dvz017. doi:10.1093/eep/dvz017

Mullen, R. D., and Behringer, R. R. (2014). Molecular genetics of Mullerian duct formation, regression and differentiation. *Sex. Dev.* 8, 281–296. doi:10.1159/000364935

Munsterberg, A., and Lovellbadge, R. (1991). Expression of the mouse anti-mullerian hormone gene suggests a role in both male and female sexual-differentiation. *Development* 113, 613–624. doi:10.1242/dev.113.2.613

Nomura, O., Nakabayashi, O., Nishimori, K., Yasue, H., and Mizuno, S. (1999). Expression of five steroidogenic genes including aromatase gene at early developmental stages of chicken male and female embryos. *J. Steroid Biochem. Mol. Biol.* 71, 103–109. doi:10.1016/s0960-0760(99)00127-2

Oreal, E., Pieau, C., Mattei, M. G., Josso, N., Picard, J. Y., Carre-Eusebe, D., et al. (1998). Early expression of AMH in chicken embryonic gonads precedes testicular SOX9 expression. *Dev. Dyn.* 212, 522–532. doi:10.1002/(SICI)1097-0177(199808)212:4<522::AID-AJA5>3.0.CO;2-J

Orvis, G. D., and Behringer, R. R. (2007). Cellular mechanisms of Mullerian duct formation in the mouse. *Dev. Biol.* 306, 493–504. doi:10.1016/j.ydbio.2007.03.027

Orvis, G. D., Jamin, S. P., Kwan, K. M., Mishina, Y., Kaartinen, V. M., Huang, S., et al. (2008). Functional redundancy of TGF-beta family type I receptors and receptor-Smads in mediating anti-Mullerian hormone-induced Mullerian duct regression in the mouse. *Biol. Reprod.* 78, 994–1001. doi:10.1095/biolreprod.107.066605

Prunskaite-Hyyrylainen, R., Skovorodkin, I., Xu, Q., Miinalainen, I., Shan, J., and Vainio, S. J. (2016). Wnt4 coordinates directional cell migration and extension of the Mullerian duct essential for ontogenesis of the female reproductive tract. *Hum. Mol. Genet.* 25, 1059–1073. doi:10.1093/hmg/ddv621

Rashedi, M., Stoll, R., and Maraud, R. (1983). Action of testis graft from puromycin- or cAMP-pretreated donor embryos on the regression of Mullerian ducts in the female chick embryo. *Gen. Comp. Endocrinol.* 50, 270–274. doi:10.1016/0016-6480(83)90227-7

Reichhart, J. M., Weniger, J. P., and Thiebold, J. (1980). Responsiveness of developing chick mullerian ducts to sex steroids. *General Comp. Endocrinol.* 40, 328.

Rodriguez-Leon, J., Rodriguez Esteban, C., Marti, M., Santiago-Josefat, B., Dubova, I., Rubiralta, X., et al. (2008). Pitx2 regulates gonad morphogenesis. *Proc. Natl. Acad. Sci. U. S. A.* 105, 11242–11247. doi:10.1073/pnas.0804904105

Roly, Z. Y., Backhouse, B., Cutting, A., Tan, T. Y., Sinclair, A. H., Ayers, K. L., et al. (2018). The cell biology and molecular genetics of Mullerian duct development. *Wiley Interdiscip. Rev. Dev. Biol.* 7, e310. doi:10.1002/wdev.310

Roly, Z. Y., Godini, R., Estermann, M. A., Major, A. T., Pocock, R., and Smith, C. A. (2020a). Transcriptional landscape of the embryonic chicken Mullerian duct. *BMC Genomics* 21, 688. doi:10.1186/s12864-020-07106-8

Roly, Z. Y., Major, A. T., Fulcher, A., Estermann, M. A., Hirst, C. E., and Smith, C. A. (2020b). Adhesion G-protein-coupled receptor, GPR56, is required for Mullerian duct development in the chick. *J. Endocrinol.* 244, 395–413. doi:10.1530/JOE-19-0419

Romanoff, A. L. (1960). *The avian embryo: structural and functional development*. New York: Macmillan.

Santana Gonzalez, L., Rota, I. A., Artibani, M., Morotti, M., Hu, Z., Wietek, N., et al. (2021). Mechanistic drivers of mullerian duct development and differentiation into the oviduct. *Front. Cell Dev. Biol.* 9, 605301. doi:10.3389/fcell.2021.605301

Smith, C. A., Andrews, J. E., and Sinclair, A. H. (1997). Gonadal sex differentiation in chicken embryos: expression of estrogen receptor and aromatase genes. *J. Steroid Biochem. Mol. Biol.* 60, 295–302. doi:10.1016/s0960-0760(96)00196-3

Smith, C. A., and Sinclair, A. H. (2004). Sex determination: insights from the chicken. *Bioessays* 26, 120–132. doi:10.1002/bies.10400

Stoll, R., Faucounau, N., and Maraud, R. (1987). Influence of an antiestrogenic drug (tamoxifen) on Mullerian duct agenesia induced by various steroidal sex hormones in the female chick embryo. *Gen. Comp. Endocrinol.* 66, 218–223. doi:10.1016/0016-6480(87)90270-x

Stoll, R., Ichas, F., Faucounau, N., and Maraud, R. (1993). Action of estradiol and tamoxifen on the Mullero-regressive activity of the chick embryonic testis assayed *in vivo* by organotypic grafting. *Anat. Embryol. Berl.* 187, 379–384. doi:10.1007/BF00185896

Stoll, R., Rashedi, M., and Maraud, R. (1975). The effect of the testicular mullerian-inhibiting hormone on ovarian development in the chick embryo. *C R. Seances Soc. Biol. Fil.* 169, 927–930.

Teng, C. S., and Teng, C. T. (1975). Studies on sex-organ development. Ontogeny of cytoplasmic oestrogen receptor in chick Mullerian duct. *Biochem. J.* 150, 191–194. doi:10.1042/bj1500191

Torres, M., Gomez-Pardo, E., Dressler, G. R., and Gruss, P. (1995). Pax-2 controls multiple steps of urogenital development. *Development* 121, 4057–4065. doi:10.1242/dev.121.12.4057

Trad, M., and Palmer, S. (2013). Mullerian duct anomalies and a case study of unicornuate uterus. *Radiol. Technol.* 84, 571–576.

Vainio, S., Heikkila, M., Kispert, A., Chin, N., and Mcmahon, A. P. (1999). Female development in mammals is regulated by Wnt-4 signalling. *Nature* 397, 405–409. doi:10.1038/17068

Van Tienhoven, A. (1983). *Reproductive physiology of vertebrates*. Ithaca, New York: Cornell University Press.

Visser, J. A., Olaso, R., Verhoef-Post, M., Kramer, P., Themmen, A. P., and Ingraham, H. A. (2001). The serine/threonine transmembrane receptor ALK2 mediates Mullerian inhibiting substance signaling. *Mol. Endocrinol.* 15, 936–945. doi:10.1210/mend.15.6.0645

Wilson, J. D. (1978). Sexual differentiation. *Annu. Rev. Physiol.* 40, 279–306. doi:10.1146/annurev.ph.40.030178.001431

Woods, J. E., and Brazzill, D. M. (1981). Plasma 17 beta-estradiol levels in the chick embryo. *Gen. Comp. Endocrinol.* 44, 37–43. doi:10.1016/0016-6480(81)90353-1

Woods, J. E., and Erton, L. H. (1978). The synthesis of estrogens in the gonads of the chick embryo. *Gen. Comp. Endocrinol.* 36, 360–370. doi:10.1016/0016-6480(78)90117-x

Woods, J. E., and Podczaski, E. S. (1974). Androgen synthesis in the gonads of the chick embryo. *Gen. Comp. Endocrinol.* 24, 413–423. doi:10.1016/0016-6480(74)90155-5

Woods, J. E., Simpson, R. M., and Moore, P. L. (1975). Plasma testosterone levels in the chick embryo. *Gen. Comp. Endocrinol.* 27, 543–547. doi:10.1016/0016-6480(75)90076-3

Yamamoto, A., Omotehara, T., Miura, Y., Takada, T., Yoneda, N., Hirano, T., et al. (2018). The mechanisms underlying the effects of AMH on Mullerian duct regression in male mice. *J. Vet. Med. Sci.* 80, 557–567. doi:10.1292/jvms.18-0023

frontiers | Frontiers in Cell and Developmental Biology

TYPE Brief Research Report
PUBLISHED 15 February 2024
DOI 10.3389/fcell.2024.1337714

OPEN ACCESS

EDITED BY
Dagmar Wilhelm,
The University of Melbourne, Australia

REVIEWED BY
Gen Yamada,
Wakayama Medical University, Japan
Martin Andres Estermann,
National Institute of Environmental Health Sciences (NIH), United States
Brendan J. Houston,
The University of Melbourne, Australia

*CORRESPONDENCE
Vincent R. Harley,
vincent.harley@hudson.org.au

RECEIVED 13 November 2023
ACCEPTED 05 February 2024
PUBLISHED 15 February 2024

CITATION
Ming Z, Bagheri-Fam S, Frost ER, Ryan JM, Vining B and Harley VR (2024), A role for TRPC3 in mammalian testis development. *Front. Cell Dev. Biol.* 12:1337714. doi: 10.3389/fcell.2024.1337714

A role for TRPC3 in mammalian testis development

Zhenhua Ming[1,2], Stefan Bagheri-Fam[1], Emily R. Frost[1], Janelle M. Ryan[1,2], Brittany Vining[1,2] and Vincent R. Harley[1,2]*

[1]Sex Development Laboratory, Hudson Institute of Medical Research, Melbourne, VIC, Australia, [2]Department of Molecular and Translational Science, Monash University, Melbourne, VIC, Australia

SOX9 is a key transcription factor for testis determination and development. Mutations in and around the *SOX9* gene contribute to Differences/Disorders of Sex Development (DSD). However, a substantial proportion of DSD patients lack a definitive genetic diagnosis. SOX9 target genes are potentially DSD-causative genes, yet only a limited subset of these genes has been investigated during testis development. We hypothesize that SOX9 target genes play an integral role in testis development and could potentially be causative genes in DSD. In this study, we describe a novel testicular target gene of SOX9, *Trpc3*. *Trpc3* exhibits high expression levels in the SOX9-expressing male Sertoli cells compared to female granulosa cells in mouse fetal gonads between embryonic day 11.5 (E11.5) and E13.5. In XY *Sox9* knockout gonads, *Trpc3* expression is markedly downregulated. Moreover, culture of E11.5 XY mouse gonads with TRPC3 inhibitor Pyr3 resulted in decreased germ cell numbers caused by reduced germ cell proliferation. *Trpc3* is also expressed in endothelial cells and Pyr3-treated E11.5 XY mouse gonads showed a loss of the coelomic blood vessel due to increased apoptosis of endothelial cells. In the human testicular cell line NT2/D1, TRPC3 promotes cell proliferation and controls cell morphology, as observed by xCELLigence and HoloMonitor real-time analysis. In summary, our study suggests that SOX9 positively regulates *Trpc3* in mouse testes and TRPC3 may mediate SOX9 function during Sertoli, germ and endothelial cell development.

KEYWORDS

SOX9, testis, sertoli cells, DSD, TRPC3, TRP, sex determination

1 Introduction

Differences/Disorders of Sex Development (DSDs) are a heterogenous group of congenital conditions in which the development of chromosomal, gonadal and/or anatomic sex is atypical (Hughes et al., 2006). A notable subset of DSDs is 46, XY DSD, where individuals possess a 46, XY chromosome complement but present with atypical male or even female external genitalia, with or without Müllerian duct derived structures (female internal genitalia) (Wisniewski et al., 2019; Reyes et al., 2023). 46, XY DSD is associated with genetic mutations in key genes involved in testis development, such as the testis-determining gene *SRY*, *SOX9*, *NR5A1*, *MAP3K1*, and *DHX37* (Eggers et al., 2016; Xu et al., 2019; Reyes et al., 2023). Despite advancements in genomic technologies, many 46, XY DSD patients lack a clinical genetic diagnosis, and numerous genes contributing to DSD remain unidentified. It is therefore important to define the basic mechanisms underlying testis development and identify genes downstream of SOX9 that mediate its functions and potentially contribute to DSD.

Mammalian testes originate from bipotential gonads, where SRY expression commences at embryonic day 11.5 (E11.5) in mice (equivalent to 7 weeks gestation in humans), initiating the male sex differentiation pathway (Koopman et al., 1990; Koopman et al., 1991). In XY mouse gonads, SRY activates the pivotal testis gene *Sox9* in supporting cells, leading to their differentiation into Sertoli cells (Vidal et al., 2001; Chaboissier et al., 2004; Barrionuevo et al., 2006; Sekido and Lovell-Badge, 2008). Sertoli cells then proliferate, migrate and surround germ cells to form testis cords. Concurrently, Leydig cells outside the testis cords begin differentiation and produce androgens, which drive the development of male internal and external genitalia (Svingen and Koopman, 2013). In the female mouse XX gonad, ovarian development is also initiated at E11.5 through RSPO1-WNT4 and FOXL2 signaling pathways (Ottolenghi et al., 2007; Chassot et al., 2008). Within the developing testis, SOX9 plays a central role in regulating target genes, directing them in fulfilling their specific functions. For instance, SOX9 directly regulates the *Amh* gene, leading to the regression of Müllerian ducts in males (Arango et al., 1999; Barrionuevo et al., 2006). SOX9 also directly regulates the expression of *Dhh* to drive Leydig cell differentiation and *Cyp26b1* to inhibit the entry of XY germ cells into meiosis (Barrionuevo et al., 2006; Kashimada et al., 2011; Rahmoun et al., 2017). Given the pivotal role of SOX9 in testis development, our previous study explored the genes affected by the absence of *Sox9* and those bound by SOX9 at the post sex determination stage (Rahmoun et al., 2017). Among these candidate target genes of SOX9, *Trpc3* (transient receptor potential cation channel subfamily C member 3) stands out prominently due to its increased expression in Sertoli cells shortly after the onset of *Sox9* transcription (Jameson et al., 2012).

TRPC3 is a membrane protein that forms a non-selective calcium permeant cation channel. It is directly activated by diacylglycerols (DAG) in response to receptor-phospholipase C (PLC) pathways (Hofmann et al., 1999; Li et al., 1999). The structure of TRPC3 includes six transmembrane domains (TM1-TM6), and cytoplasmic N- and C-termini. The C-terminus includes a highly conserved transient receptor potential (TRP) domain and a calmodulin/inositol 1,4,5-trisphosphate (IP3) receptor-binding (CIRB) region (Liu et al., 2020). TRPC3 is abundantly expressed in the cerebellum, cerebrum and the cardiovascular system with essential roles in the regulation of neurogenesis and calcium signaling (Li et al., 1999; Gonzalez-Cobos and Trebak, 2010). Dysfunctions in TRPC3 are associated with neurodegenerative diseases, cardiac hypertrophy, and ovarian cancer (Yang et al., 2009; Becker et al., 2011; Kitajima et al., 2016). TRPC3 is found in both mouse and human sperm (Treviño et al., 2001; Castellano et al., 2003) and Pyr3, a TRPC3 antagonist, can inhibit mouse sperm motility and accelerate capacitation-associated protein tyrosine phosphorylation (Ru et al., 2015). However, the role of TRPC3 in testis development remains unclear.

In this study, we analyzed *Trpc3* expression and its role in XY and XX gonads during gonad development. The *Trpc3*/TRPC3 gene and protein showed strong expression in the SOX9-expressing Sertoli cells of the fetal XY gonad. Inhibition of TRPC3 in XY gonad culture leads to a decrease in germ cell numbers attributed to reduced germ cell proliferation. This inhibition also disrupts the coelomic blood vessel and increases endothelial cell apoptosis during testicular development. *In vitro* analysis further demonstrates that TRPC3 stimulates Sertoli cell proliferation and regulates cell morphology. Our findings emphasize the necessity of SOX9 for *Trpc3* expression in Sertoli cells and suggest that TRPC3 contributes to testis development by influencing the development of Sertoli, germ, and endothelial cells.

2 Materials and methods

2.1 Mice

All animal experimentation was approved and conducted in accordance with the guidelines established by the Monash Medical Centre Animal Ethics Committee. The generation of *AMH-Cre; Sox9$^{flox/flox}$* mice was previously described (Barrionuevo et al., 2009), and these mice were maintained on a C57BL/6 background. Embryos were collected at E13.5, with the morning of plug identification designated as E0.5. Genotyping primers and PCR conditions were used as previously reported (Kist et al., 2002; Lécureuil et al., 2002; Jiménez et al., 2003).

2.2 Quantitative RT-PCR

Total RNA was extracted from fetal gonads (with mesonephros removed) at E13.5 or NT2/D1 cells using the RNeasy Mini kit (Qiagen). cDNA was synthesized using the QuantiTect reverse transcription kit (Qiagen), and quantitative PCR was performed using the QuantiNova SYBR green PCR kit (Qiagen) on a QuantStudio™ 6 Flex Real-Time PCR System (Applied Biosystems). Mouse primer sequences were as follows: *Trpc3* F: 5′TTATCGACTACCCCAAGCAA3′, *Trpc3* R: 5′CCACATCATCCCAAGAACC3′, *Tbp* F: 5′ACGGACAACTGCGTTGATTTT3′, *Tbp* R: 5′ACTTAGCTGGGAAGCCCAAC3’. Human primer sequences were as follows: *TRPC3* F: 5′TGCTGCTTTTACCACTGTAG3′, *TRPC3* R: 5′GTTGAGTAAAACGACCACCA3′, *GAPDH* F: 5′GGAGTCAACGGATTTGGTC3′, *GAPDH* R: 5′TCCATTGATGACAAGCTTCC3’. Relative expression was calculated using the delta delta cycle threshold (ΔΔCt) method with *Tbp* or *GAPDH* as the normalizing control. Statistical significance was determined using one-way ANOVA, followed by the Dunnett multiple comparisons test or unpaired Student’s t-test performed in GraphPad Prism 8.

2.3 *Ex vivo* gonad culture

Gonads with attached mesonephros were dissected from E11.5 Swiss mouse embryos. Genotyping analysis for sexing was performed using genomic DNA isolated from tail tissue, as previously described (Jiménez et al., 2003). Pairs of gonads from each embryo were cultured in hanging droplets of DMEM medium (Gibco) supplemented with 10% FBS (Bovogen) and 1% antibiotic-antimycotic (Gibco) (Ryan et al., 2011; Bernard et al., 2012). The optimal concentration of the TRPC3 inhibitor Pyr3 for gonad culture was determined based on previous studies demonstrating that 3 μM of Pyr3 induces maximal

inhibition of TRPC3-mediated Ca^{2+} influx (Kiyonaka et al., 2009; Kim et al., 2011). Our MTS assay confirmed that 3 μM Pyr3 did not adversely affect cell viability in NT2/D1 cells (data not shown). Therefore, gonads were treated with 3 μM of the TRPC3 inhibitor Pyr3 (Sigma Aldrich) or an equivalent volume of the vehicle DMSO. The explants were cultured in a humidified cell culture incubator set at 37°C with 5% CO_2. After 24 h, the drug treatment was washed off, fresh medium was replaced, and the culture was continued for either 24 or 48 h. The gonads were then harvested and fixed in 10% neutral buffered formalin for subsequent immunofluorescence staining.

2.4 Immunofluorescence

The fixed samples were processed and embedded in paraffin. Paraffin blocks were sectioned at 4 μm and mounted onto slides. Immunofluorescence analysis was conducted as previously described (Bagheri-Fam et al., 2017). Primary antibodies used were anti-TRPC3 rabbit polyclonal (ab51560, 1:50, 20 μg/mL, Abcam), anti-AMH mouse monoclonal (sc-166752, 1:100, 2 μg/mL, Santa Cruz), anti-SOX9 rabbit polyclonal (AB5535, 1:1000, 1 μg/mL, Merck), anti-DDX4 goat polyclonal (AF 2030, 1:500, 0.4 μg/mL, R&D Systems), anti-Laminin rabbit polyclonal (L9393, 1:200, 2.5 μg/mL, Merck), anti-GATA4 mouse monoclonal (sc-25310, 1:100, 2 μg/mL, Santa Cruz), anti-PECAM1 goat polyclonal (AF3628, 1:100, 2 μg/mL, R&D Systems), anti-PH3 rabbit polyclonal (06570, 1:1000, 1 μg/mL, Merck), anti-HSD3B mouse monoclonal (sc-515120, 1:100, 2 μg/mL, Santa Cruz), and anti-cleaved Caspase-3 rabbit polyclonal (9661, 1:1000, 0.052 μg/mL, Cell Signaling). The secondary antibodies used were donkey anti-rabbit Alexa Fluor 488 (A21206), donkey anti-mouse Alexa Fluor 594 (A32744), and donkey anti-goat Alexa Fluor 647 (A32849) from Thermo Fisher Scientific (1:1000, 2 μg/mL). Slides were mounted and imaged using fluorescence microscopy or confocal microscopy (Olympus Corp).

2.5 xCELLigence

The human testicular cell line NT2/D1 cells were grown in DMEM/F12 GlutaMAX medium (Gibco) supplemented with 10% FBS (Bovogen) and 1% antibiotic-antimycotic (Gibco). Culture medium was replaced every two to 3 days, and cells were subcultured at a ratio of 1:2 to 1:3 using 0.05% trypsin-EDTA (Gibco) when reaching 90%–95% confluency. NT2/D1 cells were cultured in the serum-free starvation medium for 6 h before being seeded in E-plates (Agilent Technologies) at a density of 1×10^4 cells per well. TRPC3 inhibitor Pyr3 was added at the start of the experiment. Readings were taken on the xCELLigence machine every minute for 72 h. Adhesion was analysed in the first 5 h, and proliferation was analysed in 5–72 h. All treatments were performed in quadruplicate to a total of three biological replicates. Rates of change were represented as slope (1/hr). Statistical significance was determined using one-way ANOVA followed by the Dunnett multiple comparisons test performed in GraphPad Prism 8.

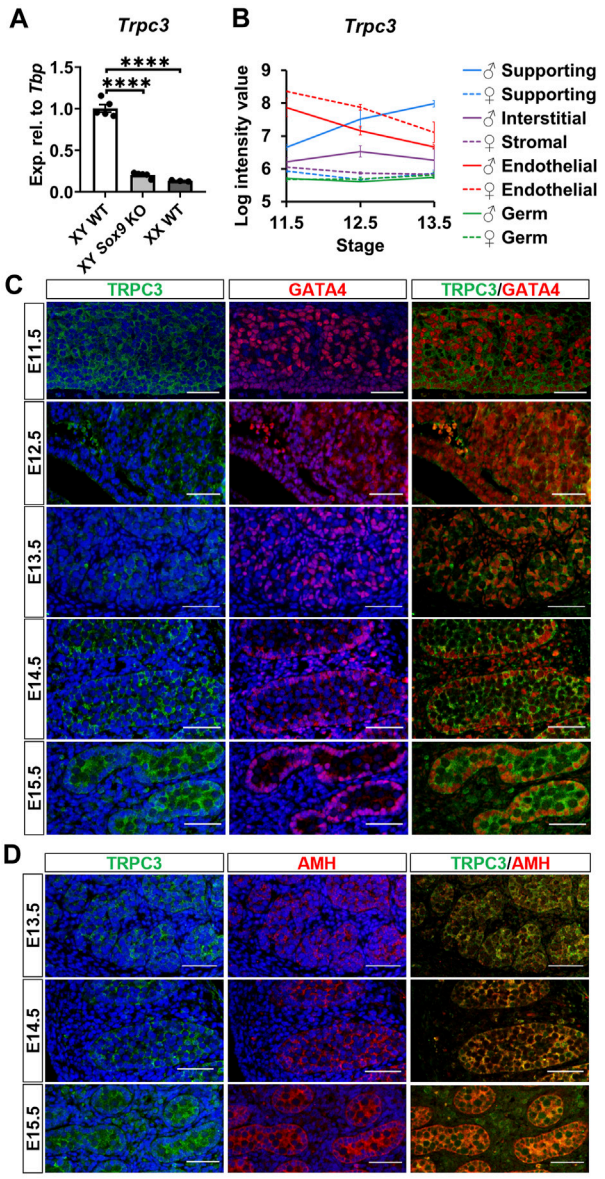

FIGURE 1
Expression of *Trpc3*/TRPC3 in the developing mouse testis. **(A)** qRT-PCR analysis confirming the downregulation of *Trpc3* in E13.5 mouse *Sox9* knockout gonads. n = 5 for XY wildtype (XY WT) and XY *Sox9* conditional knockout (XY *Sox9* KO), *n* = 3 for XX wildtype (XX WT). Transcript expression level of the *Trpc3* gene was normalized to *Tbp* and presented as relative expression. Mean ± SEM. One-way ANOVA test. ****$p < 0.0001$. **(B)** *Trpc3* RNA expression levels in developing male and female gonads from E11.5 to E13.5. The figure is generated based on the microarray dataset from Jameson et al. (2012). **(C, D)** Co-immunofluorescence staining of TRPC3 (green) with somatic cell nuclear marker GATA4 (red) and Sertoli cell cytoplasmic marker AMH (red) in the mouse testis from E11.5 to E15.5. Nuclei are visualized with the nuclear marker DAPI (blue). Scale bar = 50 μm.

2.6 HoloMonitor

The digital holographic microscope HoloMonitor (Phase Holographic Imaging AB) was used for real-time monitoring of cell morphology in culture. NT2/D1 cells were transfected with the siTRPC3 (SASI_Hs01_00195103, Merck) or the negative control

siRNA (SIC001, Merck) using Lipofectamine RNAiMAX (13778–150, Invitrogen) according to the manufacturer's instructions. After 48 h, cells were seeded into a 24-well lumox® plate (94.6110.024, Sarstedt) at 5.073×10^4 cells per well in 1.8 mL cell culture medium. After 5 h of cell adhesion, the standard plate lid was replaced with the HoloLids (71130, Phase Holographic Imaging AB). The plate was immediately placed on the stage of the HoloMonitor M4, which was kept inside a humidified incubator maintained at 37°C and 5% CO_2. HStudio 2.7 software was launched and set up according to the manufacturer's manual. Multiple cellular parameters including cell count, confluence, cell area, optical thickness, volume, irregularity, and eccentricity were analysed. Two independent experiments were conducted for each experimental group, with phase contrast and holographic images being recorded from three randomly selected areas in each experiment.

3 Results

3.1 TRPC3 is strongly expressed in Sertoli cells from E13.5

We validated the downregulation of *Trpc3* in *AMH-Cre;Sox9*$^{flox/flox}$ (*Sox9* KO) testes at E13.5, in accordance with our previous RNA-sequencing data in *Sox9* KO testes (Rahmoun et al., 2017). qRT-PCR analysis revealed an 80% reduction of *Trpc3* expression in XY *Sox9* KO testes compared to XY wildtype (WT) testes at E13.5 (Figure 1A), with *Trpc3* expression levels close to those of XX WT gonads which were 86.7% lower than XY WT. We further investigated *Trpc3* expression during testis development by screening previous microarray data of male and female developing gonads from E11.5 to E13.5 (Jameson et al., 2012) and querying expression of *Trpc3* in isolated cell lineages of the developing male or female mouse gonad (Supplementary Figure S1). The expression of *Trpc3* increases in Sertoli cells between E11.5 and E13.5, while it remains absent from female supporting cells, stromal cells, and both male and female germ cells (Figure 1B). Taken together, these data suggest *Trpc3* expression is dependent on SOX9 during sex differentiation and is minimally expressed in XX gonads at E13.5.

We further assessed TRPC3 expression and localization in the developing male gonad between E11.5 and E15.5 through co-immunofluorescence staining together with either the somatic cell marker GATA4, which is strongly expressed in the nucleus of Sertoli cells, or with the Sertoli cell cytoplasmic marker AMH. TRPC3 protein was expressed at all five time points examined (Figure 1C). At E11.5 and E12.5, TRPC3 expression was identified in somatic cells. From E13.5 onwards, TRPC3 protein was clearly expressed in the Sertoli cell membrane and cytoplasm, as indicated by its colocalization with AMH (Figure 1D). Since the *Trpc3* gene is expressed in endothelial cells between E11.5 and E13.5 (Figure 1B), we also performed co-immunostaining for TRPC3 and the endothelial cell and germ cell marker PECAM1 between E11.5 and E15.5. At E12.5, E13.5 and E15.5, weak TRPC3 staining was found in a subset of endothelial cells of the coelomic blood vessel (Supplementary Figure S2). From E14.5 onwards, weak TRPC3 staining was also detectable in interstitial cells (Figures 1C, D). Co-immunostaining for TRPC3 and the Leydig cell marker HSD3B revealed that these are Leydig cells (Supplementary Figure S2). However, since these signals were also detected in the PECAM1 channel, it is possible that they represent nonspecific background staining (Supplementary Figure S2).

3.2 Inhibition of TRPC3 leads to a reduction in germ cell numbers in cultured XY gonads

To elucidate the role of TRPC3 in gonad development, we conducted *ex vivo* gonad culture experiments in which E11.5 male and female mouse gonads were treated with the TRPC3-specific inhibitor Pyr3 for 24 h, followed by 24 and 48 h culture in fresh media. Following the culture, gonads were analyzed by immunofluorescence for cell-specific markers such as SOX9 for Sertoli cells, DDX4 for germ cells, and GATA4 for somatic cells. After 72 h of culture, Pyr3-treated XY gonads exhibited a substantial reduction in germ cell numbers (2.9-fold) when compared to control XY gonads (Figures 2A, B). At the 48-h time point, Pyr3-treated XY gonads already exhibited a reduction in germ cell numbers (1.3-fold) in comparison to control XY gonads (Figures 2A, B), whereas after 24 h, germ cell numbers were still similar in Pyr3-treated and control XY gonads (Figures 2A, B). Distinct from the male gonads, TRPC3 inhibition did not cause any changes in germ cell numbers in female gonads (Supplementary Figure S3), highlighting a sex-specific response to TRPC3 inhibition.

To elucidate the mechanisms contributing to the reduced number of germ cells in Pyr3-treated XY gonads, we examined cell proliferation and apoptosis through immunofluorescence analysis in cultured gonads, using phospho-histone H3 (PH3) for proliferation assessment and cleaved Caspase-3 (CC3) for apoptosis. After 72 h of culture, the proportion of proliferating germ cells in control XY gonads was 31.44%, whereas Pyr3-treated XY gonads exhibited a reduced percentage of 17.84% (1.76-fold reduction) (Figures 2C, D). At the 48-h time point, Pyr3-treated XY gonads already displayed a significant 1.46-fold decrease in germ cell proliferation compared to XY control gonads (31.42% *versus* 21.58%). Notably, after 24 h of culture, the percentage of proliferating germ cells between the two groups was still comparable (38.64% *versus* 39.86%). Analysis of germ cell apoptosis revealed no significant differences between XY control gonads and XY Pyr3-treated gonads at the 24, 48 and 72-h time points (Supplementary Figure S4). Collectively, these findings suggest that the reduction of the germ cell population following TRPC3 inhibition is caused by decreased germ cell proliferation. Immunofluorescence analysis for Laminin, a marker for the basal lamina of testis cords, revealed that after 48 and 72 h of culture, both control and Pyr3-treated XY gonads had formed well-defined testis cords, wherein Laminin and a closely associated layer of Sertoli cells encircled both germ cells and Sertoli cells (Supplementary Figure S5).

3.3 Inhibition of TRPC3 perturbs the coelomic blood vessel in cultured XY gonads

Given that TRPC3 is also expressed in endothelial cells and inhibition of vascularization disrupts testis cord formation and

10.3389/fcell.2024.1337714

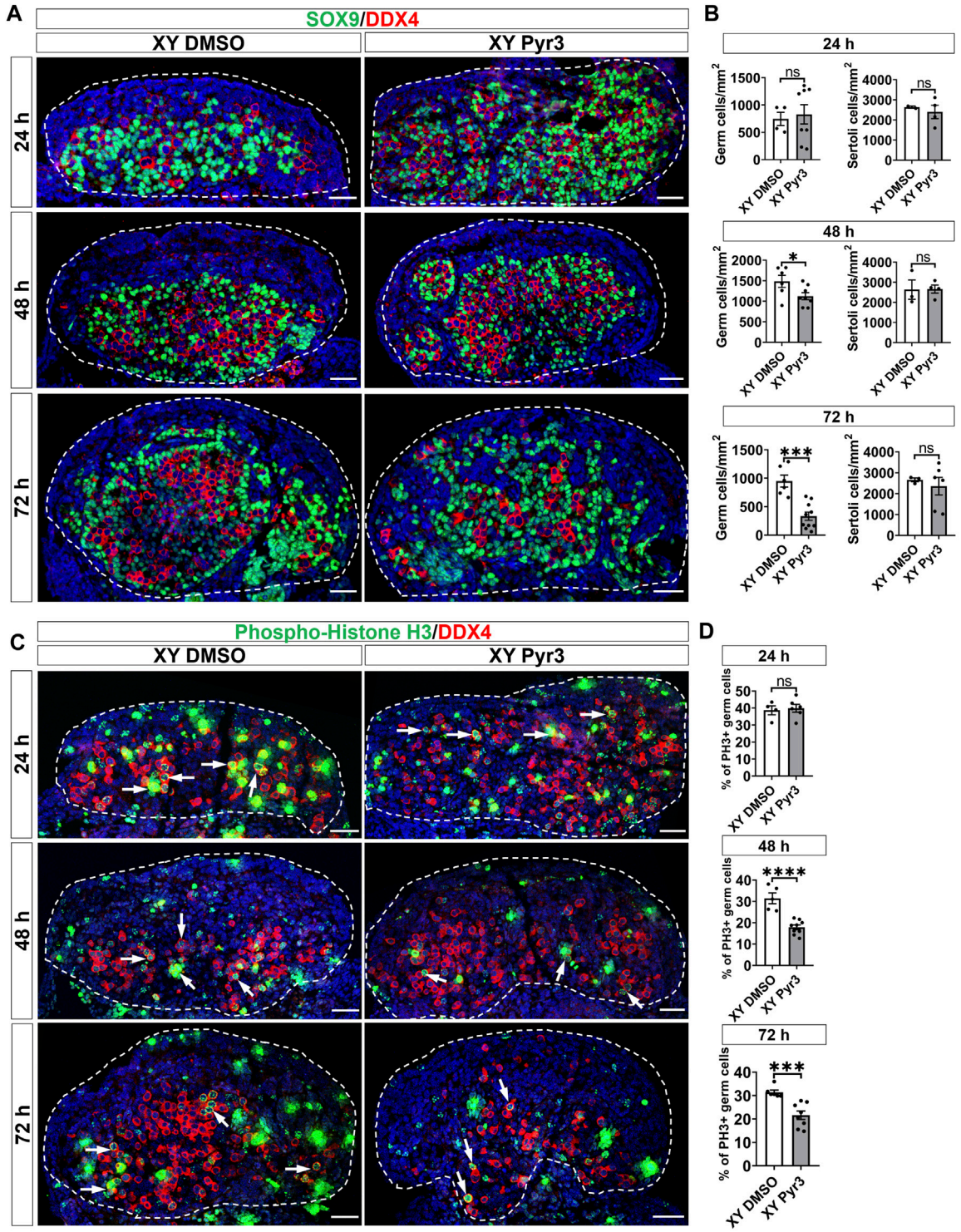

FIGURE 2
TRPC3 inhibition leads to a reduction in germ cell numbers and proliferation in cultured XY mouse gonads. **(A)** Immunofluorescence staining of male gonads after exposure to either the vehicle control DMSO or the TRPC3 inhibitor Pyr3 during *ex vivo* culture for 24, 48, and 72 h. The sections are stained for germ cell marker DDX4 (red) and Sertoli cell marker SOX9 (green). Nuclei are visualized with the nuclear marker DAPI (blue). Dashed lines outline gonads. Scale bar = 50 µm. **(B)** Quantification of germ cells and Sertoli cells in XY DMSO and XY Pyr3-treated gonads at 24-, 48- and 72-h post-culture. n = 2–4; sections counted = 2–10. Mean ± SEM. Unpaired Student's t-test. *$p < 0.05$, ***$p < 0.001$; ns, not significant. **(C)** Immunofluorescence staining for the germ cell marker DDX4 (red) and cell proliferation marker phospho-histone H3 (PH3) (green). White arrows indicate examples of proliferating germ cells. **(D)** Quantification of proliferating germ cells is performed for PH3+ germ cells relative to the total germ cell population. n = 2–4; sections counted = 4–9. Mean ± SEM. Unpaired Student's t-test. ***$p < 0.001$, ****$p < 0.0001$; ns, not significant.

10.3389/fcell.2024.1337714

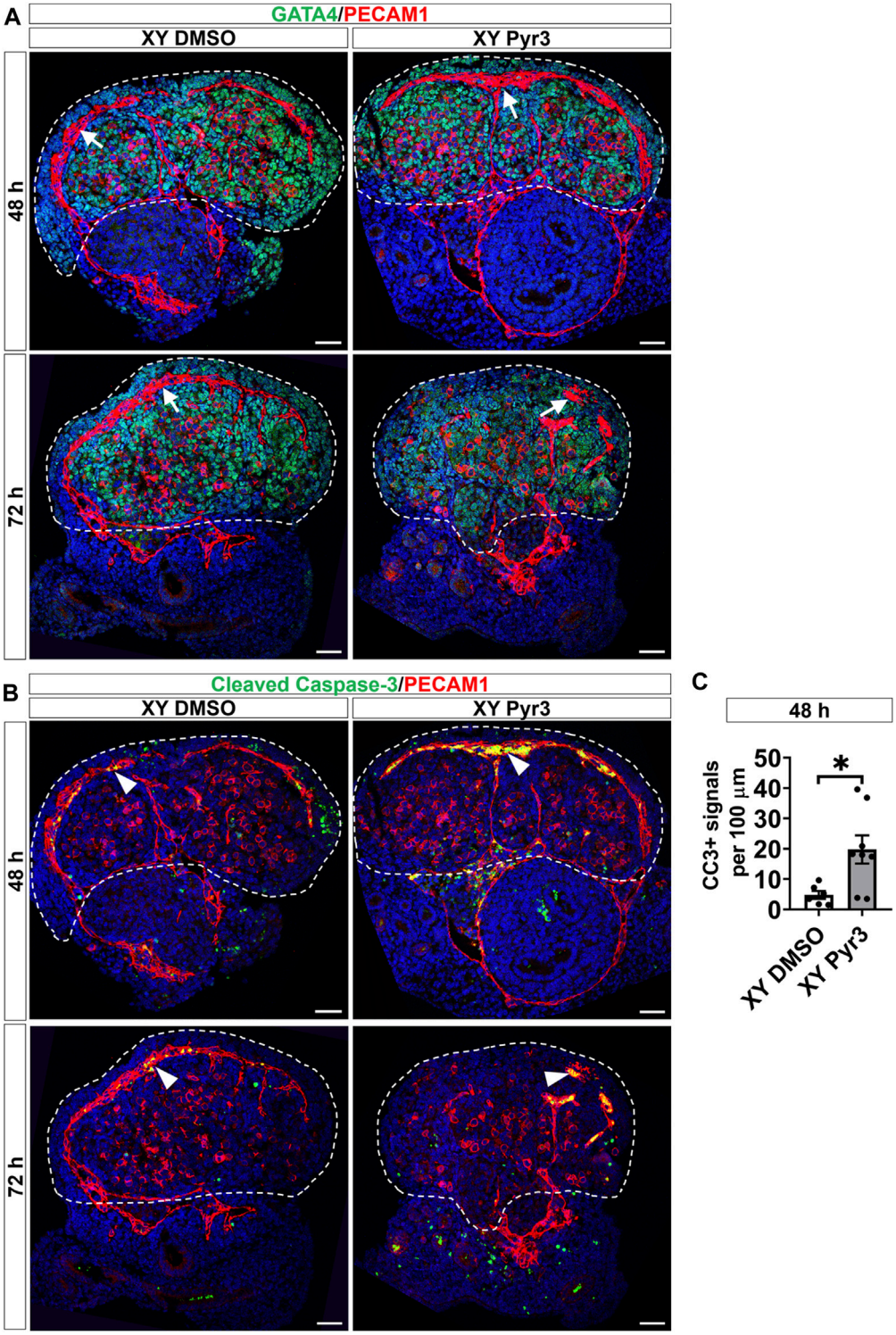

FIGURE 3
TRPC3 inhibition disrupts the coelomic blood vessel after 72 h of culture. **(A)** Immunofluorescence staining of GATA4 (green) and PECAM1 (red) in control (XY DMSO) and Pyr3-treated (XY Pyr3) gonads cultured *ex vivo* for 48 and 72 h. White arrows indicate the coelomic blood vessel. **(B)** Immunofluorescence staining of the cell apoptosis marker cleaved Caspase-3 (CC3) (green) and PECAM1 (red) in XY DMSO and XY Pyr3 gonads cultured *ex vivo* for 48 and 72 h. Arrowheads indicate examples of apoptotic endothelial cells. Nuclei are visualized with the nuclear marker DAPI (blue). Dashed lines outline gonads. Scale bar = 50 µm. **(C)** Quantification of apoptotic endothelial cells is performed for the number of CC3+ signals per 100 µm of the coelomic blood vessel. n = 3–4; sections counted = 6–8. Mean ± SEM. Unpaired Student's t-test. *$p < 0.05$.

10.3389/fcell.2024.1337714

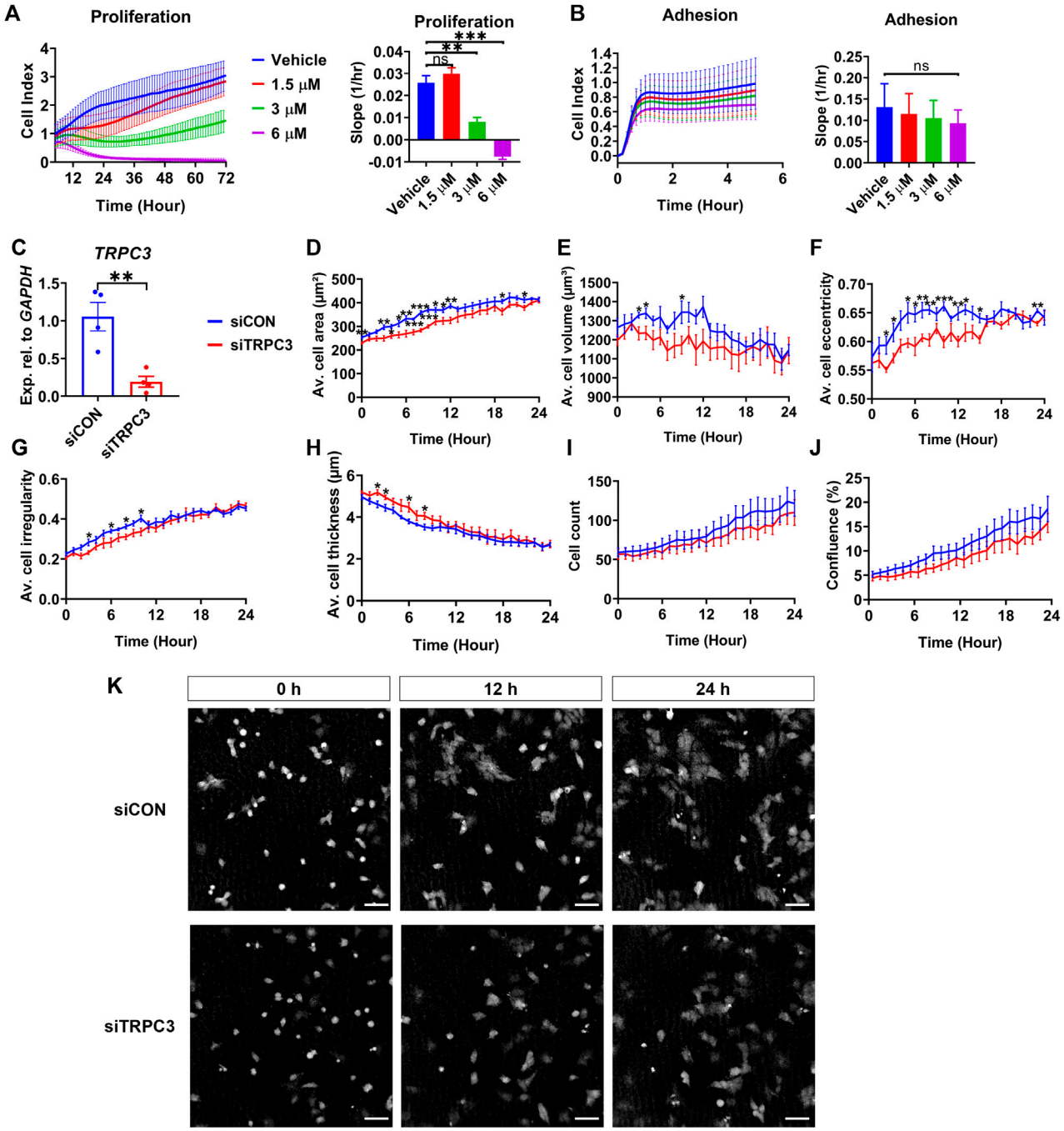

FIGURE 4
TRPC3 stimulates proliferation and controls cell morphology in NT2/D1 cells. **(A, B)** Cell proliferation (5–72 h) and cell adhesion (0–5 h) curves were generated from the xCELLigence system. Electrical impedance was measured and reported as cell index. The rate of cell proliferation or adhesion was calculated as the slope (1/hr). Mean ± SEM values were taken from three independent biological experiments. One-way ANOVA test. $^{**}p < 0.01$, $^{***}p < 0.001$; ns, not significant. **(C)** qRT-PCR analysis showing the expression levels of *TRPC3* in control (siCON) and siTRPC3 groups. Data are presented as Mean ± SEM, with statistical significance determined by unpaired Student's t-test. $^{**}p < 0.01$, n = 4. **(D–J)** HoloMonitor measurements of cell morphology include cell area, volume, eccentricity, irregularity, thickness, count, and confluence. Mean ± SEM values represent the average of two independent experiments. Unpaired Student's t-test. $^{*}p < 0.05$, $^{**}p < 0.01$, $^{***}p < 0.001$. **(K)** Holographic phase images depict cells from siCON and siTRPC3 groups at 0, 12 and 24 h. Scale bar = 50 μm.

partitioning (Bott et al., 2006; Combes et al., 2009; Cool et al., 2011), we examined the potential non-Sertoli cell effects of Pyr3 treatment on vascularization using the endothelial cell marker PECAM1. At the 48-h time point, both control and Pyr3-treated XY gonads exhibited the formation of a typical coelomic blood vessel and regular vessels between testis cords (Figure 3A). This observation suggests that TRPC3 inhibition did not disrupt vascularization at this early stage, indicating that the reduction in germ cell numbers

was unlikely due to vascular defects. However, after 72 h of culture, the coelomic vessel was disrupted in Pyr3-treated gonads when compared to control gonads (Figure 3A). This disruption suggests an altered vascularization pattern associated with TRPC3 inhibition during the later stages of culture. Subsequent analysis of endothelial cell apoptosis at the 48-h time point revealed that Pyr3-treated gonads showed a 4-fold increase in the number of cleaved Caspase-3 signals at the coelomic blood vessel when compared to control gonads (Figures 3B, C). These findings suggest that, although the coelomic blood vessel was not disturbed at the 48-h time point, it was already manifesting with increased endothelial cell apoptosis.

3.4 TRPC3 stimulates proliferation and controls cell morphology in NT2/D1 cells

To explore the impact of TRPC3 on Sertoli cell proliferation, we treated the human testicular cell line NT2/D1 with TRPC3 inhibitor Pyr3 at various concentrations, monitoring cell adhesion and proliferation in real-time over 72 h using the xCELLigence system. TRPC3 inhibition induced a dose-dependent reduction in cell proliferation, while cell adhesion remained unaffected (Figures 4A, B). To examine whether TRPC3 also regulates cell morphology over time, we silenced *TRPC3* in NT2/D1 cells using siRNA (Figure 4C) and measured cell morphology using the digital holographic microscope HoloMonitor. *TRPC3* knockdown resulted in a decrease cell area (Figure 4D), volume (Figure 4E), eccentricity (Figure 4F) and irregularity (Figure 4G), and an increase in cell thickness (Figure 4H), especially in the first 6–12 h. Both control (siCON) and *TRPC3* knockdown (siTRPC3) groups had similar initial densities with consistent increases over time, as indicated by the cell count and confluence results (Figures 4I, K). The *si*TRPC3 group showed slower cell proliferation but no significant difference compared to the control group, consistent with xCELLigence results. These findings suggest that TRPC3 stimulates Sertoli cell proliferation and controls cell morphology *in vitro*.

4 Discussion

SOX9 is a critical transcription factor in testis development, and its downstream target genes, such as *Amh*, *Dhh*, and *Cyp26b1*, play crucial roles in this process (Ming et al., 2022). We hypothesized that potential SOX9 target genes are also significant contributors to testis formation and may represent potential candidates for genetic mutations associated with human Differences/Disorders of Sex Development (DSD). In this study, we investigated the function of *Trpc3*, a putative direct target gene of SOX9, in testis development. The *Trpc3* gene is expressed in Sertoli cells from E11.5 onwards, and we found that TRPC3 protein exhibited high expression levels in Sertoli cells from at least E13.5, suggesting its involvement in early testis development. Our *ex vivo* gonad culture experiments revealed its role in supporting male germ cell development. The effects were absent in female gonads, possibly attributed to the lack of *TRPC3* expression in female granulosa or stromal cells, highlighting the sex-specific effects of TRPC3. In addition, we demonstrated that *Trpc3*/TRPC3 gene and protein are also expressed in endothelial cells. Our *ex vivo* gonad culture experiments showed that TRPC3 is required to maintain the coelomic blood vessel. Overall, our findings indicate that TRPC3 has two distinct functions in XY gonads: in Sertoli cells to stimulate germ cell proliferation and in endothelial cells to ensure their survival.

We observed a significant downregulation of *Trpc3* expression in E13.5 Sox9 KO XY gonads, showing that *Trpc3* expression is largely dependent on SOX9. Published scRNA-seq data indicate *Trpc3* expression in fetal Sertoli cells (Supplementary Figure S1); we found that expression of *Trpc3* in Sertoli cells increases within developing male gonads after sex determination. This implies the existence of a sex-specific mechanism in XY gonads that upregulates Trpc3 expression during sex differentiation. Our previous SOX9 ChIP-seq data demonstrated SOX9 binding to the proximal promoter region and intron 1 of both mouse and bovine fetal testes (Supplementary Figure S6A, B) (Rahmoun et al., 2017). DNase I hypersensitivity data from human fetal testes and fetal ovaries shows increased chromatin accessibility in this region (Supplementary Figure S6B) (Kundaje et al., 2015), and ENCODE histone modifications in NT2/D1 cells indicates active regulatory potential (Supplementary Figure S6B) (ENCODE Project Consortium, 2012). Moreover, prediction of transcription factor binding sites within the SOX9 ChIP-seq peaks revealed three potential SOX9 binding sites and one GATA4 binding site in the Trpc3/TRPC3 promoter region (Supplementary Figure S6C). Based on these data, it appears likely that SOX9 directly binds to the proximal promoter and/or intron 1 of *Trpc3*/*TRPC3* to regulate its transcription in Sertoli cells. Following the initiation of *Trpc3*/*TRPC3* expression by SOX9, other transcription factors in Sertoli cells, such as SOX8, SOX10, and GATA4, may upregulate *Trpc3*/*TRPC3* expression cooperatively (Barrionuevo and Scherer, 2010; Sekido and Lovell-Badge, 2013; Eggers et al., 2014; Viger et al., 2022). Future investigations could utilize ChIP-qPCR and luciferase assays to validate these hypotheses.

The results from our *ex vivo* gonad culture experiments, in which we treated male gonads with the TRPC3 inhibitor Pyr3, provided valuable insights into the role of *Trpc3* in the developing testis. By 48 and 72 h, Pyr3-treated XY gonads showed a reduced number of germ cells due to decreased germ cell proliferation, alongside disrupted coelomic blood vessel and increased endothelial cell apoptosis. These results suggest a potential role for TRPC3 in male fertility. One *Trpc3* KO model, the Δ202 mice, disrupted the *Trpc3* promoter due to the SV40 T antigen transgene insertion, leading to the inhibition of transcription and subsequent knockout of the TRPC3 protein. This *Trpc3* KO mouse model presented severe phenotypes, including reduced average litter size, hindlimb atrophy, and progressive paralysis, ultimately leading to the death of these mice within 3–4 months (López-Revilla et al., 2004; Rodríguez-Santiago et al., 2007). The decreased average litter size in KO mice may be a result of decreased fertility and embryo viability. This *Trpc3* KO mouse model as well as our *ex vivo* gonad culture model could potentially serve as valuable tools for future investigations into TRPC3 roles in fetal testis development. In contrast, two types of whole-body *Trpc3* KO mouse models have been reported to be viable, fertile, and phenotypically normal compared to wildtype mice (Hartmann et al., 2008; Dong et al., 2017). These *Trpc3* KO mouse models were generated through the excision of either exon 7 or exons 7 and 8 from the *Trpc3* gene using a

Cre-loxP-based strategy. Consequently, the *Trpc3* gene in these KO mice is expected to encode a truncated TRPC3 protein, which might retain some functional activity (Trebak, 2010).

Previously, a rare *TRPC3* variant (NM_001130698.2:c.2285G > A; p.Arg762His) (R762H) was identified in a patient with spinocerebellar ataxia type 41 (MIM#616410) (Fogel et al., 2015). The TRPC3 mutation falls within the highly conserved TRP box (EWKFAR) which is implicated in channel gating (Clapham, 2003; Fogel et al., 2015; Chen et al., 2021), and overexpression of the mutant TRPC3 protein led to significant cell death and increased nuclear localization of the calcium-responsive transcription factor NFAT (Fogel et al., 2015). We previously identified the same *TRPC3* R762H variant as one of only 24 candidate modifiers in a 46, XY DSD patient with an *FGF9* variant (c.583G > A; p. Asp195Asn) (Croft et al., 2023). To assess the pathogenicity of the *TRPC3* variant, knock-in mice could be generated and be crossed with *Fgf9* mutant mice to model the 46, XY DSD patient and assess the effects of both variants on testis development in mice. To test whether the mutant TRPC3 protein enhances channel activity and induces cell death, introducing *TRPC3* mutations into human cell lines such as NT2/D1 and newly generated human testis and ovary cell lines from induced pluripotent stem cells (iPSC) could provide valuable insights (Knarston et al., 2020; Gonen et al., 2023; Pierson Smela et al., 2023).

In summary, our study unveiled *Trpc3* as a novel direct target gene of SOX9, prominently expressed in Sertoli cells. Our *ex vivo* gonad culture experiments shed light on the potential role of TRPC3 in Sertoli, germ and endothelial cell development. Additionally, the *TRPC3* variant (c.2285G > A; p.Arg762His) may implicate a potential involvement of *TRPC3* in human DSD.

Data availability statement

The datasets presented in this study can be found in online repositories. The names of the repository/repositories and accession number(s) can be found in the article/Supplementary Material.

Ethics statement

Ethical approval was not required for the studies on humans in accordance with the local legislation and institutional requirements because only commercially available established cell lines were used. The animal study was approved by the Monash Medical Centre Animal Ethics Committee. The study was conducted in accordance with the local legislation and institutional requirements.

Author contributions

ZM: Conceptualization, Formal Analysis, Investigation, Methodology, Project administration, Visualization, Writing–original draft, Writing–review and editing. SB-F: Conceptualization, Data curation, Software, Supervision, Writing–review and editing. EF: Supervision, Writing–review and editing. JR: Methodology, Writing–review and editing. BV: Visualization, Writing–review and editing. VH: Conceptualization, Funding acquisition, Project administration, Resources, Supervision, Writing–review and editing.

Funding

The author(s) declare financial support was received for the research, authorship, and/or publication of this article. This research received financial support from the National Health and Medical Research Council Program Grant 2002426 and Fellowship APP1154870 awarded to VH. Additional support was provided by the China Scholarship Council (CSC) and the Australian Government Research Training Program Scholarship for ZM. We also acknowledge funding through the Victorian Government's Operational Infrastructure Support Program.

Acknowledgments

The authors acknowledge the Monash Medical Centre Animal Facility, the Medical Genomics Facility at the Monash Health Translation Precinct (MHTP), the MHTP Monash Micro Imaging, and the MHTP Monash Histology Platform. The authors also thank other members of the VH Lab for useful discussion and valuable comments.

Conflict of interest

The authors declare that the research was conducted in the absence of any commercial or financial relationships that could be construed as a potential conflict of interest.

Publisher's note

Supplementary material

The Supplementary Material for this article can be found online at: https://www.frontiersin.org/articles/10.3389/fcell.2024.1337714/full#supplementary-material

SUPPLEMENTARY FIGURE S1
UMAP (uniform manifold approximation and projection) of the cell lineages (color) in the male or female mouse gonad at ages E10.5, E11.5 and E12.5 (pooled data) scRNA-seq dataset from Garcia-Alonso et al. (Garcia-Alonso et al., 2022). In male: the Sertoli cell (chartreuse) and endothelial cell (green) clusters have been identified; in female: the pre-granulosa cell (pink) and endothelial cell (green) clusters have been identified. UMAP of gene expression shows *Sox9, Amh, Pecam1, Foxl2* and *Trpc3* gene expression across all cell lineages for either male or female embryonic mouse gonad. UMAP of stage indicates the embryonic day (E) of each derived cell within lineage clusters.

SUPPLEMENTARY FIGURE S2
Co-immunofluorescence staining of TRPC3 (green) with the endothelial cell and germ cell marker PECAM1 (red) in the mouse testis from E11.5 to E15.5, and with the Leydig cell marker HSD3B (red) at E14.5 and E15.5. Dashed

white arrows indicate possible colocalization of TRPC3 and PECAM1. Arrowheads indicate HSD3B staining. Nuclei are visualized with the nuclear marker DAPI (blue). Scale bar = 50 μm.

SUPPLEMENTARY FIGURE S3

TRPC3 inhibition has no impact on cultured XX mouse gonads. **(A)** Immunofluorescence staining of female gonads after exposure to either the vehicle control DMSO or the TRPC3 inhibitor Pyr3 during ex vivo culture for 24, 48, and 72 h. The sections are stained for germ cell marker DDX4 (red) and somatic cell marker GATA4 (green). Nuclei are visualized with the nuclear marker DAPI (blue). Dashed lines outline gonads. Scale bar = 50 μm. **(B)** Quantification of germ cells in XX DMSO and XX Pyr3-treated gonads at 24, 48 and 72 h post-culture. n = 2; sections counted = 4–10. Mean ± SEM. Unpaired Student's t-test. ns, not significant.

SUPPLEMENTARY FIGURE S4

TRPC3 inhibition does not affect germ cell apoptosis in cultured XY gonads. **(A)** Apoptosis analysis at 24, 48, and 72 h in XY gonads treated with DMSO or Pyr3 by immunofluorescence staining for the cell apoptosis marker cleaved Caspase-3 (CC3) (green) and the germ cell marker DDX4 (red). Arrowheads indicate examples of apoptotic germ cells. Nuclei are visualized with the nuclear marker DAPI (blue). Scale bar = 50 μm. Dashed lines outline gonads. **(B)** Quantification of apoptotic germ cells is performed for CC3+ germ cells relative to the total germ cell population. n = 2–4; sections counted = 5–11. Data are represented as Mean ± SEM. Unpaired Student's t-test. ns, not significant.

SUPPLEMENTARY FIGURE S5

TRPC3 inhibition has no impact on testis cord formation in cultured XY gonads. Immunofluorescence staining of Laminin (green) and GATA4 (red) in control (XY DMSO) and Pyr3-treated (XY Pyr3) gonads cultured *ex vivo* for 24, 48 and 72 h. Nuclei are visualized with the nuclear marker DAPI (blue). Yellow dashed lines outline gonads. White dashed lines outline testis cords. Scale bar = 50 μm.

SUPPLEMENTARY FIGURE S6

Analysis of SOX9 ChIP peaks in the *Trpc3/TRPC3* gene. **(A)** SOX9 ChIP-seq peaks indicate regions bound by SOX9 within the *Trpc3* gene in mouse fetal testes (Rahmoun et al., 2017), visualized using IGV. **(B)** The schematic presents key regulatory features of the *Trpc3/ TRPC3* gene visualized on the UCSC genome browser. Black boxes indicate the locations of SOX9 ChIP peaks within the *Trpc3/TRPC3* gene in mouse and bovine fetal testes (Rahmoun et al., 2017). Bioinformatic tracks from the UCSC genome browser include the DNase I hypersensitivity data from human fetal testis and ovary (Kundaje et al., 2015), the 100-vertebrate conservation track, and ENCODE histone modification peaks present in the human testicular cell line NT2/D1 (ENCODE Project Consortium, 2012). **(C)** Alignment of the *Trpc3/TRPC3* promoter regions of mouse, bovine and human. Potential SOX9 and GATA4 binding motifs were predicted by PROMO (Farré et al., 2003) and JASPAR (Rauluseviciute et al., 2024) programs. The potential binding motifs for SOX9 and GATA4 are highlighted in red and green, respectively. Nucleotide conservation between mouse, bovine and human is indicated by asterisks (*). The transcription start site (TSS) is marked with an angled arrow.

References

Arango, N. A., Lovell-Badge, R., and Behringer, R. R. (1999). Targeted mutagenesis of the endogenous mouse Mis gene promoter: *in vivo* definition of genetic pathways of vertebrate sexual development. *Cell* 99 (4), 409–419. doi:10.1016/s0092-8674(00)81527-5

Bagheri-Fam, S., Bird, A. D., Zhao, L., Ryan, J. M., Yong, M., Wilhelm, D., et al. (2017). Testis determination requires a specific FGFR2 isoform to repress FOXL2. *Endocrinology* 158 (11), 3832–3843. doi:10.1210/en.2017-00674

Barrionuevo, F., Bagheri-Fam, S., Klattig, J., Kist, R., Taketo, M. M., Englert, C., et al. (2006). Homozygous inactivation of Sox9 causes complete XY sex reversal in mice. *Biol. Reprod.* 74 (1), 195–201. doi:10.1095/biolreprod.105.045930

Barrionuevo, F., Georg, I., Scherthan, H., Lécureuil, C., Guillou, F., Wegner, M., et al. (2009). Testis cord differentiation after the sex determination stage is independent of Sox9 but fails in the combined absence of Sox9 and Sox8. *Dev. Biol.* 327 (2), 301–312. doi:10.1016/j.ydbio.2008.12.011

Barrionuevo, F., and Scherer, G. (2010). SOX E genes: SOX9 and SOX8 in mammalian testis development. *Int. J. Biochem. Cell Biol.* 42 (3), 433–436. doi:10.1016/j.biocel.2009.07.015

Becker, E. B., Fogel, B. L., Rajakulendran, S., Dulneva, A., Hanna, M. G., Perlman, S. L., et al. (2011). Candidate screening of the TRPC3 gene in cerebellar ataxia. *Cerebellum* 10 (2), 296–299. doi:10.1007/s12311-011-0253-6

Bernard, P., Ryan, J., Sim, H., Czech, D. P., Sinclair, A. H., Koopman, P., et al. (2012). Wnt signaling in ovarian development inhibits Sf1 activation of Sox9 via the Tesco enhancer. *Endocrinology* 153 (2), 901–912. doi:10.1210/en.2011-1347

Bott, R. C., McFee, R. M., Clopton, D. T., Toombs, C., and Cupp, A. S. (2006). Vascular endothelial growth factor and kinase domain region receptor are involved in both seminiferous cord formation and vascular development during testis morphogenesis in the rat. *Biol. Reprod.* 75 (1), 56–67. doi:10.1095/biolreprod.105.047225

Castellano, L. E., Treviño, C. L., Rodríguez, D., Serrano, C. J., Pacheco, J., Tsutsumi, V., et al. (2003). Transient receptor potential (TRPC) channels in human sperm: expression, cellular localization and involvement in the regulation of flagellar motility. *FEBS Lett.* 541 (1-3), 69–74. doi:10.1016/s0014-5793(03)00305-3

Chaboissier, M. C., Kobayashi, A., Vidal, V. I., Lützkendorf, S., van de Kant, H. J., Wegner, M., et al. (2004). Functional analysis of Sox8 and Sox9 during sex determination in the mouse. *Development* 131 (9), 1891–1901. doi:10.1242/dev.01087

Chassot, A. A., Ranc, F., Gregoire, E. P., Roepers-Gajadien, H. L., Taketo, M. M., Camerino, G., et al. (2008). Activation of beta-catenin signaling by Rspo1 controls differentiation of the mammalian ovary. *Hum. Mol. Genet.* 17 (9), 1264–1277. doi:10.1093/hmg/ddn016

Chen, Z., Kerwin, M., Keenan, O., and Montell, C. (2021). Conserved modules required for Drosophila TRP function *in vivo*. *J. Neurosci.* 41 (27), 5822–5832. doi:10.1523/jneurosci.0200-21.2021

Clapham, D. E. (2003). TRP channels as cellular sensors. *Nature* 426 (6966), 517–524. doi:10.1038/nature02196

Combes, A. N., Wilhelm, D., Davidson, T., Dejana, E., Harley, V., Sinclair, A., et al. (2009). Endothelial cell migration directs testis cord formation. *Dev. Biol.* 326 (1), 112–120. doi:10.1016/j.ydbio.2008.10.040

Cool, J., DeFalco, T. J., and Capel, B. (2011). Vascular-mesenchymal cross-talk through Vegf and Pdgf drives organ patterning. *Proc. Natl. Acad. Sci. U. S. A.* 108 (1), 167–172. doi:10.1073/pnas.1010299108

Croft, B., Bird, A. D., Ono, M., Eggers, S., Bagheri-Fam, S., Ryan, J. M., et al. (2023). FGF9 variant in 46,XY DSD patient suggests a role for dimerization in sex determination. *Clin. Genet.* 103 (3), 277–287. doi:10.1111/cge.14261

Dong, P., Guo, C., Huang, S., Ma, M., Liu, Q., and Luo, W. (2017). TRPC3 is dispensable for β-alanine triggered acute itch. *Sci. Rep.* 7 (1), 13869. doi:10.1038/s41598-017-12770-0

Eggers, S., Ohnesorg, T., and Sinclair, A. (2014). Genetic regulation of mammalian gonad development. *Nat. Rev. Endocrinol.* 10 (11), 673–683. doi:10.1038/nrendo.2014.163

Eggers, S., Sadedin, S., van den Bergen, J. A., Robevska, G., Ohnesorg, T., Hewitt, J., et al. (2016). Disorders of sex development: insights from targeted gene sequencing of a large international patient cohort. *Genome Biol.* 17 (1), 243. doi:10.1186/s13059-016-1105-y

ENCODE Project Consortium (2012). An integrated encyclopedia of DNA elements in the human genome. *Nature* 489 (7414), 57–74. doi:10.1038/nature11247

Farré, D., Roset, R., Huerta, M., Adsuara, J. E., Roselló, L., Albà, M. M., et al. (2003). Identification of patterns in biological sequences at the ALGGEN server: PROMO and MALGEN. *Nucleic Acids Res.* 31 (13), 3651–3653. doi:10.1093/nar/gkg605

Fogel, B. L., Hanson, S. M., and Becker, E. B. (2015). Do mutations in the murine ataxia gene TRPC3 cause cerebellar ataxia in humans? *Mov. Disord.* 30 (2), 284–286. doi:10.1002/mds.26096

Gonen, N., Eozenou, C., Mitter, R., Elzaiat, M., Stévant, I., Aviram, R., et al. (2023). *In vitro* cellular reprogramming to model gonad development and its disorders. *Sci. Adv.* 9 (1), eabn9793. doi:10.1126/sciadv.abn9793

Gonzalez-Cobos, J. C., and Trebak, M. (2010). TRPC channels in smooth muscle cells. *Front. Biosci. (Landmark Ed.)* 15 (3), 1023–1039. doi:10.2741/3660

Hartmann, J., Dragicevic, E., Adelsberger, H., Henning, H. A., Sumser, M., Abramowitz, J., et al. (2008). TRPC3 channels are required for synaptic transmission and motor coordination. *Neuron* 59 (3), 392–398. doi:10.1016/j.neuron.2008.06.009

Hofmann, T., Obukhov, A. G., Schaefer, M., Harteneck, C., Gudermann, T., and Schultz, G. (1999). Direct activation of human TRPC6 and TRPC3 channels by diacylglycerol. *Nature* 397 (6716), 259–263. doi:10.1038/16711

Hughes, I. A., Houk, C., Ahmed, S. F., and Lee, P. A. (2006). Consensus statement on management of intersex disorders. *J. Pediatr. Urol.* 2 (3), 148–162. doi:10.1016/j.jpurol.2006.03.004

Jameson, S. A., Natarajan, A., Cool, J., DeFalco, T., Maatouk, D. M., Mork, L., et al. (2012). Temporal transcriptional profiling of somatic and germ cells reveals biased lineage priming of sexual fate in the fetal mouse gonad. *PLoS Genet.* 8 (3), e1002575. doi:10.1371/journal.pgen.1002575

Jiménez, A., Fernández, R., Madrid-Bury, N., Moreira, P. N., Borque, C., Pintado, B., et al. (2003). Experimental demonstration that pre- and post-conceptional mechanisms influence sex ratio in mouse embryos. *Mol. Reprod. Dev.* 66 (2), 162–165. doi:10.1002/mrd.10345

Kashimada, K., Svingen, T., Feng, C. W., Pelosi, E., Bagheri-Fam, S., Harley, V. R., et al. (2011). Antagonistic regulation of Cyp26b1 by transcription factors SOX9/SF1 and FOXL2 during gonadal development in mice. *Faseb J.* 25 (10), 3561–3569. doi:10.1096/fj.11-184333

Kim, M. S., Lee, K. P., Yang, D., Shin, D. M., Abramowitz, J., Kiyonaka, S., et al. (2011). Genetic and pharmacologic inhibition of the Ca2+ influx channel TRPC3 protects secretory epithelia from Ca2+-dependent toxicity. *Gastroenterology* 140 (7), 2107–2115. doi:10.1053/j.gastro.2011.02.052

Kist, R., Schrewe, H., Balling, R., and Scherer, G. (2002). Conditional inactivation of Sox9: a mouse model for campomelic dysplasia. *Genesis* 32 (2), 121–123. doi:10.1002/gene.10050

Kitajima, N., Numaga-Tomita, T., Watanabe, M., Kuroda, T., Nishimura, A., Miyano, K., et al. (2016). TRPC3 positively regulates reactive oxygen species driving maladaptive cardiac remodeling. *Sci. Rep.* 6, 37001. doi:10.1038/srep37001

Kiyonaka, S., Kato, K., Nishida, M., Mio, K., Numaga, T., Sawaguchi, Y., et al. (2009). Selective and direct inhibition of TRPC3 channels underlies biological activities of a pyrazole compound. *Proc. Natl. Acad. Sci. U. S. A.* 106 (13), 5400–5405. doi:10.1073/pnas.0808793106

Knarston, I. M., Pachernegg, S., Robevska, G., Ghobrial, I., Er, P. X., Georges, E., et al. (2020). An *in vitro* differentiation protocol for human embryonic bipotential gonad and testis cell development. *Stem Cell Rep.* 15 (6), 1377–1391. doi:10.1016/j.stemcr.2020.10.009

Koopman, P., Gubbay, J., Vivian, N., Goodfellow, P., and Lovell-Badge, R. (1991). Male development of chromosomally female mice transgenic for Sry. *Nature* 351 (6322), 117–121. doi:10.1038/351117a0

Koopman, P., Münsterberg, A., Capel, B., Vivian, N., and Lovell-Badge, R. (1990). Expression of a candidate sex-determining gene during mouse testis differentiation. *Nature* 348 (6300), 450–452. doi:10.1038/348450a0

Kundaje, A., Meuleman, W., Ernst, J., Bilenky, M., Yen, A., Heravi-Moussavi, A., et al. (2015). Integrative analysis of 111 reference human epigenomes. *Nature* 518 (7539), 317–330. doi:10.1038/nature14248

Lécureuil, C., Fontaine, I., Crepieux, P., and Guillou, F. (2002). Sertoli and granulosa cell-specific Cre recombinase activity in transgenic mice. *Genesis* 33 (3), 114–118. doi:10.1002/gene.10100

Li, H. S., Xu, X. Z., and Montell, C. (1999). Activation of a TRPC3-dependent cation current through the neurotrophin BDNF. *Neuron* 24 (1), 261–273. doi:10.1016/s0896-6273(00)80838-7

Liu, X., Yao, X., and Tsang, S. Y. (2020). Post-translational modification and natural mutation of TRPC channels. *Cells* 9 (1), 135. doi:10.3390/cells9010135

López-Revilla, R., Soto-Zárate, C., Ridaura, C., Chávez-Dueñas, L., and Paul, D. (2004). Progressive paralysis associated with diffuse astrocyte anaplasia in delta 202 mice homozygous for a transgene encoding the SV40 T antigen. *Neuropathology* 24 (1), 30–37. doi:10.1111/j.1440-1789.2003.00536.x

Ming, Z., Vining, B., Bagheri-Fam, S., and Harley, V. (2022). SOX9 in organogenesis: shared and unique transcriptional functions. *Cell Mol. Life Sci.* 79 (10), 522. doi:10.1007/s00018-022-04543-4

Ottolenghi, C., Pelosi, E., Tran, J., Colombino, M., Douglass, E., Nedorezov, T., et al. (2007). Loss of Wnt4 and Foxl2 leads to female-to-male sex reversal extending to germ cells. *Hum. Mol. Genet.* 16 (23), 2795–2804. doi:10.1093/hmg/ddm235

Pierson Smela, M. D., Kramme, C. C., Fortuna, P. R. J., Adams, J. L., Su, R., Dong, E., et al. (2023). Directed differentiation of human iPSCs to functional ovarian granulosa-like cells via transcription factor overexpression. *Elife* 12, e83291. doi:10.7554/eLife.83291

Rahmoun, M., Lavery, R., Laurent-Chaballier, S., Bellora, N., Philip, G. K., Rossitto, M., et al. (2017). In mammalian foetal testes, SOX9 regulates expression of its target genes by binding to genomic regions with conserved signatures. *Nucleic Acids Res.* 45 (12), 7191–7211. doi:10.1093/nar/gkx328

Rauluseviciute, I., Riudavets-Puig, R., Blanc-Mathieu, R., Castro-Mondragon, J. A., Ferenc, K., Kumar, V., et al. (2024). JASPAR 2024: 20th anniversary of the open-access database of transcription factor binding profiles. *Nucleic Acids Res.* 52 (D1), D174–d182. doi:10.1093/nar/gkad1059

Reyes, A. P., León, N. Y., Frost, E. R., and Harley, V. R. (2023). Genetic control of typical and atypical sex development. *Nat. Rev. Urol.* 20 (7), 434–451. doi:10.1038/s41585-023-00754-x

Rodríguez-Santiago, M., Mendoza-Torres, M., Jiménez-Bremont, J. F., and López-Revilla, R. (2007). Knockout of the trcp3 gene causes a recessive neuromotor disease in mice. *Biochem. Biophys. Res. Commun.* 360 (4), 874–879. doi:10.1016/j.bbrc.2007.06.150

Ru, Y., Zhou, Y., and Zhang, Y. (2015). Transient receptor potential-canonical 3 modulates sperm motility and capacitation-associated protein tyrosine phosphorylation via [Ca2+]i mobilization. *Acta Biochim. Biophys. Sin. (Shanghai)* 47 (6), 404–413. doi:10.1093/abbs/gmv025

Ryan, J., Ludbrook, L., Wilhelm, D., Sinclair, A., Koopman, P., Bernard, P., et al. (2011). Analysis of gene function in cultured embryonic mouse gonads using nucleofection. *Sex. Dev.* 5 (1), 7–15. doi:10.1159/000322162

Sekido, R., and Lovell-Badge, R. (2008). Sex determination involves synergistic action of SRY and SF1 on a specific Sox9 enhancer. *Nature* 453 (7197), 930–934. doi:10.1038/nature06944

Sekido, R., and Lovell-Badge, R. (2013). Genetic control of testis development. *Sex. Dev.* 7 (1-3), 21–32. doi:10.1159/000342221

Svingen, T., and Koopman, P. (2013). Building the mammalian testis: origins, differentiation, and assembly of the component cell populations. *Genes Dev.* 27 (22), 2409–2426. doi:10.1101/gad.228080.113

Trebak, M. (2010). The puzzling role of TRPC3 channels in motor coordination. *Pflugers Arch.* 459 (3), 369–375. doi:10.1007/s00424-009-0740-5

Treviño, C. L., Serrano, C. J., Beltrán, C., Felix, R., and Darszon, A. (2001). Identification of mouse trp homologs and lipid rafts from spermatogenic cells and sperm. *FEBS Lett.* 509 (1), 119–125. doi:10.1016/s0014-5793(01)03134-9

Vidal, V. P., Chaboissier, M. C., de Rooij, D. G., and Schedl, A. (2001). Sox9 induces testis development in XX transgenic mice. *Nat. Genet.* 28 (3), 216–217. doi:10.1038/90046

Viger, R. S., de Mattos, K., and Tremblay, J. J. (2022). Insights into the roles of GATA factors in mammalian testis development and the control of fetal testis gene expression. *Front. Endocrinol. (Lausanne)* 13, 902198. doi:10.3389/fendo.2022.902198

Wisniewski, A. B., Batista, R. L., Costa, E. M. F., Finlayson, C., Sircili, M. H. P., Dénes, F. T., et al. (2019). Management of 46,XY differences/disorders of sex development (DSD) throughout life. *Endocr. Rev.* 40 (6), 1547–1572. doi:10.1210/er.2019-00049

Xu, Y., Wang, Y., Li, N., Yao, R., Li, G., Li, J., et al. (2019). New insights from unbiased panel and whole-exome sequencing in a large Chinese cohort with disorders of sex development. *Eur. J. Endocrinol.* 181 (3), 311–323. doi:10.1530/eje-19-0111

Yang, S. L., Cao, Q., Zhou, K. C., Feng, Y. J., and Wang, Y. Z. (2009). Transient receptor potential channel C3 contributes to the progression of human ovarian cancer. *Oncogene* 28 (10), 1320–1328. doi:10.1038/onc.2008.475

frontiers | Frontiers in Cell and Developmental Biology

TYPE Correction
PUBLISHED 15 October 2024
DOI 10.3389/fcell.2024.1484634

OPEN ACCESS

EDITED AND REVIEWED BY
Dagmar Wilhelm,
The University of Melbourne, Australia

*CORRESPONDENCE
Vincent R. Harley,
vincent.harley@hudson.org.au

RECEIVED 22 August 2024
ACCEPTED 26 September 2024
PUBLISHED 15 October 2024

CITATION
Ming Z, Bagheri-Fam S, Frost ER, Ryan JM, Vining B and Harley VR (2024) Corrigendum: A role for TRPC3 in mammalian testis development.
Front. Cell Dev. Biol. 12:1484634.
doi: 10.3389/fcell.2024.1484634

Corrigendum: A role for TRPC3 in mammalian testis development

Zhenhua Ming[1,2], Stefan Bagheri-Fam[1], Emily R. Frost[1], Janelle M. Ryan[1,2], Brittany Vining[1,2] and Vincent R. Harley[1,2]*

[1]Sex Development Laboratory, Hudson Institute of Medical Research, Melbourne, VIC, Australia, [2]Department of Molecular and Translational Science, Monash University, Melbourne, VIC, Australia

KEYWORDS

SOX9, testis, sertoli cells, DSD, TRPC3, TRP, sex determination

A Corrigendum on
A role for TRPC3 in mammalian testis development

by Ming Z, Bagheri-Fam S, Frost ER, Ryan JM, Vining B and Harley VR (2024). Front. Cell Dev. Biol. 12:1337714. doi: 10.3389/fcell.2024.1337714

In the published article, there was an error in the **Author list**, and author **Brittany Vining** was erroneously excluded. The corrected author list appears below.

"Zhenhua Ming[1,2], Stefan Bagheri-Fam[1], Emily R. Frost[1], Janelle M. Ryan[1,2], Brittany Vining[1,2] and Vincent R. Harley[1,2]"

The corrected **Author contributions** statement appears below.

"ZM: Conceptualization, Formal Analysis, Investigation, Methodology, Project administration, Visualization, Writing–original draft, Writing–review and editing. SB-F: Conceptualization, Data curation, Software, Supervision, Writing–review and editing. EF: Supervision, Writing–review and editing. JR: Methodology, Writing–review and editing. BV: Visualization, Writing–review and editing. VH: Conceptualization, Funding acquisition, Project administration, Resources, Supervision, Writing–review and editing."

In the published article, **Supplementary Figure 1** was mistakenly not included in the publication. The missing material appears below.

In the published article, the legends of the **Supplementary Figures** were mistakenly not included in the publication. The missing material appears below.

"**SUPPLEMENTARY FIGURE S1** UMAP (uniform manifold approximation and projection) of the cell lineages (color) in the male or female mouse gonad at ages E10.5, E11.5 and E12.5 (pooled data) scRNA-seq dataset from Garcia-Alonso et al. (**Garcia-Alonso et al., 2022**). In male: the Sertoli cell (chartreuse) and endothelial cell (green) clusters have been identified; in female: the pre-granulosa cell (pink) and endothelial cell (green) clusters have been identified. UMAP of gene expression shows *Sox9, Amh, Pecam1, Foxl2* and *Trpc3* gene expression across all cell lineages for either male or female embryonic mouse gonad. UMAP of stage indicates the embryonic day (E) of each derived cell within lineage clusters.

SUPPLEMENTARY FIGURE S2 Co-immunofluorescence staining of TRPC3 (green) with the endothelial cell and germ cell marker PECAM1 (red) in the mouse testis from E11.5 to E15.5, and with the Leydig cell marker HSD3B (red) at E14.5 and E15.5. Dashed white arrows indicate possible colocalization of TRPC3 and PECAM1. Arrowheads indicate HSD3B staining. Nuclei are visualized with the nuclear marker DAPI (blue). Scale bar = 50 μm.

SUPPLEMENTARY FIGURE S3 TRPC3 inhibition has no impact on cultured XX mouse gonads. **(A)** Immunofluorescence staining of female gonads after exposure to either

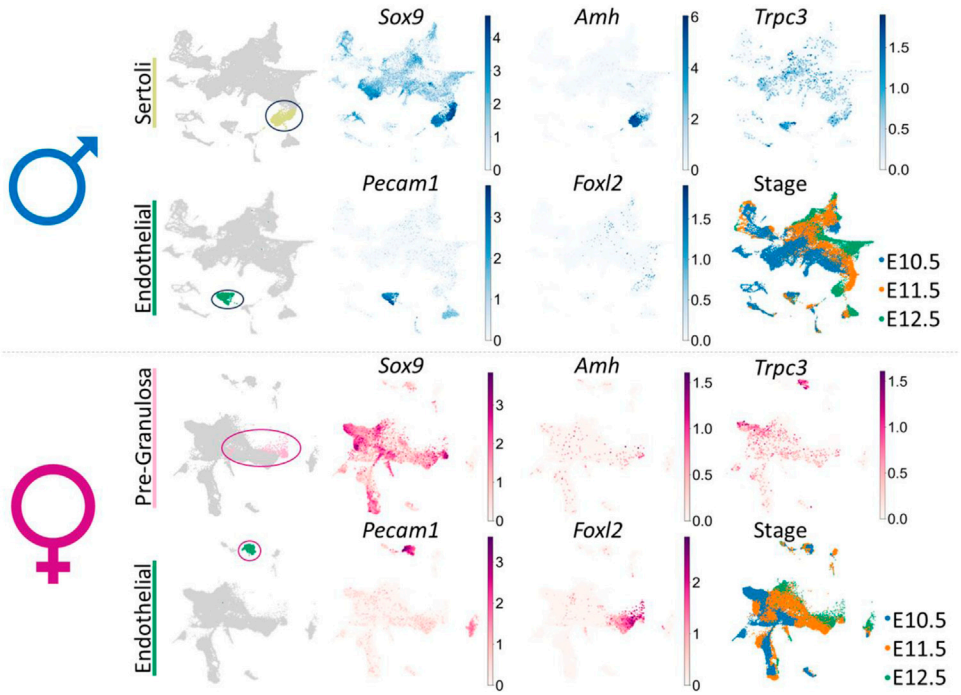

SUPPLEMENTARY FIGURE S1
UMAP (uniform manifold approximation and projection) of the cell lineages (color) in the male or female mouse gonad at ages E10.5, E11.5 and E12.5 (pooled data) scRNA-seq dataset from Garcia-Alonso et al. (**Garcia-Alonso et al., 2022**). In male: the Sertoli cell (chartreuse) and endothelial cell (green) clusters have been identified; in female: the pre-granulosa cell (pink) and endothelial cell (green) clusters have been identified. UMAP of gene expression shows *Sox9, Amh, Pecam1, Foxl2* and *Trpc3* gene expression across all cell lineages for either male or female embryonic mouse gonad. UMAP of stage indicates the embryonic day (E) of each derived cell within lineage clusters.

the vehicle control DMSO or the TRPC3 inhibitor Pyr3 during *ex vivo* culture for 24, 48, and 72 h. The sections are stained for germ cell marker DDX4 (red) and somatic cell marker GATA4 (green). Nuclei are visualized with the nuclear marker DAPI (blue). Dashed lines outline gonads. Scale bar = 50 µm. **(B)** Quantification of germ cells in XX DMSO and XX Pyr3-treated gonads at 24, 48 and 72 h post-culture. n = 2; sections counted = 4–10. Mean ± SEM. Unpaired Student's t-test. ns, not significant.

SUPPLEMENTARY FIGURE S4 TRPC3 inhibition does not affect germ cell apoptosis in cultured XY gonads. **(A)** Apoptosis analysis at 24, 48, and 72 h in XY gonads treated with DMSO or Pyr3 by immunofluorescence staining for the cell apoptosis marker cleaved Caspase-3 (CC3) (green) and the germ cell marker DDX4 (red). Arrowheads indicate examples of apoptotic germ cells. Nuclei are visualized with the nuclear marker DAPI (blue). Scale bar = 50 µm. Dashed lines outline gonads. **(B)** Quantification of apoptotic germ cells is performed for CC3+ germ cells relative to the total germ cell population. n = 2–4; sections counted = 5–11. Data are represented as Mean ± SEM. Unpaired Student's t-test. ns, not significant.

SUPPLEMENTARY FIGURE S5 TRPC3 inhibition has no impact on testis cord formation in cultured XY gonads. Immunofluorescence staining of Laminin (green) and GATA4 (red) in control (XY DMSO) and Pyr3-treated (XY Pyr3) gonads cultured *ex vivo* for 24, 48 and 72 h. Nuclei are visualized with the nuclear marker DAPI (blue). Yellow dashed lines outline gonads. White dashed lines outline testis cords. Scale bar = 50 µm.

SUPPLEMENTARY FIGURE S6 Analysis of SOX9 ChIP peaks in the *Trpc3/TRPC3* gene. **(A)** SOX9 ChIP-seq peaks indicate regions bound by SOX9 within the *Trpc3* gene in mouse fetal testes (**Rahmoun et al., 2017**), visualized using IGV. **(B)** The schematic presents key regulatory features of the *Trpc3/TRPC3* gene visualized on the UCSC genome browser. Black boxes indicate the locations of SOX9 ChIP peaks within the *Trpc3/TRPC3* gene in mouse and bovine fetal testes (**Rahmoun et al., 2017**). Bioinformatic tracks from the UCSC genome browser include the DNase I hypersensitivity data from human fetal testis and ovary (**Kundaje et al., 2015**), the 100-vertebrate conservation track, and ENCODE histone modification peaks present in the human testicular cell line NT2/D1 (**ENCODE Project Consortium, 2012**). **(C)** Alignment of the *Trpc3/TRPC3* promoter regions of mouse, bovine and human. Potential SOX9 and GATA4 binding motifs were predicted by PROMO (**Farré et al., 2003**) and JASPAR (**Rauluseviciute et al., 2024**) programs. The potential binding motifs for SOX9 and GATA4 are highlighted in red and green, respectively. Nucleotide conservation between mouse, bovine and human is indicated by asterisks (*). The transcription start site (TSS) is marked with an angled arrow."

In the published article, there was an error in **Supplementary Figure 5**. The incorrect image was published, and the numbering of the figure and its in-text citations were not accurate. The correct material appears below and is now correctly labelled as **Supplementary Figure 6**.

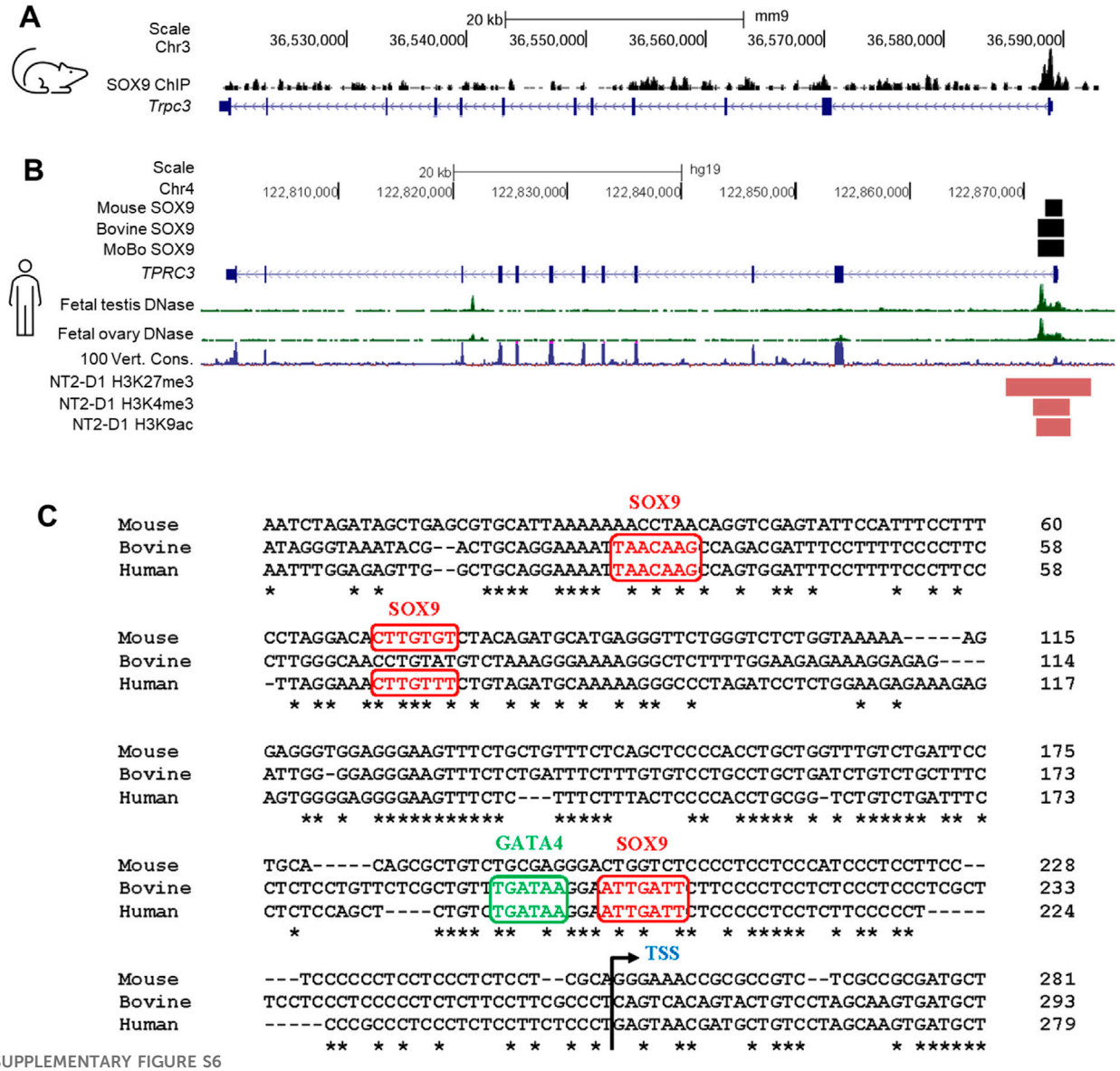

SUPPLEMENTARY FIGURE S6
Analysis of SOX9 ChIP peaks in the *Trpc3/TRPC3* gene. **(A)** SOX9 ChIP-seq peaks indicate regions bound by SOX9 within the *Trpc3* gene in mouse fetal testes (**Rahmoun et al., 2017**), visualized using IGV. **(B)** The schematic presents key regulatory features of the Trpc3/TRPC3 gene visualized on the UCSC genome browser. Black boxes indicate the locations of SOX9 ChIP peaks within the *Trpc3/TRPC3* gene in mouse and bovine fetal testes (**Rahmoun et al., 2017**). Bioinformatic tracks from the UCSC genome browser include the DNase I hypersensitivity data from human fetal testis and ovary (**Kundaje et al., 2015**), the 100-vertebrate conservation track, and ENCODE histone modification peaks present in the human testicular cell line NT2/D1 (**ENCODE Project Consortium, 2012**). **(C)** Alignment of the *Trpc3/TRPC3* promoter regions of mouse, bovine and human. Potential SOX9 and GATA4 binding motifs were predicted by PROMO (**Farré et al., 2003**) and JASPAR (**Rauluseviciute et al., 2024**) programs. The potential binding motifs for SOX9 and GATA4 are highlighted in red and green, respectively. Nucleotide conservation between mouse, bovine and human is indicated by asterisks (*). The transcription start site (TSS) is marked with an angled arrow.

In the published article, there was an error. The correct **Supplementary information** was not included, and the in-text citations of some **Supplementary Figures** were not correct.

A correction has been made to **Results**, *TRPC3 is strongly expressed in Sertoli cells from E13.5*, Paragraph 1. This sentence previously stated:

"We further investigated *Trpc3* expression during testis development by screening previous microarray data of male and female developing gonads from E11.5 to E13.5 (**Jameson et al., 2012**)."

The corrected sentence appears below:

"We further investigated *Trpc3* expression during testis development by screening previous microarray data of male and female developing gonads from E11.5 to E13.5 (**Jameson et al., 2012**) and querying expression of *Trpc3* in isolated cell lineages of the developing male or female mouse gonad (**Supplementary Figure 1**)."

A correction has been made to **Results**, *TRPC3 is strongly expressed in Sertoli cells from E13.5*, Paragraph 2. These sentences previously stated:

"At E12.5, E13.5 and E15.5, weak TRPC3 staining was found in a subset of endothelial cells of the coelomic blood vessel (**Supplementary Figure S1**). From E14.5 onwards, weak TRPC3 staining was also detectable in interstitial cells (**Figures 1C, D**). Co-immunostaining for TRPC3 and the Leydig cell marker HSD3B revealed that these are Leydig cells (**Supplementary Figure S1**). However, since these signals were also detected in the PECAM1 channel, it is possible that they represent nonspecific background staining (**Supplementary Figure S1**)."

The corrected sentences appear below:

"At E12.5, E13.5 and E15.5, weak TRPC3 staining was found in a subset of endothelial cells of the coelomic blood vessel (**Supplementary Figure S2**). From E14.5 onwards, weak TRPC3 staining was also detectable in interstitial cells (**Figures 1C, D**). Co-immunostaining for TRPC3 and the Leydig cell marker HSD3B revealed that these are Leydig cells (**Supplementary Figure S2**). However, since these signals were also detected in the PECAM1 channel, it is possible that they represent nonspecific background staining (**Supplementary Figure S2**)."

A correction has been made to **Results**, *Inhibition of TRPC3 leads to a reduction in germ cell numbers in cultured XY gonads*, Paragraph 1. This sentence previously stated:

"Distinct from the male gonads, TRPC3 inhibition did not cause any changes in germ cell numbers in female gonads (**Supplementary Figure S2**), highlighting a sex-specific response to TRPC3 inhibition."

The corrected sentence appears below:

"Distinct from the male gonads, TRPC3 inhibition did not cause any changes in germ cell numbers in female gonads (**Supplementary Figure S3**), highlighting a sex-specific response to TRPC3 inhibition."

A correction has been made to **Results**, *Inhibition of TRPC3 leads to a reduction in germ cell numbers in cultured XY gonads,* Paragraph 2. These sentences previously stated:

"Analysis of germ cell apoptosis revealed no significant differences between XY control gonads and XY Pyr3-treated gonads at the 24, 48 and 72-h time points (**Supplementary Figure S3**). Collectively, these findings suggest that the reduction of the germ cell population following TRPC3 inhibition is caused by decreased germ cell proliferation. Immunofluorescence analysis for Laminin, a marker for the basal lamina of testis cords, revealed that after 48 and 72 h of culture, both control and Pyr3-treated XY gonads had formed well-defined testis cords, wherein Laminin and a closely associated layer of Sertoli cells encircled both germ cells and Sertoli cells (**Supplementary Figure S4**)."

The corrected sentences appear below:

"Analysis of germ cell apoptosis revealed no significant differences between XY control gonads and XY Pyr3-treated gonads at the 24, 48 and 72-h time points (**Supplementary Figure S4**). Collectively, these findings suggest that the reduction of the germ cell population following TRPC3 inhibition is caused by decreased germ cell proliferation. Immunofluorescence analysis for Laminin, a marker for the basal lamina of testis cords, revealed that after 48 and 72 h of culture, both control and Pyr3-treated XY gonads had formed well-defined testis cords, wherein Laminin and a closely associated layer of Sertoli cells encircled both germ cells and Sertoli cells (**Supplementary Figure S5**)."

A correction has been made to **Discussion,** Paragraph 2. These sentences previously stated:

"We observed a significant downregulation of *Trpc3* expression in E13.5 *Sox9* KO XY gonads, showing that *Trpc3* expression is largely dependent on SOX9. We also found that expression of *Trpc3* in Sertoli cells increases within developing male gonads after sex determination. This implies the existence of a sex-specific mechanism in XY gonads that upregulates *Trpc3* expression during sex differentiation. Our previous SOX9 ChIP-seq data demonstrated SOX9 binding to the proximal promoter region and intron 1 of both mouse and bovine fetal testes (**Supplementary Figure S5A**) (**Rahmoun et al., 2017**). DNase I hypersensitivity data from human fetal testes and fetal ovaries shows increased chromatin accessibility in this region (**Supplementary Figure S5A**) (**Kundaje et al., 2015**), and ENCODE histone modifications in NT2/D1 cells indicates active regulatory potential (**Supplementary Figure S5A**) (**ENCODE Project Consortium, 2012**). Moreover, prediction of transcription factor binding sites within the SOX9 ChIP-seq peaks revealed three potential SOX9 binding sites and one GATA4 binding site in the *Trpc3*/*TRPC3* promoter region (**Supplementary Figure S5B**)."

The corrected sentences appear below:

"We observed a significant downregulation of *Trpc3* expression in E13.5 *Sox9* KO XY gonads, showing that *Trpc3* expression is largely dependent on SOX9. Published scRNA-seq data indicate *Trpc3* expression in fetal Sertoli cells (**Supplementary Figure 1**); we found that expression of *Trpc3* in Sertoli cells increases within developing male gonads after sex determination. This implies the existence of a sex-specific mechanism in XY gonads that upregulates Trpc3 expression during sex differentiation. Our previous SOX9 ChIP-seq data demonstrated SOX9 binding to the proximal promoter region and intron 1 of both mouse and bovine fetal testes (**Supplementary Figure S6A, B**) (**Rahmoun et al., 2017**). DNase I hypersensitivity data from human fetal testes and fetal ovaries shows increased chromatin accessibility in this region (**Supplementary Figure S6B**) (**Kundaje et al., 2015**), and ENCODE histone modifications in NT2/D1 cells indicates active regulatory potential (**Supplementary Figure S6B**) (**ENCODE Project Consortium, 2012**). Moreover, prediction of transcription factor binding sites within the SOX9 ChIP-seq peaks revealed three potential SOX9 binding sites and one GATA4 binding site in the *Trpc3/TRPC3* promoter region (**Supplementary Figure S6C**)."

The authors apologize for these errors and state that this does not change the scientific conclusions of the article in any way. The original article has been updated.

Publisher's note

frontiers | Frontiers in Cell and Developmental Biology

TYPE Original Research
PUBLISHED 11 March 2024
DOI 10.3389/fcell.2024.1362228

OPEN ACCESS

EDITED BY
Talia L. Hatkevich,
Duke University, United States

REVIEWED BY
Yong Zhu,
East Carolina University, United States
Matan Golan,
Agricultural Research Organization (ARO), Israel
Martin Psenicka,
University of South Bohemia, Czechia

*CORRESPONDENCE
John H. Postlethwait,
jpostle@uoregon.edu

RECEIVED 27 December 2023
ACCEPTED 20 February 2024
PUBLISHED 11 March 2024

CITATION
Wilson CA, Batzel P and Postlethwait JH (2024), Direct male development in chromosomally ZZ zebrafish.
Front. Cell Dev. Biol. 12:1362228.
doi: 10.3389/fcell.2024.1362228

Direct male development in chromosomally ZZ zebrafish

Catherine A. Wilson, Peter Batzel and John H. Postlethwait*

Institute of Neuroscience, University of Oregon, Eugene, OR, United States

The genetics of sex determination varies across taxa, sometimes even within a species. Major domesticated strains of zebrafish (*Danio rerio*), including AB and TU, lack a strong genetic sex determining locus, but strains more recently derived from nature, like Nadia (NA), possess a ZZ male/ZW female chromosomal sex-determination system. AB fish pass through a juvenile ovary stage, forming oocytes that survive in fish that become females but die in fish that become males. To understand mechanisms of gonad development in NA zebrafish, we studied histology and single cell transcriptomics in developing ZZ and ZW fish. ZW fish developed oocytes by 22 days post-fertilization (dpf) but ZZ fish directly formed testes, avoiding a juvenile ovary phase. Gonads of some ZW and WW fish, however, developed oocytes that died as the gonad became a testis, mimicking AB fish, suggesting that the gynogenetically derived AB strain is chromosomally WW. Single-cell RNA-seq of 19dpf gonads showed similar cell types in ZZ and ZW fish, including germ cells, precursors of gonadal support cells, steroidogenic cells, interstitial/stromal cells, and immune cells, consistent with a bipotential juvenile gonad. In contrast, scRNA-seq of 30dpf gonads revealed that cells in ZZ gonads had transcriptomes characteristic of testicular Sertoli, Leydig, and germ cells while ZW gonads had granulosa cells, theca cells, and developing oocytes. Hematopoietic and vascular cells were similar in both sex genotypes. These results show that juvenile NA zebrafish initially develop a bipotential gonad; that a factor on the NA W chromosome, or fewer than two Z chromosomes, is essential to initiate oocyte development; and without the W factor, or with two Z doses, NA gonads develop directly into testes without passing through the juvenile ovary stage. Sex determination in AB and TU strains mimics NA ZW and WW zebrafish, suggesting loss of the Z chromosome during domestication. Genetic analysis of the NA strain will facilitate our understanding of the evolution of sex determination mechanisms.

KEYWORDS

sex determination, gonad development, scRNA-seq, juvenile ovary, bipotential gonad, single cell transcriptomics, interstitial/stroma cells, hematopoietic cells

Introduction

Vertebrates exhibit a wide variety of sex determination mechanisms, including genetic and environmental control factors (Nagahama et al., 2021). Among fishes with genetic sex determination, some species have a single major genetic sex determinant, but others use polygenic sex determination. Unlike mammals and birds, which have evolutionarily rather stable genetic sex determinants (Ioannidis et al., 2021; Terao et al., 2022), different fish lineages can have different major sex determination genes, sometimes even in the same species or genus (Matsuda and Sakaizumi, 2016; Pan et al., 2021; Song et al., 2021). Despite the popularity of zebrafish as a model organism (Bradford et al., 2017) and substantial knowledge about its gonadogenesis (Liew and Orban, 2014; Kossack and Draper, 2019;

Aharon and Marlow, 2021), our understanding of the genetic regulation of zebrafish sex determination is insufficient.

Zebrafish gonads have been described as passing through a juvenile ovary stage, with all juveniles developing perinucleolar oocytes by about 20 days post-fertilization (dpf) (Takahashi, 1977; Uchida et al., 2002). In some individuals, these oocytes persist and the fish develops as a female, but in other individuals, oocytes die, the gonad transitions to a testis, and the fish becomes a male (Wang et al., 2007). Previous studies in zebrafish strains domesticated for mutagenesis research (Walker-Durchanek, 1980; Streisinger et al., 1981; Mullins et al., 1994) showed that germ cells, specifically oocytes, are essential for both the establishment and maintenance of female sex because zebrafish that lack germ cells become males (Slanchev et al., 2005), as do mutants that lose oocytes during meiosis (Rodriguez-Mari et al., 2010; Shive et al., 2010; Rodriguez-Mari et al., 2011; Saito et al., 2011; Beer and Draper, 2013; Dranow et al., 2013; Dranow et al., 2016; Ramanagoudr-Bhojappa et al., 2018; Takemoto et al., 2020; Blokhina et al., 2021; Islam et al., 2021). While zebrafish are gonochoristic, mutations that cause progressive oocyte loss in adults but retain some germ cells result in individuals that can first become females and later convert to a male phenotype (Dranow et al., 2013).

Mechanisms that cause some juvenile zebrafish to maintain oocytes and become females are not yet fully known, but oocyte survival and sex ratio are strongly influenced by both genetic and environmental factors. In general, stressful environments masculinize a clutch: an increased fraction of males occurs after hypoxia, high rearing density, high temperature, low nutrition, gamma rays, inbreeding, and exposure to exogenous cortisol (Walker and Streisinger, 1983; Shang et al., 2006; Lawrence et al., 2008; Abozaid et al., 2011; Ribas et al., 2017; Santos et al., 2017; Delomas and Dabrowski, 2018; Valdivieso et al., 2022). Sex phenotype has been mapped to different genetic locations in different zebrafish strains, and sex ratios are consistent in repeated matings of the same individual fish pairs, consistent with polygenic sex determination in laboratory lines (Bradley et al., 2011; Anderson et al., 2012; Howe et al., 2013; Liew and Orban, 2014; Luzio et al., 2015).

Unlike laboratory strains, zebrafish lines not long adapted to laboratory life at the time of investigation, including the Nadia (NA) strain, have a genetic ZZ/ZW sex determination system, with the major Sex-Associated Region on chromosome-4 (*sar4*) located near the telomere of the right arm of chromosome-4 (Chr4) (as displayed in Ensembl: (ensembl.org/Danio_rerio/Location/Chromosome?r=4) (Tong et al., 2010; Anderson et al., 2012; Wilson et al., 2014), a chromosome that has, in addition to the sex locus, a region that has sex-specific silencing of protein-coding gene transcription in ovaries (Wilson and Postlethwait, 2023). Individual NA strain zebrafish homozygous for Z alleles always develop as males and most ZW individuals become females, but some ZW individuals develop as males in all four strains investigated (Anderson et al., 2012; Wilson et al., 2014). In addition, WW fish in these less domesticated strains tend to become females, although some develop as males. The finding that ZZ fish do not become females suggests that the W allele is necessary but not sufficient for female development, although the hypothesis that Z dosage regulates sex (two Z doses, always male; one or zero Z chromosomes, usually female) is not formally ruled out. Because ZW fish occasionally develop as males, either masculinizing environmental factors or segregating background genetic modifiers can affect zebrafish sex determination. These results raise the question: Do ZZ zebrafish pass through the juvenile ovary stage like all fish in domesticated laboratory strains, or alternatively, do they develop directly into males? Under the hypothesis that the W carries a factor that is necessary, but insufficient, for ovarian development, ZZ fish, lacking the hypothesized W-linked ovary factor, should not form juvenile ovaries with meiotic oocytes.

To test this hypothesis, we investigated gonad development in chromosomally ZW and ZZ zebrafish from the NA strain. Results showed that 1) juvenile NA zebrafish initially develop a bipotential gonad; 2) a factor on the W chromosome, or fewer than two Z chromosomes, is essential to trigger oocyte development; and 3) ZZ zebrafish gonads develop directly into testes. These results are as expected from the hypothesis that the W chromosome contains a factor that is necessary but insufficient for female development or that the Z chromosome contains a dosage-sensitive factor that inhibits female development, with fully penetrant inhibition of ovary development in ZZ fish. Under either hypothesis, standard laboratory strains produce both males and females, as do both ZW and WW NA zebrafish, suggesting loss of the Z chromosome leading to WW populations during domestication.

Results and Discussion

Sex chromosomes and zebrafish sex development

To confirm the relationship of sex development and sex chromosomes, we crossed NA strain individuals genotyped for sex chromosomes. We evaluated 366 fish that were the offspring of eight different crosses of ZW females x ZZ males (five single pair crosses and three crosses with two males and two females). At sexual maturity, primers specific for Z- and W-chromosomes identified genotypic sex (Wilson et al., 2014), while secondary sexual characteristics distinguished phenotypic sex (for females, a rounded abdomen, and pale ventral and anal fins, and for males, a streamlined body with yellow ventral and anal fins and sex tubercles) (McMillan et al., 2013; Dai et al., 2021b). Offspring included 184 ZZ individuals (50.3%) and 182 ZW fish (49.7%), a 1:1 genotypic sex ratio ($p = 0.92$, Chi-square test). This result shows first, that in meiosis, Z and W chromosomes segregate as homologous chromosomes, and second, that ZZ and ZW genotypes are equally likely to survive. All 184 ZZ individuals were phenotypic males. Of 182 ZW fish, 128 individuals (70.3%) were phenotypic females and 54 fish (29.7%) were phenotypic males, called neomales (Ginsburger-Vogel, 1972). Families varied widely in the percent of neomales, from 6.7% to 66.7% (Figure 1A). This result would be explained either if sex determination in ZW NA strain zebrafish can be influenced by genetic factors in addition to *sar4* or if differences in environmental factors increase the likelihood of male development in NA as in laboratory strains (Liew and Orban, 2014; Valdivieso et al., 2022).

To study sex determination in chromosomally WW fish, we made three single pair matings between ZW phenotypic females

10.3389/fcell.2024.1362228

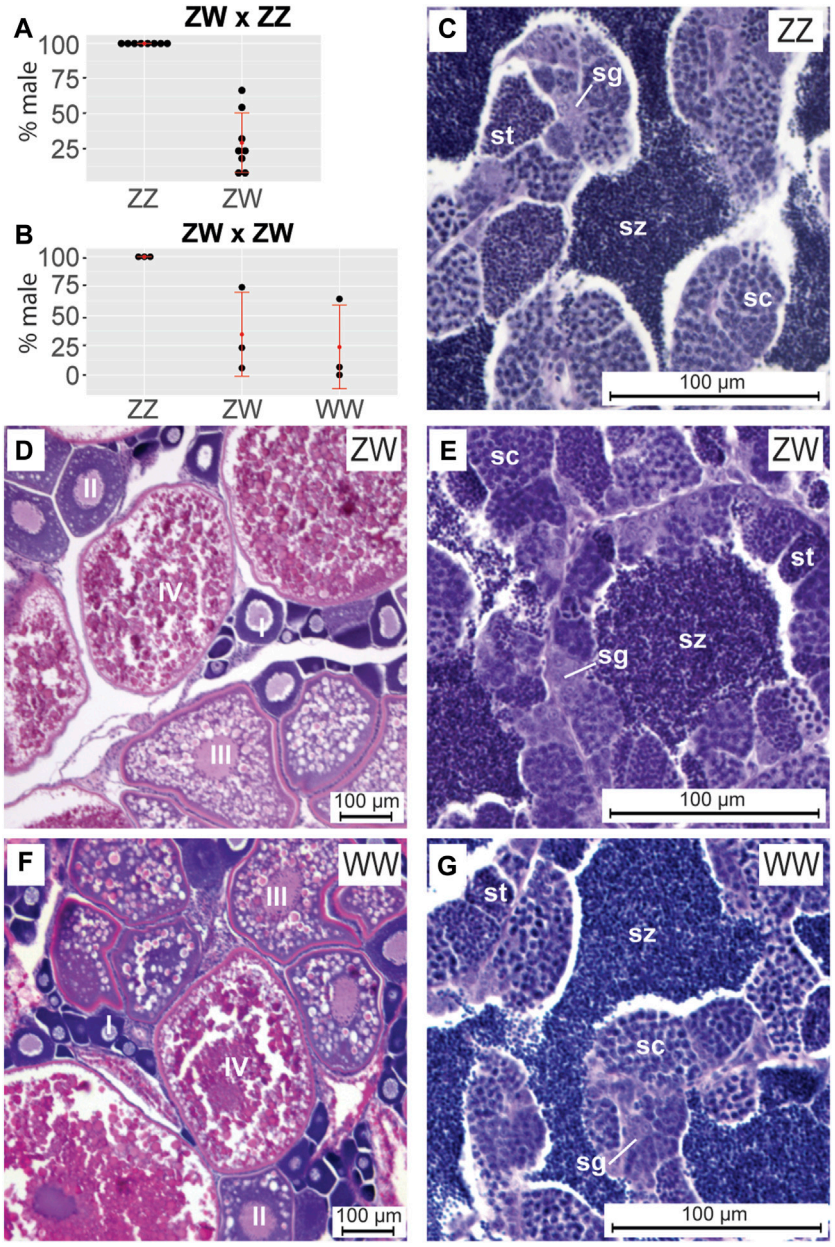

FIGURE 1
Sex ratios and gonad histology in adult ZW and ZZ zebrafish at 5 months post fertilization (mpf). **(A)** Sex phenotypes in progeny of ZW females crossed to ZZ males. Within each sex genotype, each point represents a different cross. No ZZ individuals became adult females. **(B)** Sex phenotypes in progeny of ZW females crossed to ZW neomales. No ZZ individuals became adult females. C-G. Cross sections of 5mpf adult gonads. **(C)** ZZ adult testis. **(D)** ZW ovary. **(E)** ZW neomale testis. **(F)** WW ovary. **(G)** WW neomale testis. Ovary histology for ZW and WW fish showed no clear difference and testis histology of ZZ, ZW, and WW fish was the same. Abbreviations: o, oocyte; pc, pycnotic cell; sc, spermatocyte; sg, spermatogonium; sp, spermatid; sz, spermatozoa.

and ZW neomales, resulting in a total of 158 progeny (Figure 1B). Offspring included 43 (27.2%) ZZ individuals, 74 (46.9%) ZW fish, and 41 (25.9%) WW fish, approximating a 1:2:1 genotypic ratio ($p = 0.71$, Chi square). All ZZ individuals were phenotypic males (43/43, 100%), while 30 of the 74 (40.5%) ZW fish and 10 of the 41 (25.9%) WW fish developed as neomales. The frequency of sex reversal was again highly variable among crosses, ranging between 5.9% and 74.2% (average 34.4%) for ZW and between 0% and 64.3% (average 23.7%) for WW (Figure 1B). These results show that 1) homozygous W fish have normal viability, and 2) no Z-specific genes are essential to allow a fish to develop testes.

Gonad histology in ZW, ZZ, and WW adults

Having shown that some ZW and WW fish can become neomales, we wondered if adult neomale gonads differ from those in ZZ males. Histological sections showed that at 5mpf (months post fertilization), all adult NA ZZ fish examined

(n = 4) possessed testes with germ cells organized into cysts containing mitotic spermatogonia, meiotic spermatocytes, and post-meiotic spermatids, with mature spermatozoa present in the testis lumen (Figure 1C). Abdominal sections of adult 5mpf NA ZW fish (n = 4) with female secondary sexual characteristics possessed ovaries with oocytes in various stages of development (Selman et al., 1993), including meiotic perinucleolar oocytes (Stage I), larger oocytes containing cortical alveoli (Stage II), vitellogenic oocytes accumulating yolk (Stage III), and maturing oocytes in the final stages of oogenesis (Stage IV) (Figure 1D). In contrast, in 5mpf genetic ZW neomales (n = 4), testes had morphologies not detectably different from those of ZZ males; notably, 5mpf ZW adult neomales lacked any detectable oocytes (Figure 1E). Gonads in the phenotypically female WW fish (n = 4) were also not detectably different from ovaries in ZW fish (Figure 1F), and gonads in phenotypically neomale WW fish (n = 4) were no different from testes in ZZ fish (Figure 1G). We conclude that NA strain neomales, whether ZW or WW, produce histologically normal testes with all stages of spermatogenesis like ZZ males, and by 5mpf, had no detectable oocytes.

Gonad development in ZZ and ZW juveniles

All chromosomally ZZ NA fish had normal testes as adults, but because even phenotypically male adult laboratory zebrafish pass through a juvenile ovary stage (Takahashi, 1977; Uchida et al., 2002; Wang et al., 2007), we wondered whether ZZ zebrafish do too. The hypothesis that a factor on the W chromosome or that fewer than two Z chromosomes is necessary for ovary development predicts that ZZ fish will not pass through the juvenile ovary stage. To test this prediction, we analyzed differences in gonad development in ZZ and ZW NA zebrafish over developmental time in histological sections from two separate NA families at 10, 14, 19, 22, 26, and 30dpf.

Results showed that gonads in ZZ and ZW zebrafish were morphologically indistinguishable in cross-sections of 10, 14, and 19dpf larvae. In five ZW and four ZZ fish examined at 10dpf, bilateral gonads had clusters of germ cells surrounded by somatic cells (Figures 2A, B), as for laboratory strain zebrafish (Takahashi, 1977; Uchida et al., 2002; Rodriguez-Mari et al., 2005; Wang et al., 2007; Dranow et al., 2013; Dranow et al., 2016). Gonads in both ZW and ZZ fish increased in size and in germ cell number at 14dpf and 19dpf, but gonads in ZW and ZZ fish remained morphologically indistinguishable (Figures 2C–F), again as in laboratory strains. We conclude that the morphology of ZW and ZZ gonads appeared to be bipotential up to 19dpf.

Between 19 and 22dpf, gonad development in ZW and ZZ sex genotypes began to differ. At 22dpf, gonads in nine of ten ZW individuals examined contained perinucleolar oocytes (Figure 2G), while gonads in the tenth fish examined retained the indifferent morphology of younger fish. In contrast, all ten ZZ individuals at 22dpf still possessed indifferent gonads, failing to advance detectably in developmental stage (Figure 2H). By 26dpf, gonads of all 11 ZW fish studied had perinucleolar oocytes (Figure 2I), but four of these 11 had gonads that also contained pyknotic cells representing dying oocytes (Figure 2M). Similar pyknotic cells appear in juvenile gonads transforming to adult testis in laboratory strain zebrafish and in gonads of mutants experiencing female-to-male sex reversal (Takahashi, 1977; Uchida et al., 2002; Maack and Segner, 2003; Rodriguez-Mari et al., 2010; Rodriguez-Mari et al., 2011; Dranow et al., 2016; Blokhina et al., 2021; Xie et al., 2021). Of nine 26dpf ZZ fish, three contained largely undifferentiated gonads, and the other six had clusters of spermatogonia (Figure 2J), including one with spermatocytes. At 30dpf, 10 of 12 ZW fish examined had a well-developed ovary full of perinucleolar oocytes (Figure 2K). At 30dpf, oocytes had increased in size, but had not yet entered the cortical alveolar stage [Stage II, (Selman et al., 1993)]. Two of these 12 ZW 30dpf fish, however, had gonads that were nearly all testis, including spermatogonia and spermatocytes, but also pyknotic oocyte-like cells and a few remaining oocytes (Figure 2N). We interpret these two fish as ZW individuals that had gone through the juvenile ovary stage, but by 30dpf, were transitioning to neomales.

The developmental trajectory of ZZ males differed from that of ZW neomales. At 30 dpf, gonads in one of 11 ZZ males investigated were still largely undifferentiated; three fish contained gonads with spermatogonia; gonads in four fish were still small but had both spermatogonia and spermatocytes; gonads in two individuals were larger with both spermatogonia and spermatocytes; and gonads in one ZZ male contained spermatids. All three of the ZZ fish with the most mature testes came from Family 1, which was fed paramecia instead of rotifers during development. Perinucleolar oocytes were never observed in any ZZ individual analyzed at any stage. We conclude that gonads in ZZ zebrafish of the NA strain: 1) are slower in developing sex-specific morphologies than ZW fish; 2) do not form immature oocytes; 3) do not pass through a juvenile hermaphrodite stage; and 4) develop directly into testes. This developmental trajectory differs from that of domesticated zebrafish, which all appear to pass through a juvenile hermaphrodite stage. Further, these findings are consistent with the hypothesis that a factor on the W chromosome, or alternatively, fewer than two Z chromosomes, is necessary for oocytes to develop in NA zebrafish gonads.

19dpf gonad gene expression patterns were similar in ZW and ZZ gonads

The histology investigations (Figures 1, 2) showed that at 19dpf, the morphology of ZW and ZZ gonads could not be distinguished, but at 30dpf, gonads in both ZW and ZZ fish showed signs of differentiation. To learn whether gonad transcriptomes of ZW and ZZ fish had become different at 19dpf even though gonad morphologies had not, we performed scRNA-seq on 19dpf and 30dpf gonads dissected from ZW and ZZ animals. From resulting data, we removed red blood cells and contaminating non-gonad cells, and re-clustered remaining cells. We analyzed each time point separately and then merged all four datasets (two ages by two sex genotypes). Analysis of 19dpf gonads resulted in 783 ZW cells and 1270 ZZ cells grouped into 28 clusters (Figures 3A, B, Supplementary Table S1).

Cell-type marker genes help characterize cluster identities (Qiu et al., 2021) (Supplementary Table S4). *Germ cells* are marked by a number of genes encoding RNA-binding proteins, including *dazl, adad1, ddx4*, and *dnd1* as well as novel markers including *si:ch73-167f10.1* (Fu et al., 2015; Bertho et al., 2021). Expression of these

10.3389/fcell.2024.1362228

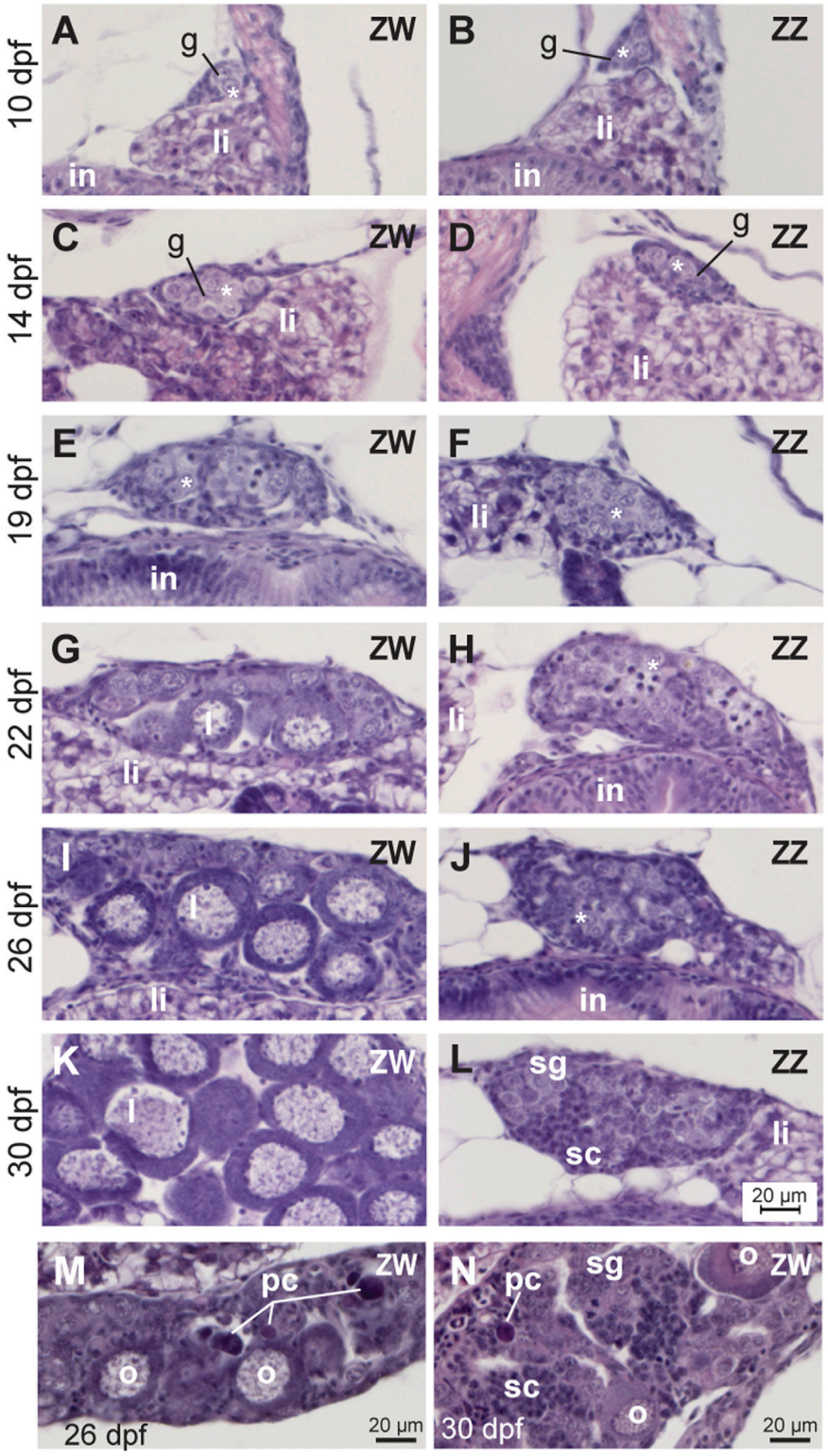

FIGURE 2
Developmental trajectory of gonads from ZW and ZZ fish. **(A,C,E,G,I,K,M,N)** ZW gonads. **(B,D,F,H,J,L)**: ZZ gonads. **(A,B)** 10dpf. **(C,D)** 14dpf. **(E,F)** 19dpf. **(G,H)** 22dpf. **(I,J)** 26dpf. **(K,L)**30dpf. At 19dpf and earlier, ZW and ZZ gonads were histologically similar, but at 22dpf and later, oocytes were developing in ZW, but not ZZ gonads. At 26dpf, some ZZ gonads showed clusters of spermatogonia, and at 30dpf, most ZZ gonads were still immature testes that were organized into cysts containing spermatogonia and spermatocytes. No ZZ gonad studied showed any oocytes at any developmental stage, but instead, showed direct development into testes. **(M)** At 26dpf, some ZW gonads were mostly ovary with a few pycnotic cells. **(N)** At 30dpf, some ZW gonads were mostly testes with a few pycnotic cells. Abbreviations: *, gonocytes; g, gonad; I and II, Stage I and Stage II oocytes; in, intestine; li, liver; o, oocyte; pc, pycnotic cell; sc, spermatocyte; sg, spermatogonium.

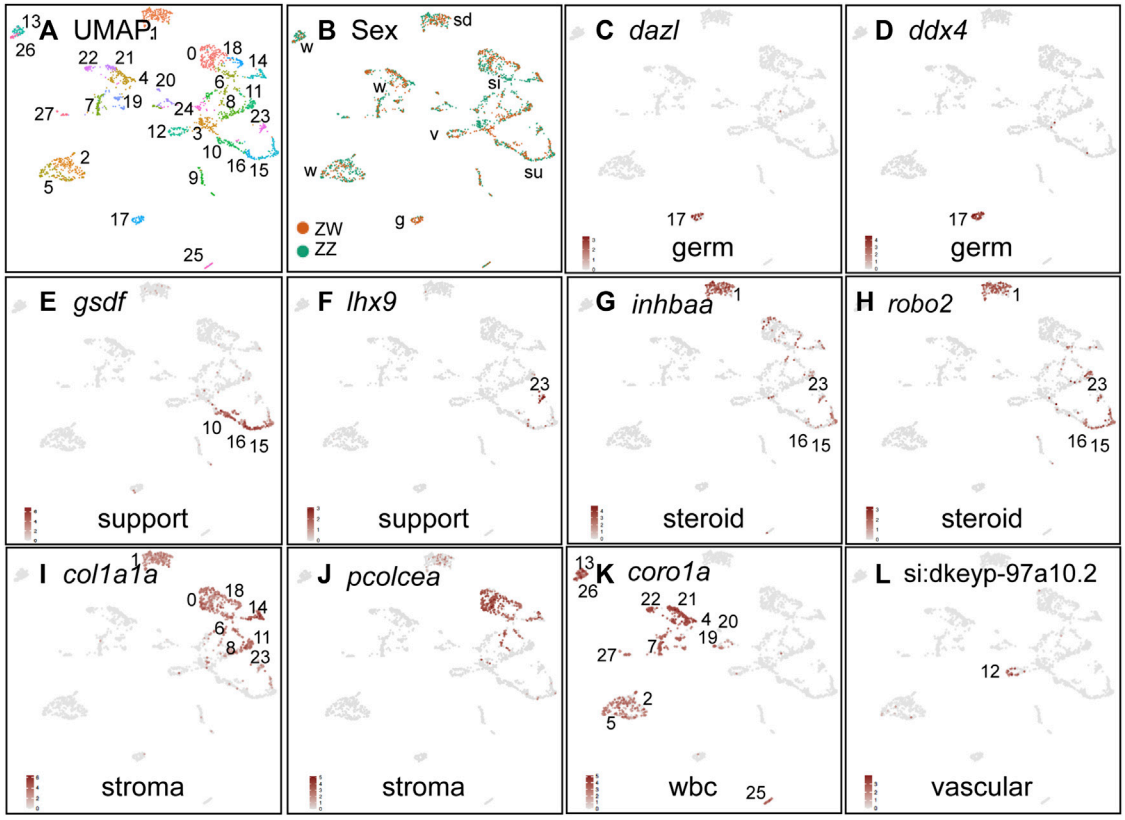

FIGURE 3
Cell-type marker genes for 19dpf ZW and ZZ gonads. **(A)** UMAP plot for 19dpf gonads combining ZW and ZZ cells. **(B)** Cells originating from ZW (red) or ZZ (blue) gonads, showing all clusters with mixtures of both sex genotypes. **(C,D)** Germ cells marked by *dazl* and *ddx4* (*vasa*) were in cluster 19c17. **(E,F)** Support cells (granulosa and Sertoli) or their precursors marked by *gsdf*, and *lhx9*. **(G,H)** Steriogenic cells (theca, Leydig) or their precursors labeled with *inhbaa* and *robo2* expression. **(I,J)** Stroma/interstitial cells marked by *col1a1a* and *pcolcea*. **(K)** White blood cells identified by *coro1a* expression. **(L)** Vasculature labeled with *si:dkeyp-97a10.2*. Abbreviations: g, germ cells; si, stroma/interstitial; sd, steroidogenic; su, support; v, vascular; w, white blood cells.

genes identified the 19dpf cluster 17 (19c17) as germ cells (Figures 3C, D, Supplementary Table S4). *Support cells*, including granulosa cells in ovaries and Sertoli cells in testes, express the fish-specific TGFb-family protein Gsdf (Sawatari et al., 2007; Gautier et al., 2011; Rondeau et al., 2013; Yan et al., 2017; Hsu and Chung, 2021), identifying three clusters (19c10, c15, and c16, Figure 3E). Cluster 19c23 strongly expressed the support cell precursor gene *lhx9* (Figure 3F) (Mazaud et al., 2002; Liu et al., 2022). *Steroidogenic cells*, including theca cells in ovaries and Leydig cells in testes, arise from *Nr5a1*-expressing precursor cells (Stevant et al., 2019; Yan et al., 2020) and express *inhbaa* and *robo2* Archambeault and Yao (2010), McClelland et al. (2015), Namwanje and Brown (2016), Lu et al. (2020), Zhao et al. (2022); these genes are expressed in 19c1, c15, c16, and c23 (Figures 3G, H, Supplementary Tables S2, S4). *Interstitial and stromal cells* express the collagen gene *col1a1a* and the procollagen cleavage enzyme *pcolcea* (Liu et al., 2022), identifying 19c0, c1, c6, c11, c14, and c18) as stromal/interstitial cells (Figures 3I, J). *Leukocytes* express *coro1a* (Song et al., 2004; Xavier et al., 2008), identifying clusters 19c2, c4, c5, c7, c13, c19, c20, c21, c22, c26, c27 (Figure 3K). *Vasculature* appears early in gonad development in XY mice (Brennan et al., 2002) and in zebrafish (Kossack et al., 2023)and it expresses *si:dkeyp-97a10.2, kdr*, and *lyve1b*, identifying 19c12 as blood vessels (Figure 3L; Supplementary Figure S4B; Supplementary Tables S2, S4) (Jackson et al., 2001; Prevo et al., 2001; Covassin et al., 2006b; Bahary et al., 2007; Gomez et al., 2009; Chen et al., 2013).

All 19dpf clusters contained both ZW and ZZ cells (Figure 3B), agreeing with the histology findings and suggesting that ZW and ZZ gonads were morphologically and transcriptionally similar at 19dpf (Figures 2E, F). Differential expression analysis of 19dpf clusters showed no significantly differentially expressed genes between ZZ and ZW genotypes in nearly all clusters; the most DE genes, mostly mitochondrial genes, appeared in 19c1, suggesting a slight difference in stress levels (Ilicic et al., 2016) in that cluster for ZW and ZZ samples (Supplementary Table S3), and confirming strong similarity of ZZ and ZW cell types at 19dpf.

30dpf gonad gene expression patterns in ZW and ZZ gonads were distinct

The histology studies had shown that ZW and ZZ gonads were morphologically different by 30dpf (Figure 2), so we wanted

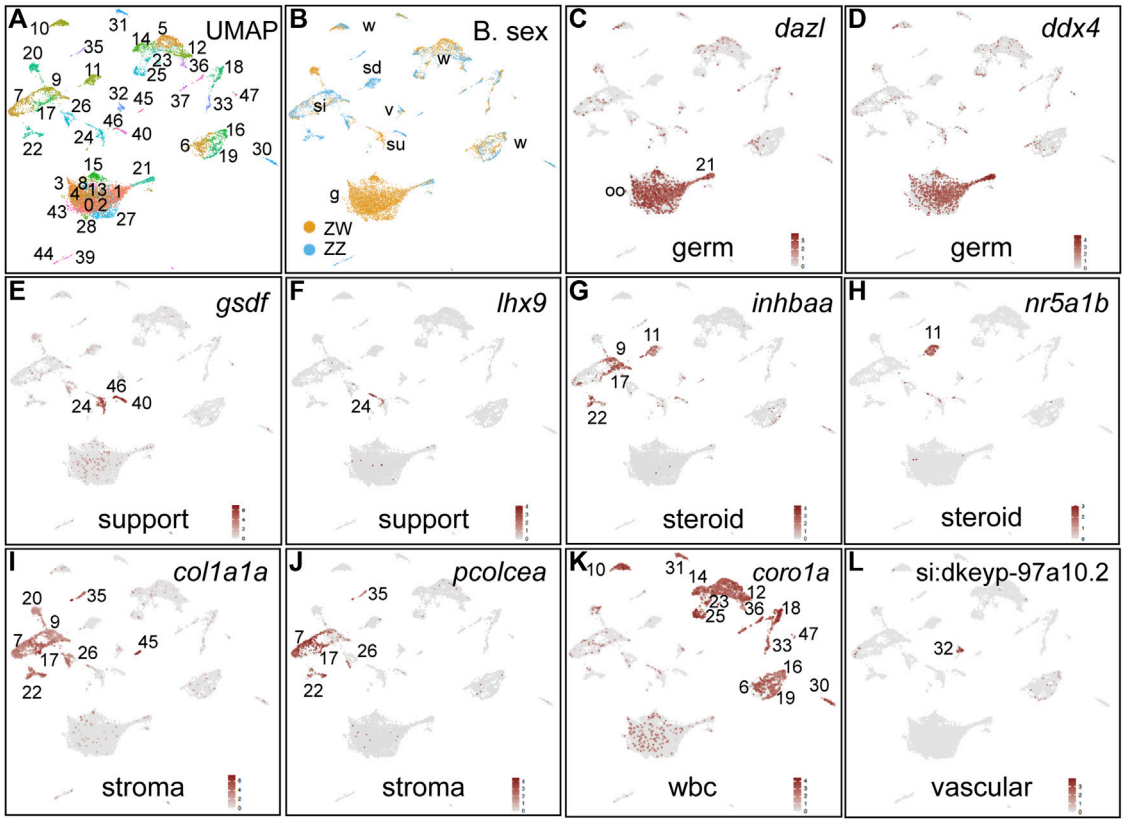

FIGURE 4
Cell-type marker genes for 30dpf ZW and ZZ gonads. **(A)** UMAP plot for 30dpf gonads combining ZW and ZZ cells. **(B)** Cells originating from ZW (gold) or ZZ (blue) gonads, showing several clusters with sex-specific genotypes. **(C,D)**. Germ cells marked by *dazl* and *ddx4* (*vasa*) expression. **(E,F)**. Support cells (granulosa and Sertoli) or their precursors marked by *gsdf* and *lhx9* expression. **(G,H)**. Steriogenic cells (theca, Leydig) or their precursors labeled with *inhbaa* and *nr5a1b* expression. **(I,J)**. Stroma/interstitial cells marked by *col1a1a* and *pcolcea* expresseion. **(K)** White blood cells identified by *coro1a* expression. **(L)** Vasculature labeled with *si:dkeyp-97a10.2* expression. Abbreviations: g, germ cells; oo, oocytes; si, stroma/interstitial; sd, steroidogenic; su, support; v, vascular; w, white blood cells.

to identify gene expression patterns in 30dpf individuals with different chromosomal sexes by single cell transcriptomics. The 30dpf gonad sample gave 7787 ZW cells and 2843 ZZ cells in 48 clusters (Figure 4A; Supplementary Tables S5, S6). In contrast to 19dpf gonads, 30dpf gonads had several clusters specific for either ZW or ZZ cells (Figure 4B). *Germ cells* were clearly labeled by *dazl* and *ddx4* in a large group of ZW-specific clusters (30c0-c4, c8, c13, c15, c27, c28, c43) and in c21 (Figures 4C, D), showing substantial proliferation of germ cells in ZW but much less in ZZ gonads. *Support cells* labeled by *gsdf* and *lhx9* identified mainly 30c24, c40, and c46 (Figures 4E, F). *Steroidogenic cells* marked by *inhbaa* and *nr5a1b* identified 30c11 for both markers, and 30c9, c17, and c22 specific for *inhbaa* (Figures 4G, H). *Interstitial/stroma cells* expressed *col1a1a* in a variety of clusters (30c7, c9, c17, c20, c22, c26, c35, c45) and *pcolcea* in most of these (Figures 4I, J). *Leukocytes* marked by *coro1a* included 14 clusters (Figure 4K). *Vascular cell* types denoted by *si:dkeyp-97a10.2* expression (Gomez et al., 2009) occupied 30c32. We conclude that by 30dpf, ZW and ZZ gonads had diverged considerably in terms of the cell types they contained, consistent with the histology results (Figure 2).

Combined datasets for age and sex genotype

Combining all four samples (two ages, each with two sex genotypes) gave 40 clusters (Figure 5A; Supplementary Table S7) with defined marker genes (Supplementary Table S8). Some clusters contained significant proportions of cells from both 19dpf and 30dpf, but many sorted out by age (Figure 5B), suggesting cell type maturation. And, as expected from the 30dpf-only analysis (Figure 5C), some clusters in the combined analysis were mostly ZW cells and others mainly ZZ cells, while many were still mixed. The analysis below provides a more detailed understanding of major cell types (Figure 5D).

Germ cells

Germ cell marker genes, including *dazl*, *ddx4,* and *dnd1* (Olsen et al., 1997; Yoon et al., 1997; Maegawa et al., 1999; Howley and Ho, 2000; Ciruna et al., 2002; Tan et al., 2002; Weidinger et al., 2003; Krovel and Olsen, 2004; Slanchev et al., 2005; Houwing et al., 2008; Saito et al., 2011; Hartung et al., 2014; Hong et al., 2016; Bertho et al., 2021) were detected in the merged 19dpf+30dpf (”1930”) data as

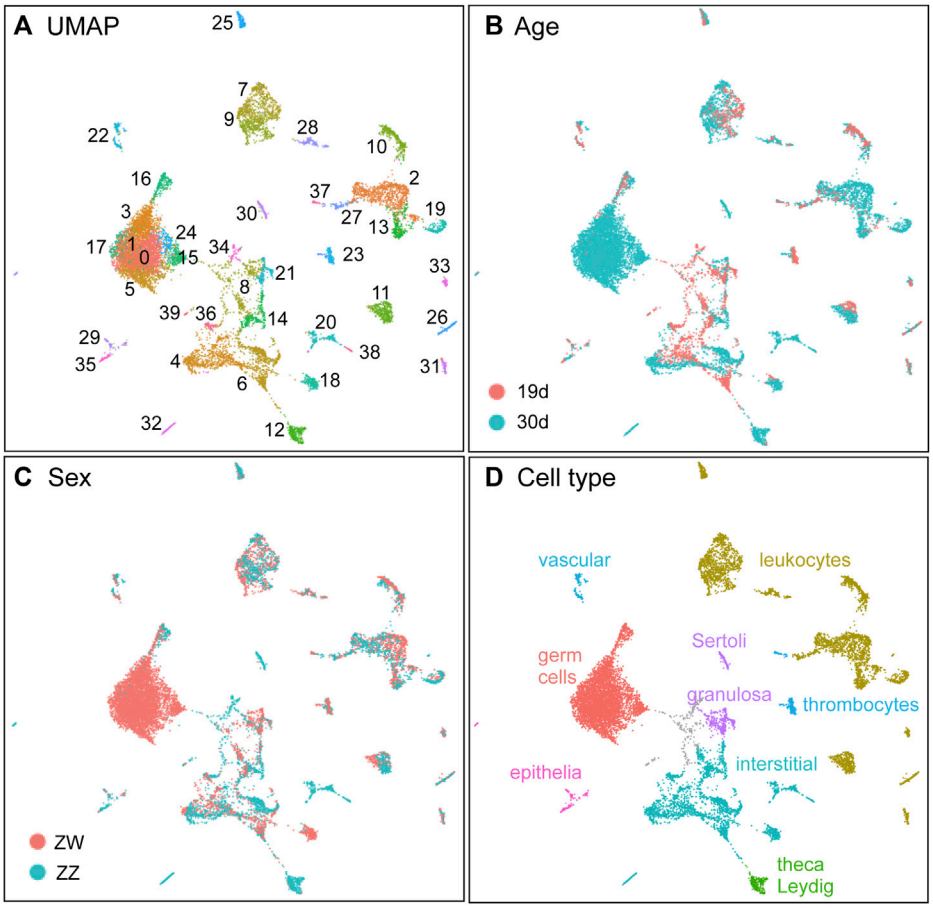

FIGURE 5
The combined dataset with two ages, each with two sex genotypes. **(A)** UMAP displaying clusters. **(B)** Samples displayed by age (19dpf, red; 30dpf, blue). **(C)** Samples displayed by sex genotype (ZW, red; ZZ, blue). **(D)** Inferred cell types.

expressed in several clusters (1930c0, c1, c3, c5, c15, c16, c17, c24) (Figures 6D–J). Cluster 1930c16 contained 19dpf cells mixed with 30dpf cells, but the large group of *dnd1*-expressing clusters contained almost exclusively 30dpf ZW cells (Figure 4B). We conclude that the large, several-cluster group of 30dpf ZW cells are developing oocytes and cluster 1930c16 cells are less mature germ cells that are generally similar in ZW and ZZ gonads.

The Vasa-encoding gene *ddx4* was strongly expressed in young germ cells of 1930c16 and less strongly in oocytes (Figure 6D), reflecting the observation that *ddx4* expression is higher in early stages of gametogenesis (Wang et al., 2007). Figures 6E–H show each of the four conditions separately in the combined 19 + 30dpf analysis. Results for germ cells (19c17 in the 19dpf-only analysis, Figures 3C, D) are shown in the box at the lower left of the 19dpf panels in Figure 6. The distribution of *ddx4*-expressing ZZ cells at 19dpf and 30dpf (Figures 6G, H) suggest that the transcriptomes of ZZ germ cells changed little between 19dpf and 30dpf, reflecting the delayed differentiation observed in ZZ gonads in our histological studies. This result also shows that ZZ germ cells did not develop an oocyte-like transcriptome, again consistent with the histology. Expression of *dnd1* supports these conclusions (Figures 6I, J).

Oocyte stages recovered are limited by the scRNA-seq protocol, which passes cells through a 40 µm filter. According to recent staging criteria (Bogoch et al., 2022), we would recover only oocytes from the earliest two stages: the symmetry-breaking stage (8–20 µm Selman Stage IA, oogonia and meiotic oocytes from leptotene to pachytene), and early Selman Stage IB, nuclear cleft, 15–50µm, oocytes from pachytene to mid-diplotene (Selman et al., 1993; Bogoch et al., 2022). Comparison of gene expression patterns with other transcriptomic analyses of zebrafish oocytes (Wong et al., 2018; Zhu et al., 2018; Can et al., 2020; Bogoch et al., 2022) are difficult because at least some of the oocyte sizes we examined were not analyzed or were mixed with larger oocytes, and in other studies, oocyte sizes were listed in relative rather than absolute terms, so comparison was not possible (Cabrera-Quio et al., 2021).

Cluster 1930c16 appears to consist of bipotential germ cells. Few genes were expressed at a higher level in 1930c16 at 19dpf than in 30dpf germ cells, but *fkbp6* was an exception (Figures 6K, L, samples separated by age, not by sex genotype). Men homozygous for pathogenic variants of *FKBP6* show arrested spermatogenesis at the round-spermatid stage and have abnormal piRNA biogenesis like mouse *Fkbp6* mutants (Xiol et al., 2012; Wyrwoll et al., 2022). piRNAs interact with Piwi proteins, including Piwil2 in zebrafish, which aids in transposon defense

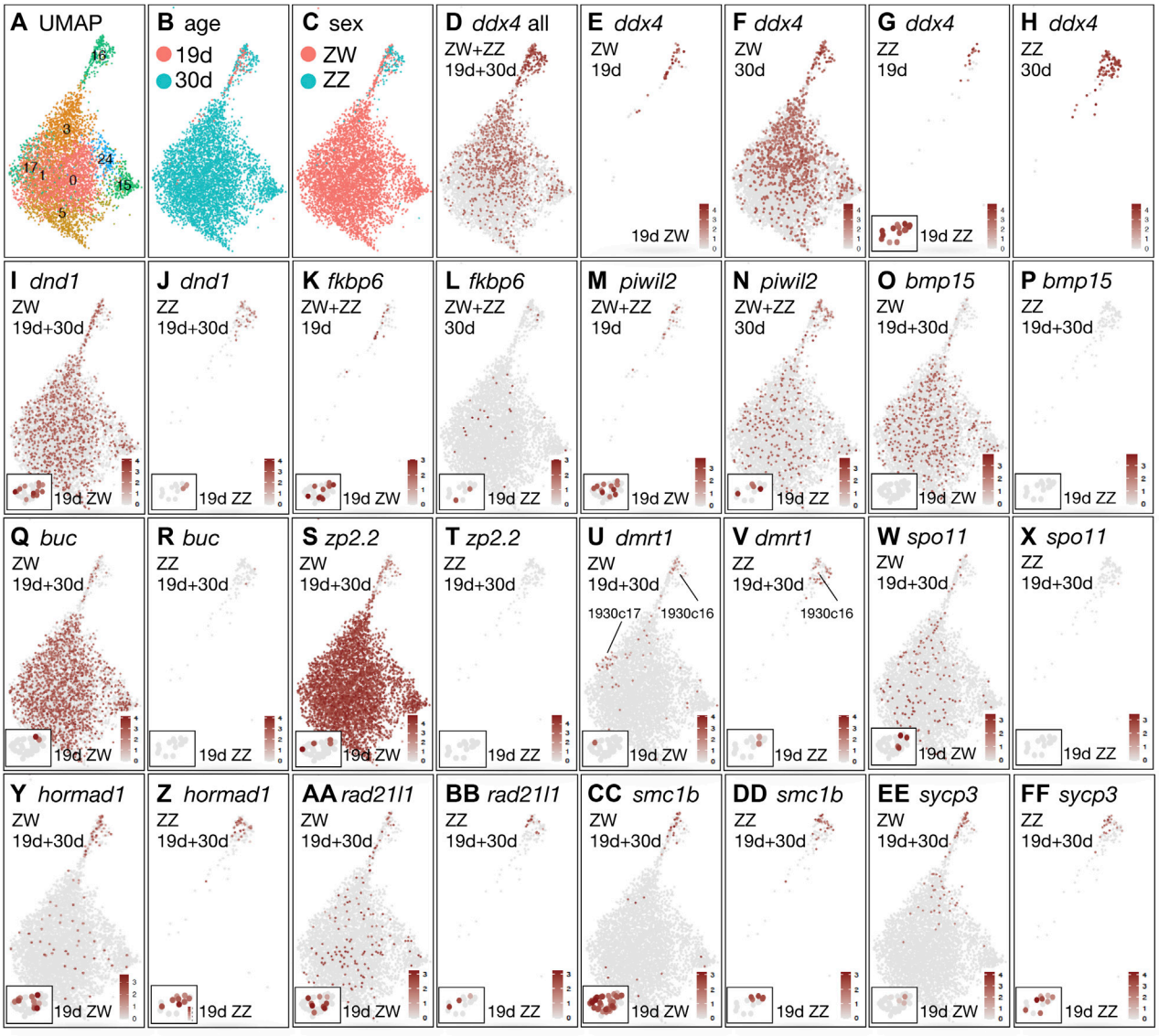

FIGURE 6
Germ cell development in the merged analysis of both ZW and ZZ cells at both 19 and 30dpf. **(A)** UMAP isolating germ cell clusters. **(B)** Germ cells marked by age (red, 19dpf; blue, 30dpf). **(C)** Germ cells marked by sex genotype (red, ZW; blue, ZZ). **(D)** *ddx4*(*vasa*) including all four conditions. **(E)** *ddx4* showing only ZW cells at 19dpf. Insert in lower left of the panel shows *ddx4* expression in the ZW germ cell cluster 19c17 in the analysis of 19dpf cells only (see Figure 3). **(F)** *ddx4,* only ZW cells at 30dpf. **(G)** *ddx4,* only ZZ cells at 19dpf. Insert in lower left of the panel shows *ddx4* expression in the ZZ germ cell cluster 19c17 from the analysis of 19dpf cells only. **(H)** *ddx4,* only ZZ cells at 30dpf. **(I)** *dnd1* ZW cells only at both 19dpf and 30dpf. **(J)** *dnd1* ZZ cells only at both 19dpf and 30dpf. **(K)** *fkbp6,* both ZW and ZZ cells only at 19dpf. **(L)** *fkbp6,* both ZW and ZZ cells only at 30dpf. **(M)** *piwil2,* ZW and ZZ cells at 19dpf. **(N)** *piwil2,* ZW and ZZ cells at 30dpf. **(O)** *bmp15,* ZW cells at both 19dpf and 30dpf. **(P)** *bmp15,* ZZ cells at both 19dpf and 30dpf. **(Q)** *buc,* ZW cells at both 19dpf and 30dpf. **(R)**. *buc,* ZZ cells at both 19dpf and 30dpf. **(S)** *zp2.2,* ZW cells at both 19dpf and 30dpf. **(T)** *zp2.2,* ZZ cells at both 19dpf and 30dpf. **(U)** *dmrt1,* ZW cells at both 19dpf and 30dpf. **(V)** *dmrt1,* ZZ cells at both 19dpf and 30dpf. **(W)** *spo11,* ZW cells at both 19dpf and 30dpf. **(X)** *spo11,* ZZ cells at both 19dpf and 30dpf. **(Y)** *hormad1,* ZW cells at both 19dpf and 30dpf. **(Z)** *hormad1,* ZZ cells at both 19dpf and 30dpf. **(AA)** *rad21l1,* ZW cells at both 19dpf and 30dpf. **(BB)** *rad21l1,* ZZ cells at both 19dpf and 30dpf. **(CC)** *smc1b,* ZW cells at both 19dpf and 30dpf. **(DD)** *smc1b*, ZZ cells at both 19dpf and 30dpf. **(EE)** *sycp3,* ZW cells at both 19dpf and 30dpf. **(FF)** *sycp3* ZZ, cells at both 19dpf and 30dpf.

(Houwing et al., 2008). Like *fkbp6, piwil2* transcripts accumulated in 1930c16 germ cells at 19dpf and 30dpf (Figures 6M, N). The expression of *fkbp6* and *piwil2* in 19dpf germ cells shows that these cells represent an early step in the pathway of gametogenesis.

Oocyte-specific genes in NA gonads tended to label strongly the *dnd1*-expressing germ-cell clusters except for 1930c16. Accumulation of *bmp15* and *gdf9* transcripts was detected only in 30dpf ZW germ cells, but not in 19dpf ZW germ cells or ZZ germ cells (Figure 6O, P, Supplementary Figure S1A, S1B). The loss of either Bmp15 or Gdf9 function blocks ovarian follicle development in zebrafish and mouse (Dong et al., 1996; Su et al., 2004; Dranow et al., 2016; Chen et al., 2022; Zhai et al., 2022). The 30dpf ZW cells also accumulated transcripts encoding the Balbiani body protein Bucky ball (*buc*), an early marker of oocyte asymmetry (Marlow and Mullins, 2008; Jamieson-Lucy et al., 2022), but few ZZ cells did, and only at a low level (Figures 6Q, R). The low or undetected expression

of *bmp15* and *gdf9* expression in 1930c16 suggests that these cells were at an earlier stage of differentiation than the large group of germ cell clusters (1930c0, c1, c3, c5, c15, c17, c24). Cells in the large group of 30dpf ZW germ cell clusters also expressed genes encoding zona pellucida egg coat proteins like Zp2.2 (Figures 6S, T). At 19dpf, the germ cell cluster 19c17 had at least one ZW germ cell expressing a zona pellucida gene [*zp2.1, zp2.2, zp2.3, zp3, zp3.2, zp3a.1, zp3a.2, zp3b, zp3d.1, zp3d.2, zp3f.1*(*si:ch211-14a17.7*), *zpcx*] but no *ZZ* germ cells expressed any *zp* gene at 19dpf; although this result was not statistically significant for any single gene (Supplementary Table S4), taken as a group, this finding would be expected if ZW germ cells were already beginning to become different from ZZ germ cells and to differentiate as oocytes even before differences were apparent histologically. Other oocyte-specific genes like *zar1* (Miao et al., 2017) (Supplementary Figures S1K, S1L) followed the same pattern.

Zebrafish orthologs of presumed fish vitellogenin receptors *vldlr* and *lrp13* (Hiramatsu N et al., 2013; Reading et al., 2014; Mushirobira et al., 2015; Morini et al., 2020) were expressed only in 30dpf ZW oocytes (Supplementary Figures S1M, S1P). Vldlr may be associated with formation of yolk oil droplets and Lrp13 with vitellogenin uptake (Hiramatsu N et al., 2013). Other suggested vitellogenin receptor candidates, like *lrp1ab, lrp2a, lrp5* and *lrp6,* were not expressed in our dataset (Zhai et al., 2022), perhaps because oocytes larger than 40 μm were excluded.

Dmrt1 is essential for normal testis differentiation in mammals and is expressed in both germ cells and Sertoli cells (Raymond et al., 1999; Raymond et al., 2000; Kim et al., 2007; Herpin et al., 2010; Matson et al., 2010; Kopp, 2012). In addition, variants of *dmrt1* are major sex determining genes in some amphibia, perhaps some snakes, in birds, and some fish (Nanda et al., 2002; Kobayashi et al., 2004; Smith et al., 2009; Janes et al., 2014; Cui et al., 2017; Mustapha et al., 2018; Ogita et al., 2020; Ioannidis et al., 2021). In NA gonads at 19dpf, *dmrt1* was expressed at low levels in both ZW and ZZ germ cells in 1930c16 (Figures 6U, V). At 30dpf, *dmrt1* expression continued in 1930c16 germ cells in both ZW and ZZ genotypes, and in addition, appeared in 30dpf ZW germ cells in 1930c17 (Figures 6U, V) along with *phospho1* and *scg3*, which were both also expressed in Sertoli cells like *dmrt1* (Supplementary Table S8). Because *in situ* hybridization in adult TU laboratory strain zebrafish showed that *dmrt1* is expressed primarily in Stage IB oocytes (Webster et al., 2017), we conclude that in our NA fish, the *dmrt1*-expressing ZW germ cells in 1930c17 represent stage 1B oocytes.

These results are consistent with the conclusion that 1) cluster 1930c16 represents largely undifferentiated germ cells that our histology studies (Figure 2) showed were present in 19dpf ZW and ZZ gonads; 2) that some of the 19dpf ZW germ cells in 1930c16 appear to have had already started expressing weakly some oocyte genes; 3) that ZZ germ cells in 1930c16 remained largely unchanged between 19dpf and 30dpf; 4) that most of the large group of 30dpf ZW-specific germ cell clusters represent Stage IA oocytes expressing strongly oocyte-specific genes; and 5) that 1930c17 represents *dmrt1*-expressing early Stage IB oocytes.

Meiosis gene functions are important for sex determination, as shown by mutations in meiosis genes that produce mostly neomale offspring (Rodriguez-Mari et al., 2010; Shive et al., 2010; Rodriguez-Mari et al., 2011; Saito et al., 2011; Ramanagoudr-Bhojappa et al., 2018; Takemoto et al., 2020; Blokhina et al., 2021; Islam et al., 2021). Meiotic recombination begins with the introduction of double-strand DNA breaks catalyzed by Spo11, Hormad1, and CCDC36 (IHO1) (Keeney, 2008; Shin et al., 2013; Stanzione et al., 2016). In zebrafish, *spo11* is necessary for homolog synapsis, for sperm production, and for preventing females from having abnormal offspring (Blokhina et al., 2019). In our samples, *spo11* expression appeared in ZW germ cells, but not in any ZZ cells, at both 19dpf and 30dpf (Figures 6W, X), and *hormad1* was expressed in 1930c16 germ cells at both ages and both sex genotypes (Figures 6Y, Z). Repair of Spo11-induced double strand breaks occurs by the DNA recombinases Dmc1 and Rad51 (Hunter, 2015) and Fanconi Anemia genes, including *fancl* and *brca2* (Grompe and D'Andrea, 2001). This process involves sister chromatid cohesion, achieved by cohesin components, including *rad21l1* in zebrafish, which is required for oogenesis but not spermatogenesis (Blokhina et al., 2021) and in our samples, was expressed at both ages in both sexes in 1930c16 (Figures 6AA, BB). Other meiosis genes, including *smc1b* (Figures 6C, D, Supplementary Figures S1C–S1F), which is essential for homolog pairing and synapsis (Islam et al., 2021), *rec8a*, and *rec8b*, and genes encoding synaptonemal complex proteins Sycp1, Sycp2, and Sycp3 (Figures 6E, F; Supplementary Figures S1G, S1H; Supplementary Table S8) are stronger markers for young germ cells in cluster 1930c16 than for oocytes in clusters 1930c0, c1, c3, c5, c15, c17, c24. The pattern for meiosis genes in general was opposite from the pattern for oocyte-specific genes, like *bmp15, buc,* and *zp2.2,* which increased from 1930c16 to the large group of oocyte clusters. How zebrafish regulate the switch from transcribing meiosis genes to maturing oocyte genes is unknown. The expression of meiosis genes in both ZW and ZZ germ cells (except for *spo11*) deepens the mystery of the mechanism in zebrafish that causes many meiotic gene mutants to tend to develop as males (*fancl, brca2, rad21l1, smc1b, sycp1, sycp2* (Rodriguez-Mari et al., 2010; Shive et al., 2010; Rodriguez-Mari et al., 2011; Saito et al., 2011; Ramanagoudr-Bhojappa et al., 2018; Takemoto et al., 2020; Blokhina et al., 2021; Islam et al., 2021), with *mlh1* and *spo11* being the exceptions (Feitsma et al., 2007; Leal et al., 2008; Blokhina et al., 2019). A hypothesis is that zebrafish females lack a synapsis checkpoint (Imai et al., 2021).

Histone H2ax phosphorylation results in foci at the sites of DNA breaks in meiosis (Hamer et al., 2003; Blokhina et al., 2021; Imai et al., 2021; Islam et al., 2021). Two H2ax histones had a reciprocal pattern of expression in NA gonads: *h2ax1*(*h2afx1*) was expressed strongly in nearly all somatic cells in all four samples and in both ZW and ZZ germ cells in 1930c16 but in few oocytes as defined by *buc* expression (Supplementary Figures S1I, S1J). Reciprocally, *h2ax*(*h2afx*) was expressed strongly in 30dpf ZW oocytes but not in somatic cells and weakly in ZZ germ cells (Supplementary Figures S1K, S1L). These results suggest that during oogenesis, histone H2ax replaces the somatic and early germ cell histone H2ax1 in zebrafish oogenesis.

Support cells

Support cells (granulosa cells in the ovary and Sertoli cells in the testis) control germ cell proliferation, differentiation, and maturation. Support cells in fish express *gsdf* both in ovaries and in testes and *gsdf* is required for oocyte maturation (Sawatari et al., 2007; Gautier et al., 2011; Imai et al., 2015; Zhang et al., 2016; Yan et al., 2017; Jiang et al., 2022). Furthermore, a variant of *gsdf* is the

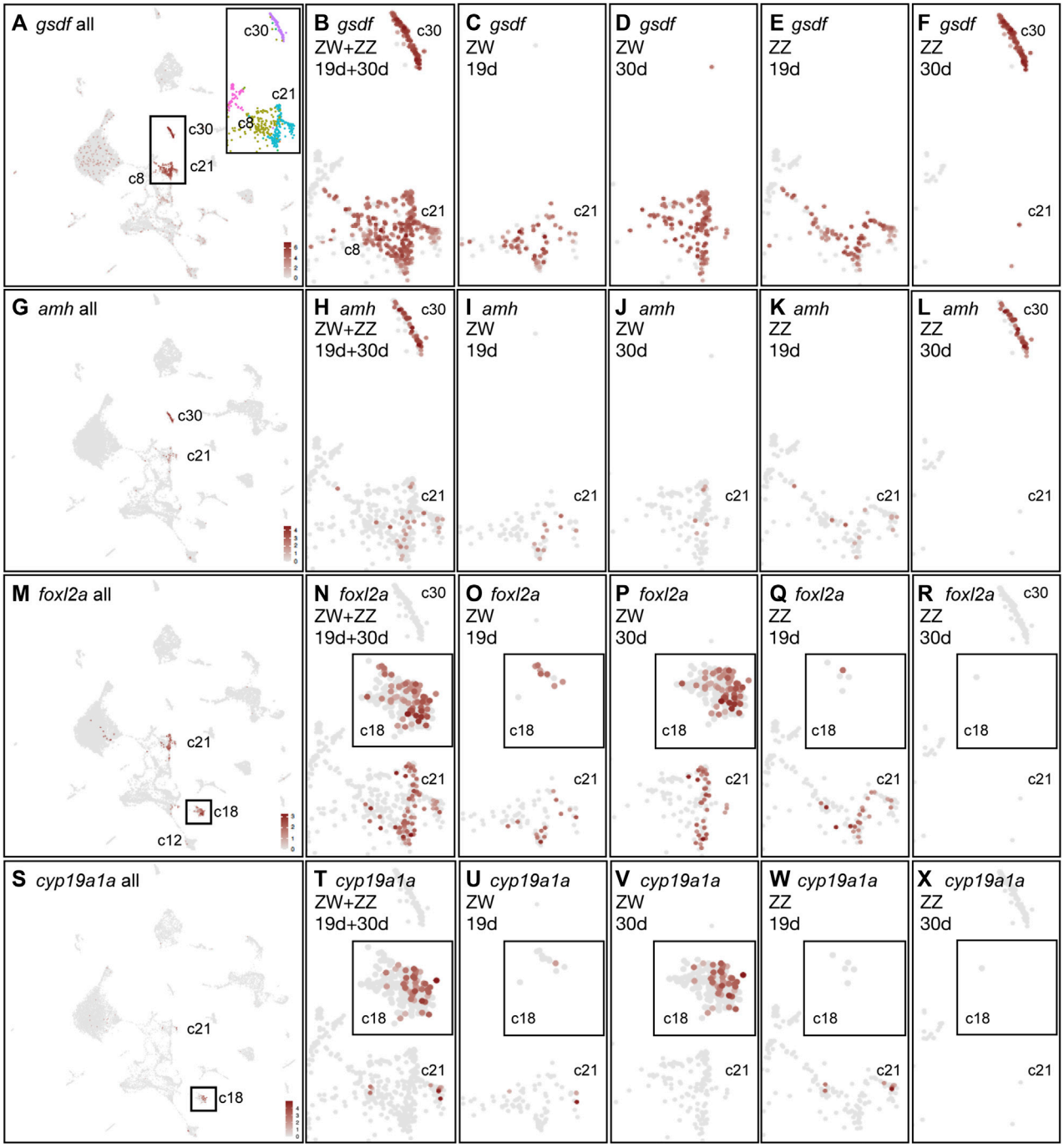

FIGURE 7
Support cell gene expression merging both time points and both sex genotypes. **(A)** *gsdf* expression across the whole combined dataset. The rectangle marks *gsdf*-expressing support cells and their precursors, expanded to show cluster assignments in color. **(B)** Enlargement of rectangle from part A, showing *gsdf* expression in clusters 1930c30, c21, and c8 combining all four conditions. **(C)** *gsdf* expression in 19dpf ZW gonads. **(D)** *gsdf* expression in 30dpf ZW cells. **(E)** *gsdf* expression in 19dpf ZZ cells. **(F)** *gsdf* expression in 30dpf ZZ cells. **(G–L)** *amh* expression in samples as described for **(B–F)**. **(M–R)** *foxl2a* expression. Box in M around 1930c18 is expanded as inserts in **(N–R)**. **(S–X)** *cyp19a1a* expression. Boxed insert in **(S)** around 1930c18 appears as inserts in **(T–X)**.

major male sex determining gene in Luzon medaka and sablefish (Myosho et al., 2012; Herpin et al., 2021). In the combined analysis, *gsdf* was expressed strongly in just three cell clusters: 1930c30, c21, and c8, identifying support cells or their precursors (Figures 7A, B). In 19dpf gonads, *gsdf* was expressed in 1930c8 and 1930c21 in both ZW and ZZ cells (Figures 7A–C, E) suggesting that these are support cell precursors and, that ZW and ZZ pre-support cells at 19dpf are transcriptionally similar (Figures 7C, E).

At 30dpf, *gsdf* expression differed substantially in ZW and ZZ gonads. Cluster 1930c30 contained almost exclusively 30dpf ZZ cells

(Figure 7F) representing Sertoli cells. In contrast, ZW cells at 30dpf occupied 1930c21 and 1930c8 (Figure 7D), suggesting that these clusters contain granulosa cells in addition to support cell precursors. Both *inha,* which is necessary for final oocyte maturation and ovulation (Lu et al., 2020), and *igf3*, which is essential for zebrafish ovarian follicles to develop beyond the primary growth stage (Xie et al., 2021), had virtually the same expression pattern as *gsdf* (Supplementary Figures S2A–S2F). These results suggest: 1) *gsdf*-expressing 30dpf ZW cells in 1930c21 represent granulosa cells; 2) *gsdf*-expressing 30dpf-ZZ cells in 1930c30 represent Sertoli cells; 3) some *gsdf*-expressing cells of both sex genotypes at 19dpf in 1930c8 and 1930c21 likely represent bipotential precursors of support cells and at 30dpf, the ZW cells represent granulosa cell precursors; 4) substantial differentiation of sex-specific cell types occurs between 19dpf and 30dpf.

Sertoli cells in fish strongly express *amh, dmrt1*, and *sox9a* (Chiang et al., 2001a; Kobayashi et al., 2004; Guo et al., 2005; Rodriguez-Mari et al., 2005; Yan et al., 2005; Lin et al., 2017; Webster et al., 2017). AntiMüllerian Hormone (Amh), secreted by Sertoli cells in mammalian testes, destroys the developing female reproductive tract, and variants of *amh* or its receptor gene *amhr2* are male sex determinants in several species of fish (Morinaga et al., 2007; Hattori et al., 2012; Kamiya et al., 2012; Li et al., 2015; Ieda et al., 2018; Pan et al., 2021). At 19dpf, a few pre-support cells of both ZW and ZZ genotypes weakly expressed *amh* (Figures 7G–I, K) and *dmrt1* (Supplementary Figures S2G–I, S2K). Recall, *dmrt1* was also expressed in germ cells, Figures 6U, V). At 30dpf, *amh* and *dmrt1* were still weakly expressed in just a few ZW cells but were strongly expressed in ZZ cells in 1930c30 (Figures 7J–L; Supplementary Figures S2J, S2L). Mammalian Sertoli cells express S*ox9,* which maintains testis development (Morais da Silva et al., 1996; Qin and Bishop, 2005; Barrionuevo et al., 2006). In our samples, *sox9a* was expressed strongly in ZZ Sertoli cells (1930c30) and was detected in some 1930c21 cells in ZW gonads and 19dpf ZZ gonads (Supplementary Figures S2M–S2R). These results support the assignment of the 30dpf ZZ-specific cluster 1930c30 as Sertoli cells and 19dpf ZZ cells in 1930c21 as support cell precursors.

Ovarian follicle cells in mammals are multi-layered, with inner granulosa cells that form gap junctions with the oocyte and transport substances, and an outer granulosa cell layer that produces estradiol (Gilchrist et al., 2008). In teleosts, however, ovarian follicle cells form a single-cell epithelium over the oocyte, but it is unclear whether this single layer provides both the transport function through gap junctions and the endocrine function or if that single cell layer consists of two cell types, one that transports substances and one that provides estradiol (Devlin and Nagahama, 2002). The mammalian granulosa gene *Foxl2* has two duplicates in zebrafish that arose in the teleost genome duplication (*foxl2a, foxl2b*) plus a third paralog, lost in mammals, that arose in a genome duplication event before the divergence of teleosts and mammals (*foxl2l,* alias *zgc:194189* or *foxl3*) (Crespo et al., 2013; Caulier et al., 2015; Bertho et al., 2016; Webster et al., 2017; Yang et al., 2017; Dai et al., 2021a; Liu et al., 2022). In our combined analysis of both ages and both sex genotypes, *foxl2a* was expressed in two clusters: in the support cell precursors in 1930c21 similar to the pattern of *gsdf* and *amh,* and additionally, in 1930c18 (Figure 7M). At 19dpf in 1930c21, expression of *foxl2a* was similar to that of *gsdf*, but weaker, and appeared in both ZW and ZZ cells (Figures 7O, Q), consistent with these cells being bipotential support cell precursors. At 30dpf, *foxl2a* was also expressed in ZW 1930c21, again consistent with these cells representing granulosa cells. A second major *foxl2a* expression domain appeared in cluster 1930c18 (Figure 7M, box; N-R, insert). Cluster 1930c18 contained few 19dpf cells and only one 30dpf ZZ cell (Figures 7N-R, insert), showing that it was a cell type that began to develop before 19dpf in both ZW and ZZ cells, but by 30dpf, it was ZW-specific.

Expression of *foxl2b* was like that of *foxl2a* (Supplementary Figures S2S, S2X). Expression of *foxl2l*, which lacks a mammalian ortholog, showed scant expression limited to Stage IA and small Stage IB oocytes; other studies show that oocytes at a more mature stage strongly express *foxl2l* (Kikuchi et al., 2020; Liu et al., 2022).

The *foxl2a*- and *foxl2b*-expressing cells in 1930c21 may be performing the transport function of mammalian granulosa cells because the gap junction connexin gene *gja11*(*cx34.5*) was specifically expressed in 1930c21 in a pattern like that of *gsdf* and *foxl2a* at 19dpf in presumed support cell precursors and at 30dpf in granulosa cells in ZW gonads. Sertoli cells in ZZ gonads also expressed *gja11* (Supplementary Figures S2Y, S2DD). *In situ* hybridization had previously detected *gja11* expression in follicle cells surrounding Stage II oocytes (cortical alveolus stage, 140–340 µm (Bogoch et al., 2022), which were not present in our samples), but not in Stage IB oocytes (Liu et al., 2022); our data detected *gja11* expression at earlier stages presumably due to increased sensitivity. The oocyte partner of Gja11 could be encoded by *gjc4a.1*(*cx44.2*) or *gjc4b*(*cx43.4*), which were expressed strongly and rather specifically in 30dpf oocytes (Santos et al., 2007) (Supplementary Figures S2KK, S2LL).

The estrogen-producing function of mammalian granulosa cells might be mediated by a cell type different from the 1930c21 cells that may perform the transport function. Gonadal aromatase, encoded by *cyp19a1a*, converts testosterone to estradiol or androstenedione to estrone (Chiang et al., 2001b; Chiang et al., 2001c; Tenugu et al., 2021). At 19dpf, a few *cyp19a1a*-expressing cells appeared with 1930c21 support cell precursors in both ZW and ZZ genotypes (Figures 7S, U, W), while at 30dpf, *cyp19a1a* was expressed in ZW cells in 1930c18 but not in ZZ cells (Figures 7V, X). The strong expression of *gsdf, foxl2a,* and *gja11* in 1930c21 and *foxl2a* and *cyp19a1a* in 1930c18 suggests that the transport function and estrogen-production function of mammalian granulosa cells may be carried out by two different follicle cell types in zebrafish 30dpf ZW ovaries.

We conclude that expression patterns of *gsdf, foxl2a, foxl2b,* and *cyp19a1a* suggest that: 1) at 19dpf, support cell precursors were similar in ZW and ZZ gonads; 2) that 30dpf ZW but not ZZ gonads maintained these common support cell precursors; 3) that granulosa cells appeared in the UMAP near support cell precursors but Sertoli cells were distant; and 4) that the aromatase function of 30dpf ovarian follicle cells was provided by a ZW cell type different from the strongly *gsdf*-expressing 30dpf ZW follicle cell type.

Steroidogenic cells

Sex steroids are important for zebrafish gonad development (Menuet et al., 2004; de Waal et al., 2009; Caulier et al., 2015; Luzio

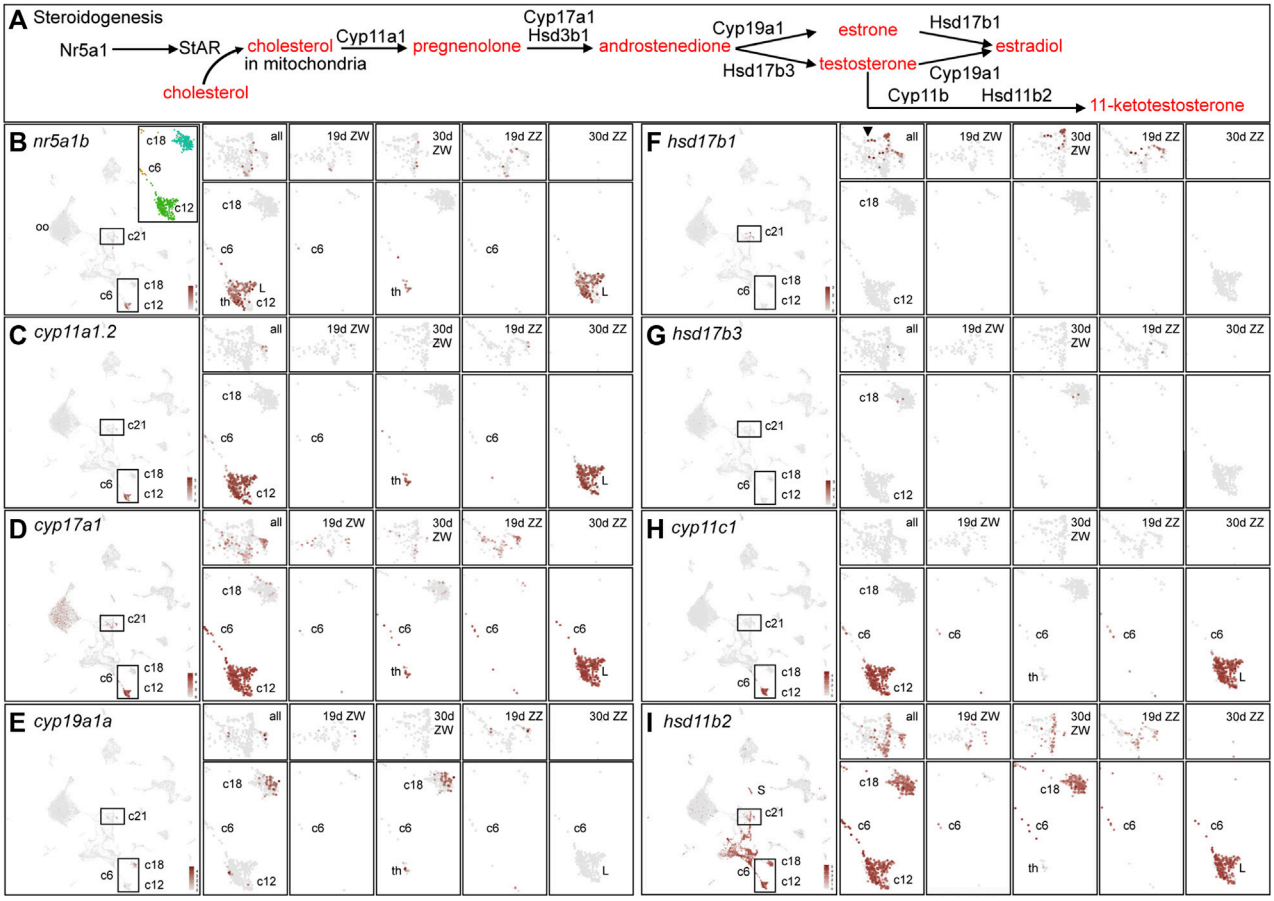

FIGURE 8
Steroidogenesis. **(A)**. An abbreviated pathway of steroidogenesis (after (Tenugu et al., 2021)). **(B)** *nr5a1b* expression. The left panel shows expression in the entire dataset. The insert shows cluster demarcation for the most relevant steroidogenic enzymes. Subsequent panels show, at the top 1930c21, the support cell precursor and granulosa cell cluster and at the bottom the clusters corresponding to the insert in the left panel. Displayed from left to right are the enlargements of all four conditions: 19dpf ZW gonads, 30dpf ZW gonads, 19dpf ZZ gonads, and 30dpf ZZ gonads. Cluster numbers are indicated. **(C)** cyp11a1.2 displayed as explained for *nr5a1b*. **(D)** *cyp17a1*. **(E)** *cyp19a1a*. **(F)**. *hsd17b1*. **(G)** *hsd17b3*. **(H)** *cyp11c1*. **(I)** *hsd11b2*. Abbreviations: L, Leydig cells; th, theca cells.

et al., 2016; Lu et al., 2017; Zhai et al., 2018), but we know little about steroidogenic cell development in ZW vs. ZZ zebrafish.

Nr5a1 and Star initiate gonadal steroidogenesis (Figure 8A, after (Tenugu et al., 2021). Nr5a1 (Steroidogenic Factor-1, SF1) is a major regulator of genes that encode gonadal steroidogenesis enzymes in theca and Leydig cells and it is one of the earliest markers of gonadal differentiation, turning on in human gonads before *SRY* (Morohashi et al., 1995; Ikeda et al., 1996; Hanley et al., 1999). Zebrafish has two co-orthologs of *Nr5a1* (*nr5a1a* and *nr5a1b*) (von Hofsten et al., 2001; Kuo et al., 2005) from the teleost genome duplication (Amores et al., 1998; Postlethwait et al., 1999; Taylor et al., 2003; Jaillon et al., 2004). Loss-of-function mutations in *nr5a1a* disrupt development strongly in the interrenal and mutations in *nr5a1b* cause more severe phenotypes in the gonad (Yan et al., 2020). At 19dpf, *nr5a1b* was expressed in a few support precursor cells (1930c21) and a few 1930c6 cells, while at 30dpf, *nr5a1b* was strongly expressed in 1930c12 but only weakly in granulosa or Sertoli cells (Figure 8B). We conclude that in 1930c12, the ZW cells are theca cells, and the ZZ cells are Leydig cells. Leydig cells in 1930c12 also specifically expressed *insl3*, *skor2*(*zgc:153395*), and *pcdh8* (Supplementary Table S8).

StAR (steroidogenic acute regulatory protein) gene transcription is turned on by Nr5a1 (Sugawara et al., 1997). In an initial step (Figure 8A), StAR brings cholesterol into the inner mitochondrial membrane (Miller and Auchus, 2011). Zebrafish adult gonads express *star* (Bauer et al., 2000; Ings and Van Der Kraak, 2006; de Waal et al., 2009), and although NA zebrafish at 19dpf had few *star*-expressing cells, at 30dpf, *star* was expressed strongly in theca and Leydig cells (1930c12) and in a few oocytes (Supplementary Figure S3B).

Cyp11a1 in mammals converts cholesterol to pregnenolone (Lai et al., 1998). Zebrafish has tandem duplicates of human *CYP11A1* (*cyp11a1.1* and *cyp11a1.2*, previously called *cyp11a1* and *cyp11a2*, respectively) (Hu et al., 2001; Goldstone et al., 2010; Parajes et al., 2013); these genes originated in a duplication event that occurred after the divergence of zebrafish and carp lineages (gene tree ENSGT00940000158575). Disruption of *cyp11a1.2* results in androgen loss, and homozygous mutants develop into feminized

males with disorganized testes and few spermatozoa (Parajes et al., 2013; Li et al., 2020a; Wang et al., 2022). At 19dpf, *cyp11a1.2* showed scant expression, but at 30dpf, it was widely expressed in ZW theca and ZZ Leydig cells and in 1930c6 (Figure 8C). In contrast, expression of the tandem duplicate *cyp11a1.1* was not detected at 19dpf (Supplementary Figure S3C) and at 30dpf, it appeared in many ZW oocytes, as expected from its known maternal expression (Hsu et al., 2002; Parajes et al., 2013; Wang et al., 2022), but it was not expressed in ZZ germ cells. The *cyp11a1.1* gene was expressed weakly in ZZ Leydig cells but in no theca cells, and weakly in a few 1930c18 cells (Supplementary Figure S3C). We conclude that the expression of *cyp11a1.1* and *cyp11a1.2* diverged after the tandem duplication event and that *cyp11a1.2* maintained the ancestral pattern in theca and Leydig cells but *cyp11a1.1* evolved stronger expression in the oocyte germ cell lineage, which does not appear to be an ancestral expression domain because medaka, which lacks the tandem duplication, does not express *cyp11a1* in oocytes (Nakamoto et al., 2010). The regulatory mechanism causing different expression patterns for these two tightly linked tandemly duplicated genes is unknown.

Cyp17a1 and Hsd3b act on the product of Cyp11a1, pregnenolone, and convert it to androstenedione (Figure 8A). Knockout of *cyp17a1* in AB zebrafish leads to loss of juvenile ovaries and an all-male population with reduced male secondary sex characteristics (Zhai et al., 2018). At 19dpf, *cyp17a1* expression was detected in many support cell precursors and in 1930c6, which may be theca/Leydig cell precursors (Figure 8D). At 30dpf, *cyp17a1* was expressed weakly in granulosa and Sertoli cells, but at a high level in ZW theca and ZZ Leydig cells, and in many oocytes (Figure 8D). Expression of *hsd3b1* was like that of *cyp17a1,* but at lower levels and in fewer cells (Supplementary Figure S3D). Expression of *hsd3b2* (Lin et al., 2015) appeared almost exclusively in oocytes, like *cyp11a1.1* (Supplementary Figure S3E).

Cyp19a1 and Hsd17b enzymes carry out the next step, converting androstenediol to estradiol (Miller and Auchus, 2011). In principle, these reactions can occur in either of two ways (Figure 8A): 1) Cyp19a1 can form estrone from which Hsd17b1 forms estradiol (E2); alternatively, 2) Hsd17b3 can form testosterone, which Cyp19a1 converts to estradiol (Figure 8A). Cyp19a1 is important for zebrafish sex development because *cyp19a1a* mutants develop mostly as males (Dranow et al., 2016; Lau et al., 2016; Yin et al., 2017; Romano et al., 2020; Wu et al., 2020). In 19dpf NA zebrafish, *cyp19a1a* expression was found in a few support cell precursors (1930c21) in both ZW and ZZ gonads (Figure 8E). At 30dpf, *cyp19a1a* expression was not detected in any ZZ cells, as expected from its role in estrogen production. Transcripts for *cyp19a1a* were present in a few ZW theca cells (Figure 8E, 1930c12), but the focus of *cyp19a1a* expression was in ZW 1930c18 cells (Figure 8E), which also strongly expressed *foxl2a* and *foxl2b* but did not strongly express *gsdf* (Figures 7A, M-R; Supplementary Figure S2S-S2X). Cluster 1930c18 ZW cells at both 19dpf and 30dpf also expressed specifically the transcription factor *arxa* (Supplementary Figure S3F), whose mammalian ortholog *Arx* is expressed in, and is necessary for, the maintenance of fetal Leydig progenitors in mouse (Miyabayashi et al., 2013) and the formation of normal genitalia and sex steroid levels in humans (Gupta et al., 2019; Basa et al., 2021). The *cyp19a1a* cluster 1930c18 also expressed strongly and specifically the G protein-coupled receptors *s1pr3a* and *gpr17*, the junctional adhesion molecule *jam2b*, and the signaling gene *wnt11* [*wnt11r* (Postlethwait et al., 2019)]. Expression of steroidogenic enzymes other than *cyp19a1a* in 1930c18 was either not detected or detected weakly, except for *hsd11b2*, which was broadly expressed in nearly all stromal/interstitial cell clusters marked by the collagen gene *col1a1a* (compare Figure 8I to Figure 9A). These results are consistent with zebrafish having two types of ovarian follicle cells, one strongly and specifically expressing *cyp19a1a, arxa, foxl2a*, *s1pr3a*, *gpr17,* and *wnt11* (1930c18), and the other expressing strongly *gsdf, foxl2a*, *lamb2l, inha,* and *igf3* (1930c21).

Hsd17b, the second estrogen-producing enzyme activity (Figure 8A), is the master sex determinant in *Seriola* fishes (Purcell et al., 2018; Koyama et al., 2019). Hsd17b activity could be provided in principle by either Hsd17b1 or Hsd17b3 (Mindnich et al., 2004; Mindnich et al., 2005). At 19dpf, *hsd17b1* expression appeared in ZZ pre-support cells but not in ZW cells in our samples (Figure 8F). By 30dpf, however, *hsd17b1* expression was detected in *gsdf*-expressing ZW granulosa cells in 1930c21 (Figure 8F) as in adult AB strain female zebrafish (Liu et al., 2022). Expression of *hsd17b1,* was not detected in the *cyp19a1a*-expressing 1930c18 ZW cells or in any 30dpf ZZ cells.

In the alternative pathway of estradiol biosynthesis (Figure 8A) and in contrast to *hsd17b1, hsd17b3* expression was low at both 19dpf and 30dpf (Figure 8G). We conclude that, as in adult AB strain zebrafish (Liu et al., 2022), *hsd17b3* appears to play a smaller role than *hsd17b1* in estrogen synthesis in juvenile zebrafish.

These results suggest that three different transcriptomic clusters are important for estrogen production in 30dpf ZW zebrafish (Supplementary Figure S3J-S3L): 1) theca cells (ZW cells in 1930c12) convert pregnenolone to androstenedione using Cyp17a1 (Figure 8D); 2) follicle cells in 1930c18 transform androstenedione to estrone catalyzed by Cyp19a1a (Figure 8E); and 3) a different type of follicle cell in 1930c21 converts estrone to estradiol by Hsd17b1 (Figure 6F). It is possible that the 1930c18 *cyp19a1a*-expressing cell type and the *hsd17b1*-expressing cell type are simply different states or stages of the same individual cells. Also, it could be that Hsd17b3 might become more important in older animals or in more mature ovarian follicles than were present in our samples.

Androgens in fish gonads include testosterone and the principal teleost androgen 11-keto-testosterone (11 KT) (Kusakabe et al., 2003; de Waal et al., 2008; Nelson et al., 2013; Tokarz et al., 2015; Tenugu et al., 2021). 11KT is produced by the enzymes Hsd17b3, Cyp11c, and Hsd11b2 (Figure 8A). In 19dpf NA zebrafish, *cyp11c1* was expressed only in a few 1930c6 cells in both ZW and ZZ gonads (Figure 8H), consistent with bi-potential gonads. At 30dpf, however, *cyp11c* was expressed strongly and specifically in ZZ Leydig cells but not in ZW theca cells (Figure 8H). Within 1930c12, ZW cells, but not ZZ cells, expressed the "estrogen genes" *cyp19a1a* (Figure 7S, Figure 8E) and *foxl2a* (Figure 7M); reciprocally, ZZ cells, but not ZW cells, expressed the "androgen gene" *cyp11c1* (Figure 8H), confirming cell assignments as theca vs. Leydig cells.

Hsd11b2 can follow Cyp11c to produce 11 KT (Figure 8A). The *hsd11b2* gene was expressed more broadly than any of the other steroidogenic enzymes discussed here (Figure 8I). At 19dpf, both ZW and ZZ gonads expressed *hsd11b2* both in pre-support cells and in 1930c6 cells (Figure 8I), as well as in several stroma/interstitial cell

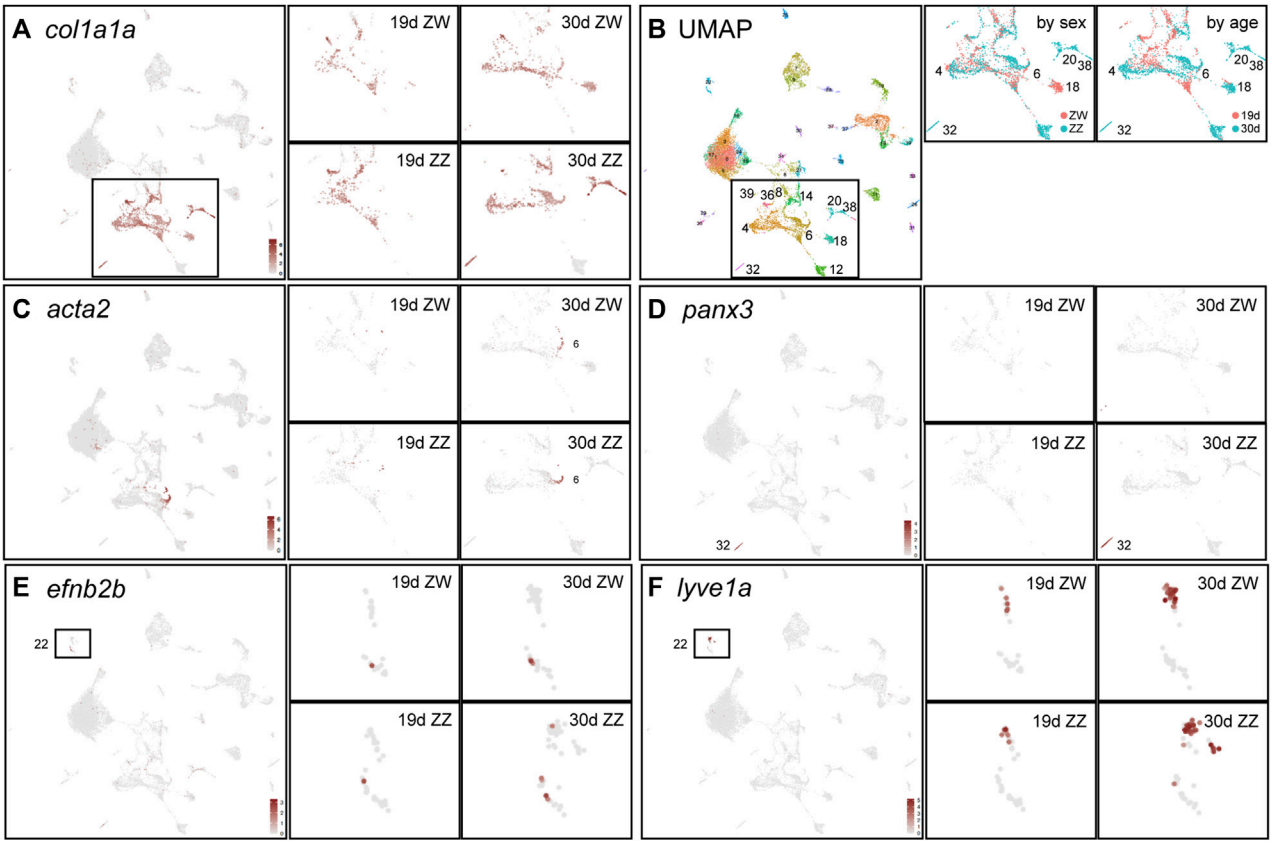

FIGURE 9
Stromal/interstitial clusters. **(A)** Expression of *col1a1a* defines stromal/interstitial cells (Liu et al., 2022). The left large panel combines cells of all four conditions for the complete dataset and the four smaller panels to the right show an enlargement of the *col1a1a*-expressing domain for each condition independently. At 19dpf, ZW and ZZ expression patterns are similar but at 30dpf, some clusters are sex-genotype specific. **(B)** The UMAP is in the left large panel; the middle panel shows the *col1a1a*-expressing region for samples separated by sex genotype (red, ZW; blue, ZZ); and the right panel shows samples separated by age (red, 19dpf; blue, 30dpf). **(C)** *acta2* expression, with panels as described for **(A)**. **(D)** *panx3* expression in the 30dpf ZZ-specific cluster 1930c32. **(E)** *efn2b* expression, indicating likely arterial endothelial cells in 1930c22 boxed in the large panel and expanded in the four condition-specific panels to the right. **(F)** *lyve1a* expression, a marker of lymphatics, labeling 1930c22.

clusters (see Figure 9). At 30dpf, *hsd11b2* was expressed in ZW gonads in granulosa cells and *cyp19a1a*-expressing 1930c18 cells, and in ZZ gonads in Sertoli cells and Leydig cells, as well as in stromal/interstitial cells (Figure 8I). *In vitro* enzyme assays show that zebrafish Hsd17b3 converts androstenedione to testosterone (Mindnich et al., 2005), but we did not specifically detect *hsd17b3* expression in ZZ NA gonads (Figure 8G). Hsd17b1 is unlikely to perform this function because, although *hsd17b1* was expressed in pre-support cells in 19dpf ZZ animals, expression was not detected at 30dpf in ZZ gonads (Figure 8F). This result suggests that at 30dpf, neither *hsd17b1* nor *hsd17b3* is likely to make a significant contribution to 11 KT formation in ZZ zebrafish, although they might at later developmental stages. A different Hsd17b enzyme might provide Hsd17b3 activity in zebrafish testes or our samples may represent a stage too early for significant production of testosterone or 11 KT. Breeding tubercles on male pectoral fins are an assay for androgen activity in zebrafish, but they first appear on males much older than those in our samples (McMillan et al., 2013; Dai et al., 2021b).

Steroid receptor genes were expressed in several steroidogenic cell types. The estrogen receptor gene *esr1* was expressed in only a few cells in NA gonads at either 19 or 30dpf, consistent with a weak effect of *esr1* mutants on ovary development (Lu et al., 2017). At 19dpf in both ZW and ZZ gonads, *esr2a* was expressed in pre-support cells and in some interstitial cells, and at 30dpf, in ZW granulosa cells, in *cyp19a1a*-expressing 1930c18 cells, in a few oocytes, and in some ZZ Leydig cells, as well as in some interstitial/stromal cells in at both ages and sex genotypes (Supplementary Figure S3G). The *esr2b* gene was expressed like *esr2a* in 30dpf ZW gonads, but also in 30dpf ZZ Sertoli cells (Supplementary Figure S3H). In addition, unique among the steroid-related gene set examined, *esr2b* was expressed strongly in19dpf ZW cells in 1930c18 (the *cyp19a1a* cluster) (Figure 8F). The androgen receptor gene *ar* was expressed with virtually the same pattern as *esr2b* (Supplementary Figure S3I). Expression of *ar* in ZZ cells is in accordance with the expectation that zebrafish *ar* mutants would mostly develop as females, and *ar* expression in ZW cells could help explain why even mutant females have reduced fertility (Crowder et al., 2018; Yu et al., 2018).

Interstitial and stromal cells

Interstitial and stromal cells provide structural support, erect barriers, transmit forces, and supply signals, thus offering functions distinct from other gonadal cell types (Kinnear et al., 2020). Many

interstitial and stromal cell types construct substantial intercellular matrix and express the collagen gene *col1a1a* (Liu et al., 2022) (Figure 9A). Sex- and age-specific clusters were prominent among *col1a1a*-expressing interstitial/stromal cells (Figure 9B). One conspicuous cluster was the 30dpf ZW-restricted *cyp19a1a*-expressing cluster 1930c18 discussed above, which has strong *col1a1a* expression (Figure 9A) and low *gsdf* expression (Figure 7A), further distinguishing the *cyp19a1a*-expressing granulosa cells in 1930c18 from the *hsd17b1*-expressing granulosa cells in 1930c21 (Figure 8F). In contrast, clusters 1930c20 and 1930c38 were 30dpf ZZ-specific (Figure 9B). These ZZ-specific clusters expressed many extracellular matrix components including the small leucine-rich proteoglycan gene *lumican* (Supplementary Figure S3A), *nog2, ccn2b*(*ctgfb*), *ccn4b*(*wisp1b*), and *ogna* (Supplementary Table S8). Cluster 1930c32 had far more ZZ cells than ZW cells at 30dpf and no cells at 19dpf, and specifically expressed the channel-forming *pannexin* gene *panx3* (Figure 9D), whose mammalian ortholog is a marker for the epididymis (Turmel et al., 2011), suggesting a role in zebrafish male gonadal ducts.

Contractile cells in 1930c6 specifically expressed the smooth muscle genes *acta2* (Figure 9C), *csrp1b, cnn1b, tpm2,* and *mylkb*. This strong expression domain appeared in 30dpf gonads and a smaller domain in 19dpf gonads, but about equally in ZW and ZZ cells. In human testes, *ACTA2, CSRP1* and other contractile protein genes are expressed in peritubular myoid cells, a layer of flattened contractile cells around seminiferous tubules that help transport spermatozoa and testicular fluid (Maekawa et al., 1996). Peritubular myoid cells also inhabit the interstitial region of fish testes (Schulz and Nóbrega, 2011). ZW cells also expressed this set of smooth muscle cell genes, as do cells in human ovaries (Fan et al., 2019).

Vascular endothelial cells line arterials, venous vessels, and lymphatics (Wolf et al., 2019; Gurung et al., 2022) and enter zebrafish gonads early in gonadogenesis (Kossack et al., 2023). For arterials, Vegf-receptor-2 (*kdr*, *kdrl*) activates Notch1 signaling (*notch1a, notch1b, notchl, dll4*) to provide Ephrin-B2 (*efnb2a, efnb2b*) at the cell surface (Villa et al., 2001; Covassin et al., 2006b; Masumura et al., 2009; Scheppke et al., 2012; Nakayama et al., 2013). Vegf-receptor, Ephrin-B2, and Notch signaling genes (e.g., *kdr,* Supplementary Figure S3B) were expressed in 1930c22 at both ages and in both sex genotypes, identifying arterial endothelium. For venous endothelium, *smarca4a* acts via CouptfII (*nr2f2*) to place Ephb4 (*ephb4a*) (Supplementary Figure S3C) and *ephb4b*) on the cell surface (Pereira et al., 2000; Wang et al., 2002; You et al., 2005; Muto et al., 2011; Davis et al., 2013; Model et al., 2014; Cui et al., 2015). The venous gene set was also expressed in 1930c22, suggesting that gonadal vein endothelial cells also appeared in this cluster. For lymphatics, *sox18* turns on Prox1 (*prox1a, prox1b*) to provide Vegfr3 (*flt4*) activity and thereby lymphatic identity supported by enriched expression of *lyve1a* (Figure 7F) and *lyve1b* (Kaipainen et al., 1995; Jackson et al., 2001; Prevo et al., 2001; Francois et al., 2008; Lee et al., 2009; Aranguren et al., 2013). We conclude that NA gonads at both 19 and 30dpf had all three types of endothelia but no vessel types appeared to be age- or sex-specific.

Gonad immune cells

Several types of white blood cells provide gonads with developmental and homeostatic functions. In mammalian testes, special lymphocytes are essential for normal testis function (Mossadegh-Keller and Sieweke, 2018; Garcia-Alonso et al., 2022). In the mammalian ovary, cytokine-mediated inflammation helps regulate ovulation (Field et al., 2014; Fan et al., 2019) and in domesticated zebrafish, activation of a specific macrophage population propels ovarian failure and masculinization (Bravo et al., 2023). To study leukocytes in developing NA gonads, we identified cells expressing the pan-leukocyte genes *coro1a,* (Figure 10A), *ptprc* (*cd45*), and *lcp1* (*l-plastin*) (Zakrzewska et al., 2010; Torraca et al., 2014) (Supplementary Table S8), all of which marked the same clusters and thus define the leukocytes in our dataset (Figure 10A).

None of the leukocyte clusters were exclusively ZW or ZZ (Figure 10B, Supplementary Table S7). Leukocyte cell types, however, partially sorted out by age, with some clusters being almost exclusively 30dpf (1930c2, c13, c19) (Figure 10C). These results suggest that at these stages, NA gonads may not have major sex-specific leukocyte populations and that between 19dpf and 30dpf, new leukocyte populations appear in the gonads.

Lymphocytes and active immunity develop at about 3 weeks post-fertilization in the interval between our sample (Lam et al., 2004). Lymphocytes and natural killer (NK) cell development in mouse and zebrafish require Ikaros (*ikzf1*), which is expressed early in the lymphocyte lineage (Winandy et al., 1995; Wang et al., 1996; Willett et al., 2001; Schorpp et al., 2006). Both sex genotypes and both ages expressed *ikzf1* in several clusters (Figure 10D). In lymphocytes, Rag1 and Rag2 help rearrange immunoglobulin genes and T-cell receptor genes; in NA gonads, *rag1* and *rag2* were expressed in 1930c27 (Figure 10E) even at 19dpf in both sex genotypes, identifying these cells as lymphoid. A few 1930c27 and adjacent 30dpf cells in 1930c2 expressed T-cell marker genes including *cd4-1* (Figure 10F), *cd8a, cd8b, zap70,* and *cd2*(*si:ch211-132g1*) (Blackburn et al., 2014; Moore et al., 2016b; Carmona et al., 2017; Shao et al., 2018). In NA gonads, the regulatory T-cell (Treg) gene *foxp3a* (Hui et al., 2017) was expressed in both ZW and ZZ gonads at 30dpf (Figure 10G), which contrasts to the testis-restricted expression of *foxp3a* in adult laboratory strain zebrafish (Li et al., 2020b)); this early *foxp3* expression in genetically female cells could explain why gonad function deteriorates in both ovary and testis in *foxp3a* mutants (Li et al., 2020b). Mixed with T-cells in 1930c2 and extending into 1930c13 were 30dpf cells expressing markers for some NK-like cells including *il2rb* (Carmona et al., 2017) (Figure 10H), suggesting that in NA zebrafish, as in mammals, gene expression in NK-like cells is similar to that in some T-cells (Bezman et al., 2012).

B-lymphocytes also appeared in both 19dpf and 30dpf gonads of both sexes in 1930c26 marked by both light and heavy immunoglobulin genes including *igl1c3* (Figure 10I), *igic1s1*, *igl3v5*, and *ighv1-4*, as well as the B-cell-specific transcription factor gene *pax5* (Cobaleda et al., 2007; Moore et al., 2016b). Cluster 1930c26 also expressed *cxcr4a,* encoding the receptor for the lymphocyte chemoattractant Cxcl12 (Bleul et al., 1996).

Myeloid cells include neutrophils, macrophages, monocytes, mast cells, eosinophils, and basophils (Wattrus and Zon, 2021). Early in myeloid development, zebrafish hematopoietic cells express *spi1a* and *spi1b* and these genes are required for macrophage specification (Bukrinsky et al., 2009; Roh-Johnson et al., 2017). NA gonads expressed *spi1a* in the 30dpf-specific cluster 1930c25 and the mixed-age clusters 1930c7, c9, and c28 (Figure 10J). Clusters 1930c7 and c9 expressed macrophage-specific genes like *mpeg1.1* and *mfap4.1*(*mfap4, zgc:77076*) (Figures 10K, L) and *marco*. Macrophages

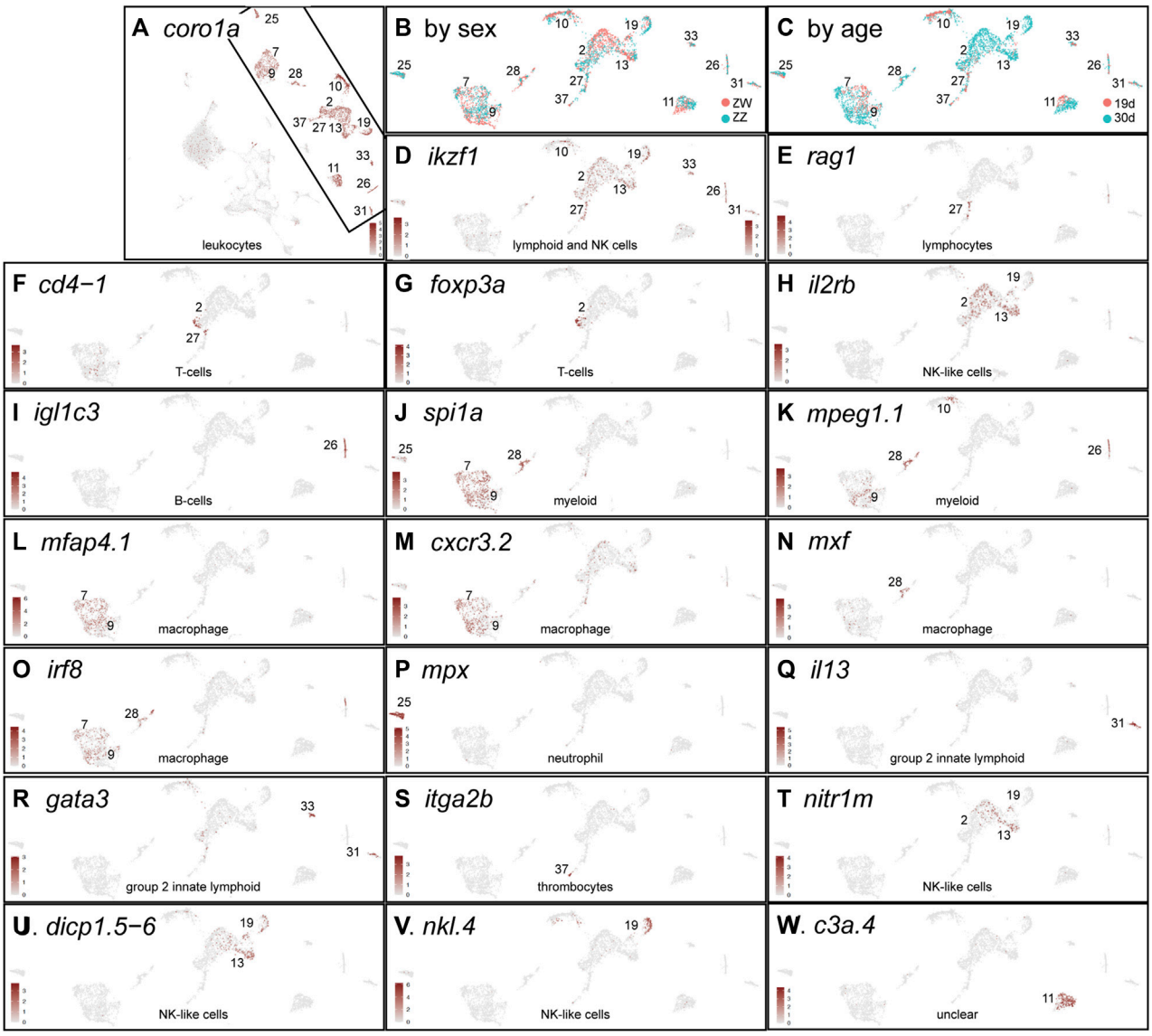

FIGURE 10
Immune cells. **(A)** *coro1a* expression identifying leukocytes displayed for all four conditions analyzed together. The remainder of the panels show the boxed region rotated counterclockwise. **(B)** Cells labeled according to sex genotype (red, ZW; blue, ZZ). **(C)** Cells labeled according to age (red, 19dpf; blue, 30dpf). **(D)** *ikzf1*. **(E)** *rag1*. **(F)** *cd4-1*. **(G)** *foxp3a*. **(H)** *il2rb*. **(I)** *igl1c3*. **(J)** *spi1a*. **(K)** *mpeg1.1*. **(L)** *mfap4.1*. **(M)** *cxcf3.2*. **(N)** *mxf*. **(O)** *irf8*. **(P)** *mpx*. **(Q)** *il13*. **(R)** *gata3*. **(S)** *itga2b*. **(T)** *nitr1m*. **(U)** *dicp1.5-6*. **(V)** *nkl.4*. **(W)** *c3a.4*.

in cluster 1930c7 and c9 were present in both sex genotypes. Macrophage migration during infection and injury in zebrafish depend on Cxcr3, but of the three *cxcr3* paralogs in zebrafish, only *cxcr3.2* is required (Sommer et al., 2020); for the gonad, this may be because *cxcr3.2* is the only one of the three paralogs expressed strongly in most 1930c7 and c9 macrophages (Figure 10M). Functionally different populations of macrophages have been identified in mammalian testes (DeFalco et al., 2015; Garcia-Alonso et al., 2022), but NA gonads did not appear to have macrophage sub-types expressing the relevant orthologs of the mammalian markers. Zebrafish gonads, however, do have multiple macrophage subtypes because 1930c28 represents a primarily 30dpf ZW population of *spi1*$^{+}$ *mpeg1.1*$^{+}$ cells that uniquely expressed *mxf* (Figure 10N) and other *myxovirus (influenza) resistance* paralogs, as well as the inflammation marker *tnfa*. Cells expressing the macrophage differentiation regulator *irf8* are present in 1930c7, c9, and c28 in both NA sex genotypes already by 19dpf (Figure 10O) and so macrophages are likely in place in NA to help remodel ovarian follicles as in laboratory strain zebrafish (Bravo et al., 2023).

Neutrophil-specific markers, including *mpx* (Figure 10P), *lyz*, and *mmp13a* were expressed strongly in 1930c25 in all four age/sex-genotype conditions. Other genes used as neutrophil markers, including *nccrp1, cebpa, cpa5, cma1, and prss1* (Tang et al., 2017; Rougeot et al., 2019), were expressed not only in 1930c25, but also strongly in several other clusters, decreasing their utility as neutrophil-specific markers in NA gonads.

Group 2 innate lymphoid cells (ILC2s, nuocytes, Th2 cells) in mammals help provide innate immunity against helminth infection and play a role in allergic airway hyperreactivity (Moro et al., 2010; Neill

et al., 2010; Barlow et al., 2012; Klein Wolterink et al., 2013). Key ILC2 genes include *IL4, IL5* (zebrafish ortholog: *csf2rb*), and *IL13* (Bottiglione et al., 2020). In zebrafish, *il4* and *il13* are essential to suppress type-1 immune responses (Bottiglione et al., 2020) and they were expressed specifically in 1930c31 (Figure 10Q). Gata3 is essential for normal expression of *IL3* and *CSF2R* (but not *IL4*) in ILC2 cells (Zhu et al., 2004), and *gata3* was expressed specifically in 1930c31 and c33 (Figure 10R). Genes strongly expressed in 1930c31 and c33 included *il11b, csf3a, gata3* and many genes annotated as 'serine-type endopeptidase activity' (including *si:dkey-78l4.2* and a dozen of its tandem duplicates), which are also strongly expressed in the 5dpf larval thymus (Farnsworth et al., 2019). We hypothesize that the ILC2-like cells in 1930c31 and c33 in zebrafish gonads may be acting to help regulate the extent of inflammation associated with developmental changes as gonads mature.

Thrombocytes appeared in 1930c37, which contained cells of both ages and sex genotypes, according to marker genes *itga2b(cd41)* (Figure 10S), *mpl, gp1bb, zfpm1* and *coagulation factor V* (*f5*) (Lin et al., 2005; Khandekar et al., 2012; Tang et al., 2017).

Natural killer (NK)-like cells may be a variant type of cytotoxic innate lymphoid cell. Zebrafish NK-like cells express NK markers like *il2rb* (Carmona et al., 2017) (Figure 10H). The 1930c2, c13, and c19 cells also expressed novel immune-type receptors (NITRs, e.g., *nitr1m*, Figure 10T) that have properties like those of mammalian natural killer receptors (NKRs) (Yoder et al., 2010). The *nitr* gene expression detected in the zebrafish ovary but not as maternal transcripts in oocytes (Yoder et al., 2010), could have been from the NK-like cells described here. Diverse immunoglobulin domain-containing protein (DICP) genes have been suggested to be associated with NK-like cells (Haire et al., 2012; Rodriguez-Nunez et al., 2016; Carmona et al., 2017) and the expression of *dicp* genes like *dicp1.5-6* (Figure 10U) in 1930c2, c13, and c19 supports this notion. The same cell set expresses NK-lysin genes: *nkl.4* expression, which is upregulated after viral infection (Pereiro et al., 2015) and increases ten-fold in *rag2*-deficient zebrafish (Moore et al., 2016a), was expressed specifically in NA gonads in 1930c19 (Figure 10V).

Cluster 1930c11 cells expressed the pan-leucocyte markers *coro1a, ptprc* (*cd45*), and *lcp1*, supporting a white blood cell identity (Figure 10A), but their specific cell type assignment is unclear. 1930c11 cells expressed many genes expressed almost exclusively in the thymus of 5dpf zebrafish (Farnsworth et al., 2019), including *c3a.4* (Figure 10W), *si:ch73-160i9.2, mfap4.9 (ENSDARG00000095746), si:dkey-203a12.7,* and *tuno4,2.* Cluster 1930c11 also expressed a number of *spink2* paralogs (*spink2.5, spink2.10, spink2.11*) that are expressed only in the zebrafish thymus at 5dpf (Farnsworth et al., 2019), while human *SPINK2* is proposed as a marker of hematopoietic stem cells (Calvanese et al., 2022). Nearly all 1930c11 genes were expressed in all four age/genotype conditions. We conclude that 1930c11 may represent an early-stage blood cell in gonads.

Conclusion

Strains of zebrafish long maintained in laboratories pass through a juvenile ovary phase in which all individuals initially form a gonad with oocytes that die in fish that become males but survive in individuals that become females (Takahashi, 1977; Uchida et al., 2002; Maack and Segner, 2003; Wang et al., 2007; Rodriguez-Mari et al., 2010). Those strains have what appears to be a polygenic sex determination mechanism (Bradley et al., 2011; Anderson et al., 2012; Howe et al., 2013; Wilson et al., 2014; Luzio et al., 2015). In contrast, in NA strain zebrafish, which have a ZW female/ZZ male chromosomal sex determination mechanism (Anderson et al., 2012; Wilson et al., 2014), ZZ individuals do not develop juvenile ovaries but instead directly develop testes (Figure 2). Although all NA strain ZW individuals initially form gonads with oocytes, some ZW fish lose these juvenile oocytes as their gonads become a testis, mimicking laboratory strains. Thus, the distinctive feature of the NA strain is the direct development of testis in ZZ fish, bypassing the juvenile ovary phase.

Because gonads in some individuals carrying the W allele initially develop oocytes that undergo apoptosis like gonads in AB and TU strains, and because oocytes do not develop in fish that lack the W chromosome, we suspect that these laboratory strains, which were cleaned of background lethal mutations by either gynogenesis or repeated inbreeding (Walker-Durchanek, 1980; Streisinger et al., 1981; Chakrabarti et al., 1983; Mullins et al., 1994), are likely chromosomally WW.

Direct testis development in ZZ NA fish raises the question of whether they transit a transcriptomic state shared with developing gonads in ZW genetic females or alternatively, if gonads in the two sex genotypes are transcriptionally different even at 19dpf when they are morphologically indistinguishable. Single-cell RNA-seq showed that at 19dpf, all clusters consisted of an intermixture of ZW and ZZ cells, but by 30dpf, sex-genotype-specific clusters had developed. The intermingling of ZW and ZZ cells in 19dpf clusters shows that at this stage, ZW and ZZ gonads in NA fish were not only morphologically similar, but also had not differentiated sex-specific cell types according to gene expression patterns in our experiments.

Despite the general bipotential nature of 19dpf NA ZW and ZZ gonads, germ cells in 19dpf ZW gonads were already expressing low levels of oocyte-specific genes, for example, eggshell (*zp*) genes, that ZZ germ cells did not express. This result suggests that ovary-specific functions had already begun in ZW, but not ZZ, fish by 19dpf. Whether those differences arise from primary differences in germ cells or subtle differences in support cells, steroidogenic cells, or stromal/interstitial cells is not yet known. The finding that 30dpf ZZ germ cells clustered with 19dpf ZZ germ cells, and that ZZ germ cells did not express spermatogenesis-specific genes, showed that ZZ germ cells generally postponed development until after 30dpf, in contrast to ZW germ cells, many of which showed oocyte-specific expression by 30dpf.

Like germ cells, ZW and ZZ support cells had very similar transcriptomes at 19dpf, but by 30dpf, ZW and ZZ support cells had differentiated into granulosa cells and Sertoli cells, respectively. The differentiated nature of the 30dpf ZZ Sertoli cells vs. the relatively undifferentiated state of the 30dpf ZZ germ cells suggests that in ZZ fish, support cell differentiation preceded germ cell differentiation.

Analysis of steroidogenic cells showed that genes encoding enzymes that catalyze the last two steps in estrogen biosynthesis are expressed in three different cell clusters: theca cells in 1930c12 expressing *cyp17a1* can produce androstenedione, which follicle cells in 1930c18 expressing *cyp19a1a* can convert to estrone, which granulosa cells in 1930c21 expressing *hsd17b1* can convert to estradiol. Whether the *cyp19a1a*-expressing cells and the *hsd17b1*-expressing cells are different states of the same cells, or alternatively, are totally different cells is unclear. The failure to find significant expression of the

testosterone-synthesizing enzyme gene *hsd17b3* in 30dpf NA gonads, mimicking findings with 40dpf AB ovaries (Liu et al., 2022), and the lack of sex tubercles at 30dpf (Dai et al., 2021b) raises the question of how or whether gonads at these stages produce testosterone.

Analysis of histological sections supported the notion that, in the four relatively natural zebrafish strains that had a ZW/ZZ *sar-4* chromosomal sex determination mechanism (Wilson et al., 2014), the W chromosome has a locus necessary, but not sufficient, for gonads to initiate oocyte development. An alternative hypothesis is that the Z chromosome has a locus that is required in two doses to prevent oocyte development. The location of the genetic sex determinant at the telomere and the enormous number of repetitive elements in the region led to a poor quality genome assembly in this region, which also lacks any of the 'usual suspects' for fish sex determination genes (e.g., Sox family, Dmrt1 variants, TGF-beta pathways) (Herpin and Schartl, 2015; Bertho et al., 2016). High quality PacBio genomic sequences from ZZ and WW individuals and detailed genetic analyses promise to lead to the molecular genetic identification of this elusive element.

Materials and methods

Fish husbandry

The NA wild-type strain (NA, ZFIN ID: ZDB-GENO-030115-2), originating from the Nadia region of India, has been raised at the University of Oregon zebrafish facility since 1999, and has been selected for maintenance of the Z chromosome since about 2012. For developmental histology, juveniles of one NA family were raised in embryo medium E2 (Westerfield, 1993) and fed paramecia from 4–10 days post-fertilization (dpf) and other families were raised in E5 and fed rotifers from 4 to 10dpf (Best et al., 2010), but results from both were comparable and were combined. After 10dpf, fish were moved to a circulating fish water system (Westerfield, 1993) and fed Zeigler Adult Zebrafish Diet. Procedures were approved by the University of Oregon IACUC protocol #18-13.

Genotyping

Animals were genotyped for Z and W chromosomes with PCR primers designed from RAD-tag sequences that contained a sex-linked marker from the published NA dataset (Fig. S1), using either the original published primer set (Wilson et al., 2014) or an improved primer set (F: CCGCGTTTATATCCTGGTAA and R: GTTGACCCAACTGGACTC TG), which amplified a 119-nucleotide (nt) fragment from NA genomic DNA. PCR conditions were: 6m 94°C; 45 cycles of 25s 94°C, 25s 61°C, 30s 72°C; followed by 10m at 72°C. The amplicon was digested with the restriction enzyme CviQI according to manufacturer's instructions (New England Biolabs). The enzyme digested the 119 nt amplicon from the Z allele to produce fragments of 43 and 76 nt, but left the W allele uncut.

Gonad histology

Fish were euthanized in ice water and the caudal fin was removed for genotyping. Fish trunks from the gills to the urogenital pore were fixed in Bouin's fixative (Sigma) for at least 48 h, then washed repeatedly with 70% ethanol. Fixed tissues were embedded in paraffin, sectioned at 7 microns, and stained with hematoxylin and eosin.

Single-cell RNA-Seq

Zebrafish were fin-clipped, genotyped for genetic sex, allowed to recover on the water system for a few days, and at 19 and 30 dpf, they were euthanized in ice water and gonads were dissected in chilled phosphate buffered saline (PBS) as described (Wang et al., 2017). Gonads from five fish per genotype were pooled in a well of a 24-well tissue culture plate and dissociated using a protocol adapted from (Covassin et al., 2006a). PBS was replaced with 1.2 mL of a solution containing 0.05% trypsin and 0.02% EDTA. Samples were incubated for 10 min at 28.5°C, pipetting up and down every 2 minutes with a 1000 µl pipette tip to manually break up tissues. Adding 200 µl of a solution containing 30% Fetal Bovine Serum and 6 mM $CaCl_2$ stopped digestion. Cells were transferred to a 1.5 mL microfuge tube and spun for 5 min at 2000 RPM (~300 RCF) at 4°C. The supernatant was removed, and cells were resuspended in a solution containing 1% fetal bovine serum, 0.8 mM CaCl2, and 1x antibiotic/antimycotic (Sigma #A5955) in L-15 medium. Cells were spun a second time for 5 min at 2,000 RPM at 4°C. The supernatant was removed, and cells were resuspended in the suspension solution, then filtered through a 40-micron strainer (Biologix #15-1040) to generate a suspension of single-cells. After microscopic visualization to check for dissociation, cells were counted with a Bio-RAD TC20 Automated Cell Counter and given to the University of Oregon Genomics and Cell Characterization Core Facility for library construction and sequencing. Libraries were prepared with Chromium v2 chemistry (10x Genomics) targeting 10,000 cells. According to manufacturer's instructions. Libraries were sequenced on an Illumina NextSeq 500.

Sequences were aligned to the zebrafish genome GRCZ11 using the Lawson zebrafish transcriptome annotation (Lawson et al., 2020) with Cell Ranger v. 6.1.1 (Zheng et al., 2017). Ambient RNA was removed with SoupX v 1.6.2 (Young and Behjati, 2020). For 19dpf individuals, ambient RNA derived from pancreas and erythrocytes, so we used the genes "hbaa1", "cpa5," "cpa1," "cel.2," "cel.1," "amy2a," "hbba1," "ela2l," "ela2," "prss1," "hbae5," and "prsS69.2" to estimate the contamination fraction. In 30dpf individuals, ambient RNA was derived from both erythrocytes and fragile oocytes, so we used the following genes to estimate the contamination fraction: "hbaa1," "hbaa2," "hbba2," "hbba1," "hbae5," "ddx4," "dnd1," "sycp1," "sycp3," and "dmc1." Data were analyzed with Seurat v. 4.2.0 (Butler et al., 2018). Non-gonad clusters, including contaminating pancreatic cells from dissection errors and erythrocytes, were excluded and gonad cells were reclustered. Differential expression analysis was performed on 19dpf clusters comparing ZZ vs. ZW genotypes using the Seurat "FindMarkers" function with the parameters min.pct = 0.05, logfc.threshold = 0.1, test.use = "MAST" (Finak et al., 2015).

Scope statement

Our manuscript "Direct Male Development in Chromosomally ZZ Zebrafish" by Wilson, Bazel, and Postlethwait is submitted to

Frontiers in Cell and Developmental Biology for the special volume entitled: *Proceedings of the ninth International Symposium on the Biology of Vertebrate Sex Determination 2023*. Our work uses histology and single-cell transcriptomics to probe the mechanisms of gonadal development in a zebrafish strain that maintains the chromosomal sex determination system found in the wild rather than in domesticated laboratory strains that lost the natural mechanism. Results show that gonads in chromosomally ZZ individuals develop directly into testes and avoid the juvenile ovary state found in gonads of all individuals in domesticated strains. Our scRNA-seq experiments revealed that gene expression in gonads at the histologically indifferent stage are highly similar in ZZ (all male) and ZW (mostly female) individuals. Eleven days later, however, when testes and ovaries are distinct morphologically, many transcriptional cell types are ZZ- or ZW-specific. This is the first work to identify genes that distinguish gonadal cell types at these early developmental states and the first to study gonad development in a zebrafish strain with the wild genetic sex determination system. This work is in the journal scope because it investigates "molecular and cellular reproduction" and "morphogenesis and patterning."

Data availability statement

The datasets presented in this study can be found in online repositories. The names of the repository/repositories and accession number(s) can be found in the article/Supplementary Material.

Ethics statement

The animal study was approved by the Institutional Animal Care and Use Committee, University of Oregon. The study was conducted in accordance with the local legislation and institutional requirements.

Author contributions

CW: Conceptualization, Formal Analysis, Investigation, Writing–original draft, Writing–review and editing, Data curation, Software. PB: Conceptualization, Data curation, Formal Analysis, Investigation, Software, Writing–review and editing. JP: Conceptualization, Formal Analysis, Investigation, Writing–review and editing, Funding acquisition, Project administration, Supervision, Writing–original draft.

Funding

The author(s) declare financial support was received for the research, authorship, and/or publication of this article. This work was funded by National Institutes of Health grant R35 GM139635.

Acknowledgments

This work benefited from access to the University of Oregon high performance computing cluster, Talapas, and the Zebrafish Information Network [(ZFIN) (RRID:SCR_002560)] and ENSEMBL Ensembl (RRID:SCR_002344) databases (Bradford et al., 2022; Martin et al., 2023).

In memoriam

We thank Ruth Bremiller (deceased), who published her first scientific paper in 1951 (White and Allen, 1951) and her 42d paper 71 years later in 2022 (Petersen et al., 2022), and Poh Kheng Loi for help with histology, and the U*niversity of Oregon's* Genomics and Cell Characterization Core *Facility* (GC3F) for library preparation and sequencing.

Conflict of interest

The authors declare that the research was conducted in the absence of any commercial or financial relationships that could be construed as a potential conflict of interest.

Publisher's note

Supplementary material

The Supplementary Material for this article can be found online at: https://www.frontiersin.org/articles/10.3389/fcell.2024.1362228/full#supplementary-material

SUPPLEMENTARY TABLE S1
Cell counts per genotype per cluster for the 19dpf single-cell dataset.

SUPPLEMENTARY TABLE S2
Cell type marker genes for 19dpf ZW and ZZ gonads.

SUPPLEMENTARY TABLE S3
Gene expression markers for 19dpf clusters. We required genes to be expressed in a minimum of 10% of cells and a minimum log fold change of 0.25.

SUPPLEMENTARY TABLE S4
Differential expression analysis comparing ZZ cells to ZW cells for each cluster at 19dpf.

SUPPLEMENTARY TABLE S5
Cell counts per genotype per cluster for the 30dpf single-cell dataset.

SUPPLEMENTARY TABLE S6
Gene expression markers for 30dpf clusters. We required genes to be expressed in a minimum of 10% of cells and a minimum log fold change of 0.25.

SUPPLEMENTARY TABLE S7
Cell counts per age per genotype per cluster for the combined 19dpf and 30dpf single-cell dataset.

SUPPLEMENTARY TABLE S8
Gene expression markers for combined 19dpf and 30dpf clusters. We required genes to be expressed in a minimum of 10% of cells and a minimum log fold change of 0.25.

SUPPLEMENTARY METHOD S1
R scripts utilizing Seurat to analyze 19dpf single-cell data.

SUPPLEMENTARY METHOD S2
R scripts utilizing Seurat to analyze 30dpf data.

SUPPLEMENTARY METHOD S3
R scripts utilizing Seurat to analyze combined single-cell data.

SUPPLEMENTARY METHOD S4
R scripts utilizing the SoupX package to remove ambient RNA.

References

Abozaid, H., Wessels, S., and Horstgen-Schwark, G. (2011). Effect of rearing temperatures during embryonic development on the phenotypic sex in zebrafish (*Danio rerio*). *Sex. Dev.* 5, 259–265. doi:10.1159/000330120

Aharon, D., and Marlow, F. L. (2021). Sexual determination in zebrafish. *Cell Mol. Life Sci.* 79, 8. doi:10.1007/s00018-021-04066-4

Amores, A., Force, A., Yan, Y. L., Joly, L., Amemiya, C., Fritz, A., et al. (1998). Zebrafish hox clusters and vertebrate genome evolution. *Science* 282, 1711–1714. doi:10.1126/science.282.5394.1711

Anderson, J. L., Rodriguez Mari, A., Braasch, I., Amores, A., Hohenlohe, P., Batzel, P., et al. (2012). Multiple sex-associated regions and a putative sex chromosome in zebrafish revealed by RAD mapping and population genomics. *PLoS One* 7, e40701. doi:10.1371/journal.pone.0040701

Aranguren, X. L., Beerens, M., Coppiello, G., Wiese, C., Vandersmissen, I., Lo Nigro, A., et al. (2013). COUP-TFII orchestrates venous and lymphatic endothelial identity by homo- or hetero-dimerisation with PROX1. *J. Cell Sci.* 126, 1164–1175. doi:10.1242/jcs.116293

Archambeault, D. R., and Yao, H. H. (2010). Activin A, a product of fetal Leydig cells, is a unique paracrine regulator of Sertoli cell proliferation and fetal testis cord expansion. *Proc. Natl. Acad. Sci. U. S. A.* 107, 10526–10531. doi:10.1073/pnas.1000318107

Bahary, N., Goishi, K., Stuckenholz, C., Weber, G., Leblanc, J., Schafer, C. A., et al. (2007). Duplicate VegfA genes and orthologues of the KDR receptor tyrosine kinase family mediate vascular development in the zebrafish. *Blood* 110, 3627–3636. doi:10.1182/blood-2006-04-016378

Barlow, J. L., Bellosi, A., Hardman, C. S., Drynan, L. F., Wong, S. H., Cruickshank, J. P., et al. (2012). Innate IL-13-producing nuocytes arise during allergic lung inflammation and contribute to airways hyperreactivity. *J. Allergy Clin. Immunol.* 129, 191–198. doi:10.1016/j.jaci.2011.09.041

Barrionuevo, F., Bagheri-Fam, S., Klattig, J., Kist, R., Taketo, M. M., Englert, C., et al. (2006). Homozygous inactivation of Sox9 causes complete XY sex reversal in mice. *Biol. Reprod.* 74, 195–201. doi:10.1095/biolreprod.105.045930

Basa, M., Vukovic, R., Sarajlija, A., Milenkovic, T., Djordjevic, M., Vucetic, B., et al. (2021). Ambiguous genitalia and lissencephaly in A 46,XY neonate with a novel variant of aristaless gene. *Acta Endocrinol. (Buchar)* 17, 402–405. doi:10.4183/aeb.2021.402

Bauer, M. P., Bridgham, J. T., Langenau, D. M., Johnson, A. L., and Goetz, F. W. (2000). Conservation of steroidogenic acute regulatory (StAR) protein structure and expression in vertebrates. *Mol. Cell Endocrinol.* 168, 119–125. doi:10.1016/s0303-7207(00)00316-6

Beer, R. L., and Draper, B. W. (2013). nanos3 maintains germline stem cells and expression of the conserved germline stem cell gene nanos2 in the zebrafish ovary. *Dev. Biol.* 374, 308–318. doi:10.1016/j.ydbio.2012.12.003

Bertho, S., Clapp, M., Banisch, T. U., Bandemer, J., Raz, E., and Marlow, F. L. (2021). Zebrafish dazl regulates cystogenesis and germline stem cell specification during the primordial germ cell to germline stem cell transition. *Development* 148, dev187773. doi:10.1242/dev.187773

Bertho, S., Pasquier, J., Pan, Q., Le Trionnaire, G., Bobe, J., Postlethwait, J. H., et al. (2016). Foxl2 and its relatives are evolutionary conserved players in gonadal sex differentiation. *Sex. Dev.* 10, 111–129. doi:10.1159/000447611

Best, J., Adatto, I., Cockington, J., James, A., and Lawrence, C. (2010). A novel method for rearing first-feeding larval zebrafish: polyculture with Type L saltwater rotifers (*Brachionus plicatilis*). *Zebrafish* 7, 289–295. doi:10.1089/zeb.2010.0667

Bezman, N. A., Kim, C. C., Sun, J. C., Min-Oo, G., Hendricks, D. W., Kamimura, Y., et al. (2012). Molecular definition of the identity and activation of natural killer cells. *Nat. Immunol.* 13, 1000–1009. doi:10.1038/ni.2395

Blackburn, J. S., Liu, S., Wilder, J. L., Dobrinski, K. P., Lobbardi, R., Moore, F. E., et al. (2014). Clonal evolution enhances leukemia-propagating cell frequency in T cell acute lymphoblastic leukemia through Akt/mTORC1 pathway activation. *Cancer Cell* 25, 366–378. doi:10.1016/j.ccr.2014.01.032

Bleul, C. C., Fuhlbrigge, R. C., Casasnovas, J. M., Aiuti, A., and Springer, T. A. (1996). A highly efficacious lymphocyte chemoattractant, stromal cell-derived factor 1 (SDF-1). *J. Exp. Med.* 184, 1101–1109. doi:10.1084/jem.184.3.1101

Blokhina, Y. P., Frees, M. A., Nguyen, A., Sharifi, M., Chu, D. B., Bispo, K., et al. (2021). Rad21l1 cohesin subunit is dispensable for spermatogenesis but not oogenesis in zebrafish. *PLoS Genet.* 17, e1009127. doi:10.1371/journal.pgen.1009127

Blokhina, Y. P., Nguyen, A. D., Draper, B. W., and Burgess, S. M. (2019). The telomere bouquet is a hub where meiotic double-strand breaks, synapsis, and stable homolog juxtaposition are coordinated in the zebrafish, *Danio rerio*. *PLoS Genet.* 15, e1007730. doi:10.1371/journal.pgen.1007730

Bogoch, Y., Jamieson-Lucy, A., Vejnar, C. E., Levy, K., Giraldez, A. J., Mullins, M. C., et al. (2022). Stage specific transcriptomic analysis and database for zebrafish oogenesis. *Front. Cell Dev. Biol.* 10, 826892. doi:10.3389/fcell.2022.826892

Bottiglione, F., Dee, C. T., Lea, R., Zeef, L. A. H., Badrock, A. P., Wane, M., et al. (2020). Zebrafish IL-4-like cytokines and IL-10 suppress inflammation but only IL-10 is essential for gill homeostasis. *J. Immunol.* 205, 994–1008. doi:10.4049/jimmunol.2000372

Bradford, Y. M., Toro, S., Ramachandran, S., Ruzicka, L., Howe, D. G., Eagle, A., et al. (2017). Zebrafish models of human disease: gaining insight into human disease at ZFIN. *ILAR J.* 58, 4–16. doi:10.1093/ilar/ilw040

Bradford, Y. M., Van Slyke, C. E., Ruzicka, L., Singer, A., Eagle, A., Fashena, D., et al. (2022). Zebrafish information network, the knowledgebase for *Danio rerio* research. *Genetics* 220, iyac016. doi:10.1093/genetics/iyac016

Bradley, K. M., Breyer, J. P., Melville, D. B., Broman, K. W., Knapik, E. W., and Smith, J. R. (2011). An SNP-based linkage map for zebrafish reveals sex determination loci. *G3 (Bethesda)* 1, 3–9. doi:10.1534/g3.111.000190

Bravo, P., Liu, Y., Draper, B. W., and Marlow, F. L. (2023). Macrophage activation drives ovarian failure and masculinization. *bioRxiv*, 2023.01.03.522645. doi:10.1101/2023.01.03.522645

Brennan, J., Karl, J., and Capel, B. (2002). Divergent vascular mechanisms downstream of Sry establish the arterial system in the XY gonad. *Dev. Biol.* 244, 418–428. doi:10.1006/dbio.2002.0578

Bukrinsky, A., Griffin, K. J., Zhao, Y., Lin, S., and Banerjee, U. (2009). Essential role of spi-1-like (spi-1l) in zebrafish myeloid cell differentiation. *Blood* 113, 2038–2046. doi:10.1182/blood-2008-06-162495

Butler, A., Hoffman, P., Smibert, P., Papalexi, E., and Satija, R. (2018). Integrating single-cell transcriptomic data across different conditions, technologies, and species. *Nat. Biotechnol.* 36, 411–420. doi:10.1038/nbt.4096

Cabrera-Quio, L. E., Schleiffer, A., Mechtler, K., and Pauli, A. (2021). Zebrafish Ski7 tunes RNA levels during the oocyte-to-embryo transition. *PLoS Genet.* 17, e1009390. doi:10.1371/journal.pgen.1009390

Calvanese, V., Capellera-Garcia, S., Ma, F., Fares, I., Liebscher, S., Ng, E. S., et al. (2022). Mapping human haematopoietic stem cells from haemogenic endothelium to birth. *Nature* 604, 534–540. doi:10.1038/s41586-022-04571-x

Can, H., Chanumolu, S. K., Gonzalez-Munoz, E., Prukudom, S., Otu, H. H., and Cibelli, J. B. (2020). Comparative analysis of single-cell transcriptomics in human and Zebrafish oocytes. *BMC Genomics* 21, 471. doi:10.1186/s12864-020-06860-z

Carmona, S. J., Teichmann, S. A., Ferreira, L., Macaulay, I. C., Stubbington, M. J., Cvejic, A., et al. (2017). Single-cell transcriptome analysis of fish immune cells provides insight into the evolution of vertebrate immune cell types. *Genome Res.* 27, 451–461. doi:10.1101/gr.207704.116

Caulier, M., Brion, F., Chadili, E., Turies, C., Piccini, B., Porcher, J. M., et al. (2015). Localization of steroidogenic enzymes and Foxl2a in the gonads of mature zebrafish (*Danio rerio*). *Comp. Biochem. Physiol. A Mol. Integr. Physiol.* 188, 96–106. doi:10.1016/j.cbpa.2015.06.016

Chakrabarti, S., Streisinger, G., Singer, F., and Walker, C. (1983). Frequency of gamma-ray induced specific locus and recessive lethal mutations in mature germ cells of the zebrafish, *Brachydanio rerio*. *Genetics* 103, 109–123. doi:10.1093/genetics/103.1.109

Chen, W., Tseng, X., Lin, G., Schreiner, A., Chen, H., Voigt, M. M., et al. (2013). The ortholog of LYVE-1 is required for thoracic duct formation in zebrafish. *CellBio* 2, 228–247. doi:10.4236/cellbio.2013.24026

Chen, W., Zhai, Y., Zhu, B., Wu, K., Fan, Y., Zhou, X., et al. (2022). Loss of growth differentiation factor 9 causes an arrest of early folliculogenesis in zebrafish – a novel insight into its action mechanism. *BioRxiv*. doi:10.1101/2022.07.01.498398

Chiang, E. F., Pai, C. I., Wyatt, M., Yan, Y. L., Postlethwait, J., and Chung, B. (2001a). Two sox9 genes on duplicated zebrafish chromosomes: expression of similar transcription activators in distinct sites. *Dev. Biol.* 231, 149–163. doi:10.1006/dbio.2000.0129

Chiang, E. F., Yan, Y. L., Guiguen, Y., Postlethwait, J., and Chung, B. (2001b). Two Cyp19 (P450 aromatase) genes on duplicated zebrafish chromosomes are expressed in ovary or brain. *Mol. Biol. Evol.* 18, 542–550. doi:10.1093/oxfordjournals.molbev.a003833

Chiang, E. F., Yan, Y. L., Tong, S. K., Hsiao, P. H., Guiguen, Y., Postlethwait, J., et al. (2001c). Characterization of duplicated zebrafish cyp19 genes. *J. Exp. Zool.* 290, 709–714. doi:10.1002/jez.1121

Ciruna, B., Weidinger, G., Knaut, H., Thisse, B., Thisse, C., Raz, E., et al. (2002). Production of maternal-zygotic mutant zebrafish by germ-line replacement. *Proc. Natl. Acad. Sci. U. S. A.* 99, 14919–14924. doi:10.1073/pnas.222459999

Cobaleda, C., Schebesta, A., Delogu, A., and Busslinger, M. (2007). Pax5: the guardian of B cell identity and function. *Nat. Immunol.* 8, 463–470. doi:10.1038/ni1454

Covassin, L. D., Villefranc, J. A., Kacergis, M. C., Weinstein, B. M., and Lawson, N. D. (2006b). Distinct genetic interactions between multiple Vegf receptors are required for development of different blood vessel types in zebrafish. *Proc. Natl. Acad. Sci. U. S. A.* 103, 6554–6559. doi:10.1073/pnas.0506886103

Covassin, L., Amigo, J. D., Suzuki, K., Teplyuk, V., Straubhaar, J., and Lawson, N. D. (2006a). Global analysis of hematopoietic and vascular endothelial gene expression by tissue specific microarray profiling in zebrafish. *Dev. Biol.* 299, 551–562. doi:10.1016/j.ydbio.2006.08.020

Crespo, B., Lan-Chow-Wing, O., Rocha, A., Zanuy, S., and Gomez, A. (2013). foxl2 and foxl3 are two ancient paralogs that remain fully functional in teleosts. *Gen. Comp. Endocrinol.* 194, 81–93. doi:10.1016/j.ygcen.2013.08.016

Crowder, C. M., Lassiter, C. S., and Gorelick, D. A. (2018). Nuclear androgen receptor regulates testes organization and oocyte maturation in zebrafish. *Endocrinology* 159, 980–993. doi:10.1210/en.2017-00617

Cui, X., Lu, Y. W., Lee, V., Kim, D., Dorsey, T., Wang, Q., et al. (2015). Venous endothelial marker COUP-tfii regulates the distinct pathologic potentials of adult arteries and veins. *Sci. Rep.* 5, 16193. doi:10.1038/srep16193

Cui, Z., Liu, Y., Wang, W., Wang, Q., Zhang, N., Lin, F., et al. (2017). Genome editing reveals dmrt1 as an essential male sex-determining gene in Chinese tongue sole (Cynoglossus semilaevis). *Sci. Rep.* 7, 42213. doi:10.1038/srep42213

Dai, S., Qi, S., Wei, X., Liu, X., Li, Y., Zhou, X., et al. (2021a). Germline sexual fate is determined by the antagonistic action of dmrt1 and foxl3/foxl2 in tilapia. *Development* 148, dev199380. doi:10.1242/dev.199380

Dai, X., Pu, D., Wang, L., Cheng, X., Liu, X., Yin, Z., et al. (2021b). Emergence of breeding tubercles and puberty onset in male zebrafish: evidence for a dependence on body growth. *J. Fish. Biol.* 99, 1071–1078. doi:10.1111/jfb.14811

Davis, R. B., Curtis, C. D., and Griffin, C. T. (2013). BRG1 promotes COUP-TFII expression and venous specification during embryonic vascular development. *Development* 140, 1272–1281. doi:10.1242/dev.087379

Defalco, T., Potter, S. J., Williams, A. V., Waller, B., Kan, M. J., and Capel, B. (2015). Macrophages contribute to the spermatogonial niche in the adult testis. *Cell Rep.* 12, 1107–1119. doi:10.1016/j.celrep.2015.07.015

Delomas, T. A., and Dabrowski, K. (2018). Effects of homozygosity on sex determination in zebrafish *Danio rerio*. *J. Fish. Biol.* 93, 1178–1187. doi:10.1111/jfb.13836

Devlin, R. H., and Nagahama, Y. (2002). Sex determination and sex differentiation in fish: an overview of genetic, physiological, and environmental influences. *Aquaculture* 208, 191–364. doi:10.1016/s0044-8486(02)00057-1

De Waal, P. P., Leal, M. C., Garcia-Lopez, A., Liarte, S., De Jonge, H., Hinfray, N., et al. (2009). Oestrogen-induced androgen insufficiency results in a reduction of proliferation and differentiation of spermatogonia in the zebrafish testis. *J. Endocrinol.* 202, 287–297. doi:10.1677/JOE-09-0050

De Waal, P. P., Wang, D. S., Nijenhuis, W. A., Schulz, R. W., and Bogerd, J. (2008). Functional characterization and expression analysis of the androgen receptor in zebrafish (*Danio rerio*) testis. *Reproduction* 136, 225–234. doi:10.1530/REP-08-0055

Dong, J., Albertini, D. F., Nishimori, K., Kumar, T. R., Lu, N., and Matzuk, M. M. (1996). Growth differentiation factor-9 is required during early ovarian folliculogenesis. *Nature* 383, 531–535. doi:10.1038/383531a0

Dranow, D. B., Hu, K., Bird, A. M., Lawry, S. T., Adams, M. T., Sanchez, A., et al. (2016). Bmp15 is an oocyte-produced signal required for maintenance of the adult female sexual phenotype in zebrafish. *PLoS Genet.* 12, e1006323. doi:10.1371/journal.pgen.1006323

Dranow, D. B., Tucker, R. P., and Draper, B. W. (2013). Germ cells are required to maintain a stable sexual phenotype in adult zebrafish. *Dev. Biol.* 376, 43–50. doi:10.1016/j.ydbio.2013.01.016

Fan, X., Bialecka, M., Moustakas, I., Lam, E., Torrens-Juaneda, V., Borggreven, N. V., et al. (2019). Single-cell reconstruction of follicular remodeling in the human adult ovary. *Nat. Commun.* 10, 3164. doi:10.1038/s41467-019-11036-9

Farnsworth, D. R., Saunders, L. M., and Miller, A. C. (2019). A single-cell transcriptome atlas for zebrafish development. *Dev. Biol.* 459, 100–108. doi:10.1016/j.ydbio.2019.11.008

Feitsma, H., Leal, M. C., Moens, P. B., Cuppen, E., and Schulz, R. W. (2007). Mlh1 deficiency in zebrafish results in male sterility and aneuploid as well as triploid progeny in females. *Genetics* 175, 1561–1569. doi:10.1534/genetics.106.068171

Field, S. L., Dasgupta, T., Cummings, M., and Orsi, N. M. (2014). Cytokines in ovarian folliculogenesis, oocyte maturation and luteinisation. *Mol. Reprod. Dev.* 81, 284–314. doi:10.1002/mrd.22285

Finak, G., Mcdavid, A., Yajima, M., Deng, J., Gersuk, V., Shalek, A. K., et al. (2015). MAST: a flexible statistical framework for assessing transcriptional changes and characterizing heterogeneity in single-cell RNA sequencing data. *Genome Biol.* 16, 278. doi:10.1186/s13059-015-0844-5

Francois, M., Caprini, A., Hosking, B., Orsenigo, F., Wilhelm, D., Browne, C., et al. (2008). Sox18 induces development of the lymphatic vasculature in mice. *Nature* 456, 643–647. doi:10.1038/nature07391

Fu, X. F., Cheng, S. F., Wang, L. Q., Yin, S., De Felici, M., and Shen, W. (2015). DAZ family proteins, key players for germ cell development. *Int. J. Biol. Sci.* 11, 1226–1235. doi:10.7150/ijbs.11536

Garcia-Alonso, L., Lorenzi, V., Mazzeo, C. I., Alves-Lopes, J. P., Roberts, K., Sancho-Serra, C., et al. (2022). Single-cell roadmap of human gonadal development. *Nature* 607, 540–547. doi:10.1038/s41586-022-04918-4

Gautier, A., Sohm, F., Joly, J. S., Le Gac, F., and Lareyre, J. J. (2011). The proximal promoter region of the zebrafish gsdf gene is sufficient to mimic the spatio-temporal expression pattern of the endogenous gene in Sertoli and granulosa cells. *Biol. Reprod.* 85, 1240–1251. doi:10.1095/biolreprod.111.091892

Gilchrist, R. B., Lane, M., and Thompson, J. G. (2008). Oocyte-secreted factors: regulators of cumulus cell function and oocyte quality. *Hum. Reprod. Update* 14, 159–177. doi:10.1093/humupd/dmm040

Ginsburger-Vogel, T. (1972). Inversion desfemelles d'Orchestiagammarella Pallqs (Crustacés Amphipodes Talitridaé) en néo-mâles fonctionnelspar greffe de glandes androgènes avant la mue de première différenciation externe du sexe. *C R. Acad. Hebd. Seances Acad. Sci. D.* 274, 3606–3609.

Goldstone, J. V., Mcarthur, A. G., Kubota, A., Zanette, J., Parente, T., Jonsson, M. E., et al. (2010). Identification and developmental expression of the full complement of Cytochrome P450 genes in Zebrafish. *BMC Genomics* 11, 643. doi:10.1186/1471-2164-11-643

Gomez, G. A., Veldman, M. B., Zhao, Y., Burgess, S., and Lin, S. (2009). Discovery and characterization of novel vascular and hematopoietic genes downstream of etsrp in zebrafish. *PLoS One* 4, e4994. doi:10.1371/journal.pone.0004994

Grompe, M., and D'Andrea, A. (2001). Fanconi anemia and DNA repair. *Hum. Mol. Genet.* 10, 2253–2259. doi:10.1093/hmg/10.20.2253

Guo, Y., Cheng, H., Huang, X., Gao, S., Yu, H., and Zhou, R. (2005). Gene structure, multiple alternative splicing, and expression in gonads of zebrafish Dmrt1. *Biochem. Biophys. Res. Commun.* 330, 950–957. doi:10.1016/j.bbrc.2005.03.066

Gupta, B., Ramteke, P., Paul, V. K., Kumar, T., and Das, P. (2019). Ambiguous genitalia associated with an extremely rare syndrome: a case report of xlag syndrome and review of the literature. *Turk Patoloji Derg.* 35, 162–165. doi:10.5146/tjpath.2017.01391

Gurung, S., Restrepo, N. K., Chestnut, B., Klimkaite, L., and Sumanas, S. (2022). Single-cell transcriptomic analysis of vascular endothelial cells in zebrafish embryos. *Sci. Rep.* 12, 13065. doi:10.1038/s41598-022-17127-w

Haire, R. N., Cannon, J. P., O'Driscoll, M. L., Ostrov, D. A., Mueller, M. G., Turner, P. M., et al. (2012). Genomic and functional characterization of the diverse immunoglobulin domain-containing protein (DICP) family. *Genomics* 99, 282–291. doi:10.1016/j.ygeno.2012.02.004

Hamer, G., Roepers-Gajadien, H. L., Van Duyn-Goedhart, A., Gademan, I. S., Kal, H. B., Van Buul, P. P., et al. (2003). DNA double-strand breaks and gamma-H2AX signaling in the testis. *Biol. Reprod.* 68, 628–634. doi:10.1095/biolreprod.102.008672

Hanley, N. A., Ball, S. G., Clement-Jones, M., Hagan, D. M., Strachan, T., Lindsay, S., et al. (1999). Expression of steroidogenic factor 1 and Wilms' tumour 1 during early human gonadal development and sex determination. *Mech. Dev.* 87, 175–180. doi:10.1016/s0925-4773(99)00123-9

Hartung, O., Forbes, M. M., and Marlow, F. L. (2014). Zebrafish vasa is required for germ-cell differentiation and maintenance. *Mol. Reprod. Dev.* 81, 946–961. doi:10.1002/mrd.22414

Hattori, R. S., Murai, Y., Oura, M., Masuda, S., Majhi, S. K., Sakamoto, T., et al. (2012). A Y-linked anti-Mullerian hormone duplication takes over a critical role in sex determination. *Proc. Natl. Acad. Sci. U. S. A.* 109, 2955–2959. doi:10.1073/pnas.1018392109

Herpin, A., Braasch, I., Kraeussling, M., Schmidt, C., Thoma, E. C., Nakamura, S., et al. (2010). Transcriptional rewiring of the sex determining dmrt1 gene duplicate by transposable elements. *PLoS Genet.* 6, e1000844. doi:10.1371/journal.pgen.1000844

Herpin, A., and Schartl, M. (2015). Plasticity of gene-regulatory networks controlling sex determination: of masters, slaves, usual suspects, newcomers, and usurpators. *EMBO Rep.* 16, 1260–1274. doi:10.15252/embr.201540667

Herpin, A., Schartl, M., Depince, A., Guiguen, Y., Bobe, J., Hua-Van, A., et al. (2021). Allelic diversification after transposable element exaptation promoted *gsdf* as the master

sex determining gene of sablefish. *Genome Res.* 31, 1366–1380. doi:10.1101/gr.274266.120

Hiramatsu, N., Luo, W., Reading, B. J., Sullivan, C. V., Mizuta, H., Ryu, Y. W., et al. (2013). Multiple ovarian lipoprotein receptors in teleosts. *Fish Physiology Biochem.* 39, 29–32. doi:10.1007/s10695-012-9612-6

Hong, N., Li, M., Yuan, Y., Wang, T., Yi, M., Xu, H., et al. (2016). Dnd is a critical specifier of primordial germ cells in the medaka fish. *Stem Cell Rep.* 6, 411–421. doi:10.1016/j.stemcr.2016.01.002

Houwing, S., Berezikov, E., and Ketting, R. F. (2008). Zili is required for germ cell differentiation and meiosis in zebrafish. *EMBO J.* 27, 2702–2711. doi:10.1038/emboj.2008.204

Howe, K., Clark, M. D., Torroja, C. F., Torrance, J., Berthelot, C., Muffato, M., et al. (2013). The zebrafish reference genome sequence and its relationship to the human genome. *Nature* 496, 498–503. doi:10.1038/nature12111

Howley, C., and Ho, R. K. (2000). mRNA localization patterns in zebrafish oocytes. *Mech. Dev.* 92, 305–309. doi:10.1016/s0925-4773(00)00247-1

Hsu, C. W., and Chung, B. C. (2021). Evolution, expression, and function of gonadal somatic cell-derived factor. *Front. Cell Dev. Biol.* 9, 684352. doi:10.3389/fcell.2021.684352

Hsu, H. J., Hsiao, P., Kuo, M. W., and Chung, B. C. (2002). Expression of zebrafish cyp11a1 as a maternal transcript and in yolk syncytial layer. *Gene Expr. Patterns* 2, 219–222. doi:10.1016/s1567-133x(02)00059-5

Hu, M. C., Chiang, E. F., Tong, S. K., Lai, W., Hsu, N. C., Wang, L. C., et al. (2001). Regulation of steroidogenesis in transgenic mice and zebrafish. *Mol. Cell Endocrinol.* 171, 9–14. doi:10.1016/s0303-7207(00)00385-3

Hui, S. P., Sheng, D. Z., Sugimoto, K., Gonzalez-Rajal, A., Nakagawa, S., Hesselson, D., et al. (2017). Zebrafish regulatory T cells mediate organ-specific regenerative programs. *Dev. Cell* 43, 659–672. doi:10.1016/j.devcel.2017.11.010

Hunter, N. (2015). Meiotic recombination: the essence of heredity. *Cold Spring Harb. Perspect. Biol.* 7, a016618. doi:10.1101/cshperspect.a016618

Ieda, R., Hosoya, S., Tajima, S., Atsumi, K., Kamiya, T., Nozawa, A., et al. (2018). Identification of the sex-determining locus in grass puffer (*Takifugu niphobles*) provides evidence for sex-chromosome turnover in a subset of Takifugu species. *PLoS One* 13, e0190635. doi:10.1371/journal.pone.0190635

Ikeda, Y., Swain, A., Weber, T. J., Hentges, K. E., Zanaria, E., Lalli, E., et al. (1996). Steroidogenic factor 1 and Dax-1 colocalize in multiple cell lineages: potential links in endocrine development. *Mol. Endocrinol.* 10, 1261–1272. doi:10.1210/mend.10.10.9121493

Ilicic, T., Kim, J. K., Kolodziejczyk, A. A., Bagger, F. O., Mccarthy, D. J., Marioni, J. C., et al. (2016). Classification of low quality cells from single-cell RNA-seq data. *Genome Biol.* 17, 29. doi:10.1186/s13059-016-0888-1

Imai, T., Saino, K., and Matsuda, M. (2015). Mutation of Gonadal soma-derived factor induces medaka XY gonads to undergo ovarian development. *Biochem. Biophys. Res. Commun.* 467, 109–114. doi:10.1016/j.bbrc.2015.09.112

Imai, Y., Olaya, I., Sakai, N., and Burgess, S. M. (2021). Meiotic chromosome dynamics in zebrafish. *Front. Cell Dev. Biol.* 9, 757445. doi:10.3389/fcell.2021.757445

Ings, J. S., and Van Der Kraak, G. J. (2006). Characterization of the mRNA expression of StAR and steroidogenic enzymes in zebrafish ovarian follicles. *Mol. Reprod. Dev.* 73, 943–954. doi:10.1002/mrd.20490

Ioannidis, J., Taylor, G., Zhao, D., Liu, L., Idoko-Akoh, A., Gong, D., et al. (2021). Primary sex determination in birds depends on DMRT1 dosage, but gonadal sex does not determine adult secondary sex characteristics. *Proc. Natl. Acad. Sci. U. S. A.* 118, e2020909118. doi:10.1073/pnas.2020909118

Islam, K. N., Modi, M. M., and Siegfried, K. R. (2021). The zebrafish meiotic cohesin complex protein Smc1b is required for key events in meiotic prophase I. *Front. Cell Dev. Biol.* 9, 714245. doi:10.3389/fcell.2021.714245

Jackson, D. G., Prevo, R., Clasper, S., and Banerji, S. (2001). LYVE-1, the lymphatic system and tumor lymphangiogenesis. *Trends Immunol.* 22, 317–321. doi:10.1016/s1471-4906(01)01936-6

Jaillon, O., Aury, J. M., Brunet, F., Petit, J. L., Stange-Thomann, N., Mauceli, E., et al. (2004). Genome duplication in the teleost fish *Tetraodon nigroviridis* reveals the early vertebrate proto-karyotype. *Nature* 431, 946–957. doi:10.1038/nature03025

Jamieson-Lucy, A. H., Kobayashi, M., James Aykit, Y., Elkouby, Y. M., Escobar-Aguirre, M., Vejnar, C. E., et al. (2022). A proteomics approach identifies novel resident zebrafish Balbiani body proteins Cirbpa and Cirbpb. *Dev. Biol.* 484, 1–11. doi:10.1016/j.ydbio.2022.01.006

Janes, D. E., Organ, C. L., Stiglec, R., O'Meally, D., Sarre, S. D., Georges, A., et al. (2014). Molecular evolution of Dmrt1 accompanies change of sex-determining mechanisms in reptilia. *Biol. Lett.* 10, 20140809. doi:10.1098/rsbl.2014.0809

Jiang, D. N., Peng, Y. X., Liu, X. Y., Mustapha, U. F., Huang, Y. Q., Shi, H. J., et al. (2022). Homozygous mutation of gsdf causes infertility in female nile Tilapia (*Oreochromis niloticus*). *Front. Endocrinol. (Lausanne)* 13, 813320. doi:10.3389/fendo.2022.813320

Kaipainen, A., Korhonen, J., Mustonen, T., Van Hinsbergh, V. W., Fang, G. H., Dumont, D., et al. (1995). Expression of the fms-like tyrosine kinase 4 gene becomes restricted to lymphatic endothelium during development. *Proc. Natl. Acad. Sci. U. S. A.* 92, 3566–3570. doi:10.1073/pnas.92.8.3566

Kamiya, T., Kai, W., Tasumi, S., Oka, A., Matsunaga, T., Mizuno, N., et al. (2012). A trans-species missense SNP in Amhr2 is associated with sex determination in the tiger pufferfish, *Takifugu rubripes* (fugu). *PLoS Genet.* 8, e1002798. doi:10.1371/journal.pgen.1002798

Keeney, S. (2008). Spo11 and the formation of DNA double-strand breaks in meiosis. *Genome Dyn. Stab.* 2, 81–123. doi:10.1007/7050_2007_026

Khandekar, G., Kim, S., and Jagadeeswaran, P. (2012). Zebrafish thrombocytes: functions and origins. *Adv. Hematol.* 2012, 857058. doi:10.1155/2012/857058

Kikuchi, M., Nishimura, T., Ishishita, S., Matsuda, Y., and Tanaka, M. (2020). foxl3, a sexual switch in germ cells, initiates two independent molecular pathways for commitment to oogenesis in medaka. *Proc. Natl. Acad. Sci. U. S. A.* 117, 12174–12181. doi:10.1073/pnas.1918556117

Kim, S., Bardwell, V. J., and Zarkower, D. (2007). Cell type-autonomous and non-autonomous requirements for Dmrt1 in postnatal testis differentiation. *Dev. Biol.* 307, 314–327. doi:10.1016/j.ydbio.2007.04.046

Kinnear, H. M., Tomaszewski, C. E., Chang, F. L., Moravek, M. B., Xu, M., Padmanabhan, V., et al. (2020). The ovarian stroma as a new frontier. *Reproduction* 160, R25–R39. doi:10.1530/REP-19-0501

Klein Wolterink, R. G., Serafini, N., Van Nimwegen, M., Vosshenrich, C. A., De Bruijn, M. J., Fonseca Pereira, D., et al. (2013). Essential, dose-dependent role for the transcription factor Gata3 in the development of IL-5+ and IL-13+ type 2 innate lymphoid cells. *Proc. Natl. Acad. Sci. U. S. A.* 110, 10240–10245. doi:10.1073/pnas.1217158110

Kobayashi, T., Matsuda, M., Kajiura-Kobayashi, H., Suzuki, A., Saito, N., Nakamoto, M., et al. (2004). Two DM domain genes, DMY and DMRT1, involved in testicular differentiation and development in the medaka, *Oryzias latipes*. *Dev. Dyn.* 231, 518–526. doi:10.1002/dvdy.20158

Kopp, A. (2012). Dmrt genes in the development and evolution of sexual dimorphism. *Trends Genet.* 28, 175–184. doi:10.1016/j.tig.2012.02.002

Kossack, M. E., and Draper, B. W. (2019). Genetic regulation of sex determination and maintenance in zebrafish (*Danio rerio*). *Curr. Top. Dev. Biol.* 134, 119–149. doi:10.1016/bs.ctdb.2019.02.004

Kossack, M. E., Tian, L., Bowie, K., and Plavicki, J. S. (2023). More than germ cells: vascular development in the early zebrafish 1 (*Danio rerio*) gonad. *bioRxiv*, 2023.01.18.524593. doi:10.1101/2023.01.18.524593

Koyama, T., Nakamoto, M., Morishima, K., Yamashita, R., Yamashita, T., Sasaki, K., et al. (2019). A SNP in a steroidogenic enzyme is associated with phenotypic sex in Seriola fishes. *Curr. Biol.* 29, 1901–1909. doi:10.1016/j.cub.2019.04.069

Krovel, A. V., and Olsen, L. C. (2004). Sexual dimorphic expression pattern of a splice variant of zebrafish vasa during gonadal development. *Dev. Biol.* 271, 190–197. doi:10.1016/j.ydbio.2004.04.004

Kuo, M. W., Postlethwait, J., Lee, W. C., Lou, S. W., Chan, W. K., and Chung, B. C. (2005). Gene duplication, gene loss and evolution of expression domains in the vertebrate nuclear receptor NR5A (Ftz-F1) family. *Biochem. J.* 389, 19–26. doi:10.1042/BJ20050005

Kusakabe, M., Nakamura, I., and Young, G. (2003). 11beta-hydroxysteroid dehydrogenase complementary deoxyribonucleic acid in rainbow trout: cloning, sites of expression, and seasonal changes in gonads. *Endocrinology* 144, 2534–2545. doi:10.1210/en.2002-220446

Lai, W. W., Hsiao, P. H., Guiguen, Y., and Chung, B. C. (1998). Cloning of zebrafish cDNA for 3beta-hydroxysteroid dehydrogenase and P450scc. *Endocr. Res.* 24, 927–931. doi:10.3109/07435809809032708

Lam, S. H., Chua, H. L., Gong, Z., Lam, T. J., and Sin, Y. M. (2004). Development and maturation of the immune system in zebrafish, *Danio rerio*: a gene expression profiling, *in situ* hybridization and immunological study. *Dev. Comp. Immunol.* 28, 9–28. doi:10.1016/s0145-305x(03)00103-4

Lau, E. S., Zhang, Z., Qin, M., and Ge, W. (2016). Knockout of zebrafish ovarian aromatase gene (cyp19a1a) by TALEN and CRISPR/Cas9 leads to all-male offspring due to failed ovarian differentiation. *Sci. Rep.* 6, 37357. doi:10.1038/srep37357

Lawrence, C., Ebersole, J. P., and Kesseli, R. V. (2008). Rapid growth and out-crossing promote female development in zebrafish (*Danio rerio*). *Environ. Biol. Fishes* 81, 239–246. doi:10.1007/s10641-007-9195-8

Lawson, N. D., Li, R., Shin, M., Grosse, A., Yukselen, O., Stone, O. A., et al. (2020). An improved zebrafish transcriptome annotation for sensitive and comprehensive detection of cell type-specific genes. *Elife* 9, e55792. doi:10.7554/eLife.55792

Leal, M. C., Feitsma, H., Cuppen, E., Franca, L. R., and Schulz, R. W. (2008). Completion of meiosis in male zebrafish (*Danio rerio*) despite lack of DNA mismatch repair gene mlh1. *Cell Tissue Res.* 332, 133–139. doi:10.1007/s00441-007-0550-z

Lee, S., Kang, J., Yoo, J., Ganesan, S. K., Cook, S. C., Aguilar, B., et al. (2009). Prox1 physically and functionally interacts with COUP-TFII to specify lymphatic endothelial cell fate. *Blood* 113, 1856–1859. doi:10.1182/blood-2008-03-145789

Liew, W. C., and Orban, L. (2014). Zebrafish sex: a complicated affair. *Brief. Funct. Genomics* 13, 172–187. doi:10.1093/bfgp/elt041

Li, M., Sun, Y., Zhao, J., Shi, H., Zeng, S., Ye, K., et al. (2015). A tandem duplicate of anti-mullerian hormone with a missense SNP on the Y chromosome is essential for male sex determination in nile Tilapia, *Oreochromis niloticus*. *PLoS Genet.* 11, e1005678. doi:10.1371/journal.pgen.1005678

Lin, H. F., Traver, D., Zhu, H., Dooley, K., Paw, B. H., Zon, L. I., et al. (2005). Analysis of thrombocyte development in CD41-GFP transgenic zebrafish. *Blood* 106, 3803–3810. doi:10.1182/blood-2005-01-0179

Lin, J. C., Hu, S., Ho, P. H., Hsu, H. J., Postlethwait, J. H., and Chung, B. C. (2015). Two zebrafish hsd3b genes are distinct in function, expression, and evolution. *Endocrinology* 156, 2854–2862. doi:10.1210/en.2014-1584

Li, N., Oakes, J. A., Storbeck, K. H., Cunliffe, V. T., and Krone, N. P. (2020a). The P450 side-chain cleavage enzyme Cyp11a2 facilitates steroidogenesis in zebrafish. *J. Endocrinol.* 244, 309–321. doi:10.1530/JOE-19-0384

Lin, Q., Mei, J., Li, Z., Zhang, X., Zhou, L., and Gui, J. F. (2017). Distinct and cooperative roles of *amh* and *dmrt1* in self-renewal and differentiation of male germ cells in zebrafish. *Genetics* 207, 1007–1022. doi:10.1534/genetics.117.300274

Liu, Y., Kossack, M. E., Mcfaul, M. E., Christensen, L. N., Siebert, S., Wyatt, S. R., et al. (2022). Single-cell transcriptome reveals insights into the development and function of the zebrafish ovary. *Elife* 11, e76014. doi:10.7554/eLife.76014

Li, X., Zhang, F., Wu, N., Ye, D., Wang, Y., Zhang, X., et al. (2020b). A critical role of *foxp3a*-positive regulatory T cells in maintaining immune homeostasis in zebrafish testis development. *J. Genet. Genomics* 47, 547–561. doi:10.1016/j.jgg.2020.07.006

Lu, H., Cui, Y., Jiang, L., and Ge, W. (2017). Functional analysis of nuclear estrogen receptors in zebrafish reproduction by genome editing approach. *Endocrinology* 158, 2292–2308. doi:10.1210/en.2017-00215

Lu, H., Zhao, C., Zhu, B., Zhang, Z., and Ge, W. (2020). Loss of inhibin advances follicle activation and female puberty onset but blocks oocyte maturation in zebrafish. *Endocrinology* 161, bqaa184. doi:10.1210/endocr/bqaa184

Luzio, A., Coimbra, A. M., Benito, C., Fontainhas-Fernandes, A. A., and Matos, M. (2015). Screening and identification of potential sex-associated sequences in *Danio rerio*. *Mol. Reprod. Dev.* 82, 756–764. doi:10.1002/mrd.22508

Luzio, A., Matos, M., Santos, D., Fontainhas-Fernandes, A. A., Monteiro, S. M., and Coimbra, A. M. (2016). Disruption of apoptosis pathways involved in zebrafish gonad differentiation by 17α-ethinylestradiol and fadrozole exposures. *Aquat. Toxicol.* 177, 269–284. doi:10.1016/j.aquatox.2016.05.029

Maack, G., and Segner, H. (2003). Morphological development of the gonads in zebrafish. *J. Fish Biol.* 62, 895–906. doi:10.1046/j.1095-8649.2003.00074.x

Maegawa, S., Yasuda, K., and Inoue, K. (1999). Maternal mRNA localization of zebrafish DAZ-like gene. *Mech. Dev.* 81, 223–226. doi:10.1016/s0925-4773(98)00242-1

Maekawa, M., Kamimura, K., and Nagano, T. (1996). Peritubular myoid cells in the testis: their structure and function. *Arch. Histol. Cytol.* 59, 1–13. doi:10.1679/aohc.59.1

Marlow, F. L., and Mullins, M. C. (2008). Bucky ball functions in Balbiani body assembly and animal-vegetal polarity in the oocyte and follicle cell layer in zebrafish. *Dev. Biol.* 321, 40–50. doi:10.1016/j.ydbio.2008.05.557

Martin, F. J., Amode, M. R., Aneja, A., Austine-Orimoloye, O., Azov, A. G., Barnes, I., et al. (2023). Ensembl 2023. *Nucleic Acids Res.* 51, D933–D941. doi:10.1093/nar/gkac958

Masumura, T., Yamamoto, K., Shimizu, N., Obi, S., and Ando, J. (2009). Shear stress increases expression of the arterial endothelial marker ephrinB2 in murine ES cells via the VEGF-Notch signaling pathways. *Arterioscler. Thromb. Vasc. Biol.* 29, 2125–2131. doi:10.1161/ATVBAHA.109.193185

Matson, C. K., Murphy, M. W., Griswold, M. D., Yoshida, S., Bardwell, V. J., and Zarkower, D. (2010). The mammalian doublesex homolog DMRT1 is a transcriptional gatekeeper that controls the mitosis versus meiosis decision in male germ cells. *Dev. Cell* 19, 612–624. doi:10.1016/j.devcel.2010.09.010

Matsuda, M., and Sakaizumi, M. (2016). Evolution of the sex-determining gene in the teleostean genus Oryzias. *Gen. Comp. Endocrinol.* 239, 80–88. doi:10.1016/j.ygcen.2015.10.004

Mazaud, S., Oreal, E., Guigon, C. J., Carre-Eusebe, D., and Magre, S. (2002). Lhx9 expression during gonadal morphogenesis as related to the state of cell differentiation. *Gene Expr. Patterns* 2, 373–377. doi:10.1016/s1567-133x(02)00050-9

Mcclelland, K. S., Bell, K., Larney, C., Harley, V. R., Sinclair, A. H., Oshlack, A., et al. (2015). Purification and transcriptomic analysis of mouse fetal Leydig cells reveals candidate genes for specification of gonadal steroidogenic cells. *Biol. Reprod.* 92, 145. doi:10.1095/biolreprod.115.128918

Mcmillan, S. C., Xu, Z. T., Zhang, J., Teh, C., Korzh, V., Trudeau, V. L., et al. (2013). Regeneration of breeding tubercles on zebrafish pectoral fins requires androgens and two waves of revascularization. *Development* 140, 4323–4334. doi:10.1242/dev.095992

Menuet, A., Le Page, Y., Torres, O., Kern, L., Kah, O., and Pakdel, F. (2004). Analysis of the estrogen regulation of the zebrafish estrogen receptor (ER) reveals distinct effects of ERalpha, ERbeta1 and ERbeta2. *J. Mol. Endocrinol.* 32, 975–986. doi:10.1677/jme.0.0320975

Miao, L., Yuan, Y., Cheng, F., Fang, J., Zhou, F., Ma, W., et al. (2017). Translation repression by maternal RNA binding protein Zar1 is essential for early oogenesis in zebrafish. *Development* 144, 128–138. doi:10.1242/dev.144642

Miller, W. L., and Auchus, R. J. (2011). The molecular biology, biochemistry, and physiology of human steroidogenesis and its disorders. *Endocr. Rev.* 32, 81–151. doi:10.1210/er.2010-0013

Mindnich, R., Deluca, D., and Adamski, J. (2004). Identification and characterization of 17 beta-hydroxysteroid dehydrogenases in the zebrafish, *Danio rerio*. *Mol. Cell Endocrinol.* 215, 19–30. doi:10.1016/j.mce.2003.11.010

Mindnich, R., Haller, F., Halbach, F., Moeller, G., Hrabe De Angelis, M., and Adamski, J. (2005). Androgen metabolism via 17beta-hydroxysteroid dehydrogenase type 3 in mammalian and non-mammalian vertebrates: comparison of the human and the zebrafish enzyme. *J. Mol. Endocrinol.* 35, 305–316. doi:10.1677/jme.1.01853

Miyabayashi, K., Katoh-Fukui, Y., Ogawa, H., Baba, T., Shima, Y., Sugiyama, N., et al. (2013). Aristaless related homeobox gene, Arx, is implicated in mouse fetal Leydig cell differentiation possibly through expressing in the progenitor cells. *PLoS One* 8, e68050. doi:10.1371/journal.pone.0068050

Model, L. S., Hall, M. R., Wong, D. J., Muto, A., Kondo, Y., Ziegler, K. R., et al. (2014). Arterial shear stress reduces eph-b4 expression in adult human veins. *Yale J. Biol. Med.* 87, 359–371.

Moore, F. E., Garcia, E. G., Lobbardi, R., Jain, E., Tang, Q., Moore, J. C., et al. (2016a). Single-cell transcriptional analysis of normal, aberrant, and malignant hematopoiesis in zebrafish. *J. Exp. Med.* 213, 979–992. doi:10.1084/jem.20152013

Moore, J. C., Mulligan, T. S., Yordan, N. T., Castranova, D., Pham, V. N., Tang, Q., et al. (2016b). T cell immune deficiency in *zap70* mutant zebrafish. *Mol. Cell Biol.* 36, 2868–2876. doi:10.1128/MCB.00281-16

Morais Da Silva, S., Hacker, A., Harley, V., Goodfellow, P., Swain, A., and Lovell-Badge, R. (1996). Sox9 expression during gonadal development implies a conserved role for the gene in testis differentiation in mammals and birds. *Nat. Genet.* 14, 62–68. doi:10.1038/ng0996-62

Morinaga, C., Saito, D., Nakamura, S., Sasaki, T., Asakawa, S., Shimizu, N., et al. (2007). The *hotei* mutation of medaka in the anti-Mullerian hormone receptor causes the dysregulation of germ cell and sexual development. *Proc. Natl. Acad. Sci. U. S. A.* 104, 9691–9696. doi:10.1073/pnas.0611379104

Morini, M., Lafont, A. G., Maugars, G., Baloche, S., Dufour, S., Asturiano, J. F., et al. (2020). Identification and stable expression of vitellogenin receptor through vitellogenesis in the European eel. *Animal* 14, 1213–1222. doi:10.1017/S1751731119003355

Morohashi, K., Hatano, O., Nomura, M., Takayama, K., Hara, M., Yoshii, H., et al. (1995). Function and distribution of a steroidogenic cell-specific transcription factor, Ad4BP. *J. Steroid Biochem. Mol. Biol.* 53, 81–88. doi:10.1016/0960-0760(95)00041-w

Moro, K., Yamada, T., Tanabe, M., Takeuchi, T., Ikawa, T., Kawamoto, H., et al. (2010). Innate production of T(H)2 cytokines by adipose tissue-associated c-Kit(+)Sca-1(+) lymphoid cells. *Nature* 463, 540–544. doi:10.1038/nature08636

Mossadegh-Keller, N., and Sieweke, M. H. (2018). Testicular macrophages: guardians of fertility. *Cell Immunol.* 330, 120–125. doi:10.1016/j.cellimm.2018.03.009

Mullins, M. C., Hammerschmidt, M., Haffter, P., and Nusslein-Volhard, C. (1994). Large-scale mutagenesis in the zebrafish: in search of genes controlling development in a vertebrate. *Curr. Biol.* 4, 189–202. doi:10.1016/s0960-9822(00)00048-8

Mushirobira, Y., Mizuta, H., Luo, W., Todo, T., Hara, A., Reading, B. J., et al. (2015). Molecular cloning and partial characterization of a low-density lipoprotein receptor-related protein 13 (Lrp13) involved in vitellogenin uptake in the cutthroat trout (*Oncorhynchus clarki*). *Mol. Reprod. Dev.* 82, 986–1000. doi:10.1002/mrd.22579

Mustapha, U. F., Jiang, D.-N., Liang, Z.-H., Gu, H.-T., Yang, W., Chen, H.-P., et al. (2018). Male-specific Dmrt1 is a candidate sex determination gene in spotted scat (*Scatophagus argus*). *Aquaculture* 495, 351–358. doi:10.1016/j.aquaculture.2018.06.009

Muto, A., Yi, T., Harrison, K. D., Davalos, A., Fancher, T. T., Ziegler, K. R., et al. (2011). Eph-B4 prevents venous adaptive remodeling in the adult arterial environment. *J. Exp. Med.* 208, 561–575. doi:10.1084/jem.20101854

Myosho, T., Otake, H., Masuyama, H., Matsuda, M., Kuroki, Y., Fujiyama, A., et al. (2012). Tracing the emergence of a novel sex-determining gene in medaka, *Oryzias luzonensis*. *Genetics* 191, 163–170. doi:10.1534/genetics.111.137497

Nagahama, Y., Chakraborty, T., Paul-Prasanth, B., Ohta, K., and Nakamura, M. (2021). Sex determination, gonadal sex differentiation, and plasticity in vertebrate species. *Physiol. Rev.* 101, 1237–1308. doi:10.1152/physrev.00044.2019

Nakamoto, M., Fukasawa, M., Orii, S., Shimamori, K., Maeda, T., Suzuki, A., et al. (2010). Cloning and expression of medaka cholesterol side chain cleavage cytochrome P450 during gonadal development. *Dev. Growth Differ.* 52, 385–395. doi:10.1111/j.1440-169X.2010.01178.x

Nakayama, A., Nakayama, M., Turner, C. J., Hoing, S., Lepore, J. J., and Adams, R. H. (2013). Ephrin-B2 controls PDGFRβ internalization and signaling. *Genes Dev.* 27, 2576–2589. doi:10.1101/gad.224089.113

Namwanje, M., and Brown, C. W. (2016). Activins and inhibins: roles in development, physiology, and disease. *Cold Spring Harb. Perspect. Biol.* 8, a021881. doi:10.1101/cshperspect.a021881

Nanda, I., Kondo, M., Hornung, U., Asakawa, S., Winkler, C., Shimizu, A., et al. (2002). A duplicated copy of DMRT1 in the sex-determining region of the Y chromosome of the medaka, *Oryzias latipes*. *Proc. Natl. Acad. Sci. U. S. A.* 99, 11778–11783. doi:10.1073/pnas.182314699

Neill, D. R., Wong, S. H., Bellosi, A., Flynn, R. J., Daly, M., Langford, T. K., et al. (2010). Nuocytes represent a new innate effector leukocyte that mediates type-2 immunity. *Nature* 464, 1367–1370. doi:10.1038/nature08900

Nelson, D. R., Goldstone, J. V., and Stegeman, J. J. (2013). The cytochrome P450 genesis locus: the origin and evolution of animal cytochrome P450s. *Philos. Trans. R. Soc. Lond B Biol. Sci.* 368, 20120474. doi:10.1098/rstb.2012.0474

Ogita, Y., Mawaribuchi, S., Nakasako, K., Tamura, K., Matsuda, M., Katsumura, T., et al. (2020). Parallel evolution of two *dmrt1*-derived genes, *dmy* and *dm-W*, for vertebrate sex determination. *iScience* 23, 100757. doi:10.1016/j.isci.2019.100757

Olsen, L. C., Aasland, R., and Fjose, A. (1997). A *vasa*-like gene in zebrafish identifies putative primordial germ cells. *Mech. Dev.* 66, 95–105. doi:10.1016/s0925-4773(97)00099-3

Pan, Q., Feron, R., Jouanno, E., Darras, H., Herpin, A., Koop, B., et al. (2021). The rise and fall of the ancient northern pike master sex determining gene. *Elife* 10, e62858. doi:10.7554/eLife.62858

Parajes, S., Griffin, A., Taylor, A. E., Rose, I. T., Miguel-Escalada, I., Hadzhiev, Y., et al. (2013). Redefining the initiation and maintenance of zebrafish interrenal steroidogenesis by characterizing the key enzyme cyp11a2. *Endocrinology* 154, 2702–2711. doi:10.1210/en.2013-1145

Pereira, F. A., Tsai, M. J., and Tsai, S. Y. (2000). COUP-TF orphan nuclear receptors in development and differentiation. *Cell Mol. Life Sci.* 57, 1388–1398. doi:10.1007/PL00000624

Pereiro, P., Varela, M., Diaz-Rosales, P., Romero, A., Dios, S., Figueras, A., et al. (2015). Zebrafish Nk-lysins: first insights about their cellular and functional diversification. *Dev. Comp. Immunol.* 51, 148–159. doi:10.1016/j.dci.2015.03.009

Petersen, A. M., Small, C. M., Yan, Y. L., Wilson, C., Batzel, P., Bremiller, R. A., et al. (2022). Evolution and developmental expression of the sodium-iodide symporter (NIS, slc5a5) gene family: implications for perchlorate toxicology. *Evol. Appl.* 15, 1079–1098. doi:10.1111/eva.13424

Postlethwait, J. H., Navajas Acedo, J., and Piotrowski, T. (2019). Evolutionary origin and nomenclature of vertebrate wnt11-family genes. *Zebrafish* 16, 469–476. doi:10.1089/zeb.2019.1760

Postlethwait, J., Amores, A., Force, A., and Yan, Y. L. (1999). The zebrafish genome. *Methods Cell Biol.* 60, 149–163.

Prevo, R., Banerji, S., Ferguson, D. J., Clasper, S., and Jackson, D. G. (2001). Mouse LYVE-1 is an endocytic receptor for hyaluronan in lymphatic endothelium. *J. Biol. Chem.* 276, 19420–19430. doi:10.1074/jbc.M011004200

Purcell, C. M., Seetharam, A. S., Snodgrass, O., Ortega-Garcia, S., Hyde, J. R., and Severin, A. J. (2018). Insights into teleost sex determination from the *Seriola dorsalis* genome assembly. *BMC Genomics* 19, 31. doi:10.1186/s12864-017-4403-1

Qin, Y., and Bishop, C. E. (2005). Sox9 is sufficient for functional testis development producing fertile male mice in the absence of Sry. *Hum. Mol. Genet.* 14, 1221–1229. doi:10.1093/hmg/ddi133

Qiu, Y., Wang, J., Lei, J., and Roeder, K. (2021). Identification of cell-type-specific marker genes from co-expression patterns in tissue samples. *Bioinformatics* 37, 3228–3234. doi:10.1093/bioinformatics/btab257

Ramanagoudr-Bhojappa, R., Carrington, B., Ramaswami, M., Bishop, K., Robbins, G. M., Jones, M., et al. (2018). Multiplexed CRISPR/Cas9-mediated knockout of 19 Fanconi anemia pathway genes in zebrafish revealed their roles in growth, sexual development and fertility. *PLoS Genet.* 14, e1007821. doi:10.1371/journal.pgen.1007821

Raymond, C. S., Kettlewell, J. R., Hirsch, B., Bardwell, V. J., and Zarkower, D. (1999). Expression of Dmrt1 in the genital ridge of mouse and chicken embryos suggests a role in vertebrate sexual development. *Dev. Biol.* 215, 208–220. doi:10.1006/dbio.1999.9461

Raymond, C. S., Murphy, M. W., O'Sullivan, M. G., Bardwell, V. J., and Zarkower, D. (2000). Dmrt1, a gene related to worm and fly sexual regulators, is required for mammalian testis differentiation. *Genes Dev.* 14, 2587–2595. doi:10.1101/gad.834100

Reading, B. J., Hiramatsu, N., Schilling, J., Molloy, K. T., Glassbrook, N., Mizuta, H., et al. (2014). Lrp13 is a novel vertebrate lipoprotein receptor that binds vitellogenins in teleost fishes. *J. Lipid Res.* 55, 2287–2295. doi:10.1194/jlr.M050286

Ribas, L., Valdivieso, A., Diaz, N., and Piferrer, F. (2017). Appropriate rearing density in domesticated zebrafish to avoid masculinization: links with the stress response. *J. Exp. Biol.* 220, 1056–1064. doi:10.1242/jeb.144980

Rodriguez-Mari, A., Canestro, C., Bremiller, R. A., Nguyen-Johnson, A., Asakawa, K., Kawakami, K., et al. (2010). Sex reversal in zebrafish fancl mutants is caused by Tp53-mediated germ cell apoptosis. *PLoS Genet.* 6, e1001034. doi:10.1371/journal.pgen.1001034

Rodriguez-Mari, A., Wilson, C., Titus, T. A., Canestro, C., Bremiller, R. A., Yan, Y. L., et al. (2011). Roles of *brca2* (*fancd1*) in oocyte nuclear architecture, gametogenesis, gonad tumors, and genome stability in zebrafish. *PLoS Genet.* 7, e1001357. doi:10.1371/journal.pgen.1001357

Rodriguez-Mari, A., Yan, Y. L., Bremiller, R. A., Wilson, C., Canestro, C., and Postlethwait, J. H. (2005). Characterization and expression pattern of zebrafish Anti-Mullerian hormone (*Amh*) relative to *sox9a, sox9b*, and *cyp19a1a*, during gonad development. *Gene Expr. Patterns* 5, 655–667. doi:10.1016/j.modgep.2005.02.008

Rodriguez-Nunez, I., Wcisel, D. J., Litman, R. T., Litman, G. W., and Yoder, J. A. (2016). The identification of additional zebrafish DICP genes reveals haplotype variation and linkage to MHC class I genes. *Immunogenetics* 68, 295–312. doi:10.1007/s00251-016-0901-6

Roh-Johnson, M., Shah, A. N., Stonick, J. A., Poudel, K. R., Kargl, J., Yang, G. H., et al. (2017). Macrophage-Dependent cytoplasmic transfer during melanoma invasion *in vivo*. *Dev. Cell* 43, 549–562. doi:10.1016/j.devcel.2017.11.003

Romano, S., Kaufman, O. H., and Marlow, F. L. (2020). Loss of dmrt1 restores zebrafish female fates in the absence of cyp19a1a but not rbpms2a/b. *Development* 147, dev190942. doi:10.1242/dev.190942

Rondeau, E. B., Messmer, A. M., Sanderson, D. S., Jantzen, S. G., Von Schalburg, K. R., Minkley, D. R., et al. (2013). Genomics of sablefish (*Anoplopoma fimbria*): expressed genes, mitochondrial phylogeny, linkage map and identification of a putative sex gene. *BMC Genomics* 14, 452. doi:10.1186/1471-2164-14-452

Rougeot, J., Torraca, V., Zakrzewska, A., Kanwal, Z., Jansen, H. J., Sommer, F., et al. (2019). RNAseq profiling of leukocyte populations in zebrafish larvae reveals a *cxcl11* chemokine gene as a marker of macrophage polarization during mycobacterial infection. *Front. Immunol.* 10, 832. doi:10.3389/fimmu.2019.00832

Saito, K., Siegfried, K. R., Nusslein-Volhard, C., and Sakai, N. (2011). Isolation and cytogenetic characterization of zebrafish meiotic prophase I mutants. *Dev. Dyn.* 240, 1779–1792. doi:10.1002/dvdy.22661

Santos, E. M., Workman, V. L., Paull, G. C., Filby, A. L., Van Look, K. J., Kille, P., et al. (2007). Molecular basis of sex and reproductive status in breeding zebrafish. *Physiol. Genomics* 30, 111–122. doi:10.1152/physiolgenomics.00284.2006

Santos, D., Luzio, A., and Coimbra, A. M. (2017). Zebrafish sex differentiation and gonad development: a review on the impact of environmental factors. *Aquat. Toxicol.* 191, 141–163. doi:10.1016/j.aquatox.2017.08.005

Sawatari, E., Shikina, S., Takeuchi, T., and Yoshizaki, G. (2007). A novel transforming growth factor-beta superfamily member expressed in gonadal somatic cells enhances primordial germ cell and spermatogonial proliferation in rainbow trout (*Oncorhynchus mykiss*). *Dev. Biol.* 301, 266–275. doi:10.1016/j.ydbio.2006.10.001

Scheppke, L., Murphy, E. A., Zarpellon, A., Hofmann, J. J., Merkulova, A., Shields, D. J., et al. (2012). Notch promotes vascular maturation by inducing integrin-mediated smooth muscle cell adhesion to the endothelial basement membrane. *Blood* 119, 2149–2158. doi:10.1182/blood-2011-04-348706

Schorpp, M., Bialecki, M., Diekhoff, D., Walderich, B., Odenthal, J., Maischein, H. M., et al. (2006). Conserved functions of Ikaros in vertebrate lymphocyte development: genetic evidence for distinct larval and adult phases of T cell development and two lineages of B cells in zebrafish. *J. Immunol.* 177, 2463–2476. doi:10.4049/jimmunol.177.4.2463

Schulz, R. W., and Nóbrega, R. H. (2011). "The reproductive organs and processes | anatomy and histology of fish testis," in *Encyclopedia of fish physiology. From genome to environment*. Editor A. P. Farrell (San Diego: Academic Press).

Selman, K., Wallace, R. A., Sarka, A., and Qi, X. (1993). Stages of oocyte development in the zebrafish, *Brachydanio rerio*. *J. Morphol.* 218, 203–224. doi:10.1002/jmor.1052180209

Shang, E. H., Yu, R. M., and Wu, R. S. (2006). Hypoxia affects sex differentiation and development, leading to a male-dominated population in zebrafish (*Danio rerio*). *Environ. Sci. Technol.* 40, 3118–3122. doi:10.1021/es0522579

Shao, T., Shi, W., Zheng, J. Y., Xu, X. X., Lin, A. F., Xiang, L. X., et al. (2018). Costimulatory function of Cd58/Cd2 interaction in adaptive humoral immunity in a zebrafish model. *Front. Immunol.* 9, 1204. doi:10.3389/fimmu.2018.01204

Shin, Y. H., Mcguire, M. M., and Rajkovic, A. (2013). Mouse HORMAD1 is a meiosis i checkpoint protein that modulates DNA double-strand break repair during female meiosis. *Biol. Reprod.* 89, 29. doi:10.1095/biolreprod.112.106773

Shive, H. R., West, R. R., Embree, L. J., Azuma, M., Sood, R., Liu, P., et al. (2010). brca2 in zebrafish ovarian development, spermatogenesis, and tumorigenesis. *Proc. Natl. Acad. Sci. U. S. A.* 107, 19350–19355. doi:10.1073/pnas.1011630107

Slanchev, K., Stebler, J., De La Cueva-Mendez, G., and Raz, E. (2005). Development without germ cells: the role of the germ line in zebrafish sex differentiation. *Proc. Natl. Acad. Sci. U. S. A.* 102, 4074–4079. doi:10.1073/pnas.0407475102

Smith, C. A., Roeszler, K. N., Ohnesorg, T., Cummins, D. M., Farlie, P. G., Doran, T. J., et al. (2009). The avian Z-linked gene DMRT1 is required for male sex determination in the chicken. *Nature* 461, 267–271. doi:10.1038/nature08298

Sommer, F., Torraca, V., Kamel, S. M., Lombardi, A., and Meijer, A. H. (2020). Frontline Science: antagonism between regular and atypical Cxcr3 receptors regulates macrophage migration during infection and injury in zebrafish. *J. Leukoc. Biol.* 107, 185–203. doi:10.1002/JLB.2HI0119-006R

Song, H. D., Sun, X. J., Deng, M., Zhang, G. W., Zhou, Y., Wu, X. Y., et al. (2004). Hematopoietic gene expression profile in zebrafish kidney marrow. *Proc. Natl. Acad. Sci. U. S. A.* 101, 16240–16245. doi:10.1073/pnas.0407241101

Song, W., Xie, Y., Sun, M., Li, X., Fitzpatrick, C. K., Vaux, F., et al. (2021). A duplicated *amh* is the master sex-determining gene for Sebastes rockfish in the Northwest Pacific. *Open Biol.* 11, 210063. doi:10.1098/rsob.210063

Stanzione, M., Baumann, M., Papanikos, F., Dereli, I., Lange, J., Ramlal, A., et al. (2016). Meiotic DNA break formation requires the unsynapsed chromosome axis-binding protein IHO1 (CCDC36) in mice. *Nat. Cell Biol.* 18, 1208–1220. doi:10.1038/ncb3417

Stevant, I., Kuhne, F., Greenfield, A., Chaboissier, M. C., Dermitzakis, E. T., and Nef, S. (2019). Dissecting cell lineage specification and sex fate determination in gonadal somatic cells using single-cell transcriptomics. *Cell Rep.* 26, 3272–3283. doi:10.1016/j.celrep.2019.02.069

Streisinger, G., Walker, C., Dower, N., Knauber, D., and Singer, F. (1981). Production of clones of homozygous diploid zebra fish (*Brachydanio rerio*). *Nature* 291, 293–296. doi:10.1038/291293a0

Su, Y. Q., Wu, X., O'Brien, M. J., Pendola, F. L., Denegre, J. N., Matzuk, M. M., et al. (2004). Synergistic roles of BMP15 and GDF9 in the development and function of the oocyte-cumulus cell complex in mice: genetic evidence for an oocyte-granulosa cell regulatory loop. *Dev. Biol.* 276, 64–73. doi:10.1016/j.ydbio.2004.08.020

Sugawara, T., Kiriakidou, M., Mcallister, J. M., Holt, J. A., Arakane, F., and Strauss, J. F. (1997). Regulation of expression of the steroidogenic acute regulatory protein (StAR) gene: a central role for steroidogenic factor 1. *Steroids* 62, 5–9. doi:10.1016/s0039-128x(96)00152-3

Takahashi, H. (1977). Juvenile hermaphroditism in the zebrafish, *Brachydanio rerio*. *Bull. Fac. Fish. Hokkaido Univ.* 28, 57–65.

Takemoto, K., Imai, Y., Saito, K., Kawasaki, T., Carlton, P. M., Ishiguro, K. I., et al. (2020). Sycp2 is essential for synaptonemal complex assembly, early meiotic recombination and homologous pairing in zebrafish spermatocytes. *PLoS Genet.* 16, e1008640. doi:10.1371/journal.pgen.1008640

Tan, C. H., Lee, T. C., Weeraratne, S. D., Korzh, V., Lim, T. M., and Gong, Z. (2002). *ziwi*, the zebrafish homologue of the Drosophila *piwi*: co-localization with *vasa* at the embryonic genital ridge and gonad-specific expression in the adults. *Gene Expr. Patterns* 2, 257–260. doi:10.1016/s1567-133x(02)00052-2

Tang, Q., Iyer, S., Lobbardi, R., Moore, J. C., Chen, H., Lareau, C., et al. (2017). Dissecting hematopoietic and renal cell heterogeneity in adult zebrafish at single-cell resolution using RNA sequencing. *J. Exp. Med.* 214, 2875–2887. doi:10.1084/jem.20170976

Taylor, J. S., Braasch, I., Frickey, T., Meyer, A., and Van De Peer, Y. (2003). Genome duplication, a trait shared by 22000 species of ray-finned fish. *Genome Res.* 13, 382–390. doi:10.1101/gr.640303

Tenugu, S., Pranoty, A., Mamta, S., and Senthilkumaran, B. (2021). Development and organisation of gonadal steroidogenesis in bony fishes - a review. *Aquac. Fish.* 6, 223–246. doi:10.1016/j.aaf.2020.09.004

Terao, M., Ogawa, Y., Takada, S., Kajitani, R., Okuno, M., Mochimaru, Y., et al. (2022). Turnover of mammal sex chromosomes in the Sry-deficient Amami spiny rat is due to male-specific upregulation of Sox9. *Proc. Natl. Acad. Sci. U. S. A.* 119, e2211574119. doi:10.1073/pnas.2211574119

Tokarz, J., Moller, G., Hrabe De Angelis, M., and Adamski, J. (2015). Steroids in teleost fishes: a functional point of view. *Steroids* 103, 123–144. doi:10.1016/j.steroids.2015.06.011

Tong, S. K., Hsu, H. J., and Chung, B. C. (2010). Zebrafish monosex population reveals female dominance in sex determination and earliest events of gonad differentiation. *Dev. Biol.* 344, 849–856. doi:10.1016/j.ydbio.2010.05.515

Torraca, V., Masud, S., Spaink, H. P., and Meijer, A. H. (2014). Macrophage-pathogen interactions in infectious diseases: new therapeutic insights from the zebrafish host model. *Dis. Model Mech.* 7, 785–797. doi:10.1242/dmm.015594

Turmel, P., Dufresne, J., Hermo, L., Smith, C. E., Penuela, S., Laird, D. W., et al. (2011). Characterization of pannexin1 and pannexin3 and their regulation by androgens in the male reproductive tract of the adult rat. *Mol. Reprod. Dev.* 78, 124–138. doi:10.1002/mrd.21280

Uchida, D., Yamashita, M., Kitano, T., and Iguchi, T. (2002). Oocyte apoptosis during the transition from ovary-like tissue to testes during sex differentiation of juvenile zebrafish. *J. Exp. Biol.* 205, 711–718. doi:10.1242/jeb.205.6.711

Valdivieso, A., Wilson, C. A., Amores, A., Da Silva Rodrigues, M., Nobrega, R. H., Ribas, L., et al. (2022). Environmentally-induced sex reversal in fish with chromosomal vs. polygenic sex determination *Environ. Res.* 213, 113549. doi:10.1016/j.envres.2022.113549

Villa, N., Walker, L., Lindsell, C. E., Gasson, J., Iruela-Arispe, M. L., and Weinmaster, G. (2001). Vascular expression of Notch pathway receptors and ligands is restricted to arterial vessels. *Mech. Dev.* 108, 161–164. doi:10.1016/s0925-4773(01)00469-5

Von Hofsten, J., Jones, I., Karlsson, J., and Olsson, P. E. (2001). Developmental expression patterns of FTZ-F1 homologues in zebrafish (*Danio rerio*). *Gen. Comp. Endocrinol.* 121, 146–155. doi:10.1006/gcen.2000.7582

Walker, C., and Streisinger, G. (1983). Induction of mutations by gamma-rays in pregonial germ cells of zebrafish embryos. *Genetics* 103, 125–136. doi:10.1093/genetics/103.1.125

Walker-Durchanek, R. C. (1980). *Induction of germ line mutations by irradiation of zebrafish embryos*. Masters, University of Oregon, Eugene OR USA.

Wang, J. H., Nichogiannopoulou, A., Wu, L., Sun, L., Sharpe, A. H., Bigby, M., et al. (1996). Selective defects in the development of the fetal and adult lymphoid system in mice with an Ikaros null mutation. *Immunity* 5, 537–549. doi:10.1016/s1074-7613(00)80269-1

Wang, X. G., Bartfai, R., Sleptsova-Freidrich, I., and Orban, L. (2007). The timing and extent of 'juvenile ovary' phase are highly variable during zebrafish testis differentiation. *J. Fish Biol.* 70, 33–44. doi:10.1111/j.1095-8649.2007.01363.x

Wang, X., Chen, S., Zhang, W., Ren, Y., Zhang, Q., and Peng, G. (2017). Dissection of larval zebrafish gonadal tissue. *J. Vis. Exp.*, 55294. doi:10.3791/55294

Wang, Y., Ye, D., Zhang, F., Zhang, R., Zhu, J., Wang, H., et al. (2022). Cyp11a2 is essential for oocyte development and spermatogonial stem cell differentiation in zebrafish. *Endocrinology* 163, bqab258. doi:10.1210/endocr/bqab258

Wang, Z., Miura, N., Bonelli, A., Mole, P., Carlesso, N., Olson, D. P., et al. (2002). Receptor tyrosine kinase, EphB4 (HTK), accelerates differentiation of select human hematopoietic cells. *Blood* 99, 2740–2747. doi:10.1182/blood.v99.8.2740

Wattrus, S. J., and Zon, L. I. (2021). Blood in the water: recent uses of zebrafish to study myeloid biology. *Curr. Opin. Hematol.* 28, 43–49. doi:10.1097/MOH.0000000000000627

Webster, K. A., Schach, U., Ordaz, A., Steinfeld, J. S., Draper, B. W., and Siegfried, K. R. (2017). Dmrt1 is necessary for male sexual development in zebrafish. *Dev. Biol.* 422, 33–46. doi:10.1016/j.ydbio.2016.12.008

Weidinger, G., Stebler, J., Slanchev, K., Dumstrei, K., Wise, C., Lovell-Badge, R., et al. (2003). Dead end, a novel vertebrate germ plasm component, is required for zebrafish primordial germ cell migration and survival. *Curr. Biol.* 13, 1429–1434. doi:10.1016/s0960-9822(03)00537-2

Westerfield, M. (1993). *The zebrafish book: a guide for the laboratory use of zebrafish (Brachydanio rerio)*. Eugene, OR: M. Westerfield.

White, R. T., and Allen, R. A. (1951). An improved clinical microtome for sectioning frozen tissue. *Stain Technol.* 26, 137–138. doi:10.3109/10520295109113195

Willett, C. E., Kawasaki, H., Amemiya, C. T., Lin, S., and Steiner, L. A. (2001). Ikaros expression as a marker for lymphoid progenitors during zebrafish development. *Dev. Dyn.* 222, 694–698. doi:10.1002/dvdy.1223

Wilson, C. A., High, S. K., Mccluskey, B. M., Amores, A., Yan, Y. L., Titus, T. A., et al. (2014). Wild sex in zebrafish: loss of the natural sex determinant in domesticated strains. *Genetics* 198, 1291–1308. doi:10.1534/genetics.114.169284

Wilson, C. A., and Postlethwait, J. H. (2023). A maternal-to-zygotic-transition gene block on the zebrafish sex chromosome. *bioRxiv*, 2023.12.06.570431. doi:10.1101/2023.12.06.570431

Winandy, S., Wu, P., and Georgopoulos, K. (1995). A dominant mutation in the *Ikaros* gene leads to rapid development of leukemia and lymphoma. *Cell* 83, 289–299. doi:10.1016/0092-8674(95)90170-1

Wolf, K., Hu, H., Isaji, T., and Dardik, A. (2019). Molecular identity of arteries, veins, and lymphatics. *J. Vasc. Surg.* 69, 253–262. doi:10.1016/j.jvs.2018.06.195

Wong, Q. W., Sun, M. A., Lau, S. W., Parsania, C., Zhou, S., Zhong, S., et al. (2018). Identification and characterization of a specific 13-miRNA expression signature during follicle activation in the zebrafish ovary. *Biol. Reprod.* 98, 42–53. doi:10.1093/biolre/iox160

Wu, K., Song, W., Zhang, Z., and Ge, W. (2020). Disruption of dmrt1 rescues the all-male phenotype of the cyp19a1a mutant in zebrafish - a novel insight into the roles of aromatase/estrogens in gonadal differentiation and early folliculogenesis. *Development* 147, dev182758. doi:10.1242/dev.182758

Wyrwoll, M. J., Gaasbeek, C. M., Golubickaite, I., Stakaitis, R., Oud, M. S., Nagirnaja, L., et al. (2022). The piRNA-pathway factor FKBP6 is essential for spermatogenesis but dispensable for control of meiotic LINE-1 expression in humans. *Am. J. Hum. Genet.* 109, 1850–1866. doi:10.1016/j.ajhg.2022.09.002

Xavier, C. P., Eichinger, L., Fernandez, M. P., Morgan, R. O., and Clemen, C. S. (2008). Evolutionary and functional diversity of coronin proteins. *Subcell. Biochem.* 48, 98–109. doi:10.1007/978-0-387-09595-0_9

Xie, Y., Huang, D., Chu, L., Liu, Y., Sun, X., Li, J., et al. (2021). Igf3 is essential for ovary differentiation in zebrafish†. *Biol. Reprod.* 104, 589–601. doi:10.1093/biolre/ioaa218

Xiol, J., Cora, E., Koglgruber, R., Chuma, S., Subramanian, S., Hosokawa, M., et al. (2012). A role for Fkbp6 and the chaperone machinery in piRNA amplification and transposon silencing. *Mol. Cell* 47, 970–979. doi:10.1016/j.molcel.2012.07.019

Yan, Y. L., Desvignes, T., Bremiller, R., Wilson, C., Dillon, D., High, S., et al. (2017). Gonadal soma controls ovarian follicle proliferation through Gsdf in zebrafish. *Dev. Dyn.* 246, 925–945. doi:10.1002/dvdy.24579

Yan, Y.-L., Titus, T., Desvignes, T., Bremiller, R., Batzel, P., Sydes, J., et al. (2020). *A fish with no sex: gonadal and adrenal functions partition between zebrafish NR5A1 co-orthologs. GENETICS/2020/303676*.

Yan, Y. L., Willoughby, J., Liu, D., Crump, J. G., Wilson, C., Miller, C. T., et al. (2005). A pair of Sox: distinct and overlapping functions of zebrafish sox9 co-orthologs in craniofacial and pectoral fin development. *Development* 132, 1069–1083. doi:10.1242/dev.01674

Yang, Y. J., Wang, Y., Li, Z., Zhou, L., and Gui, J. F. (2017). Sequential, divergent, and cooperative requirements of Foxl2a and Foxl2b in ovary development and maintenance of zebrafish. *Genetics* 205, 1551–1572. doi:10.1534/genetics.116.199133

Yin, Y., Tang, H., Liu, Y., Chen, Y., Li, G., Liu, X., et al. (2017). Targeted disruption of aromatase reveals dual functions of *cyp19a1a* during sex differentiation in zebrafish. *Endocrinology* 158, 3030–3041. doi:10.1210/en.2016-1865

Yoder, J. A., Turner, P. M., Wright, P. D., Wittamer, V., Bertrand, J. Y., Traver, D., et al. (2010). Developmental and tissue-specific expression of NITRs. *Immunogenetics* 62, 117–122. doi:10.1007/s00251-009-0416-5

Yoon, C., Kawakami, K., and Hopkins, N. (1997). Zebrafish vasa homologue RNA is localized to the cleavage planes of 2- and 4-cell-stage embryos and is expressed in the primordial germ cells. *Development* 124, 3157–3165. doi:10.1242/dev.124.16.3157

You, L. R., Lin, F. J., Lee, C. T., Demayo, F. J., Tsai, M. J., and Tsai, S. Y. (2005). Suppression of Notch signalling by the COUP-TFII transcription factor regulates vein identity. *Nature* 435, 98–104. doi:10.1038/nature03511

Young, M. D., and Behjati, S. (2020). SoupX removes ambient RNA contamination from droplet-based single-cell RNA sequencing data. *Gigascience* 9, giaa151. doi:10.1093/gigascience/giaa151

Yu, G., Zhang, D., Liu, W., Wang, J., Liu, X., Zhou, C., et al. (2018). Zebrafish androgen receptor is required for spermatogenesis and maintenance of ovarian function. *Oncotarget* 9, 24320–24334. doi:10.18632/oncotarget.24407

Zakrzewska, A., Cui, C., Stockhammer, O. W., Benard, E. L., Spaink, H. P., and Meijer, A. H. (2010). Macrophage-specific gene functions in Spi1-directed innate immunity. *Blood* 116, e1–e11. doi:10.1182/blood-2010-01-262873

Zhai, G., Shu, T., Xia, Y., Lu, Y., Shang, G., Jin, X., et al. (2018). Characterization of sexual trait development in *cyp17a1*-deficient zebrafish. *Endocrinology* 159, 3549–3562. doi:10.1210/en.2018-00551

Zhai, Y., Zhao, C., Geng, R., Wu, K., Yuan, M., Ai, N., et al. (2022). Phenotypical rescue of Bmp15 deficiency by mutation of inhibin a (inha) provides novel clues to how Bmp15 controls zebrafish folliculogenesis. *bioRxiv*. preprint. doi:10.1101/2022.12.30.522301

Zhang, X., Guan, G., Li, M., Zhu, F., Liu, Q., Naruse, K., et al. (2016). Autosomal gsdf acts as a male sex initiator in the fish medaka. *Sci. Rep.* 6, 19738. doi:10.1038/srep19738

Zhao, C., Zhai, Y., Geng, R., Wu, K., Song, W., Ai, N., et al. (2022). Genetic analysis of activin/inhibin β subunits in zebrafish development and reproduction. *PLoS Genet.* 18, e1010523. doi:10.1371/journal.pgen.1010523

Zheng, G. X., Terry, J. M., Belgrader, P., Ryvkin, P., Bent, Z. W., Wilson, R., et al. (2017). Massively parallel digital transcriptional profiling of single cells. *Nat. Commun.* 8, 14049. doi:10.1038/ncomms14049

Zhu, B., Pardeshi, L., Chen, Y., and Ge, W. (2018). Transcriptomic analysis for differentially expressed genes in ovarian follicle activation in the zebrafish. *Front. Endocrinol. (Lausanne)* 9, 593. doi:10.3389/fendo.2018.00593

Zhu, J., Min, B., Hu-Li, J., Watson, C. J., Grinberg, A., Wang, Q., et al. (2004). Conditional deletion of Gata3 shows its essential function in T(H)1-T(H)2 responses. *Nat. Immunol.* 5, 1157–1165. doi:10.1038/ni1128

frontiers | Frontiers in Cell and Developmental Biology

TYPE Original Research
PUBLISHED 19 June 2024
DOI 10.3389/fcell.2024.1343800

OPEN ACCESS

EDITED BY
Dagmar Wilhelm,
The University of Melbourne, Australia

REVIEWED BY
Rasoul Godini,
Monash University, Australia
Francis Poulat,
Université de Montpellier, France
Joohyung Lee,
Monash University, Australia

*CORRESPONDENCE
Per-Erik Olsson,
per-erik.olsson@oru.se

†These authors share first authorship

‡PRESENT ADDRESSES
Subrata Pramanik,
Jyoti and Bhupat Mehta School of Health Sciences and Technology, Indian Institute of Technology Guwahati, Guwahati, Assam 781039, India; Centre for Nanotechnology, Indian Institute of Technology Guwahati, Guwahati 781039, Assam, India

RECEIVED 24 November 2023
ACCEPTED 05 June 2024
PUBLISHED 19 June 2024

CITATION
Paylar B, Pramanik S, Bezabhe YH and Olsson P-E (2024), Temporal sex specific brain gene expression pattern during early rat embryonic development.
Front. Cell Dev. Biol. 12:1343800.
doi: 10.3389/fcell.2024.1343800

Temporal sex specific brain gene expression pattern during early rat embryonic development

Berkay Paylar†, Subrata Pramanik†‡, Yared H. Bezabhe and Per-Erik Olsson*

Biology, The Life Science Center, School of Science and Technology, Örebro University, Örebro, Sweden

Background: The classical concept of brain sex differentiation suggests that steroid hormones released from the gonads program male and female brains differently. However, several studies indicate that steroid hormones are not the only determinant of brain sex differentiation and that genetic differences could also be involved.

Methods: In this study, we have performed RNA sequencing of rat brains at embryonic days 12 (E12), E13, and E14. The aim was to identify differentially expressed genes between male and female rat brains during early development.

Results: Analysis of genes expressed with the highest sex differences showed that *Xist* was highly expressed in females having XX genotype with an increasing expression over time. Analysis of genes expressed with the highest male expression identified three early genes, *Sry2, Eif2s3y*, and *Ddx3y*.

Discussion: The observed sex-specific expression of genes at early development confirms that the rat brain is sexually dimorphic prior to gonadal action on the brain and identifies *Sry2* and *Eif2s3y* as early genes contributing to male brain development.

KEYWORDS

neuronal, sex chromosome, RNA sequencing, sexual dimorphism, differentiation

1 Introduction

Sexual dimorphism, including maternal care, sexual behavior, brain function, structure, and susceptibility to neurological disorders is evident in humans as well as in nonhuman species. Studies of human male and female brains have revealed sex differences in connectome, methylome, and transcriptome profiles (Ingalhalikar et al., 2014; Xu et al., 2014). Despite extensive advancement in neuroscience, the molecular regulation of these sex differences remains unclear.

The classical model of brain sex differentiation that placed gonadal steroid hormones as the main drivers in establishing male and female neural networks was derived from earlier studies (Phoenix et al., 1959; Arnold, 2009). This model states that the chromosomal constitution (XX or XY) determines the gonadal sex and that the hormone secreted by the gonads programs the brain neural network differently (Phoenix et al., 1959; Arnold, 2009).

The initiation of sex differentiation is governed by the sex determining region Y (Sry) master regulator gene located on the Y chromosome, that signals for the activation of the male sex differentiation pathway and the formation of testes (Koopman, 2005). The earliest gonadal expression of Sry is at around E10.5 in mouse, and peaks at E11.5 to initiate testis differentiation (Sim et al., 2008). It has also been observed that Sry is present in the mouse

brain at E11 (Mayer et al., 2000). In rats, multiple Sry copies were identified by Turner and co-workers (Turner et al., 2007). They observed that among the different Sry homologues, Sry2 had the highest expression in rat testis and adrenal glands at 15 weeks of age. In a separate study, it was observed that the expression of Sry2 in rat gonads began from E11, as revealed by transcriptional analysis (Prokop et al., 2020). In humans the expression of Sry is observed first at E41 to peak on E44 (Hanley et al., 2000). Studies using the four-core mouse model indicate that Sry may be needed for proper masculinization of the animal, both gonadal and neuronal (Arnold, 2009). A study in chicken also indicate that male and female brains are sexually dimorphic prior to gonadal development (Lee et al., 2009).

Studies on zebra finch has been instrumental in revealing the involvement of genetic elements in neuronal cell sex differentiation. In a study on zebra finch, Gahr and Metzdorf, showed that androgen treatment of female birds did not fully masculinize the song center (Gahr and Metzdorf, 1999). Furthermore, an involvement of genetic factors in brain sex development was evident from a study of a gynandromorphic zebra finch (Arnold, 2003). Despite the whole brain being under the influence of the same gonadal hormones, the zebra finch still developed histologically identifiable song centers in the male side of the brain while the female side of the brain remained feminine (Arnold, 2003). In addition, aromatase inhibitor treatment, that induced testicular tissue in the genetic female zebra finch, failed to masculinize the song system that remained feminine (Wade and Arnold, 1996).

To identify genes involved in brain sexual development Dewing and coworkers performed a study using embryonic mouse heads and microarray analysis (Dewing et al., 2003) They observed sex differences in gene expression at embryonic day 10.5 (E10.5) were observed in the head region. DEAD-box RNA helicase y (Ddx3y; Dby) and eukaryotic translation initiation factor 2 subunit 3y (Eif2s3y) were identified as having the highest male biased gene expression at 10.5 dpc (days post coitum), while X-inactive specific transcript (Xist) showed the highest female bias. While studies on human brain sex differences are limited and generally obtained from mid-gestational developmental stages, they do provide information on brain sex differences (Reinius and Jazin, 2009; Johansson et al., 2016). Analysis of gene expression of sex-chromosome linked genes showed 11 Y-chromosome linked genes that were upregulated in comparison to their X-chromosome homologues in females. Further analysis of two of these genes (Pcdh11y and Nlgn4y) showed that these genes were predominantly expressed in different glial and neuronal cell populations in the CNS. In line with this it has also been shown that the microglia cell displays sex differences with males exhibiting higher microglia count than females throughout the neonatal period (Bordt et al., 2020).

To further elucidate the mechanisms leading to differential transcription in the developing male and female brain, and to identify genes showing sex dependent regulation in the developing rodent brain, we performed a transcriptomic analysis of rat brain during the period of gonadal activation. We selected three embryonic stages to determine sex differences in gene expression in the brain. These were stage E12 prior to gonadal activation (Prokop et al., 2020), E13 at the time of gonadal activation, and at E14 following gonadal activation (Val et al., 2003).

The temporal expression from E12 to E14 revealed two Y-chromosome genes with the highest expression levels at E12, Sry2, and Eif2s3y. As Sry2 showed sex biased gene expression at all three developmental stages, locally expressed Sry cannot be excluded as a regulator of gene expression in the brain prior to testis differentiation. Our results support that there are genetic sex differences in developing brains prior to hormone action and suggest that these differences may be involved in the differential development of male and female brains.

2 Materials and methods

2.1 Sample processing, genotyping, and RNA sequencing

Brain samples from Sprague Dawley rats (*Rattus norvegicus*) were obtained from Brain Bits (United States). The Spraque Dawley rats represent an outbred strain that was selected to allow for determination of responses related to a normal population of the species. Following sampling the brains were maintained in Hibernate™-E Medium (ThermoFisher Scientific, United States) and were shipped on ice. Directly following receiving the samples they were transferred to −80°C. Three males and three females were used to obtain brain samples from each developmental stage. For genotyping, tissue samples from the body were extracted using a DNA isolation kit (Zymo Research, United States). DNA was quantified using NanoDrop (Denovix, United States) and qPCR was performed for *Xist* and *Sry*, to confirm the sex of the sample and to validate brain specific expression. The primer sequences used for *Sry* and *Xist* are listed in Table 1. The qPCR reaction conditions were as follows: 95°C for 5 min followed by 35 cycles of 95°C for 10 s, 55°C for 15 s, and 72°C for 1 min. The PCR product was run on 1% agarose gel. Following genotyping, three individuals per sex and stage were used for RNA sequencing.

The samples were homogenized in Tri Reagent (Sigma) and RNA extraction was performed using Directzol RNA extraction kit (Zymo Research, United States). RNA samples were quantified using NanoDrop (Denovix, United States), and the quality was analyzed using RNA denaturing gel. RNA at a concentration of 50 ng/μL with a OD 260/280 between 1.8 and 2.0, OD 260/230 between 2.0 and 2.2 were sent to GATC Biotech/Eurofins for RNA sequencing. RNA samples with a RNA integrity number equal to or exceeding eight were used for sequencing, Sequencing was performed using Illumina platform to generate 2 × 51 bp reads.

2.2 Data analysis

The raw data files were first analyzed for sequence quality using pre-alignment QA/QC. Reads were trimmed from three prime ends based on quality score and the average Phred score for the reads was determined for all replicates. The reads were aligned to the rat genome (Rnor_6.0) using BWA-MEM alignment algorithm followed by quantification to alignment model using Partek genomic software (Partek Inc., St. Louis, United States). BWA was chosen due to its well described alignment accuracy and handling of false negative results which is usually observed by

TABLE 1 Primers used for qRT-PCR analysis.

Gene name	Gene symbol	Forward (5′→3′)	Reverse (5′→3′)
Sex determining region on the Y chromosome	Sry	gctgcacaccagtcctccaag	cagggtcggtcaccagtgatatca
X-inactive specific transcript	Xist	ggagtcgttcctcacaccag	gcagcattctgtcgagcca

other algorithms with short sequence reads (Wu et al., 2019; Alganmi and Abusamra, 2023). The gene expression counts were normalized using the Counts Per Million reads (CPM) method, followed by 1.0e-4 addition. This adjustment is particularly important for genes located on the Y chromosome, as they do not exhibit any expression in female samples. Lowest gene coverage of 10 was employed to filter out low expressed genes. The resulting normalized counts were used to identify differentially regulated genes using DESeq2 (Anders and Huber, 2010). Analysis of the number of reads of Y chromosome genes was performed by calculating reads per million using Integrated Genomics Viewer version 2.12 (Robinson et al., 2011). Manual inspection of the reads of *Sry* genes was performed to ascertain localization at the correct position and ensured that the low read counts were not merely noise.

Hierarchical clustering and heatmaps were generated for each stage with the average linkage cluster distance metric, in conjunction with the Euclidean point distance metric (https://www.bioinformatics.com.cn/en). Standardized gene expression values (z-scores) were used to visualize each stage. Principal component analysis (PCA) was utilized to visualize relationships between various embryonic stages (Partek Inc., St. Louis, United States). To ensure uniform feature contribution in the construction of the PCA, 18 principal components (normalized counts) underwent a logarithmic transformation with a base of two and a transform offset of 1.

Venn diagrams were individually created using jvenn (https://jvenn.toulouse.inrae.fe/app/index.html) for male and female rats at each developmental stage, illustrating the unique gene sets for each sex. Furthermore, the overlapping genes across different stages were highlighted. Key Y-chromosome gene expression profiles were derived through the utilization of counts per million, allowing for the visualization of gene expression patterns across successive developmental stages.

Bubble plots were created to highlight GO annotations and KEGG pathway analysis for each embryonic stage by employing identified differentially expressed genes (DEGs) using an online data analysis and visualization platform (https://www.bioinformatics.com.cn/en). Terms and pathways were ranked based on their enrichment score and the top 10 enriched terms and pathways are presented. A color gradient was employed to indicate the percentage of sex ratios for the given term. Pathways that were overrepresented in males and females were indicated by red and a green coloring, respectively.

Relationships between proteins encoded by the DEGs at the embryonic stages were visualized using STRING database version 12.0 (Szklarczyk et al., 2019). Networks were individually created for each developmental stage. Interactions were predicted based on a confidence score computed by combining the probabilities from experimental, co-expression, co-occurrence, neighborhood, text mining, and database evidence corrected for the probability of randomly observing an interaction. Interactions with a medium confidence score (0.4) are shown. The thickness of the connecting lines indicates the strength of the interaction. Proteins were assigned to one of three clusters according to their global interaction score. Clusters were created with the KMEANS algorithm. Interactions between clusters are shown by dotted lines. Analysis was performed using False Discovery Rate (FDR <0.1) without limiting to 1.5 times fold change. Gene ontology and pathway enrichment was done in Reactome using Human orthologues (Fabregat et al., 2018) to determine whether the genes were separated into specific categories.

2.3 Statistical analysis

Candidate DEGs were initially identified based on a p-value threshold of less than 0.05. To control for multiple testing, the FDR step-up method was utilized, with a criterion of an FDR step-up value less than or equal to 0.1. Additionally, a fold change requirement of less than −1.5 or greater than 1.5 was applied to identify DEGs. This approach ensured the selection of genes that are both statistically significant and show substantial changes in expression levels. Significant interactions among gene sets were determined at $p \leq 0.05$. Statistical analysis was performed using One way ANOVA followed by Tukey's multiple comparison post-test using the GraphPad Prism eight software (GraphPad software, Boston, United States). The differences were considered significant when the p-value was <0.05 ($*p < 0.05$; $**p < 0.01$).

3 Results

3.1 Alignment results

Comprehensive QA/QC results for samples used in this study are shown in Table 2. Key metrics, including coverage, alignment, average coverage depth, average sequence length, average sequence quality, and %GC content, have been summarized. High alignment percentages around 97% indicate robust alignment to the reference genome, ensuring the reliability of the sequencing data. Moreover, the stable average sequence length at approximately 50.97 base pairs emphasized the uniformity of sequenced fragments, that allowed robust downstream data analysis. The average sequence quality scores, ranging from 36.19 to 39.21, reflect the accuracy of base calling, with higher scores indicating lower sequencing errors. Furthermore, the %GC content, consistently ranging from 48.54% to 50.84%, suggested a homogeneous base composition among the samples.

3.2 Differentially expressed genes in rat brain

Analysis of differentially expressed genes in rat brains from E12 to E14 was performed to identify sex differences during early embryogenesis. The number of genes with higher read counts in

TABLE 2 Alignment statistics.

Sample	Coverage	Aligned	Average Depth	Average Length	Average Quality	%GC
E12 Male-1	4.88925	97.78	21.7383	50.9759	36.1853	49.0329
E12 Male-2	6.1667	97.94	17.9316	50.9761	36.1916	48.7357
E12 Male-3	5.3285	97.88	17.0218	50.9763	36.1915	49.164
E12 Female-1	6.2791	97.87	21.1414	50.9762	36.1913	48.8289
E12 Female-2	5.72136	97.96	19.2717	50.9765	36.1973	48.8719
E12 Female-3	6.45545	97.92	18.091	50.9764	36.2007	48.6667
E13 Male-1	4.87876	97.66	11.8507	50.9636	38.5991	50.1077
E13 Male-2	4.88408	97.49	11.5121	50.9566	38.3518	50.1377
E13 Male-3	5.27774	97.72	11.9268	50.9632	38.5984	49.4595
E13 Female-1	7.36217	97.76	14.9687	50.9672	38.7602	49.7626
E13 Female-2	5.22015	97.77	11.0533	50.9629	38.591	49.2864
E13 Female-3	5.29042	97.64	10.6814	50.9627	38.5698	49.4276
E14 Male-1	9.24112	97.71	15.558	50.9652	38.6291	50.6518
E14 Male-2	6.60427	97.55	11.7672	50.9691	39.0414	49.8576
E14 Male-3	7.62769	97.65	13.6377	50.9824	39.2096	49.9381
E14 Female-1	9.08841	97.66	17.3476	50.9704	38.9529	49.2044
E14 Female-2	4.68918	97.57	9.4766	50.9624	38.5578	50.8363
E14 Female-3	5.09087	97.67	11.9699	50.9628	38.6121	49.8906

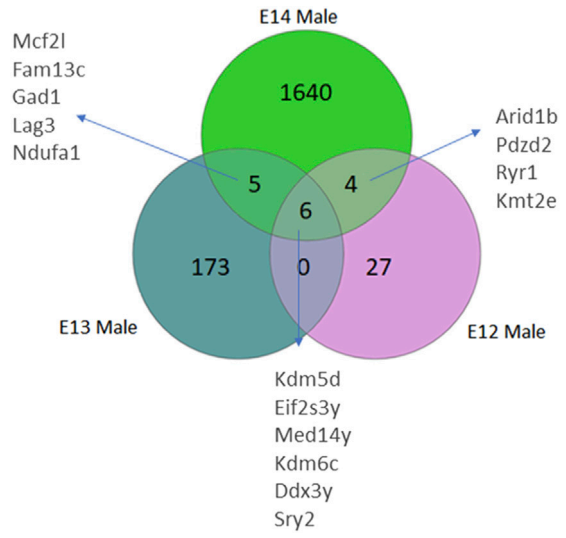

FIGURE 1
Venn diagrams illustrate the number of differentially expressed genes (DEGs) in male rats, categorized by their developmental stage. DEGs were identified based on an adjusted *p*-value <0.05, following False Discovery Rate (FDR) correction. DEGs common to multiple stages are also annotated.

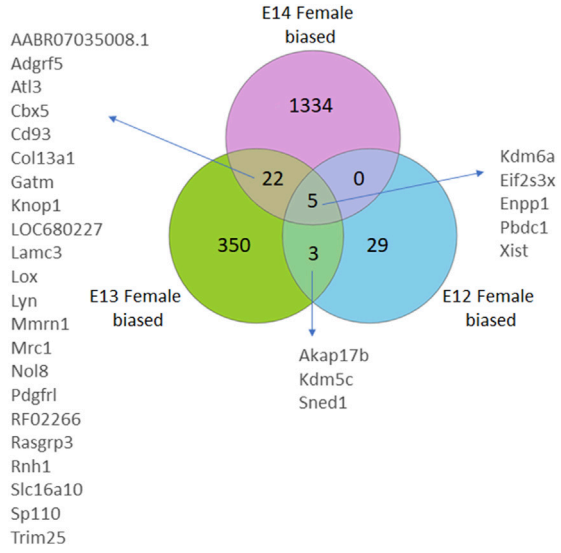

FIGURE 2
Venn diagrams illustrate the number of differentially expressed genes (DEGs) in female rats, categorized by their developmental stage. DEGs were identified based on an adjusted *p*-value <0.05, following False Discovery Rate (FDR) correction. DEGs common to multiple stages are also annotated.

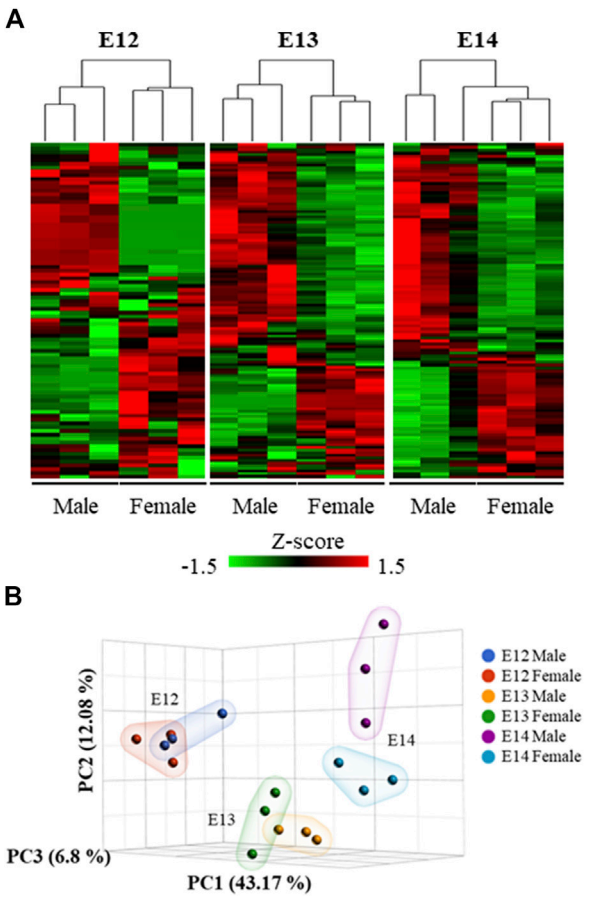

FIGURE 3
Hierarchical clustering and heat map of the differentially expressed genes. **(A)** The expression patterns at the three studied developmental stages were visualized using standardized gene expression values (z-scores). **(B)** 3D scatter plot illustrates the results of a Principal Component Analysis (PCA) performed on gene expression data from male and female embryos at different developmental stages.

male brains compared to female brains increased from E12 to E14 (Figure 1; Supplementary Figure S1). At E12, only 37 genes had higher read counts in males, and this number increased to 184 at E13 and 1,655 genes at E14 (Supplementary Table S2). Of these genes, six Y-chromosome genes were differentially expressed at all three developmental stages. In addition, there is an overlap of five DEGs between stages E13 and E14. Furthermore, a set of four genes exhibits differential expression at both E12 and E14. It was interesting to note that there were no overlapping genes between E12 and E13 except for the six Y-chromosome genes.

The gene expression profile in female brains followed a similar pattern with the numbers of female biased genes increasing from E12 to E14 (Figure 2; Supplementary Figure S1). Here, four X-chromosome genes, and one autosomal gene, had significantly higher read counts in female brain at all three developmental stages. Moreover, an overlap of three genes was observed between E12 and E13, and 22 DEGs were common between E13 and E14. Notably, there were no common DEGs between E12 and E14 except for the four X chromosome genes, and one autosomal gene, that overlapped in all three stages.

Analysis of the overall gene expression pattern clearly grouped the brains into male and female (Figure 3A). A separation between the sexes at the later stages is apparent from the PCA analysis where the two sexes are clearly separated at E14 (Figure 3B).

Analysis of abundance and changes in Y chromosome genes was performed by calculating reads per million instead of fold change as these genes are not present in females (Supplementary Figure S2). Manual inspection of the *Sry* reads located at the correct position ensured that the low read counts were not merely noise. The highest expression of the *Sry* genes was observed for *Sry2* (Supplementary Figure S2A). The expression levels of *Sry2* were highest at E12 (Figure 4A). The brain specific expression of *Sry* genes was verified by qPCR, confirming that *Sry* expression was highest at E12 (Supplementary Figure S3). The remaining *Sry* genes showed much lower expression and no stage specific differences (Supplementary Figure S2B-I). It is interesting to note that *Sry2* is located within an *Kdm5d* gene intron in opposite direction of *Kdm5d* (Supplementary Figure S2J). The other Y-chromosome genes that were overlapping between all three stages are shown in Figure 4. Of these, *Eif2s3y* showed a similar expression pattern as *Sry2*, with downregulation from E12 to E14 (Figure 4B). *Ddx3y* (Figure 4C), *Kdm5d* (Figure 4D), and Kdm6c (Figure 4E) showed statistically significant upregulation from E12 to E14. The *Med14y* gene was upregulated from E13 to E14 (Figure 4F), together with the X-chromosome linked *Med14* gene.

Four X-chromosome linked genes, *Kdm6a*, *Eifs3x*, *Pbdc1* and *Xist* were present at all developmental stages with higher expression in females than in males (Figure 5). Of these, *Xist* was upregulated during embryogenic development in female brain and showed no expression in male brain (Figure 5A). The brain specific expression of *Xist* was verified by qPCR, confirming the upregulation from E12 to E14 (Supplementary Figure S2). *Kdm6a* was only downregulated in female brains at E14 (Figure 5B). *Eif2s3x*, and *Pbdc1* were downregulated in both male and female brains (Figures 5C, E). Also present at all developmental stages was *Enpp1*, coding for an enzyme involved in ATP cleavage, located on chromosome 1. *Enpp1* showed higher expression in female brains at E12 and E13 (Figure 5D). At E14 *Enpp1* was downregulated in both sexes and no sex difference remained. While *Kdm6a* was upregulated at all three developmental stages, the *Kdm5c* gene showed female biased expression at E12 and E13. Both the X-linked *Akap17b* gene and the *Sned1* gene (chromosome 9) showed female biased expression at E12 and E13. There were no common autosomal DEGs between all three developmental stages. However, several autosomal genes associated with proper neuronal functions had higher read counts in male brains at E12 (Supplementary Table S1). These include neuregulin 1 (*Nrg1*, normal development of nervous system), amyloid beta precursor protein (*App*, neural plasticity, and synapse formation), DnaJ Heat Shock Protein Family (*Hsp40*) Member A3 (*Dnaja3*, associated with Alzheimer disease), interleukin one receptor type 1 (*Il1r1*, neuron migration), and neuroligin 1 (*Nlgn1*, synapse function). In addition, ethanolamine kinase 2 (*Etnk2*) which is involved in choline metabolism also had higher read counts in the male rat brain at E12. In female brains, three genes stood out as

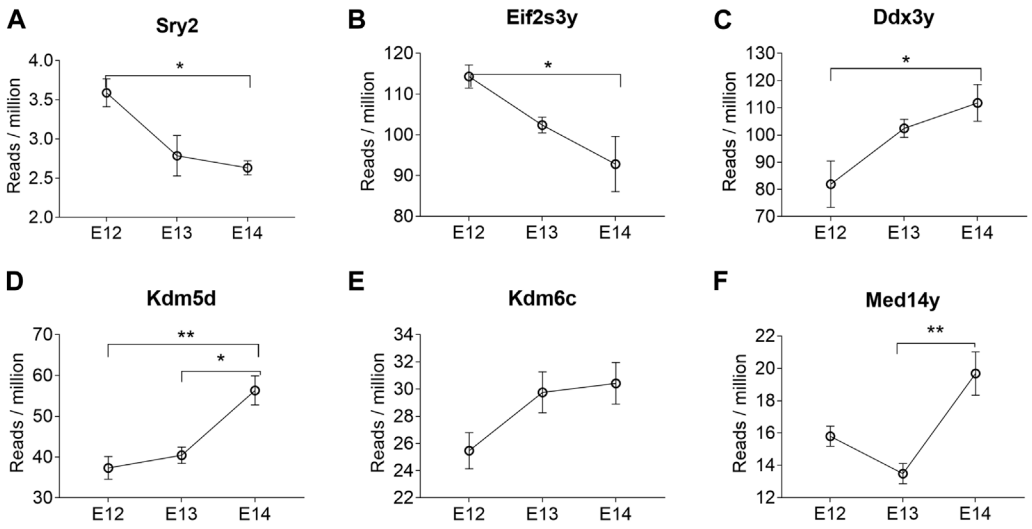

FIGURE 4
Y chromosome genes differentially expressed at all three developmental stages in male rat brains. The reads per million of DEGs at all three developmental stages are shown. Statistical analysis was performed using One way ANOVA followed by Tukey's multiple comparison post-test (*p < 0.05 and **p < 0.01) (n = 3, mean ± SEM).

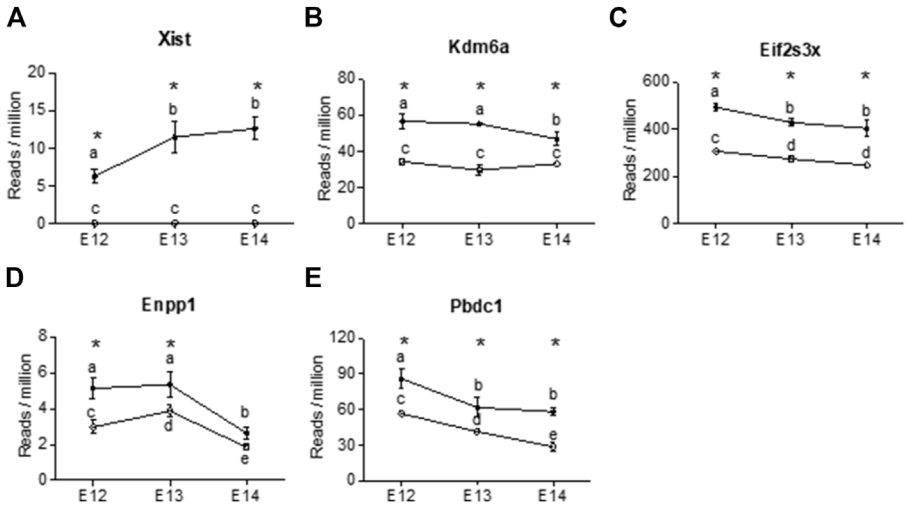

FIGURE 5
X chromosome genes were differentially expressed at all three developmental stages in female rat brain (closed circles). The reads per million of DEGs at all three developmental stages are shown For male brains (open circles) only three of the genes showed differences in reads per million between developmental stages. **(A)** Xist, **(B)** Kdm6a, **(C)** Eifs2s3x, **(D)** Enpp1, **(E)** Pbdc2. Statistical analysis was performed using One way ANOVA followed by Tukey's multiple comparison post-test. Different letters were used to denote the level of significance between stages, and asterisk was used to denote statistical differences between sexes at p < 0.05 (n = 3, mean ± SEM).

highly expressed at E12. These were *Somatostatin* (*Sst*), *Cytochrome P450 26b1* (*Cyp26b1*) and (*Cyp2j4*).

3.3 Sex and stage specific effects on biological processes

Gene Ontology (GO) enrichment analysis showed consistent and evolving patterns across the three distinct embryonic stages (Figure 6). Biological processes (BP) crucial to development and regulation, such as developmental process, regulation of nervous system development, and neuron differentiation, exhibited sustained enrichment. However, the interplay of sex-specific influences within these enriched processes emerged when sex ratios were considered for the pathways. At the E12 stage, genes associated with the enriched processes displayed a higher expression in males, emphasizing a potential male gene dominance in these developmental pathways at this point. Interestingly, this dynamic shifted during the E13 stage, with a notable trend towards female gene regulation, suggesting a

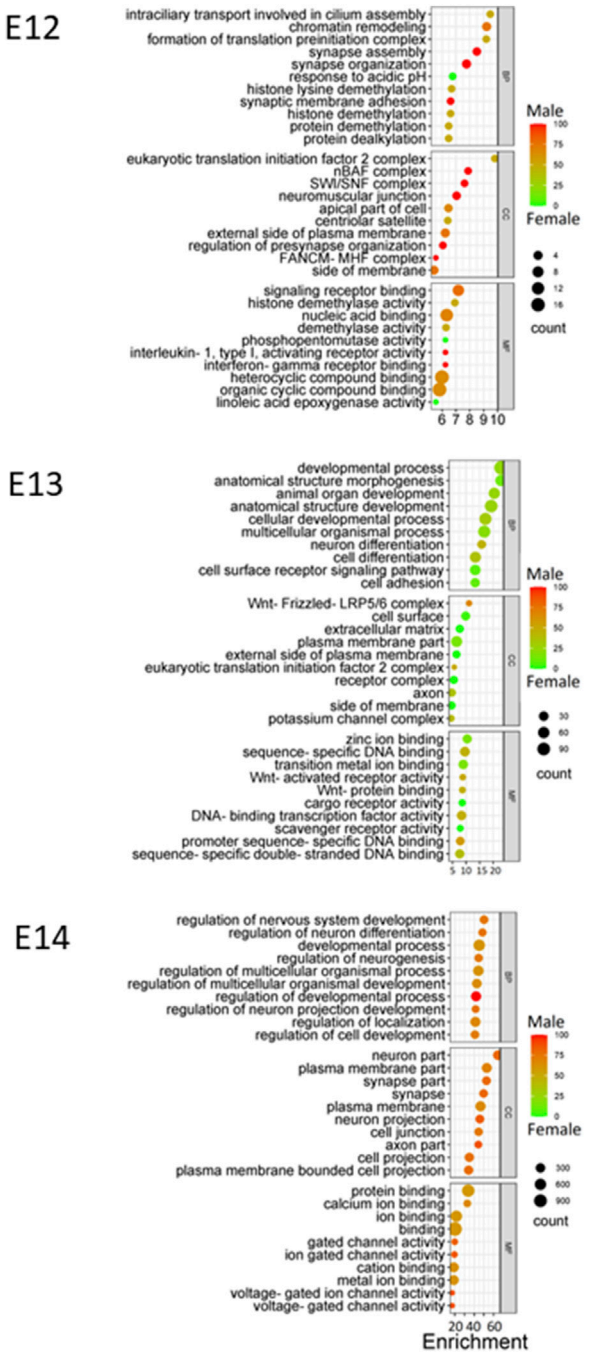

FIGURE 6
GO enrichment at E12 to E14. Bubble plots were constructed to visually represent Gene Ontology (GO) annotations for each embryonic stage utilizing DEGs identified at each stage, providing a comprehensive overview of the functional categories that are enriched during development. Enriched biological processes (BP), cellular components (CC), and molecular functions (MF) are presented using color gradient to represent the percentage of sex bias for given terms. Red color indicates male dominated enrichment while green color indicates female dominated enrichment.

transitional period in the influence of different sexes. Finally, by the E14 stage, there was a reversion to a male influence, indicating the complexity and variability of sex-specific contributions to development across different stages.

Throughout the embryonic stages, certain cellular components (CC) were consistently enriched. The plasma membrane part, synapse part, and neuron part emerged as recurrently enriched components (Figure 6). Moreover, molecular functions (MF) that encompass binding and receptor activity, including zinc ion binding, sequence-specific DNA binding, and signaling receptor binding, were also consistently enriched across stages. Additionally, the variations in sex percentage involvement across processes, components, and functions provide an intriguing opportunity for further investigation into the interplay between genetics, sex-specific influences, and developmental outcomes.

3.4 Brain sex development leads to differentially enriched pathways

The analysis of enriched pathways in the KEGG database showed significant sex differences across the embryonic stages, which is in line with the dynamic nature of embryonic development (Table 3; Supplementary Figure S4). The *p*-values associated with these pathways provided a measure of statistical significance. Some pathways, particularly at later stages, displayed exceptionally low *p*-values, suggesting high statistical significance. In contrast, pathways at E12, such as riboflavin metabolism, exhibited relatively higher *p*-values, indicating less statistically significant associations. The analysis revealed that certain pathways are particularly associated with specific embryonic stages. Notably, embryonic stage E13 was characterized by pathways related to disease and viral infections such as gastric cancer, proteoglycans in cancer, and human papillomavirus infection. In contrast, at embryonic stage E14, neural and cellular processes dominated, with nicotine addiction and glutamatergic synapse showing noteworthy significance. The number of genes associated with these pathways varied significantly between stages and they increased in number as the development of the embryo progressed (Table 3). This was in line with the increasing number of DEGs for consecutive stages. Although the *p*-values and gene counts differed, several pathways, such as extracellular matrix (ECM)-receptor interaction and Focal adhesion, were enriched in both E13 and E14 indicating that these pathways play significant roles in both stages of embryonic development. At embryonic stage E14, a distinct cluster of pathways related to cardiac function and signaling was observed. Pathways such as Hypertrophic cardiomyopathy and Arrhythmogenic right ventricular cardiomyopathy indicated a critical period for the development of the cardiac system during this stage (Table 3).

3.5 Predicted stage specific functional protein networks during sex differentiation of the brain

Functional gene network of neural development genes showed significant associations/interactions among differentially expressed genes in the three developmental stages (Supplementary Figure S5). In each stage, three distinct clusters were identified. There were also interactions among protein products within or between neighboring clusters. Interacting proteins contribute to a shared function, an

10.3389/fcell.2024.1343800

TABLE 3 Enrichment of KEGG pathways among DEGs from E12 to E14.

E12					
Pathway	Enrichment	List	Female biased	Male biased	Male%
Riboflavin metabolism	3.73	7	1	0	0
Inflammatory mediator regulation of TRP channels	3.46	91	1	1	50
Serotonergic synapse	3.26	102	1	1	50
Pantothenate and CoA biosynthesis	2.94	17	1	0	0
E13					
Gastric cancer	11.15	132	8	3	27
Proteoglycans in cancer	9.92	181	10	2	17
Human papillomavirus infection	9.33	292	11	4	27
PI3K-Akt signaling pathway	9.3	293	13	2	13
Signaling pathways regulating pluripotency of stem cells	6.69	126	6	2	25
MicroRNAs in cancer	6.27	135	7	1	13
Hippo signaling pathway	6.18	137	6	2	25
Breast cancer	6.18	137	6	2	25
Cushing's syndrome	6.14	138	6	2	25
Basal cell carcinoma	5.98	55	3	2	40
Hepatocellular carcinoma	5.28	160	6	2	25
ECM-receptor interaction	4.9	72	5	0	0
Glutamatergic synapse	4.84	104	5	1	17
Pathways in cancer	4.72	468	12	3	20
Focal adhesion	4.5	184	8	0	0
E14					
Nicotine addiction	17.33	20	1	16	94
Glutamatergic synapse	10.25	84	3	23	88
DNA replication	9.39	22	12	0	0
Protein digestion and absorption	9	55	11	8	42
GABAergic synapse	8.29	64	2	18	90
Morphine addiction	7.95	66	2	18	90
Relaxin signaling pathway	7.38	98	11	14	56
Axon guidance	7.31	141	5	27	84
Arrhythmogenic right ventricular cardiomyopathy (ARVC)	6.75	52	6	10	63
Taste transduction	6.48	38	0	13	100
ECM-receptor interaction	6.34	60	14	3	18
Dilated cardiomyopathy (DCM)	6.28	66	6	12	67
Focal adhesion	6.19	159	24	9	27
Hypertrophic cardiomyopathy (HCM)	6.19	61	6	11	65
Synaptic vesicle cycle	6.14	45	1	13	93
Insulin secretion	5.9	63	3	14	82

indication of biological interactions. In all developmental stages, Y chromosome genes showed a distinct network and interacted with X-linked genes. At embryonic stage E12, multiple interactions were observed among autosomal proteins involved in signal transduction and neural development and function. In E13, highly expressed genes involved in the development of the reproductive system, produced a distinct network. At embryonic stage E14, a large network of highly expressed genes involved in neural development and gene expression was observed. The reactome analysis furthermore indicates pathway similarities and differences between the three stages (Supplementary Figure S6). At E12 and E13 both developmental biology and signal transduction pathways are enriched, while at E14 developmental and extracellular matrix organization is augmented.

4 Discussion

In the present study our aim was to further the understanding of early key events in the process of sex differentiation of the brain. Earlier studies on zebra finch (Agate et al., 2003), mouse (Dewing et al., 2003), and chicken (Lee et al., 2009) suggest involvement of genetic signals in the development of male and female brain neuronal networks. By performing a temporal analysis of gene expression patterns in the early developing brain, around the time of gonadal sex differentiation we were able to determine temporal the regulation of differentially expressed genes. The gene expression pattern gave insight into the increased specialization of the brain, occurring from E12 to E14 and revealed sex biased enriched pathways related to nicotine and morphine addiction.

From experiments using the four-core mouse model it is apparent that Sry is needed for sex differentiation of both gonadal and somatic cells (Arnold, 2009). However, until now it has been unclear if *Sry* is expressed in neuronal cells during sex differentiation of the brain. RNA sequencing of rat embryonic brains revealed the presence of *Sry2* with the highest expression already at the first studied embryonal stage, E12. The expression of *Sry* in rat gonads is detectable at E11 with the expression of *Sry2* followed by the upregulation of other *Sry1*, *Sry3C* and *Sry4a* at E12 (Prokop et al., 2020). At later stages, *Sry4a* appears to be the main form expressed in rat testis (Prokop et al., 2020). Sequence analysis of the different *Sry* isoforms in rat shows that they differ in amino acid sequence with *Sry2* having two point mutations (H4Q and R21H) in the first helix of the HMG box, leading to reduced nuclear translocation (Prokop et al., 2013; Prokop et al., 2016). This has led to questioning the ability of *Sry2* to translocate to the nucleus and activate gene transcription. However, it has been shown that transfection of Chinese hamster ovarian (CHO) cell lines with the *Sry2* transcript results in activation of downstream genes (Milsted et al., 2010; Prokop et al., 2016). In the earlier study *Sry2* was compared to *Sry1* and *Sry3* for its ability to regulate the renin-angiotensin system (Milsted et al., 2010). While *Sry1* and *Sry3* were more potent than *Sry2* it remains that all three isoforms could regulate the renin-angiotensin system. In the later study expression of the *Sry1*, *Sry2* and *Sry3* isoforms in CHO cells resulted in translocation to the nucleus all three isoforms, with *Sry2* showing equal distribution between nucleus and cytosol (Prokop et al., 2016). Thus, while *Sry2* appears to be less efficient at nuclear translocation and activation of downstream gene regulation it still is functional.

In mice testis, *Sry* first appears at 10.5 dpc, peaks at 11.5 dpc, and by 12.5 dpc the expression is undetectable (Larney et al., 2014). *Sry* has previously been reported to be expressed in adult mouse and human male brains (Mayer et al., 1998; Vawter et al., 2004; Dewing et al., 2006; Czech et al., 2012). In male rat gonads, *Sry* expression peaks at E12 (Prokop et al., 2020). However, at this stage the gonad is still underdeveloped (Val et al., 2003). Hence, it can be assumed that steroid secretion is still not initiated from the testis at E13. Thus, it can be concluded that the differential gene expression profiles observed for rat brains at E12 occur prior to hormonal actions on the brain.

In mice brain at E10.5 it was observed that *Eif2s3y* and *Dby* (*Ddx3y*) had the highest fold differential expression in males (Dewing et al., 2003). The remaining genes indicated to be differentially expressed were not located on the Y chromosome (Dewing et al., 2003). In the present study, we identified an increasing number of male biased genes from E12 to E14. There were six Y-chromosome genes showing differential expression at all developmental stages. Besides *Sry2*, we also identified both *Eif2s3y* and *Ddx3y* as early upregulated genes in the male brain. Of these two genes, *Eif2s3y* showed a similar expression profile as *Sry2*, with the highest expression at E12. Overexpression of *Eif2s3y* in mouse neurons has been shown to lead to autism-like behavior in male mice (Zhang et al., 2021). Several autosomal genes (*Nrg1*, *App*, *Dnaja3*, *Il1r1*, *Arid1b*, and *Nlgn1b*) that were upregulated at E12 are also associated with neuronal functions (Mucke et al., 1996; Stefansson et al., 2004; Tabarean et al., 2006; Martinez-Mir et al., 2013; Ka et al., 2016; Zhou et al., 2020). These results show that the early gene expression pattern in male mice is closely connected to neuronal outcomes in adult males.

In the present study we identified four Y chromosome genes, expressed at all three stages, with homologues on the X chromosome that escape X chromosome inactivation. These were *ddx3y*, *eif2s3y*, *kdm5d*, and *kdm6c*. In female brain the X chromosome homologues to three of these genes, *eif2s3x*, *kdm5c*, and *kdm6a* showed female biased expression, suggesting that the Y chromosome homologues could complement the expression of the X chromosome genes. However, it is worth noting that for all four Y chromosome genes it has been established that their functions are overlapping, but not identical, to their X chromosome counterpart (Mayfour et al., 2019; Shen et al., 2022; Dicke et al., 2023; Li et al., 2023; Liu et al., 2023; Rock et al., 2023). Thus, the sex differences in regulation of these genes may lead to sex specific functions. *Ddx3y* showed increasing expression in brain from E12 to E14. *Ddx3y* and *Kdm6c*, are both located in the AZFa region of the Y-chromosome. The AZFa, b, and c regions on the Y-chromosome have been identified to be required for normal spermatogenesis (Vog et al., 1996). In the AZFa region, it has been suggested that *Ddx3y* is the main gene responsible for infertility (Foresta et al., 2000). In male gonads, *Ddx3y* is expressed in spermatogonia before meiosis and *Ddx3x* is expressed in spermatids (Rauschendorf et al., 2014). Deletion of *Ddx3y* disrupts germ cell development and leads to infertility in males (Ramathal et al., 2015; Dicke et al., 2023). The increased

expression of *Ddx3y* from E12 to E14 in rat brain indicate that this gene has key functions in male brain development.

Kdm5d and *Kdm6c* were both present at all three developmental stages with *Kdm5d* being upregulated from E12 to E14. The functions of both genes have been shown to differ from their X chromosome homologues (Meyfour et al., 2019; Rock et al., 2023). These genes are active demethylases, acting on Lys 27 of histone H3 (Shpargel et al., 2012; Walport et al., 2014). *Kdm6c* shows >88% similarity with *Kdm6a* and has recently been shown to be an active demethylase, demethylating H3K27, but with lower activity than KDM6A (Walport et al., 2014). Kdm6a regulation of H3K27me3 has been indicated to be an important regulator in embryonic stem cells (Welstead et al., 2012). It was also shown that Kdm6c complemented Kdm6a during cellular differentiation. Both genes have been demonstrated to be important for male neurogenesis (Pottmeier et al., 2020).

While few Y-chromosome genes overlapping in males between all three stages, the number of X-chromosome and autosomal genes increased over time in male brains. At E12, *Foxo4* was the only X-chromosome gene upregulated in the male brain. *Foxo4* is a member of the FOXO family that regulates genes involved in metabolism (Liu et al., 2020). In a study on triple knock-out mice, the loss of *Foxo4*, together with *Foxo1* and *Foxo3*, was shown to reduce insulin responses in male, but not female mice (Penniman et al., 2019). In pathway enrichment analysis, Foxo4 and T-box transcription factor 20 (Tbx20) enriched carcinogenesis developmental process in E12, indicating a crucial role of the genes in the early heart development in male. While FOXO4 along with NKX2-5, and MEF2C bind the promoter of the MYOCD (Myocardin) gene, TBX20 and ISL1: LDB1 complex bind the anterior heart field enhancer of the MEF2C gene during cardiogenesis (Takeuchi et al., 2005; Creemers et al., 2006). The role of *Foxo4* in male brain development is of interest for further studies. In female brains *Xist* showed the highest expression with an upregulation from 12 to E13. In addition to *Xist*, *Kdm5c* also showed increased expression at E13. The Y chromosome homologue, kdm5d, showed increased expression first at E14. It is worth noting that *Kdm5c*, but not *Kdm5d*, has been shown to be involved in the activation of *Xist* (Samanta et al., 2022).

Transcriptome analysis revealed that the progression from E12 to E14 resulted in increased specialization of the brain. Following male biased gene expression at E12 there was a shift toward female biased expression at E13 and again a shift back to male biased expression at E14 (Figure 6). A possible rational for this may be that the reprograming of the male brain at E12 requires more time to activate the new downstream genes compared to a continued differentiation of female neurons. Although it has not been explicitly demonstrated, research suggests that cell proliferation rates in the amygdala of rats may be higher in females compared to males (Krebs-Kraft et al., 2010). The GO enrichment analysis reveals dynamic patterns across embryonic stages, highlighting the role of sex in shaping developmental pathways. The consistent enrichment of certain cellular components and molecular functions underscores their importance in embryonic development. The enrichment of biological processes crucial to development and regulation, such as developmental process, regulation of nervous system development, and neuron differentiation, aligns with the understanding that these processes are fundamental to embryogenesis (Zhang et al., 2019).

Analysis of sex biased enriched pathways showed a strong male bias for nicotine and morphine addiction as well as GABAergic and glutamateric synapses at E14. The neuronal signalling is overlapping for these systems, and it has earlier been shown that they exhibit male biased expression in adults (D'Souza and Markou, 2013; Morgan and Ataras, 2022; Medrano et al., 2023). Nicotine exposure can lead to sex-dependent regulation of signalling pathways (Lee et al., 2021). This suggests that the sex biased effects on adults are established already during early development.

The Reactome pathway analysis indicated that the expression of *Rac1* and *Rock1* resulted in enriched semaphorin 4D. Semaphorin 4D axon guidance molecule influence cell migration and axon guidance which are essential for the proper formation and function of the nervous system (Jongbloets et al. 2014). These results show that axon guidance in nervous system development begin at E12. No neuronal development pathways were enriched during E13. We also observed enriched RHOH GTPase cycle, which regulates the proliferation, survival, migration, and engraftment of hematopoietic progenitor cells and specifically T cell development (Li et al., 2002; Yi et al., 2005). Rho GTPase activation is also associated with increased cancer cell invasiveness and associated with the development and progression of various cancers, including breast cancer, lung cancer, and skin cancer (Murray et al., 2014; Butera et al., 2020).

At E14, NCAM signaling for neurite out-growth and the L1CAM interaction axon guidance pathways were significantly overrepresented by DEGs. Three of the 4 DEGs in the NCAM signaling for neurite out-growth, *Cacna1i*, *Cacna1d*, and *Cacna1h*, were upregulated at E14. Similarly, four of the 5 DEGs, *Dlg3*, *Dcx*, *Ank3*, and *L1cam*, that enriched the L1CAM interactions were upregulated. The NCAM and L1CAMs are involved in the formation and maintenance of the nervous system. These neural adhesion molecules act as coreceptors for integrins, growth factors and axon guidance/axon pathfinding receptorsduring nervous system development (Schmid and Maness, 2008; Russell and Bashaw, 2018).

In the present study, we have mapped temporal expression patterns in male and female rat brains. The result shows that a limited number of Y-chromosome and X-chromosome genes are involved in all three studied embryonic stages, forming a cluster of interacting genes. In contrast, the expression of autosomal genes was highly stage specific with no gene involved in all three stages. This suggests that once the signaling for sex determination has been activated, there is a progression in functions that will be developed. In addition, the shift from male to female and back to male gene bias from E12 to E14, indicates that the shift from female to male brain requires more time than the direct development of the female brain. The present study reveals that one of the *Sry* genes, *Sry2,* peaked at E12 or earlier, together with *Eif2s3y*. This is followed by the upregulation of *Ddx3y* and *Kdm5d*. The results suggest that *Sry2* is involved in the early sex differentiation cascade for the male brain.

Data availability statement

The datasets presented in this study can be found in online repositories. The names of the repository/repositories and accession number(s) can be found below: https://www.ncbi.nlm.nih.gov/, PRJNA1046089.

Ethics statement

Ethical approval was not required for the studies on animals in accordance with the local legislation and institutional requirements because only commercially available established cell lines were used.

Author contributions

BP: Data curation, Formal Analysis, Investigation, Methodology, Validation, Writing–original draft, Writing–review and editing. SP: Formal Analysis, Investigation, Methodology, Writing–original draft, Writing–review and editing. YB: Formal Analysis, Investigation, Methodology, Writing–review and editing. P-EO: Conceptualization, Formal Analysis, Funding acquisition, Investigation, Project administration, Resources, Supervision, Writing–original draft, Writing–review and editing.

Funding

The author(s) declare that financial support was received for the research, authorship, and/or publication of this article. This study was financed by the Swedish Research Council (Grant number 2019-04455) and Örebro University.

Acknowledgments

We are grateful to Dr. Carina Modig for proofreading the manuscript.

Conflict of interest

The authors declare that the research was conducted in the absence of any commercial or financial relationships that could be construed as a potential conflict of interest.

Publisher's note

Supplementary material

The Supplementary Material for this article can be found online at: https://www.frontiersin.org/articles/10.3389/fcell.2024.1343800/full#supplementary-material

References

Agate, R. J., Grisham, W., Wade, J., Mann, S., Wingfield, J., Schanen, C., et al. (2003). The gender of the voice within: the neural origin of sex differences in the brain. *Curr. Opin. Neurobiol.* 13 (6), 759–764. doi:10.1016/j.conb.2003.10.005

Alganmi, N., and Abusamra, H. (2023). Evaluation of an optimized germline exomes pipeline using BWA-MEM2 and Dragen-GATK tools. *PLOS ONE* 18, e0288371. doi:10.1371/journal.pone.0288371

Anders, S., and Huber, W. (2010). Differential expression analysis for sequence count data. *Genome Biol.* 11 (10), R106. doi:10.1186/gb-2010-11-10-r106

Arnold, A. P. (2009). The organizational-activational hypothesis as the foundation for a unified theory of sexual differentiation of all mammalian tissues. *Horm. Behav.* 55 (5), 570–578. doi:10.1016/j.yhbeh.2009.03.011

Bordt, E. A., Ceasrine, A. M., and Bilbo, S. D. (2020). Microglia and sexual differentiation of the developing brain: a focus on ontogeny and intrinsic factors. *Glia* 68 (6), 1085–1099. doi:10.1002/glia.23753

Butera, A., Cassandri, M., Rugolo, F., Agostini, M., and Melino, G. (2020). The ZNF750–RAC1 axis as potential prognostic factor for breast cancer. *Cell Death Discov.* 6 (1), 135. doi:10.1038/s41420-020-00371-2

Creemers, E. E., Sutherland, L. B., McAnally, J., Richardson, J. A., and Olson, E. N. (2006). Myocardin is a direct transcriptional target of Mef2, Tead and Foxo proteins during cardiovascular development. *Development* 133 (21), 4245–4256. doi:10.1242/dev.02610

Czech, D. P., Lee, J., Sim, H., Parish, C. L., Vilain, E., and Harley, V. R. (2012). The human testis-determining factor *SRY* localizes in midbrain dopamine neurons and regulates multiple components of catecholamine synthesis and metabolism. *J. Neurochem.* 122 (2), 260–271. doi:10.1111/j.1471-4159.2012.07782.x

Dewing, P., Chiang, C. W., Sinchak, K., Sim, H., Fernagut, P. O., Kelly, S., et al. (2006). Direct regulation of adult brain function by the male-specific factor *SRY*. *Curr. Biol.* 16 (4), 415–420. doi:10.1016/j.cub.2006.01.017

Dewing, P., Shi, R. T., Horvath, S., and E. Vilain, E. (2003). Sexually dimorphic gene expression in mouse brain precedes gonadal differentiation. *Brain Res. Mol. Brain Res.* 118 (1-2), 82–90. doi:10.1016/s0169-328x(03)00339-5

Dicke, A. K., Pilatz, A., Wyrwoll, M. J., Punab, M., Ruckert, C., Nagirinaja, L., et al. (2023). Ddx3y is likely the key spermatogenic factor in the AZFa region that contributes to human non-obstructive azoospermia. *Commun. Biol.* 6, 350. doi:10.1038/s42003-023-04714-4

D'Sousa, M. S., and Markou, A. (2013). The "Stop" and "go" of nicotine dependence: role of GABA and Glutamate. *Cold Spring Harb. Perspect. Med.* 3, a012146. doi:10.1101/cshperspect.a012146

Fabregat, A., Jupe, S., Matthews, L., Sidiropoulos, K., Gillespie, M., Garapati, P., et al. (2018). The reactome pathway knowledgebase. *Nucleic Acids Res.* 46 (D1), D649–D655. doi:10.1093/nar/gkx1132

Foresta, C., Ferlin, A., and Moro, E. (2000). Deletion and expression analysis of AZFa genes on the human Y chromosome revealed a major role for DBY in male infertility. *Hum. Mol. Genet.* 9 (8), 1161–1169. doi:10.1093/hmg/9.8.1161

Gahr, M., and Metzdorf, R. (1999). The sexually dimorphic expression of androgen receptors in the song nucleus hyperstriatalis ventrale pars caudale of the zebra finch develops independently of gonadal steroids. *J. Neurosci.* 19 (7), 2628–2636. doi:10.1523/JNEUROSCI.19-07-02628.1999

Hanley, N. N., Hagan, D. M., Clement-Jones, M., Ball, S. G., Srachan, T., Salas-Cortés, L., et al. (2000). *Sry, Sox9*, and *Dax1* expression patterns during human sex determination and gonadal development. *Mech. Dev.* 91, 403–407. doi:10.1016/s0925-4773(99)00307-x

Ingalhalikar, M., Smith, A., Parker, D., Satterthwaite, T. D., Elliott, M. A., Ruparel, K., et al. (2014). Sex differences in the structural connectome of the human brain. *PNAS* 111 (2), 823–828. doi:10.1073/pnas.1316909110

Johansson, M. M., Lundin, E., Qian, X., Mirzazadeh, M., Halvardson, J., Darj, E., et al. (2016). Spatial sexual dimorphism of X and Y homolog gene expression in the human central nervous system during early male development. *Biol. Sex. Diff.* 7, 5. doi:10.1186/s13293-015-0056-4

Jongbloets, B. C., Jeroen, R., and Pasterkamp, R. J. (2014). Semaphorin signalling during development. *Development* 141, 3292–3297. doi:10.1242/dev.105544

Ka, M., Chopra, D. A., Dravid, M. S., and Kim, W. Y. (2016). Essential roles for ARID1B in dendritic arborization and spine morphology of developing pyramidal neurons. *J. Neurosci.* 36 (9), 2723–2742. doi:10.1523/JNEUROSCI.2321-15.2016

Koopman, P. (2005). Sex determination: a tale of two Sox genes. *Trends Genet.* 21 (7), 367–370. doi:10.1016/j.tig.2005.05.006

Krebs-Kraft, D. L., Hill, M. N., Hillard, C. J., and McCarthy, M. M. (2010). Sex difference in cell proliferation in developing rat amygdala mediated by endocannabinoids has implications for social behavior. *PNAS* 107 (47), 20535–20540. doi:10.1073/pnas.1005003107

Larney, C., Bailey, T. L., and P. Koopman, P. (2014). Switching on sex: transcriptional regulation of the testis-determining gene *Sry*. *Development* 141 (11), 2195–2205. doi:10.1242/dev.107052

Lee, A. M., Mansuri, M. S., Wilson, R. S., Lam, T. T., Nairn, A. C., and Picciotto, M. R. (2021). Sex differences in the ventral tegmental area and nucleus accumbens proteome at baseline and following nicotine exposure. *Front. Mol. Neurosci.* 14 (14), 657064. doi:10.3389/fnmol.2021.657064

Lee, S. I., Lee, W. K., Shin, J. H., Han, B. K., Moon, S., Cho, S., et al. (2009). Sexually dimorphic gene expression in the chick brain before gonadal differentiation. *Poult. Sci.* 88 (5), 1003–1015. doi:10.3382/ps.2008-00197

Li, X., Bu, X., Lu, B., Avraham, H., Flavell, R. A., and Lim, B. (2002). The hematopoiesis-specific GTP-binding protein RhoH is GTPase deficient and modulates activities of other Rho GTPases by an inhibitory function. *Mol. Cell Biol.* 22 (4), 1158–1171. doi:10.1128/mcb.22.4.1158-1171.2002

Li, Y., Wu, W., Xu, W., Wang, Y., Wan, S., Cjen, W., et al. (2023). *Eif2s3y* alleviated LPS-induced damage to mouse testis and maintained spermatogenesis by negatively regulating *Adamts5*. *Theriogenology* 211, 65–75. doi:10.1016/j.theriogenology.2023.08.003

Liu, W., Li, N., Zhang, M., Arisha, A. H., and Hua, J. (2023). The role of Eif2s3y in mouse spermatogenesis and ESC. *Curr. Stem Cell Res. Ther.* 17, 750–755. doi:10.2174/1574888X16666211102091513

Liu, W., Yong, L., and Luo, B. (2020). Current perspective on the regulation of FOXO4 and its role in disease progression. *Cell Mol. Life Sci.* 77, 651–663. doi:10.1007/s00018-019-03297-w

Martinez-Mir, A., González-Pérez, A., Gayán, J., Antúnez, C., Marín, J., Boada, J. M., et al. (2013). Genetic study of neurexin and neuroligin genes in Alzheimer's disease. *J. Alzheimers Dis.* 35 (2), 403–412. doi:10.3233/JAD-122257

Mayer, A., Lahr, G., Swaab, D. F., Pilgrim, C., and Reisert, I. (1998). The Y-chromosomal genes *SRY* and ZFY are transcribed in adult human brain. *Neurogenetics* 1 (4), 281–288. doi:10.1007/s100480050042

Mayer, A., Mosler, G., Just, W., Pilgrim, C., and Reisert, I. (2000). Developmental profile of *Sry* transcripts in mouse brain. *Neurogenetics* 3 (1), 25–30. doi:10.1007/s100480000093

Mayfour, A., Pahlavan, S., Ansari, H., Baharvand, H., and Salekdeh, G. H. (2019). Down-regulation of a male-specific H3K4 demethylase, kdm5d, impairs cardiomyocyte differentiation. *J. Proteome* 18, 4277–4282. doi:10.1021/acs.jproteome.9b00395

Medrano, M. C., Darlot, F., Cador, M., and Caille, S. (2023). Poor inhibitory control predicts sex-specific vulnerability to nicotine rewarding properties in mice. *Psycopharmacology* 240, 1973–1986. doi:10.1007/s00213-023-06418-3

Milsted, A., Underwood, A. C., Dunmire, J., DelPuerto, H. L., Martins, A. S., Ely, D. L., et al. (2010). Regulation of multiple renin-angiotensin system genes by Sry. *J. Hypertens.* 28 (19), 59–64. doi:10.1097/HJH.0b013e328332b88d

Morgan, M. M., and Ataras, K. (2022). Sex differences in the impact of pain, morphine administration and morphine withdrawal on quality of life in rats. *Pharmacol. Biochem. Behav.* 219, 173451. doi:10.1016/j.pbb.2022.173451

Mucke, L., Abraham, C. R., and Masliah, E. (1996). Neurotrophic and neuroprotective effects of hAPP in transgenic mice. *Ann. N. Y. Acad. Sci.* 17 (777), 82–88. doi:10.1111/j.1749-6632.1996.tb34405.x

Murray, D. W., Didier, S., Chan, A., Paulino, V., Van Aelst, L., Ruggieri, R., et al. (2014). Guanine nucleotide exchange factor Dock7 mediates HGF-induced glioblastoma cell invasion via Rac activation. *Br. J. Cancer* 110 (5), 1307–1315. doi:10.1038/bjc.2014.39

Penniman, C. M., Suarez Beltran, P. A., Bhardwaj, G., Junck, T. L., Jena, J., Poro, K., et al. (2019). Loss of FoxOs in muscle reveals sex-based differences in insulin sensitivity but mitigates diet-induced obesity. *Mol. Metab.* 30, 203–220. doi:10.1016/j.molmet.2019.10.001

Phoenix, C. H., Goy, R. W., Gerall, A. A., and Young, W. C. (1959). Organizing action of prenatally administered testosterone propionate on the tissues mediating mating behavior in the female Guinea pig. *Endocrinol* 65, 369–382. doi:10.1210/endo-65-3-369

Pottmeier, P., Doszyn, O., Peuckert, C., and Jazin, E. (2020). Increased expression of Y-encoded demethylases during differentiation of human male neural stem cells. *Stem Cells Dev.* 29 (23), 1497–1509. doi:10.1089/scd.2020.0138

Prokop, J. W., Chhetri, S. B., van Veen, J. E., Chen, X., Underwood, A. C., Uhl, K., et al. (2020). Transcriptional analysis of the multiple *Sry* genes and developmental program at the onset of testis differentiation in the rat. *Biol. Sex. Differ.* 11 (1), 28–8. doi:10.1186/s13293-020-00305-8

Prokop, J. W., Tsaih, S.-W., Faber, A. B., Boehme, S., Underwood, A. C., Troyer, S., et al. (2016). The phenotypic impact of the male-specific region of chromosome-Y in inbred mating: the role of genetic variants and gene duplications in multiple inbred rat strains. *Biol. Sex. Diff.* 7, 10. doi:10.1186/s13293-016-0064-z

Prokop, J. W., Underwood, A. C., Turner, M. E., Miller, N., Pietrzak, D., Scott, S., et al. (2013). Analysis of Sry duplications on the *Rattus norvegicus* Y-chromosome. *BMC Genomics* 14, 792. doi:10.1186/1471-2164-14-792

Ramathal, C., Angulo, B., Sukhwani, M., Cui, J., Durruthy-Durruthy, J., Fang, F., et al. (2015). DDX3Y gene rescue of a Y chromosome AZFa deletion restores germ cell formation and transcriptional programs. *Sci. Rep.* 5, 15041. doi:10.1038/srep15041

Rauschendorf, M. A., Zimmer, J., Ohnmacht, C., and Vogt, P. H. (2014). DDX3X, the X homologue of AZFa gene DDX3Y, expresses a complex pattern of transcript variants only in the male germ line. *Mol. Hum. Reprod.* 20 (12), 1208–1222. doi:10.1093/molehr/gau081

Reinius, B., and Jazin, E. (2009). Prenatal sex differences in the human brain. *Mol. Psychiatry* 14, 988–989. doi:10.1038/mp.2009.79

Robinson, J. T., Thorvaldsdóttir, H., Winckler, W., Guttman, M., Lander, E. S., Gad Getz, G., et al. (2011). Integrative genomics viewer. *Nat. Biotechnol.* 29, 24–26. doi:10.1038/nbt.1754

Rock, K. D., Folts, L. M., Zierden, H. C., Marx-Rattner, R., Leu, N. A., Nugent, B. M., et al. (2023). Developmental transcriptomic patterns can be altered by transgenic overexpression of Uty. *Sci. Rep.* 13, 21082. doi:10.1038/s41598-023-47977-x

Russell, S. A., and Bashaw, G. J. (2018). Axon guidance pathways and the control of gene expression. *Dev. Dyn.* 247, 571–580. doi:10.1002/dvdy.24609

Samanta, M. K., Gayen, S., Harris, C., Maclary, E., Murata-Nakamura, Y., Malcore, R. M., et al. (2022). Activation of Xist by an evolutionarily conserved function of kdm5c demethylase. *Nat. Commun.* 13, 2602. doi:10.1038/s41467-022-30352-1

Schmid, R. S., and Maness, P. F. (2008). L1 and NCAM adhesion molecules as signaling coreceptors in neuronal migration and process outgrowth. *Curr. Opin. Neurobiol.* 18, 245–250. doi:10.1016/j.conb.2008.07.015

Shen, H., Yanas, A., Owens, M. C., Zhang, C., Fritsch, C., Fare, C. M., et al. (2022). Sexually dimorphic RNA helicases DDX3X and DDX3Y differentially regulate RNA metabolism through phase separation. *Mol. Cell* 82, 2588–2603.e9. doi:10.1016/j.molcel.2022.04.022

Shpargel, K. B., Sengoku, T., Yokohama, S., and Magnuson, T. (2012). UTX and UTY demonstrate histone demethylase-independent function in mouse embryonic development. *PLOS Genet.* 8 (9), e1002964. doi:10.1371/journal.pgen.1002964

Sim, H., Argentaro, A., and Harley, V. R. (2008). Boys, girls and shuttling of *SRY* and SOX9. *Trends Endocrinol. Metab.* 19 (6), 213–222. doi:10.1016/j.tem.2008.04.002

Stefansson, H., Steinthorsdottir, V., Thorgeirsson, T. E., Gulcher, J. R., and Stefansson, K. (2004). Neuregulin 1 and schizophrenia. *Ann. Med.* 36 (1), 62–71. doi:10.1080/07853890310017585

Szklarczyk, D., Gable, A. L., Lyon, D., Junge, A., Wyder, S., Huerta-Cepas, J., et al. (2019). STRING v11: protein-protein association networks with increased coverage, supporting functional discovery in genome-wide experimental datasets. *Nucleic Acids Res.* 47 (D1), D607–D613. doi:10.1093/nar/gky1131

Tabarean, I. V., Korn, H., and Barfai, T. (2006). Interleukin-1beta induces hyperpolarization and modulates synaptic inhibition in preoptic and anterior hypothalamic neurons. *Neuroscience* 141, 1685–1695. doi:10.1016/j.neuroscience.2006.05.007

Takeuchi, J. K., Mileikovskaia, M., Koshiba-Takeuchi, K., Heidt, A. B., Mori, A. D., Arruda, E. P., et al. (2005). Tbx20 dose-dependently regulates transcription factor networks required for mouse heart and motoneuron development. *Development* 132 (10), 2463–2474. doi:10.1242/dev.01827

Turner, M. E., Martin, C., Martins, A. S., Dunmire, J., Farkas, J., Ely, D. L., et al. (2007). Genomic and expression analysis of multiple *Sry* loci from a single *Rattus norvegicus* Y chromosome. *BMC Genet.* 8 (11), 11. doi:10.1186/1471-2156-8-11

Val, P., Lefrançois-Martinez, A. M., Veyssière, G., and Martinez, A. (2003). SF-1 a key player in the development and differentiation of steroidogenic tissues. *Nucl. Recept* 1 (1), 8. doi:10.1186/1478-1336-1-8

Vawter, M. P., Evans, S., Choudary, P., Tomita, H., Meador-Woodruff, J., Molnar, M., et al. (2004). Gender-specific gene expression in post-mortem human brain: localization to sex chromosomes. *Neuropsychopharmacology* 29 (2), 373–384. doi:10.1038/sj.npp.1300337

Vog, P., Edelmann, A., Kirsch, S., Henegariu, O., Hirschmann, P., Kiesewetter, F., et al. (1996). Human Y chromosome azoospermia factors (AZF) mapped to different subregions in Yq11. *Hum. Mol. Genet.* 5 (7), 933–943. doi:10.1093/hmg/5.7.933

Wade, J., and Arnold, A. P. (1996). Functional testicular tissue does not masculinize development of the zebra finch song system. *PNAS* 93 (11), 5264–5268. doi:10.1073/pnas.93.11.5264

Walport, L. J., Hopkinson, R. J., Vollmar, M., Madden, S. K., Gileadi, C., Oppermann, U., et al. (2014). Human UTY(KDM6C) is a male-specific N-methyl lysyl demethylase. *J. Biol. Chem.* 289 (26), 18302–18313. doi:10.1074/jbc.M114.555052

Welstead, G. G., Creyghton, M.-P., Bilodeau, S., Cheng, A. W., Markoulaki, S., Young, R. A., et al. (2012). X-lin ked H3K27me3 demethylase Utx is required for embryonic development in a sex-specific manner. *PNAS* 109 (32), 13004–13009. doi:10.1073/pnas.1210787109

Wu, X., Heffelfinger, C., Zhao, H., and Dellaporta, S. L. (2019). Benchmarking variant identification tools for plant diversity discovery. *BMC Genomics* 20, 701. doi:10.1186/s12864-019-6057-7

Xu, H., Wang, F., Liu, Y., Yu, Y., Gelernter, J., and Zhang, H. (2014). Sex-biased methylome and transcriptome in human prefrontal cortex. *Hum. Mol. Genet.* 23 (5), 1260–1270. doi:10.1093/hmg/ddt516

Yi, G., Jasti, A. C., Jansen, M., and Siefring, J. E. (2005). RhoH, a hematopoietic-specific Rho GTPase, regulates proliferation, survival, migration, and engraftment of hematopoietic progenitor cells. *Blood* 105 (4), 1467–1475. doi:10.1182/blood-2004-04-1604

Zhang, M., Zhou, Y., Jiang, Y., Lu, Z., Xiao, X., Ning, J., et al. (2021). Profiling of sexually dimorphic genes in neural cells to identify Eif2s3y, whose overexpression causes autism-like behaviors in male mice. *Front. Cell Dev. Biol.* 9, 669798. doi:10.3389/fcell.2021.669798

Zhang, X., Gan, Y., Zou, G., Guan, J., and Zhou, S. (2019). Genome-wide analysis of epigenetic dynamics across human developmental stages and tissues. *BMC Genomics* 20 (Suppl. 2), 221. doi:10.1186/s12864-019-5472-0

Zhou, C., Taslima, F., Abdelhamid, M., Kim, S. W., Akatsu, H., Michikawa, M., et al. (2020). Beta-amyloid increases the expression levels of Tid1 responsible for neuronal cell death and amyloid beta production. *Mol. Neurobiol.* 57, 1099–1114. doi:10.1007/s12035-019-01807-2

Frontiers in
Cell and Developmental Biology

Explores the fundamental biological processes of life, covering intracellular and extracellular dynamics.

The world's most cited developmental biology journal, advancing our understanding of the fundamental processes of life. It explores a wide spectrum of cell and developmental biology, covering intracellular and extracellular dynamics.

Discover the latest Research Topics

See more →

Frontiers

Avenue du Tribunal-Fédéral 34
1005 Lausanne, Switzerland
frontiersin.org

Contact us

+41 (0)21 510 17 00
frontiersin.org/about/contact